Tropical Water Quality Hub

National Environmental Science Programme

Final Report

# Testing and implementation of an improved water quality index for the 2016 and 2017 Great Barrier Reef Report Cards

Cedric Robillot, Murray Logan, Mark Baird, Jane Waterhouse, Katherine Martin and Britta Schaffelke

Australian Government

Australian Institute of Marine Science

# Testing and implementation of an improved water quality index for the 2016 and 2017 Great Barrier Reef Report Cards

Cedric Robillot[5], Murray Logan[1], Mark Baird[2], Jane Waterhouse[3], Katherine Martin[4] and Britta Schaffelke[1]

[1] Australian institute of Marine Science
[2] CSIRO Oceans and Atmosphere
[3] School of Marine and Tropical Biology, James Cook University
[4] Great Barrier Reef Marine Park Authority
[5] eReefs, Great Barrier Reef Foundation



Supported by the Australian Government's
National Environmental Science Program

Project 3.2.5 Testing and implementation of an improved water quality index for the 2016 and 2017 Great Barrier Reef Report Cards

National Library of Australia Cataloguing-in-Publication entry:
978-1-925514-18-6

This report should be cited as:
Robillot, C., Logan, M., Baird, M., Waterhouse J., Martin, K. and Schaffelke, B. (2018) *Testing and implementation of an improved water quality index for the 2016 and 2017 Great Barrier Reef Report Cards – Detailed technical report.* Report to the National Environmental Science Program. Reef and Rainforest Research Centre Limited, Cairns (150pp.).

Published by the Reef and Rainforest Research Centre on behalf of the Australian Government's National Environmental Science Program (NESP) Tropical Water Quality (TWQ) Hub.

The Tropical Water Quality Hub is part of the Australian Government's National Environmental Science Program and is administered by the Reef and Rainforest Research Centre Limited (RRRC). The NESP TWQ Hub addresses water quality and coastal management in the World Heritage listed Great Barrier Reef, its catchments and other tropical waters, through the generation and transfer of world-class research and shared knowledge.



Cover photographs: Gary Cranitch; MODIS - NASA

This report is available for download from the NESP Tropical Water Quality Hub website:
http://www.nesptropical.edu.au

# CONTENTS

# LIST OF TABLES

# LIST OF FIGURES

# ACRONYMS

**AIMS** ..... Australian Institute of Marine Science
**BOM**..... Bureau of Meteorology
**CSIRO**..... Commonwealth Scientific and Industrial Research Organisation
**DERM** ..... Department of Environment and Resource Management
**EEC**s..... Essential Ecosystem Characteristics
**FU** ..... Functional Unit
**GBR**..... Great Barrier Reef
**GBRF**..... Great Barrier Reef Foundation
**GBRMP**..... Great Barrier Reef Marine Park
**GBRMPA**..... Great Barrier Reef Marine Park Authority
**IMOS**..... Integrated Marine Observing System
**ISP** ..... Independent Science Panel
**JCU**..... James Cook University
**MMP**..... Marine Monitoring Program
**MODIS** ..... Moderate Resolution Imaging Spectroradiometer
**NAP** ..... Non-algal particulates
**NESP** ..... National Environmental Science Program
**P2R**..... Paddock 2 Reef
**RRRC**..... Reef and Rainforest Research Centre Limited
**TSS**..... Total Suspended Solids
**TWQ**..... Tropical Water Quality
**WQIP** ..... Water Quality Improvement Plan

# ACKNOWLEDGEMENTS

We thank Peter Doherty, Roger Shaw, Hugh Yorkston, Carl Mitchell and the Reef 2050 Water Quality Improvement Plan (WQIP) Independent Science Panel for their scientific advice. We thank Carol Honchin and Bronwyn Houlden from the Great Barrier Reef Marine Park Authority (GBRMPA) for guidance on marine water quality guidelines and boundaries of water bodies. We thank Eric Lawrey from the Australian Institute of Marine Science for assistance with the management of data on eAtlas. We thank Emlyn Jones, Jennifer Skerratt, Nugzar Margvelashvili, Farhan Rizwi and Mike Herzfeld from CSIRO for the implementation of the eReefs models and data assimilation scheme.

The eReefs Project is a collaboration between the Great Barrier Reef Foundation (GBRF), Bureau of Meteorology (BOM), Commonwealth Scientific and Industrial Research Organisation (CSIRO), Australian Institute of Marine Science (AIMS) and the Queensland Government, supported by funding from the Australian Government's Caring for our Country, the Queensland Government, the BHP Billiton Mitsubishi Alliance, and the Science Industry Endowment Fund. Atmospherically-corrected MODIS products were sourced from the Integrated Marine Observing System (IMOS) - IMOS is supported by the Australian Government through the National Collaborative Research Infrastructure Strategy and the Super Science Initiative."

This research was supported by the Australian Government's National Environmental Science Program (NESP) Tropical Water Quality (TWQ) Hub, administered in North Queensland by the Reef and Rainforest Research Centre Ltd (RRRC), and by the Great Barrier Reef Marine Park Authority.

# GLOSSARY

| | |
|---|---|
| **AIMS FLNTU** | Data from continuous deployments of Combination Fluorometer and Turbidity Sensors (WET Labs Environmental Characterization Optics (ECO) FLNTUSB (Fluorescence, NTU) loggers), collected by AIMS as part of the MMP |
| **AIMS In situ** | Data from analysis of direct water samples (collected manually, using Niskin bottles) collected by AIMS as part of the MMP |
| **Chlorophyll-a** | The green pigment found in cyanobacteria, algae and plants. Chlorophyll-a concentration is widely used as a proxy for phytoplankton biomass as a measure of the productivity of marine systems, eutrophication status and to indicate nutrient availability |
| **eReefs BGC** | eReefs biogeochemical model of the Great Barrier Reef as described in http://ereefs.info |
| **Indicator** | An overall characteristic of interest, e.g. water quality |
| **Index** | Standardized representation of a measure typically expressed relative to a benchmark, guideline or threshold |
| **Measure** | A numerical value of an environmental response that has been measured (directly in field) or obtained by calculation from other measures. |
| **Metric** | Mathematical formulation or expression used to generate an index |
| **MMP** | Marine Monitoring Program |
| **NOx** | Dissolved oxidised nitrogen, the sum of nitrate and nitrite |
| **NTU** | Nephelometric Turbidity Units |
| **Region** | Natural Resource Management (NRM) Region |
| **Satellite** | Data derived from Bureau of Meteorology MODIS satellite imagery |
| **Secchi Depth** | The depth at which a 8-inch (20cm) disk of alternating white and black quadrants is no longer visible from the surface of fluid |
| **Subindicator** | A major component of interest of the Indicator, a grouping of a set of measures, e.g. Water Clarity |
| **TSS** | Total Suspended Solids, a measure for the concentration of particulate matter in the water. |
| **Turbidity** | A measure of light scattering caused mainly by suspended solids, algae, microorganisms and other particulate matter, conventionally measured using a sensor (nephelometer) as Nephelometric Turbidity Units (NTU). |
| **Water Body** | One of the five water bodies as defined by the Great Barrier Reef Marine Park Authority in GBRMPA (2010) |
| **Zone** | Combination of Region and Water Body |

# EXECUTIVE SUMMARY

The Reef 2050 Water Quality Improvement Plan (Reef Plan) guides how industry, government and the community will work together to improve the quality of water flowing to the Great Barrier Reef (GBR). Nested under the water quality theme of Reef 2050, it is a joint commitment of the Australian and Queensland governments to address all land-based run-off flowing from the catchments adjacent to the GBR. The plan sets the strategic priorities for the whole Reef catchment. Regional Water Quality Improvement Plans, developed by regional natural resource management bodies, support the plan in providing locally relevant information and guiding local priority actions within regions Progress towards the goal and target is assessed and described through the annual Reef Report Card (Report Card), which is based on a range of monitoring programs summarising improvements in land management practices, progress towards pollutant targets, and the condition of the GBR and its catchments. The information in this report determines the success of actions and identifies whether further measures need to be taken to address water quality in the Great Barrier Reef. In previous Report Cards (until 2015), marine water quality was reported using a metric based on satellite remote sensing of near surface concentrations of chlorophyll and total suspended solids. This provided a wide spatial and temporal coverage of marine water quality which cannot be achieved with in situ observations.

More specifically, in previous Report Cards, marine water quality was assessed using near-surface concentrations of Chlorophyll-a (Chl-a) and non-algal particulates (NAP)[1] as indicators determined from satellite remote sensing. Index scores for these indicators were calculated based on the relative area of the inshore water body that did or did not exceed the relevant GBRMPA Water Quality Guidelines. Scores for Chl-a and NAP were aggregated (averaged) into a final metric value subsequently converted into a final grade on a five-point uniform scale (very good, good, moderate, poor, very poor) for each region. This final grade describes the overall water quality condition across the Great Barrier Reef and within each individual region. The water quality metric used underpinning previous Report Cards (until 2015) presented a number of significant shortcomings:

- It was solely based on remote sensing-derived data. Concerns were raised about the appropriateness of relying on remote sensing exclusively to evaluate inshore water quality, considering well-documented challenges in obtaining accurate estimates from optically complex waters and the fact that valid satellite observations are limited in the wet season due to cloud cover;
- It was limited to reporting on two indicators and did not incorporate other water quality data collected through the Marine Monitoring Program and IMOS;
- It appeared relatively insensitive to large terrestrial inputs such as the impact of rainfall on the volume and quality of water entering the GBR lagoon, most likely due to the binary assessment of compliance relative to the water quality guidelines and aggregation and averaging over large spatial and temporal scales;

In 2016, based on the limitations described above, the Reef Plan Independent Science Panel (ISP) expressed a lack of confidence in the water quality metric used in Report Cards (until 2015) and recommended that a new approach be identified for Report Card 2016 and future

[1] reported as Total Suspended Solids (TSS) which includes suspended solids and particulate nutrients

Report Cards. The ISP also acknowledged substantial advancements in modelling water quality through the eReefs biogeochemical models and the fact that recent research and method development[2] had improved our ability to construct report card metrics. To address the above shortcomings, the ISP requested that:

- the e-Reefs marine biogeochemical model be tested for its ability to deliver a better water quality assessment than the current practice based on remote sensing;
- the GBRMPA water quality guidelines be reviewed to incorporate new evidence collected over the last 6-8 years in understanding coral and seagrass responses to chronic and acute pressures, ecosystem health, recovery and resilience;
- the utility of observational data streams from in-situ monitoring is analysed for potential inclusion in Report Card;
- the current practice of scoring relative to water quality guidelines and aggregating data over fixed spatial and temporal scales be improved to incorporate the magnitude, frequency and duration of exceedance rather than using average annual exceedance counts;
- the inclusion of photic depth, as derived from satellite data, into the metric be evaluated since light is the important driver for coral and seagrass productivity. The most appropriate measure of photic depth can be evaluated and related to seagrass and coral responses; and
- options for combining indicator scores into a single metric are evaluated, including a statistical assessment of potential metrics.

These recommendations led to the funding of this NESP Tropical Water Quality Hub Project 3.2.5: Testing and implementation of an improved water quality index for the 2016 and 2017 Great Barrier Reef Report Cards. Run as a collaboration between GBRMPA, AIMS, CSIRO and James Cook University (JCU), the high-level objectives for this project were to identify and assess alternative strategies to integrate available monitoring and modelling data into an improved metric, adopt these findings into Report Card 2016, and provide recommendations for further improvements to the metric in subsequent report cards. To achieve these objectives and meet the timelines of Report Card 2016, significant improvements had to be demonstrated by April 2017.

[2] Such as a Reef Rescue-funded project on data integration (Brando et al. 2013) and data aggregation methods developed for and used in the recent Gladstone Healthy Harbour Partnership report card

# 1.0 DATA SOURCES

Report cards are typically compiled and communicated annually. However, the time window that constitutes a year differs from report card to report card. Many environmental report cards communicate on data collected within a financial year. This schedule provides a reporting window that is consistent with other management and governmental considerations. Others use a time window that naturally aligns with the cycle of some major underlying environmental gradient - such as wet/dry season. For this project, we are adopting using the same water year (1st Oct < 30 Sept) definition as the AIMS inshore Water Quality Marine Monitoring Program (Lønborg et al., 2016).

The Great Barrier Reef Marine Park (GBRMP), spans nearly 14° of latitude, covers approximately 344,400km$^2$ and in so doing spans multiple jurisdictions with differing pressures and management strategies. Furthermore, the GBR also spans a substantial longitudinal range being bounded by the Queensland coastline in the west and the outer reef in the east. Hence, it is useful to partition the GBR into smaller more homogeneous zones representing combinations of region and water body. For this project, we will adopt six regions (Cape York, Wet Tropics, Dry Tropics, Mackay Whitsunday, Fitzroy and Burnett Mary) and four water bodies (Enclosed Coastal, Open Coastal, Midshelf and Offshore), see Figure 1. Following the recommendations of the Independent Science Panel (ISP), the Enclosed Coastal zone will be excluded from the majority of high level summary products. Nevertheless, it will be present in exploratory data analysis products for the sake of transparency as well as to provide some form of validation and justification for ISP's recommendations.

**Table 1: Great Barrier Reef spatial zones and associated regions and water bodies.**

| Spatial Reporting Zone | Zone | Region | Water body |
|---|---|---|---|
| Enclosed_Coastal_Cape_York | Enclosed_Coastal_Cape York | Cape York | Enclosed Coastal |
| Enclosed_Coastal_Terrain_NRM | Enclosed_Coastal_Wet Tropics | Wet Tropics | Enclosed Coastal |
| Enclosed_Coastal_Burdekin_Dry_Tropics_NRM | Enclosed_Coastal_Dry Tropics | Dry Tropics | Enclosed Coastal |
| Enclosed_Coastal_Mackay_Whitsunday_NRM_Group | Enclosed_Coastal_Mackay Whitsunday | Mackay Whitsunday | Enclosed Coastal |
| Enclosed_Coastal_Fitzroy_Basin_Association | Enclosed_Coastal_Fitzroy | Fitzroy | Enclosed Coastal |
| Enclosed_Coastal_Burnett_Mary_Regional_Group_for_NRM | Enclosed_Coastal_Burnett Mary | Burnett Mary | Enclosed Coastal |
| Open_Coastal_Cape_York | Open_Coastal_Cape York | Cape York | Open Coastal |
| Open_Coastal_Terrain_NRM | Open_Coastal_Wet Tropics | Wet Tropics | Open Coastal |
| Open_Coastal_Burdekin_Dry_Tropics_NRM | Open_Coastal_Dry Tropics | Dry Tropics | Open Coastal |
| Open_Coastal_Mackay_Whitsunday_NRM_Group | Open_Coastal_Mackay Whitsunday | Mackay Whitsunday | Open Coastal |
| Open_Coastal_Fitzroy_Basin_Association | Open_Coastal_Fitzroy | Fitzroy | Open Coastal |
| Open_Coastal_Burnett_Mary_Regional_Group_for_NRM | Open_Coastal_Burnett Mary | Burnett Mary | Open Coastal |
| Midshelf_Cape_York | Midshelf_Cape York | Cape York | Midshelf |
| Midshelf_Terrain_NRM | Midshelf_Wet Tropics | Wet Tropics | Midshelf |
| Midshelf_Burdekin_Dry_Tropics_NRM | Midshelf_Dry Tropics | Dry Tropics | Midshelf |
| Midshelf_Mackay_Whitsunday_NRM_Group | Midshelf_Mackay Whitsunday | Mackay Whitsunday | Midshelf |
| Midshelf_Fitzroy_Basin_Association | Midshelf_Fitzroy | Fitzroy | Midshelf |
| Midshelf_Burnett_Mary_Regional_Group_for_NRM | Midshelf_Burnett Mary | Burnett Mary | Midshelf |
| Offshore_Cape_York | Offshore_Cape York | Cape York | Offshore |
| Offshore_Terrain_NRM | Offshore_Wet Tropics | Wet Tropics | Offshore |
| Offshore_Burdekin_Dry_Tropics_NRM | Offshore_Dry Tropics | Dry Tropics | Offshore |
| Offshore_Mackay_Whitsunday_NRM_Group | Offshore_Mackay Whitsunday | Mackay Whitsunday | Offshore |
| Offshore_Fitzroy_Basin_Association | Offshore_Fitzroy | Fitzroy | Offshore |
| Offshore_Burnett_Mary_Regional_Group_for_NRM | Offshore_Burnett Mary | Burnett Mary | Offshore |

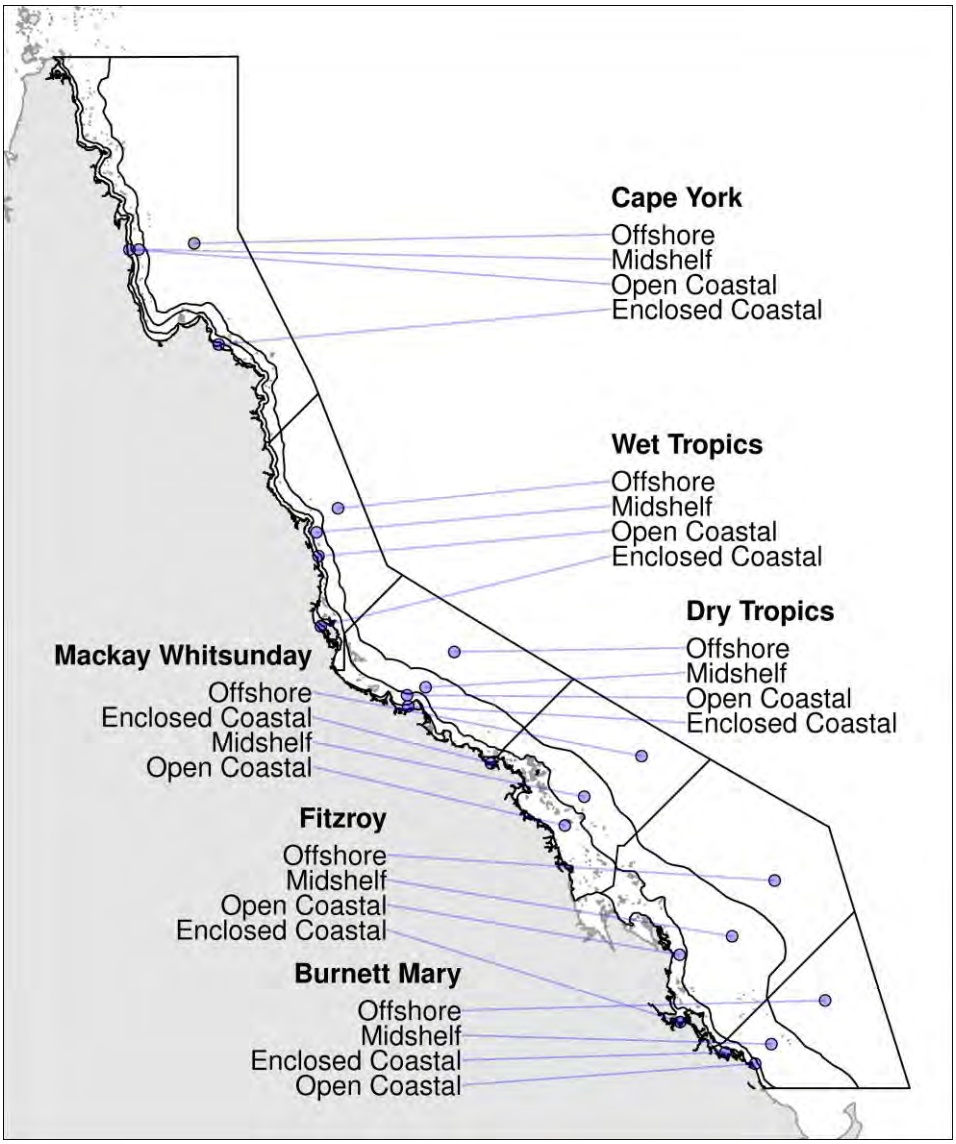


**Figure 1: Great Barrier Reef Zones (Regions and Water Bodies).**

**Table 2: Overview of used data sources**

| Source | Custodian | Description |
|---|---|---|
| AIMS Insitu | AIMS | AIMS inshore monitoring program Niskin data |
| AIMS FLNTU | AIMS | AIMS inshore monitoring program FLNTU logger data |
| Satellite | BOM | BOM: Catalog http://ereeftds.bom.gov.au/ereefs/tds/catalog/ereef/mwq/P1D/2002/catalog.html |
| eReefs | eReefs | First application of BGC data assimilation that is being used for GBR report card 7. |
| eReefs926 | eReefs | eReefs: http://dapds00.nci.org.au/thredds/catalog/fx3/gbr4_bgc_926/catalog.html |

## 1.1 Indicators

One of the biggest challenges of report card development is the selection of appropriate indicators from amongst a potentially very large candidate pool. Since the outcomes, conclusions and implications are all dependent on the indicators selected, the selection process is one of the most influential steps and has justifiably received a great deal of attention.

As part of their ecosystem report card framework, Harwell et al. (1999) urged that the alignment of scientific information with societal goals and objectives should be the guiding principle of indicator selection. In their frame- work, clearly articulated societal goals and objectives (a combination of societal values and scientific knowledge, such as restored and sustainable wetland system) are translated into Essential Ecosystem Characteristics (EECs) that represent a set of generic attributes that further refine the broad goals (such as water quality, sediment quality, habitat quality, ecological processes). The EEC's are then further translated into a set of scientific informed indicators that are measured or monitored to indicate the status of trends or states associated with the EEC's.

There have since been numerous studies that have focused on providing more formal, objective criterion for indicator selection (Dauvin et al., 2008; Emerson et al., 2012; Flint et al., 2012; James et al., 2012). Whilst the specifics vary, most can be broadly encapsulated by a Dauvin et al. (2008)'s contextual implementation of the Doran (1981)'s SMART (Simple, Measurable, Achievable, Realistic, and Time limited) principle. A 'good' indicator should be representative, easily interpreted, broadly comparable, sensitive to change and have a reference or guideline value. To be 'useful', an indicator must be approved by international consensus, be well grounded and documented, have a reasonable cost/benefit ratio and have adequate historical and on-going spatial-temporal coverage. Flint et al. (2012) and James et al. (2012) further developed numerical scoring systems to help evaluate indicators objectively. Nevertheless, (Neary, 2012) warned against the potential to manipulate an index by saturating with inappropriate or biased indicators and whilst recommending that an index comprise of at least seven indicators, they did advocate that the type of indicator is more important than the number of indicators.

Since final outcomes are likely to be highly influenced by indicator choice, the robustness and sensitivity of both indicators and final outcomes to changes in ecosystem health should be understood if not formally investigated as part of the indicator selection process (Dobbie and Dail, 2013). Sensitivity analyses can involve:

- simulating changes in the underlying data of different magnitudes and estimating the resulting sensitivity (percentage or probability of change) expressed by the indicator
- estimating the effect of past perturbations on the indicator hind casted from on historical data

As stressed above, indicators should align intimately with report card objectives. Yet in the more broad ecosystem report card frameworks, such indicators are often too general to be measurable. Therefore, in such cases, the indicators are further sub-divided into progressively more specific measures. For example, an indicator of water quality might comprise sub-indicators of nutrients, metals and physico-chemistry which in turn might be represented by more specific measures such as total nitrogen, mercury, dissolved oxygen, pH etc.

The resulting design is a hierarchical structure in which sub-indicators (etc) are nested within indicators and spatial scales are nested from entire regions, sub-regions or zones down to individual sites or sampling units. One of the strengths of such a hierarchical report card framework is that the inherent inbuilt redundancy allows for the addition, deletion or exchange of finer scale items (sites and actual measured variables) with minimum disruption to the actual report indicators. That is, the indicator is relatively robust to some degree of internal makeup. Furthermore, by abstracting away the fine details of an indicator, similar indicators from different report cards (each potentially comprising different sampling designs) are more directly comparable. For example, in different report cards that include water quality, a water quality indicator of 'water clarity' might comprise different Measures (e.g. suspended solids, NTU, Secchi depth etc) collected from different sources (e.g. satellite, in situ loggers or hand samples), yet provided each of these water clarity indicators are well calibrated, it should be possible to compare state and trend across the report cards.

**Table 3: Example of Water Quality Measure hierarchy specifying which Measures contribute to which Subindicators and which Subindicators contribute to which Indicators.**

| Indicator | Subindicator | Measure | Label | Units |
|---|---|---|---|---|
| Water Quality | Productivity | chl | Chlorophyll | $\mu gL^{-1}$ |
| Water Quality | Water Clarity | nap | TSS | $mgL^{-1}$ |
| Water Quality | Water Clarity | ntu | NTU | NTU |
| Water Quality | Water Clarity | sd | Secchi | m |
| Water Quality | Nutrients | NOx | NOx | $\mu gL^{-1}$ |

## 1.2 AIMS in situ samples

The AIMS component of MMP inshore water quality monitoring sampling program has been designed to quantify spatial and temporal patterns in inshore water quality, particularly in the context of catchment loads. Details of the sampling design are outlined in (Lønborg et al., 2016). From 2006<2014, AIMS visited 20 sites, three times per year (roughly corresponding to wet, early and late dry seasons), see Figures 2 and 3. The sites were largely selected along approximate north-south transects proximal to major rivers so as to provide samples along an expected water quality gradients (exposure to runoff). Following a review in 2014, the design was modified to intensify the spatial (32 sites) and temporal (typically between 5 and 10 samples per year) coverage of the sampling program. In particular, additional sampling effort was applied around three priority focal areas (Russell-Mulgrave, Tully and Burdekin).

**Table 4: Measures collected in AIMS MMP insitu inshore water quality monitoring program. NOx is the sum of NO2 and NO3. Data used are annual means of depth weighted averages per site.**

| Measure | Variable | Description | Abbreviation | Conversion | Units |
|---|---|---|---|---|---|
| Chlorophyll-a | DRIFTCHL_UGPERL.wm | Chlorophyll-a (µg/L) | chl | x1 | $\mu gL^{-1}$ |
| Total Suspended Solids | TSS_MGPERL.wm | Suspended solids (mg/L) | nap | x1 | $mgL^{-1}$ |
| Secchi Depth | SECCHI_DEPTH.wm | Secchi depth (m) | sd | x1 | m |
| NOx | NOX.wm | Nitrite and Nitrate measured by micoanalyser (µM/L) | NOx | x14 | $\mu gL^{-1}$ |

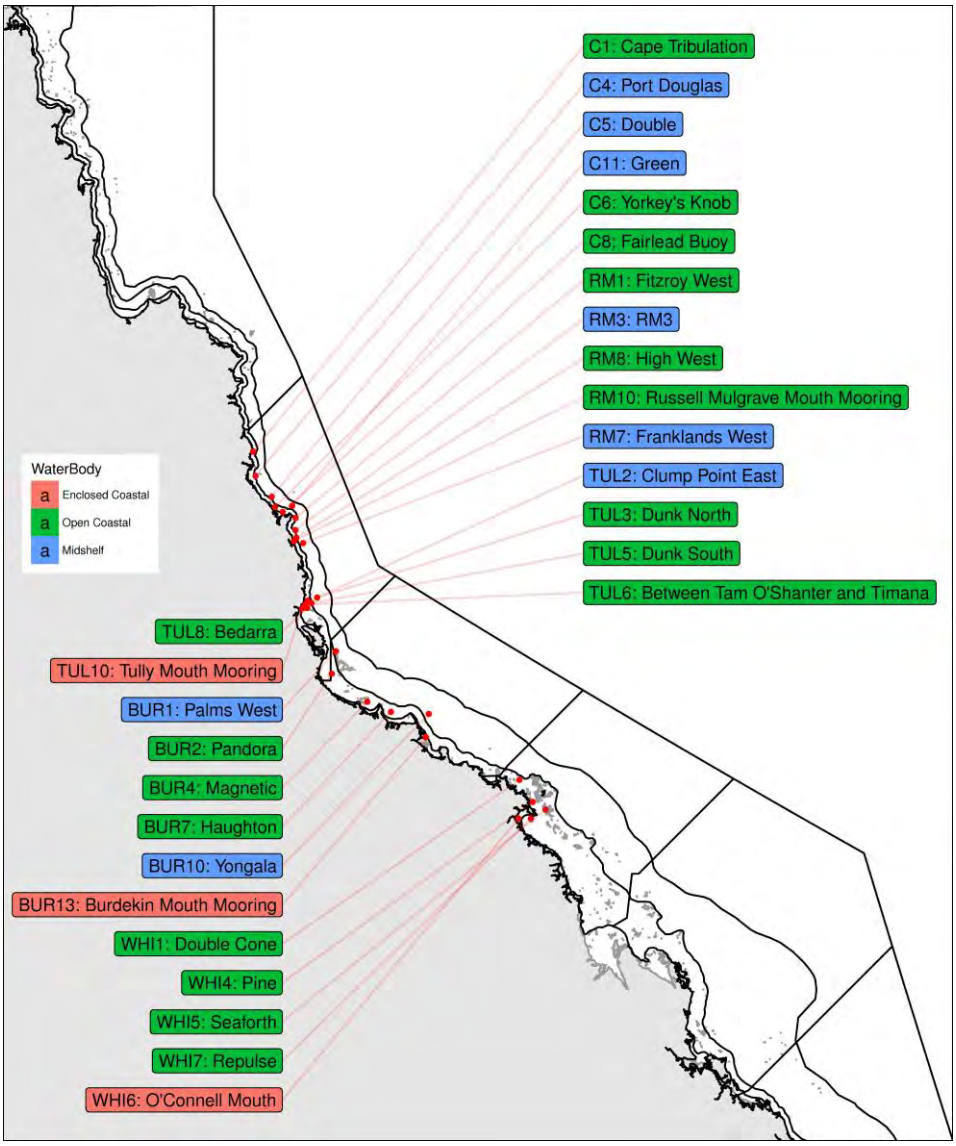


**Figure 2: Map of AIMS in situ sample sites.**

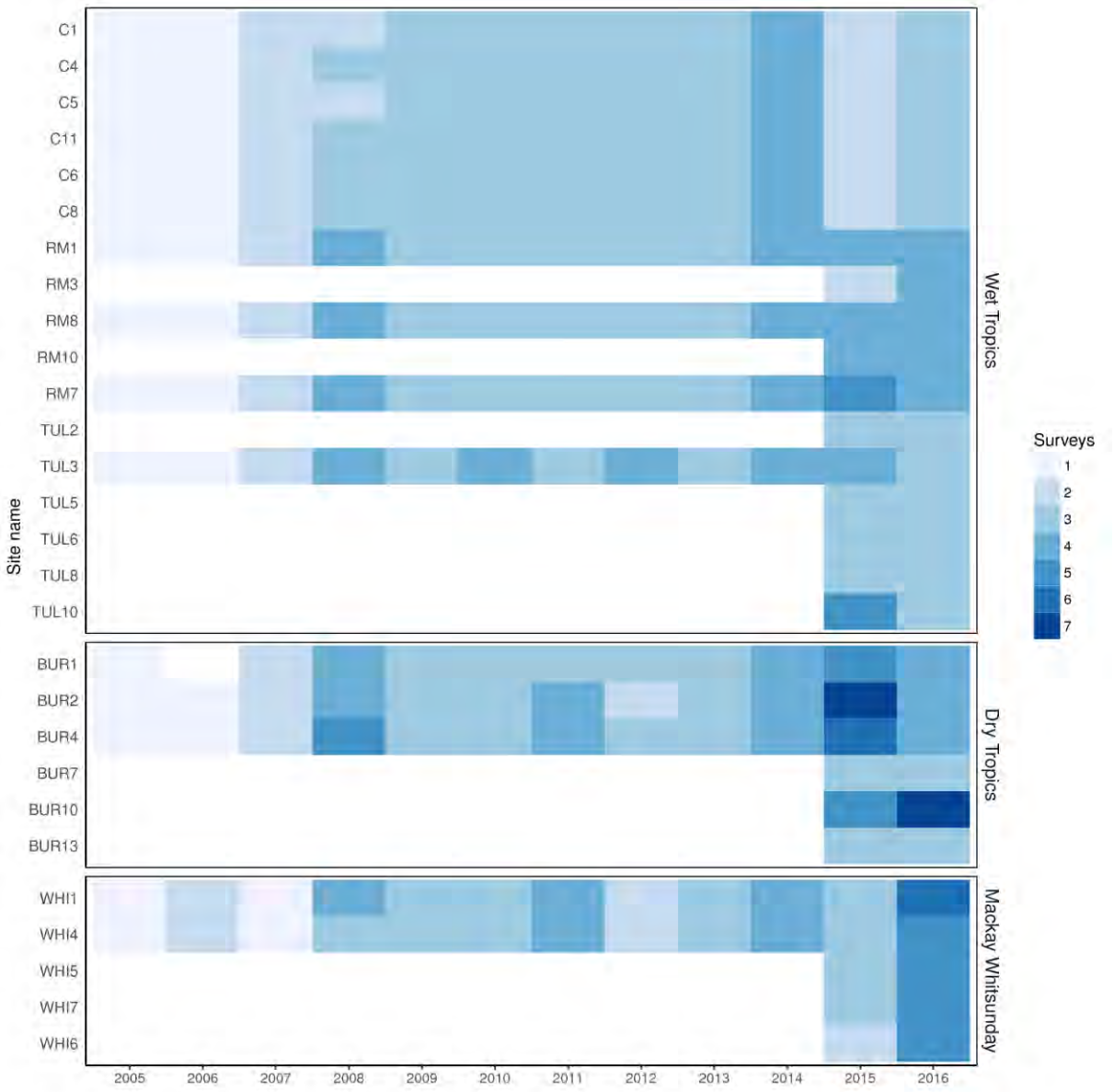


**Figure 3: Spatial and temporal distribution of AIMS insitu samples. Sites names follow Great Barrier Reef Marine Park Authority (GBRMPA) and sites are arranged north to south into the focal Regions. Blue shading of tiles denotes the number of surveys conducted in the year at each site.**

## 1.3 AIMS FLNTU samples

Combination continuous Flourometer and Turbidity Sensors (hereafter FLNTU) loggers were deployed at 15 of the AIMS MMP inshore water quality monitoring sites.

**Table 5: Measures collected in AIMS MMP flntu inshore water quality monitoring program. Data used are daily means per site.**

| Measure | Variable | Description | Abbreviation | Conversion | Units |
|---|---|---|---|---|---|
| Chlorophyll-a | CHL_QA_AVG | Daily mean chlorophyll fluorescence | chl | CHL_QA_AVG x1 | $\mu g L^{-1}$ |
| NTU | NTU_QA_AVG | Daily mean turbidity | ntu | NTU_QA_AVG x1 | NTU |

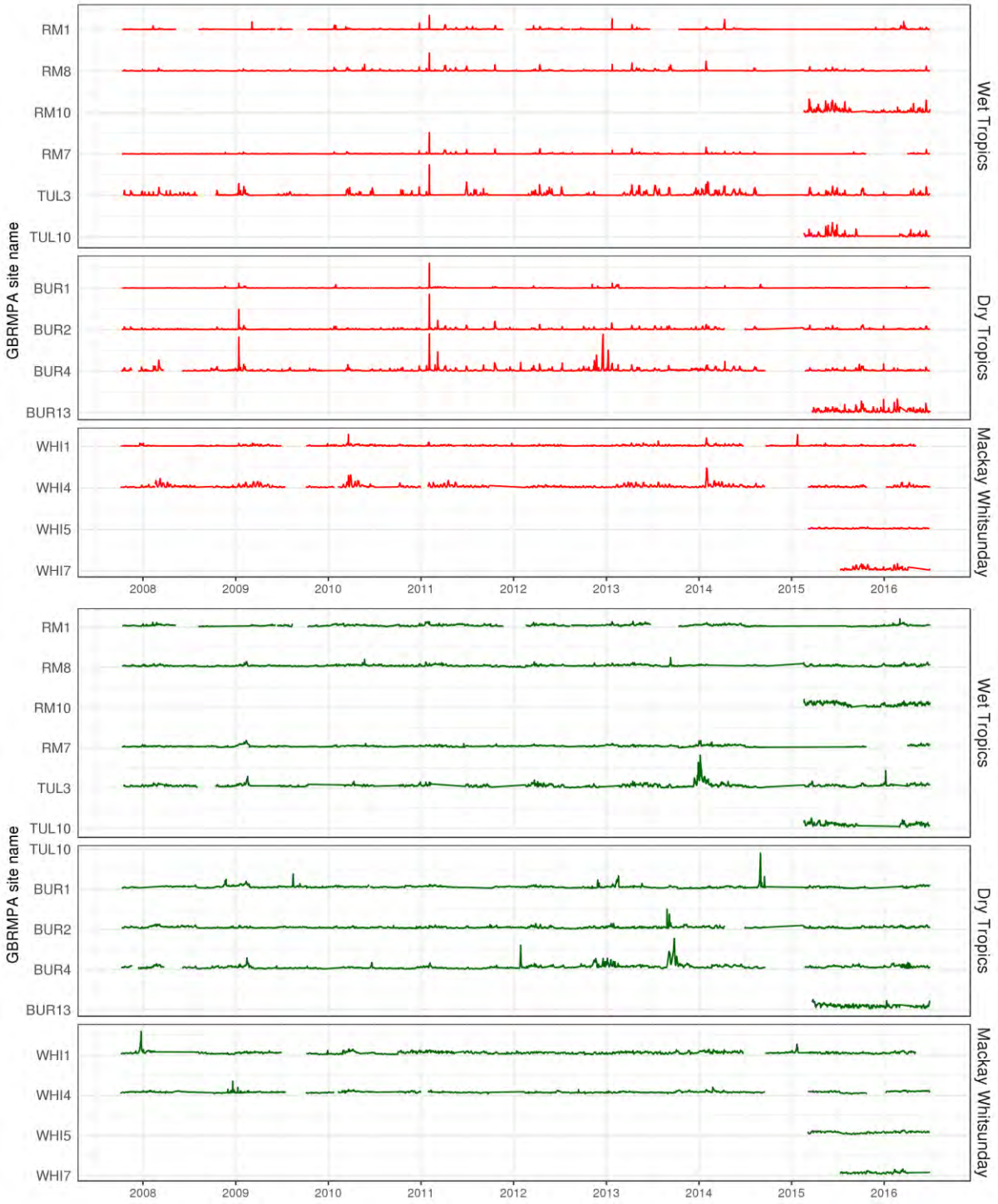


**Figure 4: Spatial and temporal distribution of AIMS FLNTU samples (Red: NTU, Green: Chlorophyll-a). Sites names follow Great Barrier Reef Marine Park Authority (GBRMPA) and sites are arranged north to south into the focal Regions.**

## 1.4 Remote sensing (BOM satellite)

Daily (July 2002<Dec 2016, 1 × 1$km^2$ resolution) Moderate Resolution Imaging Spectroradiometer (MODIS satel- lite) imagery (hereafter referred to as Satellite) data were obtained by downloading NETCDF files from the thredds server (http://ereeftds.bom.gov.au/ereefs/tds/catalog/ereef/mwq/P1D/2002/catalog.html). The data referred to herein relates to the individual measures considered in the data exploration component of the project, and is distinct from the surface reflectance data used in the eReefs data assimilation scheme discussed below in section 1.5.

**Table 6: Measures collected from MODIS satellite imaging. Data used are daily means per pixel. Variable and Description pertain to the eReefs source. Conversion indicates the conversion applied on data to conform to threshold Units. Abbreviation provides a consistent key across data. MIM refers to the robust and scalable matrix inversion method used to handle the variability in optical properties of satellite imagery**

| Measure | Variable | Description | Abbreviation | Conversion | Units |
|---|---|---|---|---|---|
| Chlorophyll-a | Chl_MIM | Near surface concentration based on empirical relationship established between in situ measurements and blue-to-green band ratios | Chl | Chl_MIM x1 | $\mu gL^{-1}$ |
| Non-Algal Particles | Nap_MIM | Total suspended solids based on relationship established between in situ measurements and the absorption concentration of non-algal particles | Nap | Nap_MIM x1 | $mgL^{-1}$ |
| Secchi Depth | SD_MIM | Secchi depth based on empirical relationship established between in situ measurements and estimated depth at which 10% of surface light still available | Sd | SD_MIM x1 | M |

## 1.5 eReefs coupled hydrodynamic – biogeochemical model

The eReefs coupled hydrodynamic, sediment and BGC modelling system involves the application of a range of physical, chemical and biological process descriptions to quantify the rate of change of physical and biological variables (Fig. 5, Schiller et al. (2014)). The processes descriptions are generally based either on a fundamental understanding of the process (such as the effect of gravity on circulation) or measurements when the process is isolated (such as the maximum division rate of phytoplankton cells at 25°C in a laboratory mono-culture). The model also requires as inputs external forcings, such as observed river flows and pollutant loads. Thus, the model can be run without observations from the marine environment and in this mode is quite skillful (Skerratt et al. (submitted 9 Nov. 2017) and below). This mode which does not use observations from the marine environment as the simulation is undertaken is referred to as the non-assimilating simulation. Most of the eReefs marine biogeochemical simulations are non-assimilating.

Despite being already skillful, the predictive skill of the model can be improved by assimilating marine observations into an ensemble (i.e. a large number (108) of similar but not identical) of model simulations. The form of data assimilation we chose, and that is commonly used in weather forecasting, involves updating of the state of the model as the simulation progresses (Fig. 6). State updating involves first looking for a mismatch between the state of the ensemble members and the observations over the previous 5 days. Ocean colour, the observation of water-leaving irradiance at 8 individual wavebands, provides the only data set with sufficient temporal (daily) and spatial (1 km) resolution, providing upwards of 13 million pixels on a cloud-

free day. For this comparison, we have chosen to use the mismatch between the model's prediction of the ratio of the water-leaving irradiance at 443 nm (blue) and 551 nm (green) and the observation of the same quantities from the MODIS sensor on NASA's Aqua satellite. The eReefs biogeochemical model is the first published model to assimilate raw ocean colour observations (Jones et al., 2016). The data assimilation algorithm uses the model-observation mismatch, as well as statistically-quantified dynamical properties of model, to periodically alter the values in the 108 member ensemble, resulting the ensemble mean gaining a closer match to the observations. The outcome of this modelling system is referred to in the field of data assimilation as a reanalysis.

Below we describe the model itself, and then particular data assimilation system.

### *1.5.1 eReefs coupled model description and forcing*

The hydrodynamic model is a fully 3-D finite-difference baroclinic model based on the 3-D equations of momentum, continuity and conservation of heat and salt, employing the hydrostatic and Boussinesq assumptions (Herzfeld, 2006; Herzfeld et al., 2015). The sediment transport model adds a multilayer sediment bed to the hydrodynamic model grid and simulates sinking, deposition and resuspension of multiple size classes of suspended sediment (Margvelashvili, 2009; Margvelashvili et al., 2016). The complex BGC model simulates optical, nutrient, plankton, benthic organisms (seagrass, macroalgae and coral), detritus, chemical and sediment dynamics across the whole GBR region, spanning estuarine systems to oligotrophic offshore reefs (Fig. 5, Baird et al. (2016)). An expanded description of the BGC model is available at https://ereefs.info, with a brief description of the optical model in Appendix B. Briefly, the BGC model considers four groups of microalgae (small and large phytoplankton, Trichodesmium and microphytobenthos), two zooplankton groups, three macrophytes types (seagrass types corresponding to Zostera and Halophila, macroalgae) and coral communities.

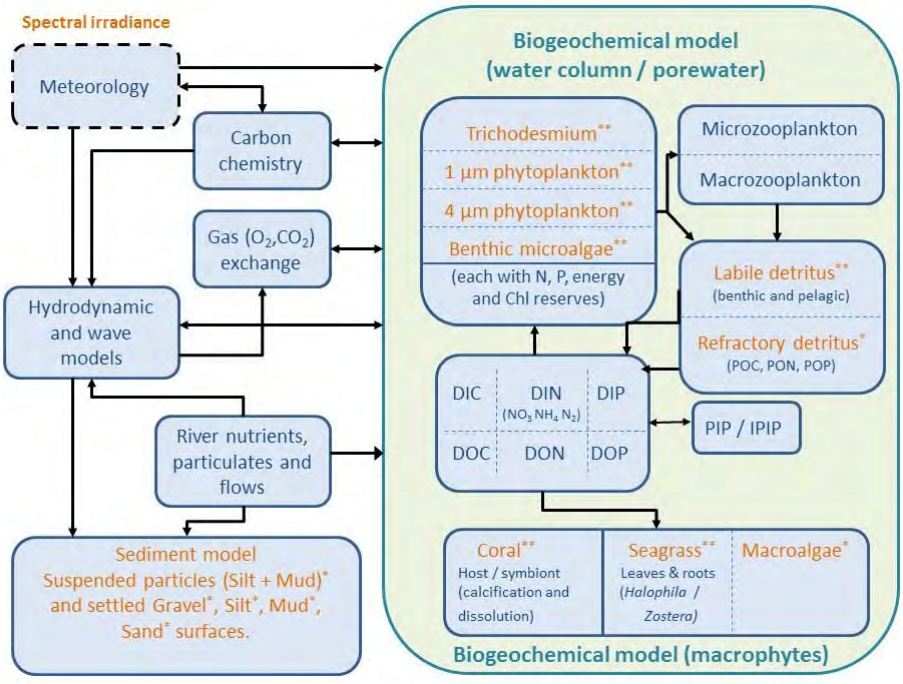


**Figure 5: Schematic showing eReefs coupled hydrodynamic biogeochemical model.**

Photosynthetic growth is determined by concentrations of dissolved nutrients (nitrogen and phosphorous) and photosynthetically active radiation. Microalgae contain two pigments (chlorophyll a and an accessory pigment) and have variable carbon : pigment ratios determined using a photoadaptation model (described in Baird et al. (2013). Overall, the model contains 23 optically active constituents (Baird et al. (2016); and http://ereefs.info).

The model is forced with freshwater inputs at 21 rivers along the GBR and the Fly River in southwest Papua New Guinea. River flows are obtained from the DERM (Department of Environment and Resource Management) gauging network. Nutrient concentrations flowing in from the ocean boundaries were obtained from the CSIRO Atlas of Regional Seas (CARS) 2009 climatology (Ridgway et al., 2002).

The nutrient loads (TSS, PN, PP, DIN,DIP) for the 21 rivers were obtained from the process-based Source models used for Paddock 2 Reef (P2R) load reduction estimates (Waters et al., 2014). The P2R represents land uses and landscape processes in a variety of ways, often based upon spatially explicit farm-scale models that are included through a system of bespoke pre-processing and transfer tools. These P2R Source models also include flow related in-stream processing of pollutants, thus altering loads as fluxes transfer throughout the network. P2R modelling includes scenarios designed to represent ‘baseline’ (or ‘current condition’) and ‘pre-development’ catchment loads. In this report we only use ’baseline’ condition. The reliance of the base P2R Source models on external, farm scale sub-models, means that they cannot be easily modified to extend the period covered by the report card. Thus we only use the P2R outputs from Jan 2011 - July 2014.

In order to provide daily timeseries predictions of pollutant loads past July 2014, the reliance on external submodels was replaced by pollutant generation models that estimate daily loads through monthly varying concentrations (‘EMC/DWC’). The particular concentration values for each pollutant for each Functional Unit (FU) within each sub catchment have been calculated by analysing the monthly runoff volumes and pollutant loads from the P2R Source models defined in Waters et al. (2014). The network transport and in-stream processing mechanisms are unaltered from the base P2R Source models. These monthly concentration pollutant generation models allow the model predictions to be extended by providing updated rainfall runoff model inputs (i.e. the runoff of the day), without the need to also update many thousands of farm scale sub-models. Simple comparisons of predicted loads indicates that the monthly varying concentration approach works reasonably well for sediment and associated particulate nutrient, and less well for pollutants that are usually reliant on farm scale representation of management inputs.

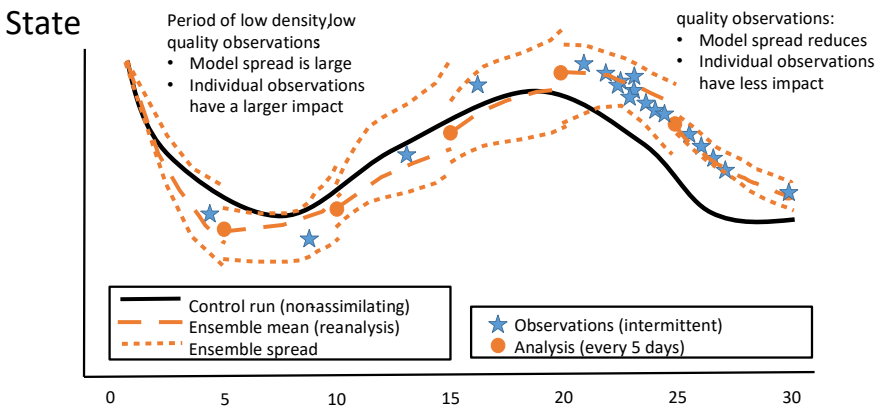


**Figure 6: Schematic showing the evolution of the model ensemble over 6 assimilation cycles using the Ensemble Karman Filter (EnKF) system. The non-assimilating control run (black line) is capturing the gross cycle in the observations (blue stars), but errors remain that observations can constrain. At the initial time, all ensemble members, and the control run, have similar values. In the first five days the 108 members develop a spread, with the control run being different to the ensemble mean, but within the ensemble spread. At 5 days, the first state updating occurs. In the first 5 days there was only one observations, being above the ensemble mean. At day 5, a new state for the entire ensemble is calculated (the analysis being the mean of the updated ensemble) based on the mismatch between the ensemble members and observations. The updated state is closer to the model if the ensemble spread is small, or to the observations if they are dense with few errors. At day 5, because of the small positive mismatch, the ensemble spread is only slightly narrowed, and the mean increased. The ensemble members all restart from these new updated states. The next four analysis steps proceed much like the first. For the fifth analysis step, high density observation were available over the previous 5 days, so the analysis is weighted heavily toward the observations, and the model spread is constrained significantly. Looking at the error between the ensemble mean and the observations over the entire period we see that the data assimilation system has provided an improved estimate of the state (the mean of the ensemble) relative to the control run, and achieved this using the model that contains the processes we understanding to describe system.**

### *1.5.2 Assimilation system*

#### *1.5.2.1 Assimilation of ocean colour*

Ocean colour was chosen as the data set to assimilate due to its availability over the entire GBR at high temporal and spatial density. Ocean colour has often been used for biogeochemical data assimilation (Kidston et al., 2013). In global biogeochemical data assimilation applications, the observation - model mismatch used has often been satellite estimates of *in situ* chlorophyll concentration versus model predicted chlorophyll concentration (Ford et al., 2012). This approach is problematic in coastal waters such as the GBR, where chlorophyll concentration is often overestimated by satellite algorithms due to bottom reflectance or absorption by non-phytoplankton components (Schroeder et al., 2012). So it is not possible in this application to base the data assimilation system on the mismatch of model chlorophyll against satellite estimates of *in situ* chlorophyll. Instead, we have pioneered the use of remote-sensing reflectance as the variable to determine the mismatch between the observed and modelled quantities (Jones et al., 2016).

Remote-sensing reflectance, $R_{rs}$, is the ratio of the water-leaving irradiance in the direction of a satellite to the water entering radiance. In this sense it is a 'raw' satellite observation. The value of $R_{rs}$ varies with wavelength and is measured in $sr^{-1}$ (sr = steradians, the SI unit of solid angle, where the solid angle in all direction on a spherical surface is $4\pi$ sr). In the open ocean

at blue wavelengths the value is around 0.03 $sr^{-1}$ (Baird et al., 2016). That is, 3 % of the light that entered the ocean within 1 $m^2$ emerged travelling in the direction within a solid angle of 1 sr (i.e. 1/4π of a sphere).

The model contains 23 optically active constituents (shaded orange in Fig. 5, see also Baird et al. (2016)). For each of these constituents the optical model calculates the rate of absorption, scattering and backscattering. To calculate $R_{rs}$ at the surface, we need to consider the light returning from multiple depths, and from the bottom. Rather than using a computationally expensive radiative transfer model, we approximate $R_{rs}$ based on an optical-depth weighted scheme (Baird et al., 2016). The model sums the return from each depth (and the bottom) to give the surface $R_{rs}$ . As shown in Baird et al. (2016), this calculation is sufficiently accurate that the primary reason for the mismatch between observed and modelled $R_{rs}$ is errors in the coupled hydrodynamic-biogeochemical model prediction of optically-active constituents. This is, of course, the result we wanted - it means that when the assimilation system updates the optically-active biogeochemical constituents in order to minimise the mismatch between observed and modelled $R_{rs}$ , it is changing the components of the model that have the greatest errors, and in doing so improving the solution of those parts that we most care about - the optically-active components that determine water clarity.

When testing the data assimilation system, we found that the best quantity to assimilate was the ratio of the remote-sensing reflectance at 443 and 551 nm. In fact, this ratio is the same one used in the NASA OC3M algorithm that we mentioned above is NOT a good measure of *in situ* chlorophyll in coastal waters! So how can it be that OC3M is a poor predictor of *in situ* chlorophyll in coastal waters, yet assimilating the mismatch between simulated OC3M and satellite-observed OC3M achieves the best skill for *in situ* chlorophyll when compared against independent *in situ* observations? The answer lies in that simulated OC3M is calculated using the ratio of two simulated $R_{rs}$ , in the same manner in which observed OC3M is calculated using the ratio of two observed $R_{rs}$ . Fig. 7 shows the *in situ* chlorophyll concentration, the simulated OC3M and the NASA observed OC3M for the Cape York region on a relatively clear day. The *in situ* chlorophyll concentration in coastal regions along this coast is $\sim$ 0.5 mg $m^{-3}$ (Fig. 7 left). The simulated OC3M, calculated from simulated $R_{rs}$ , is greater along the coastal fringe due to the absorption of blue light from CDOM, and addition bottom reflection of green light (Fig. 7 centre). The observed OC3M, also affected by CDOM absorption and the bottom, looks more like the simulated OC3M than the *in situ* chlorophyll concentration (Fig. 7 right). Further, where there are differences, the primary cause is the error in the simulated water-column optically-active constituents like chlorophyll. Thus by producing the same simulated and observed quantity, we have improved the ability of the assimilation system to update the optically-active model constituent that is in error.

OC3M uses the ratio of above-surface remote-sensing reflectance as a combination of three wavelengths, R′, which is given by:

$$R' = \log_{10} (\max [R_{rs,443}, R_{rs,488}] / R_{rs,551}) \quad (1)$$

The ratio R′ is used in the OC3M algorithm to estimate surface chlorophyll, $Chl_{OC3}$, with coefficients from the 18 March 2010 reprocessing:

$$Chl_{OC3} = 10^{0.283 + R'(-2.753 + R'(1.457 + R'(0.659 - 1.403R')))} \quad (2)$$

obtained from **oceancolor.gsfc.nasa.gov/REPROCESSING/R2009/ocv6/**. Using, OC3M we gain the benefit of assimilating directly the mismatch between the simulated OC3M (based on simulated remote-sensing reflectance) and the observed remote-sensing reflectance; and we use a quantity that has meaning in the water quality community (mass concentration of chlorophyll). To re-state, because we use the simulated remote-sensing reflectance to calculate OC3M, the system is not affected by the inaccuracies in the relationship between in situ chlorophyll and satellite-derived OC3M. And our assimilation system's prediction of chlorophyll is the simulated *in situ* chlorophyll concentration (and not OC3M).

The accuracy of the modelling systems also requires that the model and observations are closely matched in space and time. This is because remote-sensing reflectance is a function of solar angle (and therefore time of day), and because the optical properties of coastal waters can vary quickly due to a range of processes such as phytoplankton chlorophyll synthesis, movement of fronts, wind driven-upwelling, river plume structure changes etc. We used the flexible outputting time of the model, and the asynchronous assimilation routines in the EnKF-C package (Sakov, 2017), to closely align the observations and models. In doing so we were able to meet the ±30 minutes matching requirements used for the calibration / validation of ocean colour satellite products.

The Aqua satellite overpasses the GBR between 1130 and 1530 locally. In order to match the model output to within 30 minutes of the overpass, the model remote-sensing reflectance was output at 1200, 1300, 1400 and 1500 daily. For the calculations of remote-sensing reflectance, the water column calculations of the light field (and $R_{rs}$) was redone on the output time assuming the entire grid is at 150◦E, while in fact it varies from 142◦31'E to 156◦51'E. Thus the maximum error in calculating solar angle for the purposes of outputting $R_{rs}$, in the Torres Strait, is about 30 minutes (this small error will be corrected in the next phase of eReefs). The light field calculation was also done at wavelengths at the centre of the MODIS ocean colour bands to avoid any small interpolations from the spectrally-resolved model that has a 20 nm resolution.

The observations also need to be spatially aligned. The observations are at approximately ~1 km resolution (up to 2 km on the edges of the swath), with location varying spatially with each different satellite swath. Meanwhile the model cells are stationary, are ~16 $km^2$, and are defined on the curvilinear grid. The observations are grouped into a "superobservation" for each model cell. The superobservation contains all observations that were closer to a particular cell centre than any other cell centre. The position of the superobservation is the mean of the observations it is composed of, and will be close to, but not exactly the same, as the location of the cell centre. The assimilation system then accounts for the now small misalignment in time and space when considering the mismatch between the model and observation.

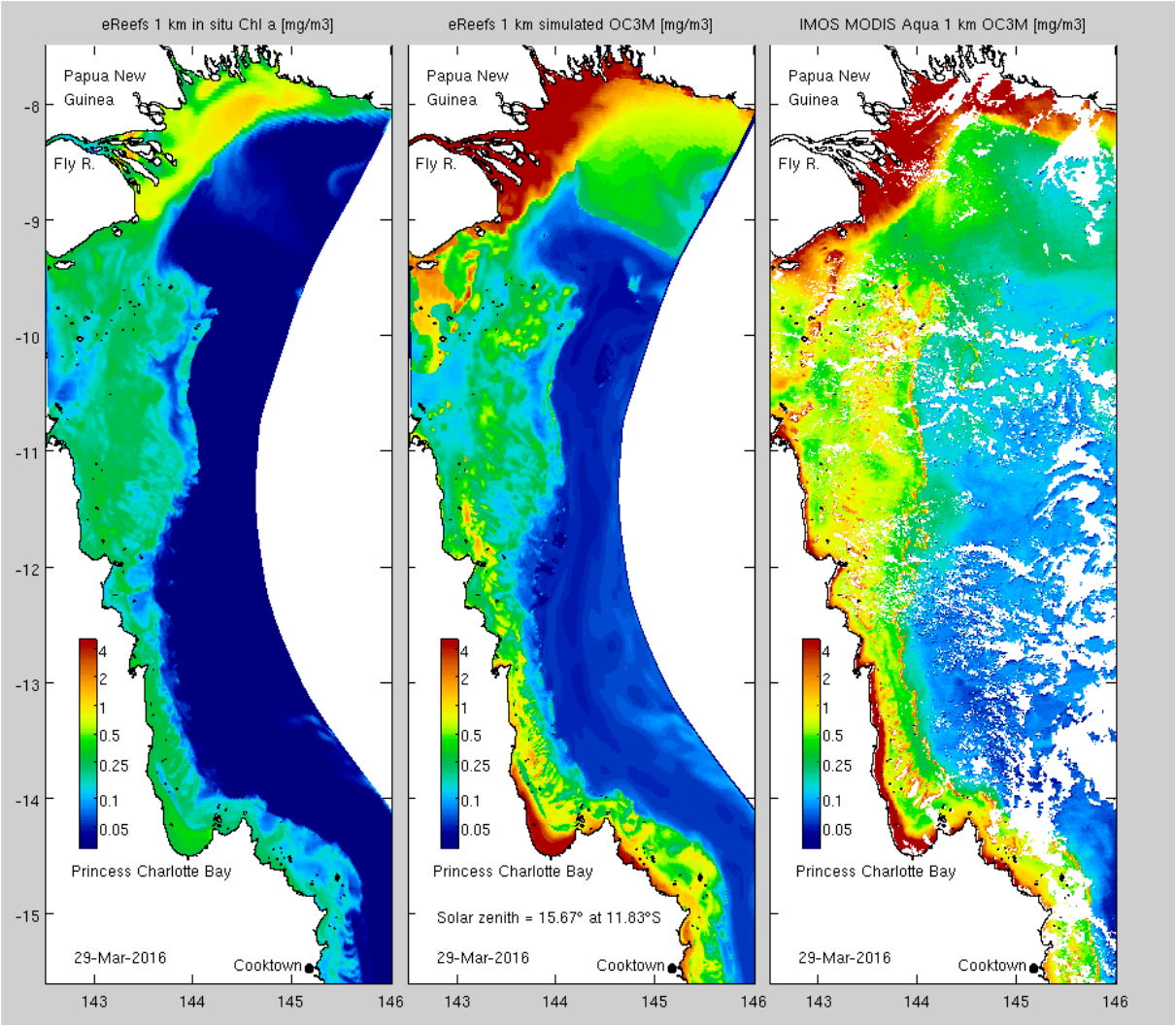


**Figure 7: Example of the estimates of OC3M in the Cape York region on the 29 March 2016 using the 1 km GBR1 model and the NASA Aqua MODIS sensor: in situ chlorophyll concentration (left), the simulated OC3M (centre) and the NASA observed OC3M (right).**

### *1.5.2.2 Ensemble member design*

The assimilation system used in this study is the Deterministic Ensemble Kalman Filter (DEnKF) that requires an ensemble of model runs that approximate the uncertainty in the model solution. The uncertainty in the model solution arises from uncertainty in the model initial conditions, boundary conditions, surface forcing and model parameterisations. The ensemble members differ in the values of the quadratic mortality rate coefficient of small zooplankton, in the loads of nutrients delivered in the rivers (as a multiple of the SOURCE catchments specified loads), and in the PAR light forcing (again as a multiple of the Bureau of Meteorology short wave radiation prediction). These relatively small differences, which are undertaken on the most uncertain biological parameter, and most sensitive forcing parameters, provide a spread of ensemble members that the Karman Filter can operate on. For a further description of the numerical schemes in the assimilation system see (Jones et al., 2016). A number of modifications have been made to improve the accuracy and efficiency of the system, including transferring the the EnKF-C software.

### 1.5.3 Summary results

The non-assimilating version of the model has been compared to observations previously (ereefs.info, Baird et al. (2016) and Skerratt et al. (submitted 9 Nov. 2017)). The results produced in the reanalysis are compared directly to observations available at http://ereefs.info showing comparisons to hundreds of time-series. Further, later components of this document compare the metric calculated using the non-assimilating model, the assimilating model, satellite observations and in situ observations. Here we will just show a few snapshot results to aid in the understanding of the performance of the data assimilation relative to the non-assimilating run.

#### 1.5.3.1 Assessment of Chlorophyll concentration at MMP sites

In our assessment of the skill of the eReefs biogeochemical models, we have considered the most important property to be the prediction of in situ chlorophyll concentration at the MMP sites. For this there are two measures - the chlorophyll extractions at the sampling sites, and the calibrated chlorophyll fluorescence on the moorings. While the extractions are considered the most accurate, the fluorescence time-series is continuous. When the two are lined up in time (they are slightly separated in space), the mismatch between the observed chlorophyll extractions and the observed chlorophyll fluorescence is 0.2 mg $m^3$. We use this 0.2 mg $m^3$ as indicative of the error of the observations.

It is important to note that the in situ chlorophyll concentration observations were not assimilated into the model. That is, they were observation withheld just for the model assessment. In fact, the mismatch between observed and modelled quantities used in the assimilation system is neither an in situ measurement, nor a chlorophyll concentration. The assimilated quantity was the ratio of remote-sensing reflectance at blue and green wavelengths. Thus, we can be confident that if the assimilation system has improved the prediction of in situ chlorophyll concentration then it has improved the overall biogeochemical model.

At 13 of the 14 MMP site, the assimilation of satellite-observed remote-sensing reflectance improved the prediction in situ chlorophyll concentration (Fig. 8, top). On average the assimilation reduced the error from 0.34 to 0.29 mg $m^3$, bring it 30 % closer to the observation error (the limit of our ability to quantify an improvement in the model). The worst two site remained the most coastal sites, Geoffrey Bay and Dunk Island, for which the 4 km model poorly resolves local processes, and for which the assimilation system would provide little information to water column due to the optically-shallow and complex waters. The best site was Double Cone Island off Airlie Beach. At Double Cone Island, a time-series shows the improvement in the chlorophyll fluorescence due to the assimilation (Fig. 8, bottom). During a particularly cloud-free period in the second half of 2015, the assimilation system does a remarkable job of both removing model bias and capturing variability in the model.

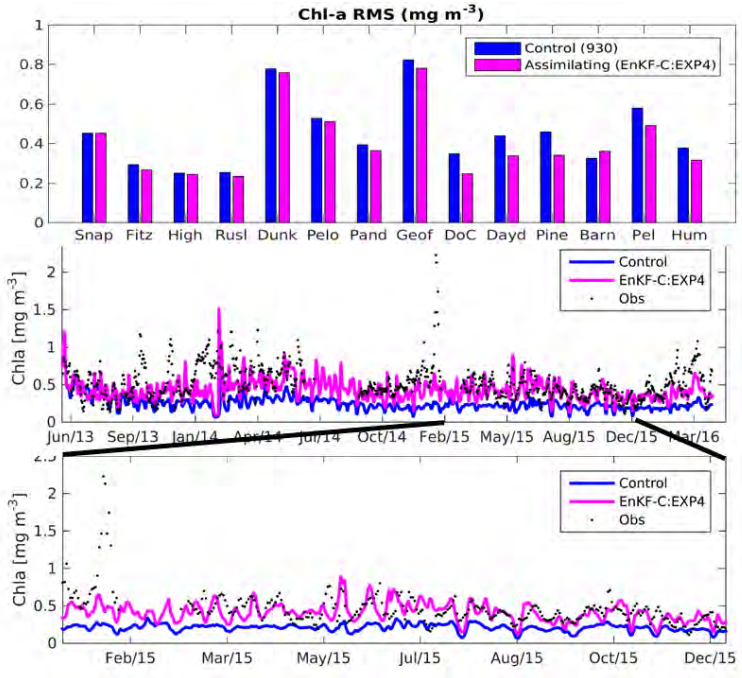


**Figure 8: Comparison of the non-assimilating (blue) and assimilating (pink) runs at the MMP sites. The instantaneous state root mean square error at the 14 MMP sites (top). The approximate error in the observations is 0.2 mg m$^3$. At Double Cone Island in the Whitsundays (off Airlie Beach), a time-series of the observations (black dots) and simulations is shown for the whole simulations (centre) and the a 1 year period (bottom).**

**Table 7: eReefs regional biogeochemical simulation catalog.**

| Simulation name | Herein name | Date range | Delivery | Notes/Improvements |
|---|---|---|---|---|
| GBR4_H1p85_B1p0_Cbas_Dhnd | eReefs926 | Jan 1, 2011 < Jun 30, 2014 | Available on NCI | Simulation delivered as part of SIEF project (previously known as 926). Skill assessment available in SIEF report. |
| GBR4_H2p0_B2p0_Chyd_Dhnd | | Jan 1, 2011 < present, 2014 | | Second publicly-release (mid 2017) long run being used for GBRF resilience and NESP TWQ Hub projects. |
| GBR4_H2p0_B1p9_Chyd_Dran | eReefs | May 1, 2013 < Oct 1, 2016 | | First application of BGC data assimila- tion that is being used for GBR report card 7. |

In this context, the **eReefs** model refers to the GBR4_H2p0_B1p9_Chyd_Dran model (see TableB2) for the catalog and model descriptions and Table9 for a description of the variables and processing).

This source of data only extends back to 2014. Whilst the eReefs GBR4_H2p0_B1p9_Chyd_Dran model tech- nically does contain 2013 calendar year data, the current project partitions time into water years in which the full 2013 water year starts in October 2012. Therefore as the 2013 is not a complete 12 months of data, it is excluded from analyses. Unfortunately, this means that any signals associated with the 2010-2011 floods are unavailable.

**Table 8: Measures collected from eReefs assimilated model. Data used are daily means per pixel. Variable and Description pertain to the eReefs source. Conversion indicates the conversion applied on data to conform to threshold Units. Abbreviation provides a consistent key across data.**

| Measure | Variable | Description | Abbreviation | Conversion | Units |
|---|---|---|---|---|---|
| Chlorophyll-a | Chl_a_um | Sum of Chlorophyll concentration of four microalgae types ($mg/m^3$) | chl | Chl_a_um x1 | $\mu gL^{-1}$ |
| Non-Algal Particles | EFI | EFI = NAP and is the sum of Mud and Fine Sediment | nap | EFI x1000 | $mgL^{-1}$ |
| Secchi Depth | Kd_490 | Kd_490 is calculated from the scattering and absorbing properties of all optical-active constituents,and includes the cosine zenith angle on vertical attenuation. | sd | 1/Kd_490 | m |
| NOx | NO3 | Concentration of Nitrate. As Nitrite is not represented in the model, NO3 = $[NO^-]_3 + [NO^-]_2$ ($mg/m^3$) | NOx | NO3 x1 | $\mu gL^{-1}$ |

## 1.6 eReefs926

In this context, the eReefs926 model refers to the GBR4_H1p85_B1p0_Cbas_Dhnd model (see TableB2). This model provides alternative formulation and importantly does extend back to the full 2013 water year thereby providing some coverage closer to the 2010-2011 flood period. Variables used as per Table 9.

## 1.7 Thresholds

An environmental health metric represents the state or condition relative to some reference, threshold or expectation. Most of the current water quality indices compare values to a set of specifically selected guidelines. These guidelines are either formulated specifically from long-term historical data appropriate to the spatial and temporal domain of interest or else are based on ANZEC guidelines (Australian and New Zealand Environment and Conservation Council, 2000).

Typically there are strict guidelines on how these guidelines should be applied. In particular, the guidelines associated with various measures used in various report cards throughout the Great Barrier Reef should be applied to annually aggregated data - not individual observations. Since this project intends to generate indices on the scale of individual observations, we have decided to refer to the guidelines as thresholds so as to avoid contradicting the terms of use of guidelines.

The thresholds used for each Measure within each Region and Water body are indicated in Table A1 (page 157). Note, that whilst the application of seasonal thresholds could potentially remove some uncertainty, in the absence of clear consensus on how to define wet and dry seasons and what the associated set of thresholds would be, seasonal thresholds are not used in this project.

# 2.0 EXPLORATORY DATA ANALYSIS

Exploratory data analysis is vital for informing data processing and analysis as well as establishing assumptions and limitations. Of particular importance for the current project is the spatial and temporal distribution and variability of the various data Measures and Sources. As such, a series of exploratory plots have been generated (see https://eatlas.org.au/nesp-twq-3/3-2-5-analysis-catalogue). In the interest of keeping the main text free of copious graphics, we have elected to present only a small fraction of the exploratory data analyses figures here. The figures presented will act as exemplars of general format and predominant features or patterns.

## 2.1 All data

Figures 9 - 12 display the temporal distribution of Chlorophyll-a, TSS, Secchi depth and NOx observations for the Wet Tropics Open Coastal Zone from AIMS insitu, AIMS FLNTU, Satellite, eReefs and eReefs926 sources.

All of the figures are presented with log-transformed y-axes as the data are typically positively skewed. This is expected for parameters that have a natural minimum (zero), yet no theoretical maximum. It does however mean that these distributional properties should be considered during the analyses. In particular, for mean based aggregations, outliers and skewed distributions can impart unrepresentative influence on outcomes.

Each of the data sources present different variability characteristics. The scale of the range of AIMS insitu data is predominantly and approximately less than or equal to the scale of the half/twice the associated threshold value (Fig. 9-12a). The AIMS FLNTU logger data (Fig. 9-12b) have a larger range than the AIMS insitu data - presumably because the former data collection frequency captures most of the peaks and troths whereas the latter are unlikely to do so. Furthermore, whilst the AIMS insitu data are predominantly collected during the dry season, the AIMS FLNTU loggers collect data across the entire year and are therefore likely to record a greater proportion of the full variation in conditions. Of course it is important when interpreting these diagnostic plots to focus mainly on the violin plots and less on the dots (representing individual observations). This is because the dots do not provide an indication of the density and it is easy to allow outliers to distort out impression of the variability of the data.

Similarly, the scale of the range eReefs and eReefs926 data (Fig. 9-12d-e) is approximately equal to the scale of the range of the span from half/twice the threshold value. This reflects both a more complete time series and broader spatial extent represented in the data. In contrast to the AIMS insitu and to a lesser extent the AIMS FLNTU and eReefs data, the scale of the range of the Satellite is relatively large - typically a greater span than the range of half/twice threshold value (Fig. 9-12c).

The Satellite, eReefs and eReefs926 data series all start and end part of the way through a water year. For annually aggregated data, this is likely to result in unrepresentative estimates and thus only full water years will be analysed.

a) AIMS insitu

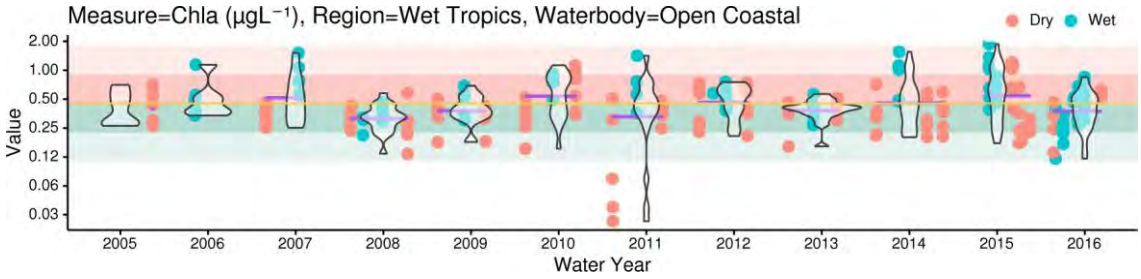


b) AIMS FLNTU

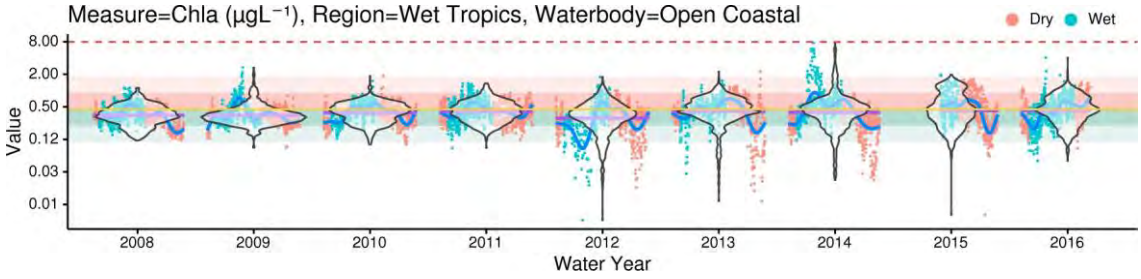


c) Satellite

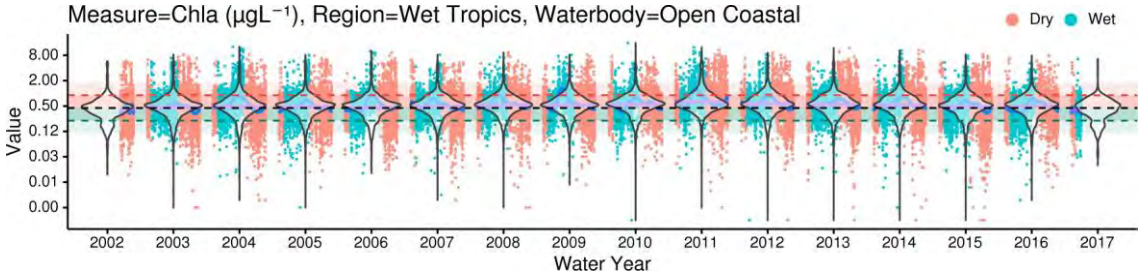


d) eReefs

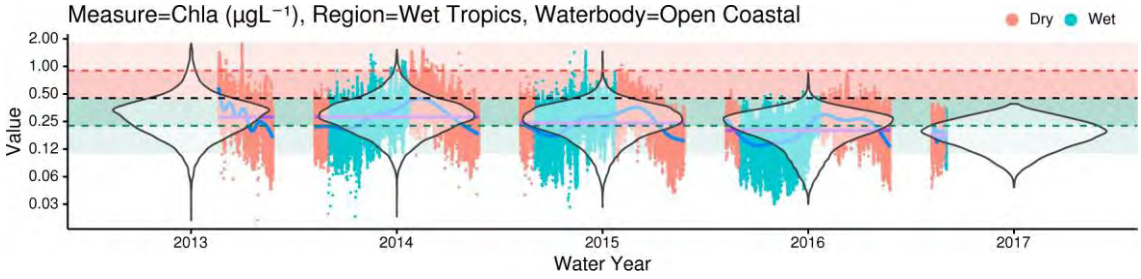


e) eReefs926

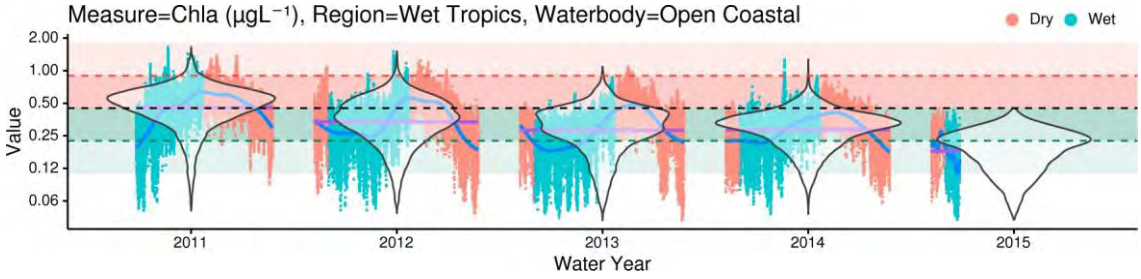


**Figure 9: Observed (logarithmic axis with violin plot overlay) Chlorophyll-a data for the Wet Tropics Open Coastal Zone from a) AIMS insitu, b) AIMS FLNTU, c) Satellite, d) eReefs and e) eReefs926. Observations are ordered over time and colored conditional on season as Wet (blue symbols) and Dry (red symbols). Blue smoother represents Generalized Additive Mixed Model within a water year and purple line represents average within the water year. Horizontal red, black and green dashed lines denote the twice threshold, threshold and half threshold values respectively. Red and green background shading indicates the range (10% shade: x4,/4; 30% shade: x2,/2) above and below threshold respectively.**

a) AIMS insitu

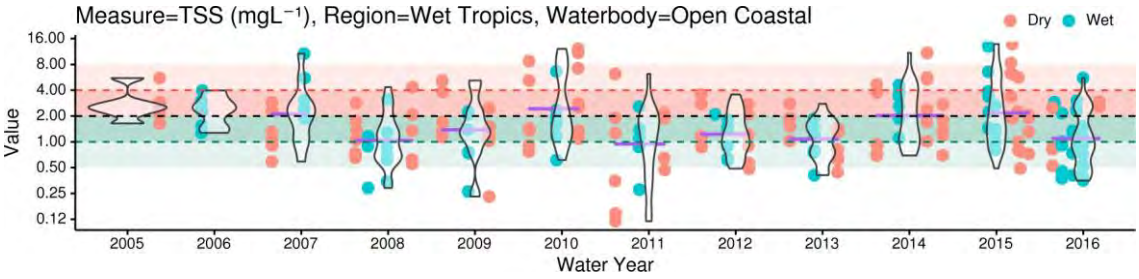


b) AIMS FLNTU

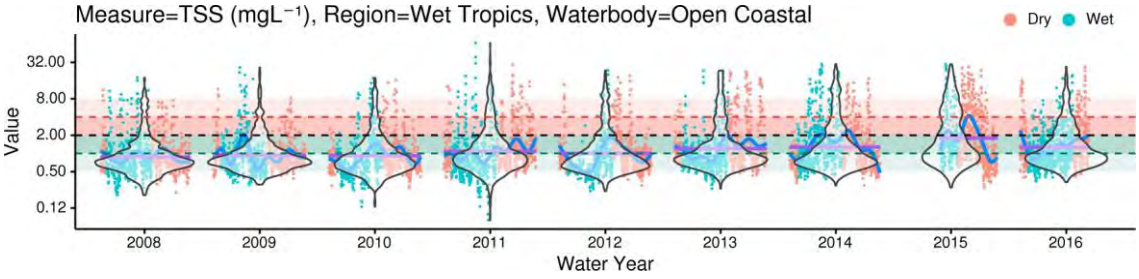


c) Satellite

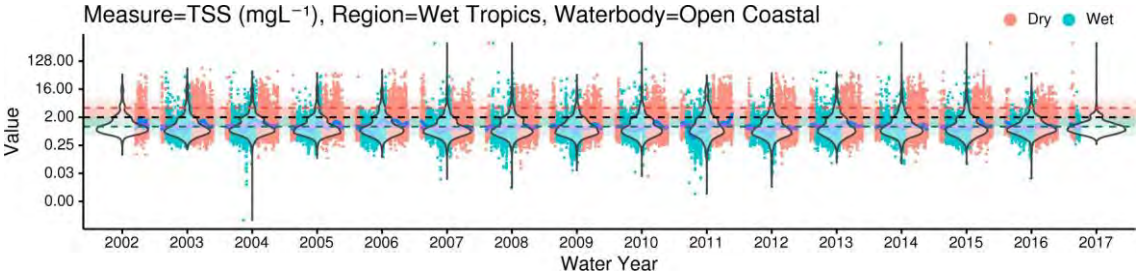


d) eReefs

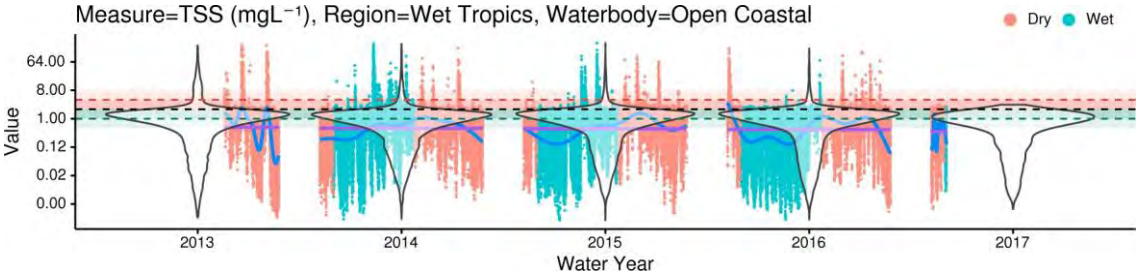


e) eReefs926

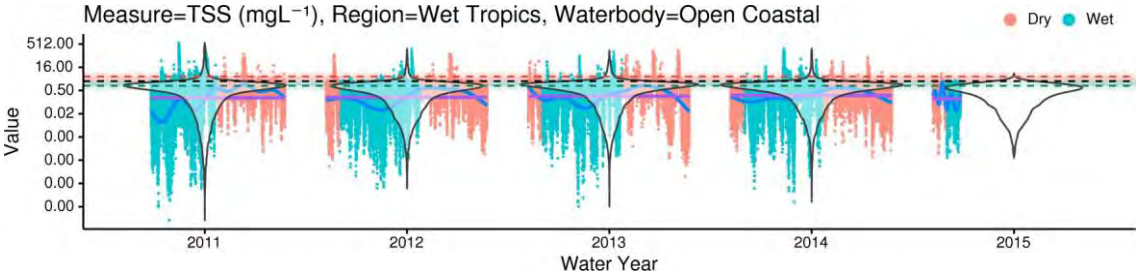


**Figure 10: Observed (logarithmic axis with violin plot overlay) TSS data for the Wet Tropics Open Coastal Zone from a) AIMS insitu, b) AIMS FLNTU, c) Satellite, d) eReefs and e) eReefs926. Observations are ordered over time and colored conditional on season as Wet (blue symbols) and Dry (red symbols). Blue smoother represents Generalized Additive Mixed Model within a water year and purple line represents average within the water year. Horizontal red, black and green dashed lines denote the twice threshold, threshold and half threshold values respectively. Red and green background shading indicates the range (10% shade: x4,/4; 30% shade: x2,/2) above and below threshold respectively.**

a) AIMS insitu

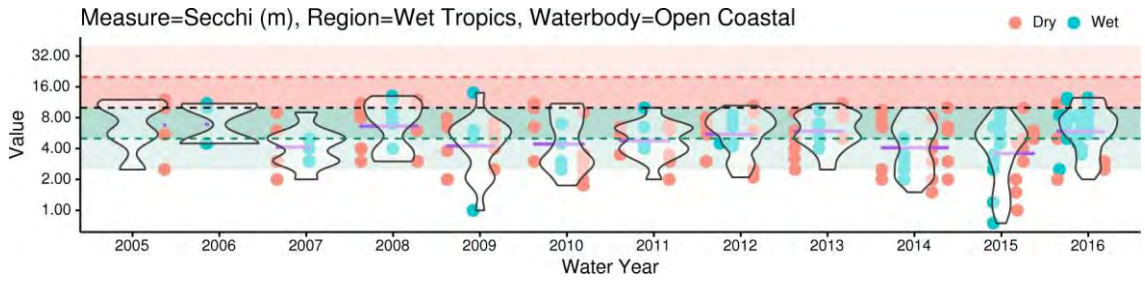


b) AIMS FLNTU

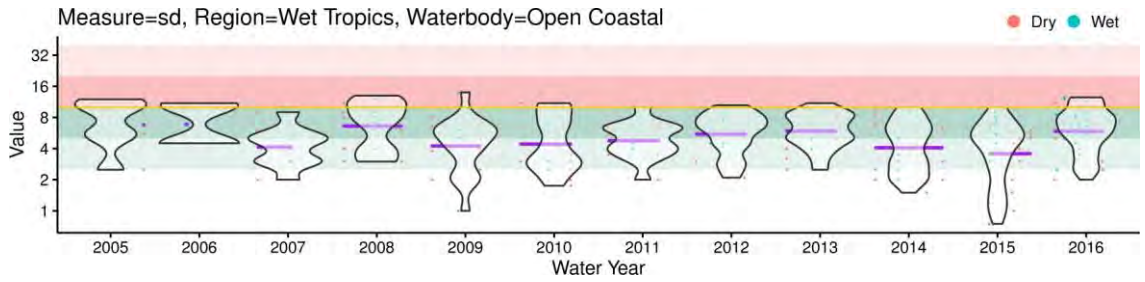


c) Satellite

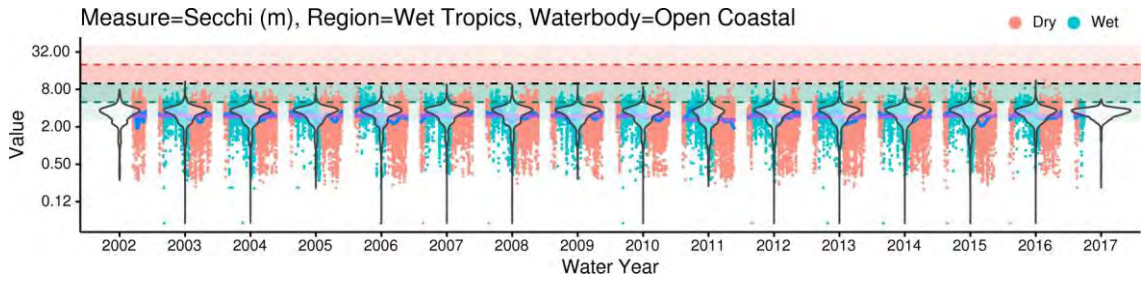


d) eReefs

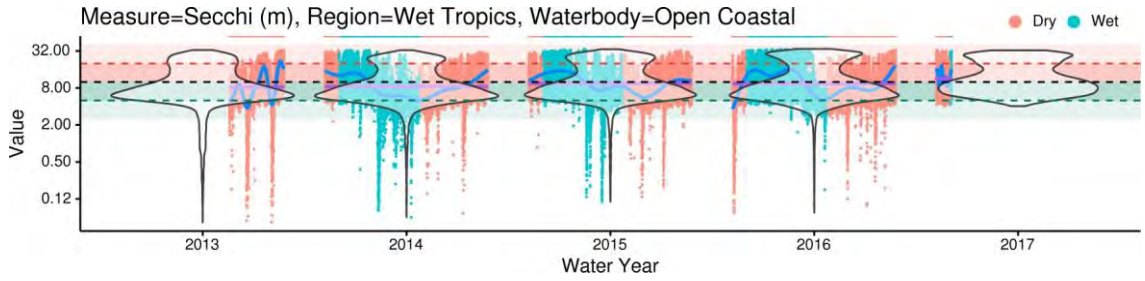


e) eReefs926

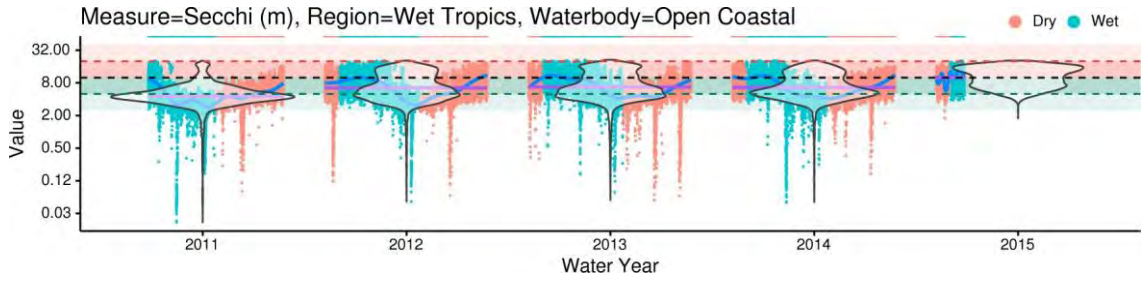


**Figure 11: Observed (logarithmic axis with violin plot overlay) Secchi depth data for the Wet Tropics Open Coastal Zone from a) AIMS insitu, b) AIMS FLNTU, c) Satellite, d) eReefs and e) eReefs926. Observations are ordered over time and colored conditional on season as Wet (blue symbols) and Dry (red symbols). Blue smoother represents Generalized Additive Mixed Model within a water year and purple line represents average within the water year. Horizontal red, black and green dashed lines denote the twice threshold, threshold and half threshold values respectively. Red and green background shading indicates the range (10% shade: x4,/4; 30% shade: x2,/2) above and below threshold respectively.**

a) AIMS insitu

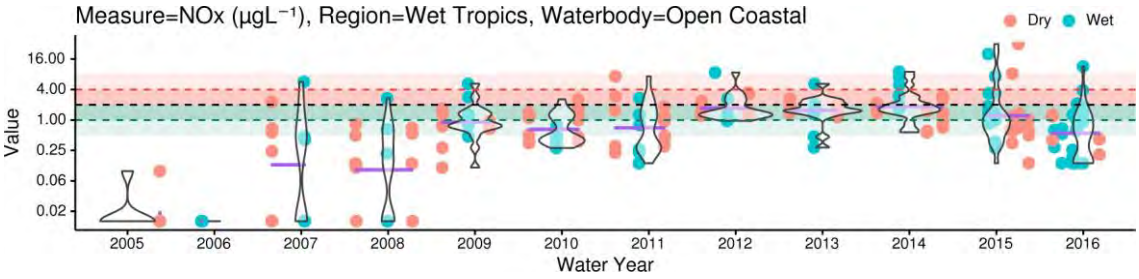


b) eReefs

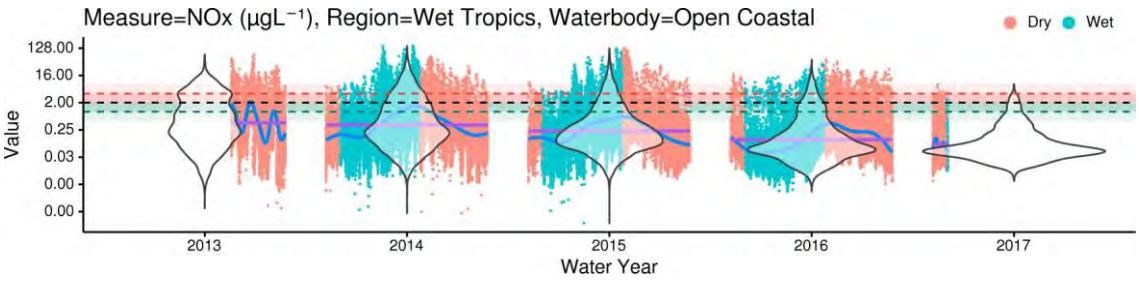


c) eReefs926

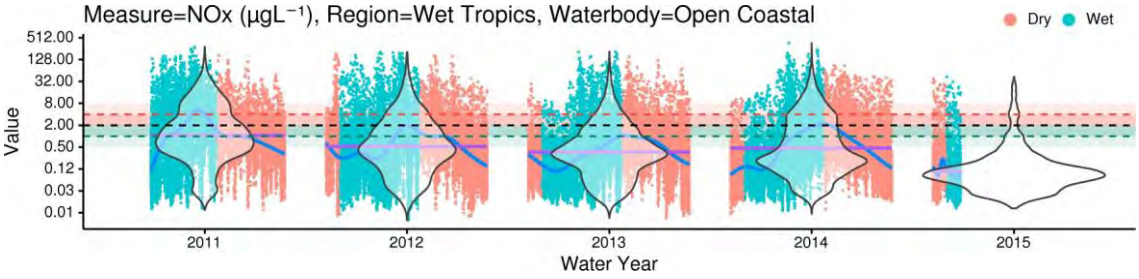


**Figure 12: Observed (logarithmic axis with violin plot overlay) NOx data for the Wet Tropics Open Coastal Zone from a) AIMS insitu, b) eReefs and c) eReefs926. Observations are ordered over time and colored conditional on season as Wet (blue symbols) and Dry (red symbols). Blue smoother represents Generalized Additive Mixed Model within a water year and purple line represents average within the water year. Horizontal red, black and green dashed lines denote the twice threshold, threshold and half threshold values respectively. Red and green background shading indicates the range (10% shade: x4,/4; 30% shade: x2,/2) above and below threshold respectively.**

## 2.3 Monthly data

Figures 13 - 18 provide finer temporal resolution by displaying the temporal distribution of Chlorophyll-a, TSS, Secchi depth and NOx observations for the each month within Wet Tropics Open Coastal Zone from AIMS insitu, AIMS FLNTU, Satellite, eReefs and eReefs926 sources.

The monthly violin plots do not add any additional insights with respect to understanding the characteristics of the underlying data to help guide the selection of appropriate indexation formulation or perhaps even Measure/Source selection. Rather, they provide a less compacted view of the underlying data from which patterns highlighted in Section 2.2 might be more easily appreciated.

a) AIMS insitu

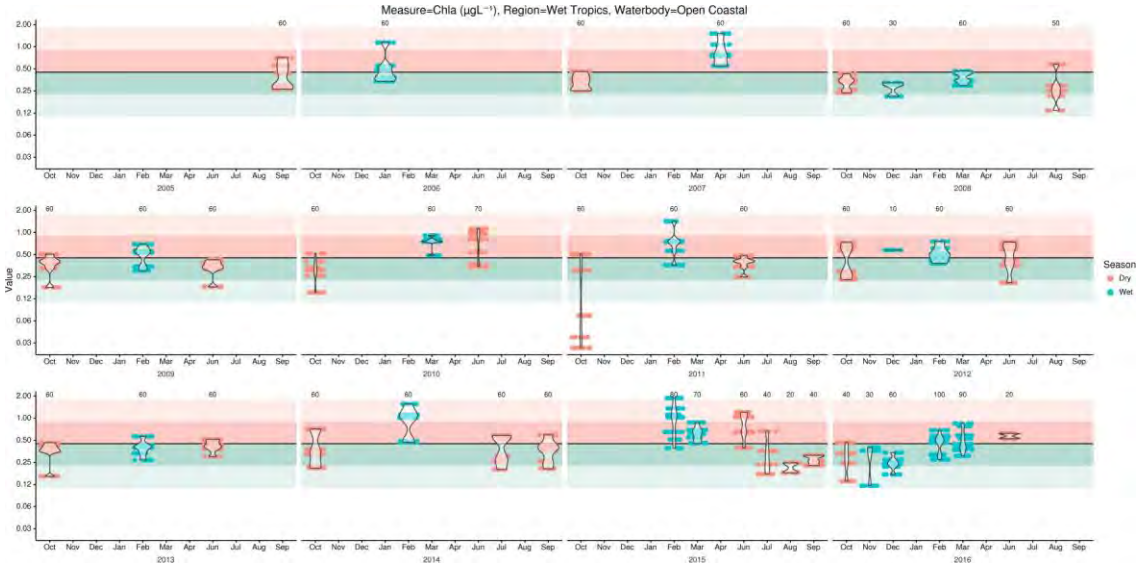


b) AIMS FLNTU

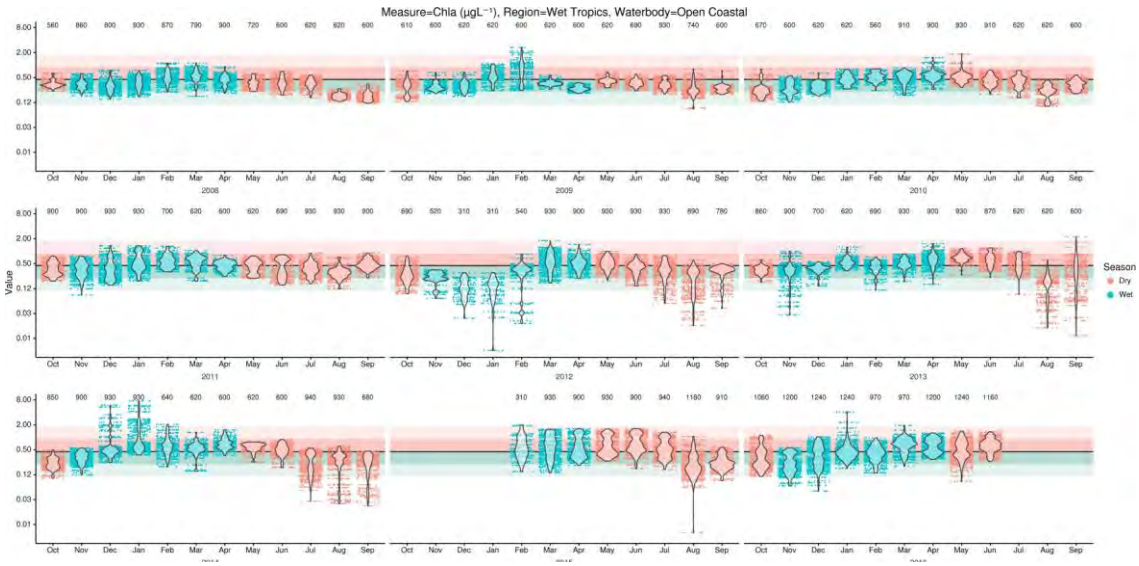


**Figure 13: Observed (logarithmic axis with violin plot overlay) Chlorophyll-a data for the Wet Tropics Open Coastal Zone from a) AIMS insitu, b) AIMS FLNTU. Observations grouped into months are ordered over time and coloured conditional on season as Wet (blue symbols) and Dry (red symbols). Sample sizes represented as numbers above violins and horizontal black dashed line denotes threshold value. Red and green background shading indicates the range (10% shade: x4,/4; 30% shade: x2,/2) above and below threshold respectively.**

a) Satellite

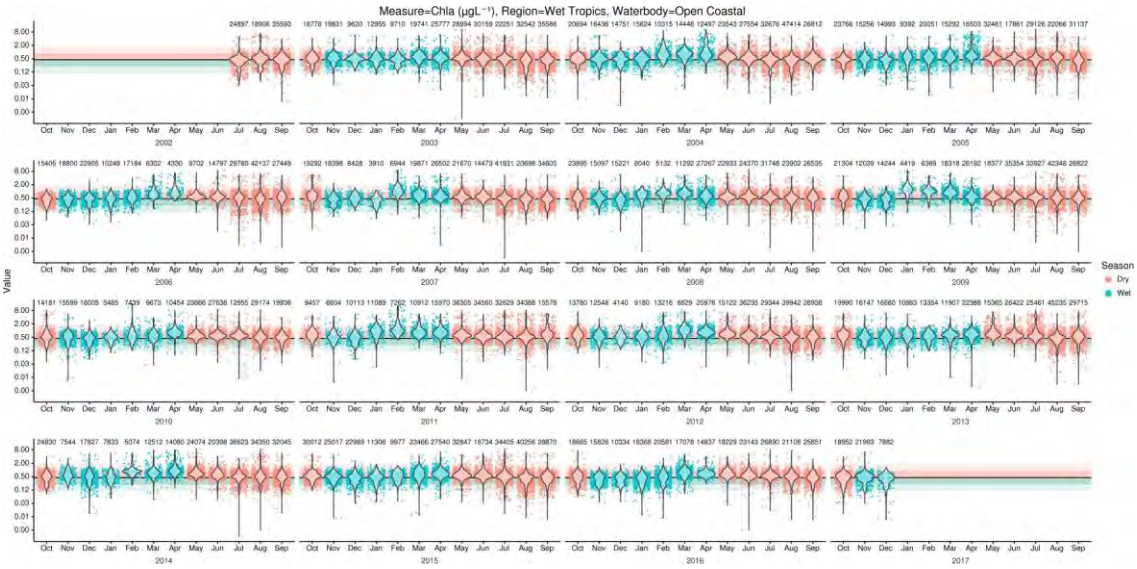


b) eReefs

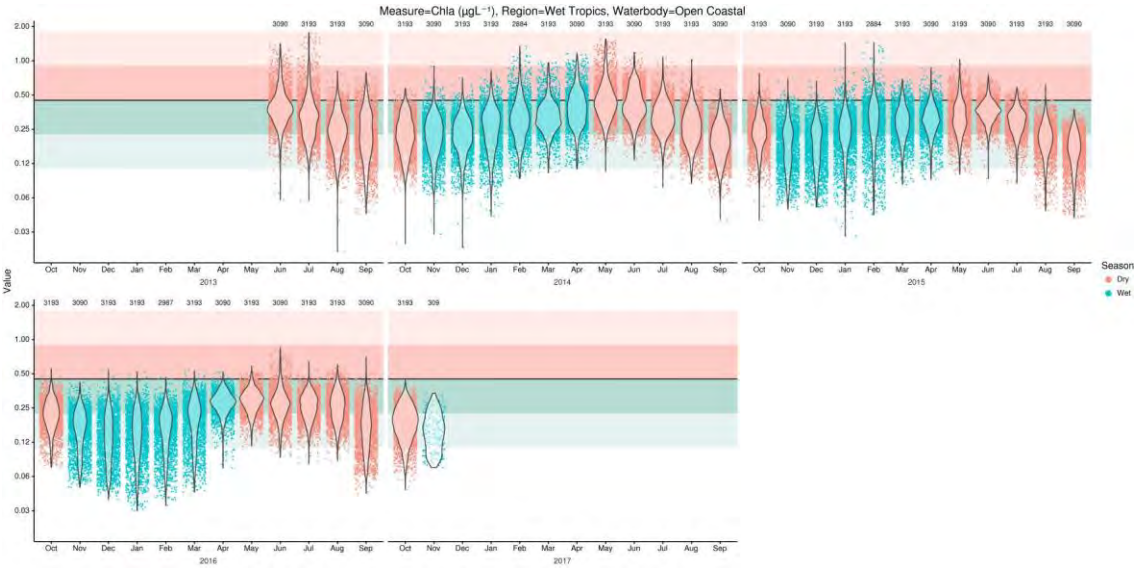


**Figure 14: Observed (logarithmic axis with violin plot overlay) Chlorophyll-a data for the Wet Tropics Open Coastal Zone from a) Satellite, b) eReefs. Observations grouped into months are ordered over time and coloured conditional on season as Wet (blue symbols) and Dry (red symbols). Sample sizes represented as numbers above violins and horizontal black dashed line denotes threshold value. Red and green background shading indicates the range (10% shade: x4,/4; 30% shade: x2,/2) above and below threshold respectively.**

a) AIMS insitu

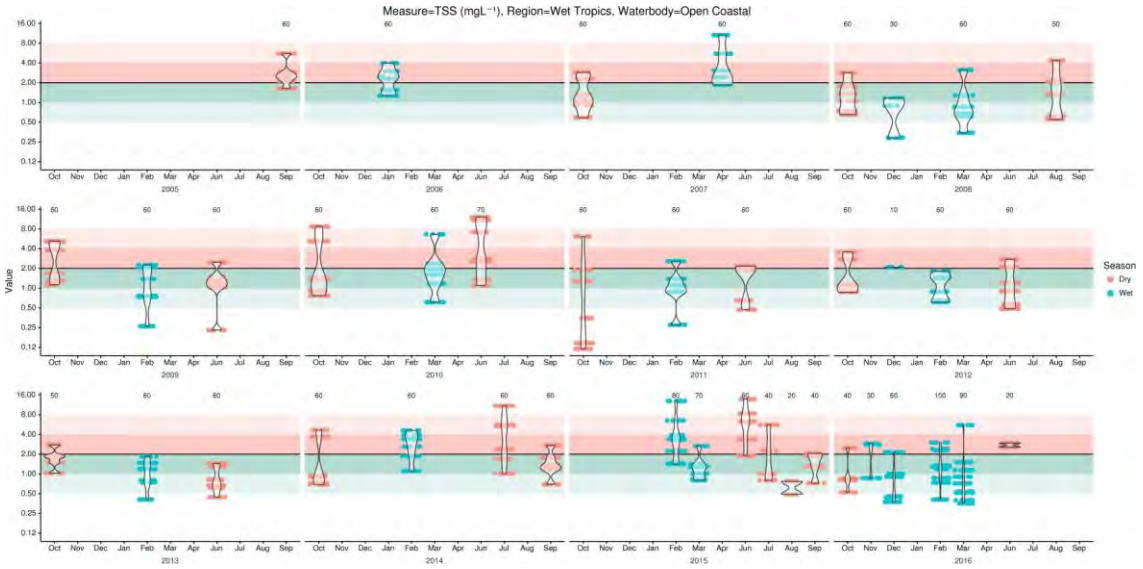


b) AIMS FLNTU

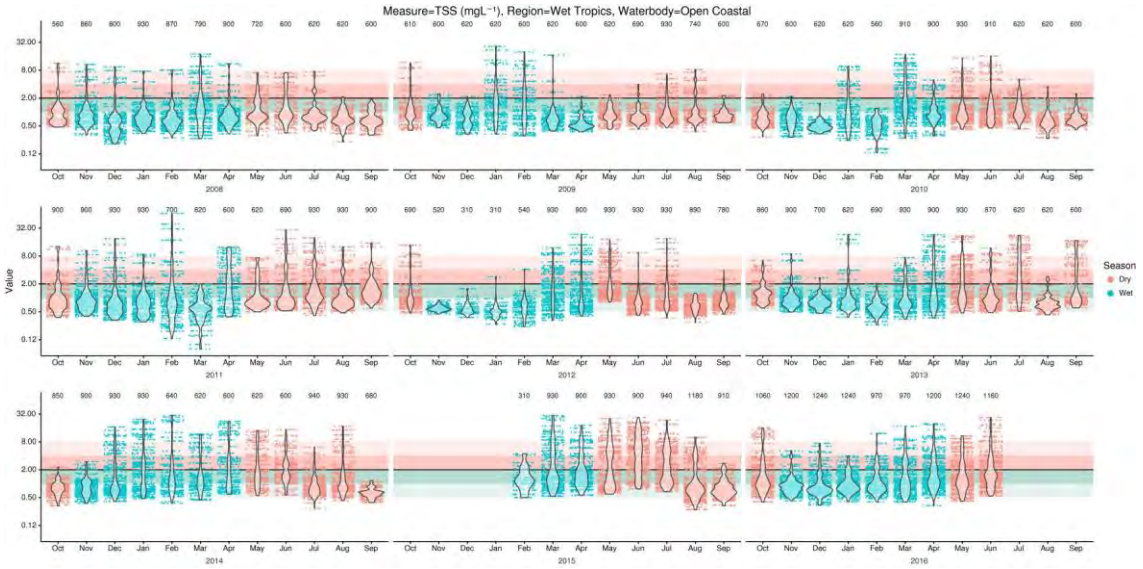


**Figure 15: Observed (logarithmic axis with violin plot overlay) TSS data for the Wet Tropics Open Coastal Zone from a) AIMS insitu, b) AIMS FLNTU. Observations grouped into months are ordered over time and coloured conditional on season as Wet (blue symbols) and Dry (red symbols). Sample sizes represented as numbers above violins and horizontal black dashed line denotes threshold value. Red and green background shading indicates the range (10% shade: x4,/4; 30% shade: x2,/2) above and below threshold respectively.**

a) Satellite

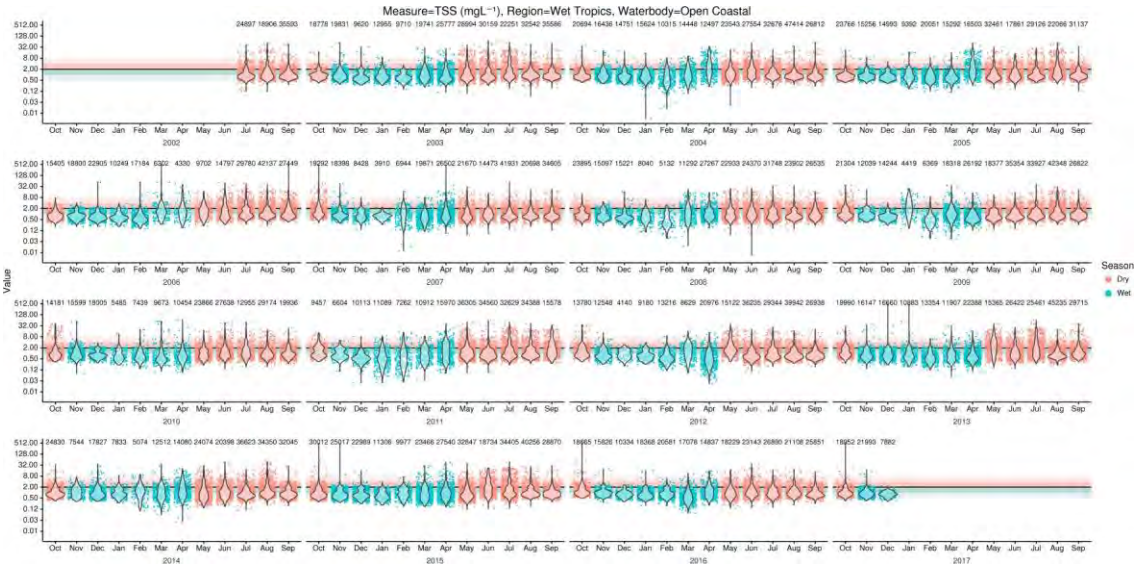


b) eReefs

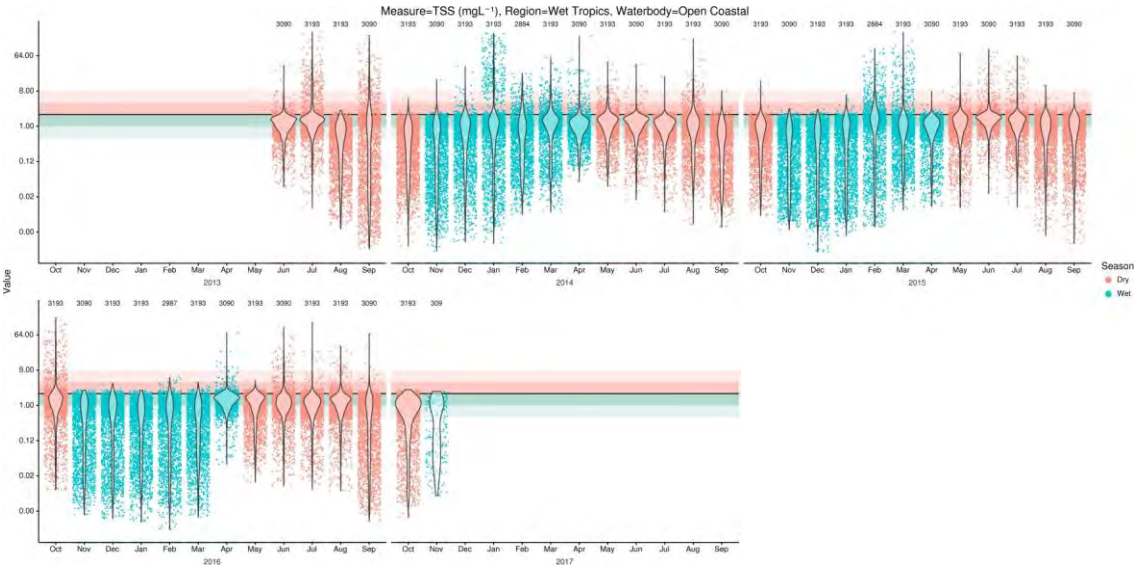


**Figure 16: Observed (logarithmic axis with violin plot overlay) TSS data for the Wet Tropics Open Coastal Zone from a) Satellite, b) eReefs. Observations grouped into months are ordered over time and coloured conditional on season as Wet (blue symbols) and Dry (red symbols). Sample sizes represented as numbers above violins and horizontal black dashed line denotes threshold value. Red and green background shading indicates the range (10% shade: x4,/4; 30% shade: x2,/2) above and below threshold respectively.**

a) AIMS insitu

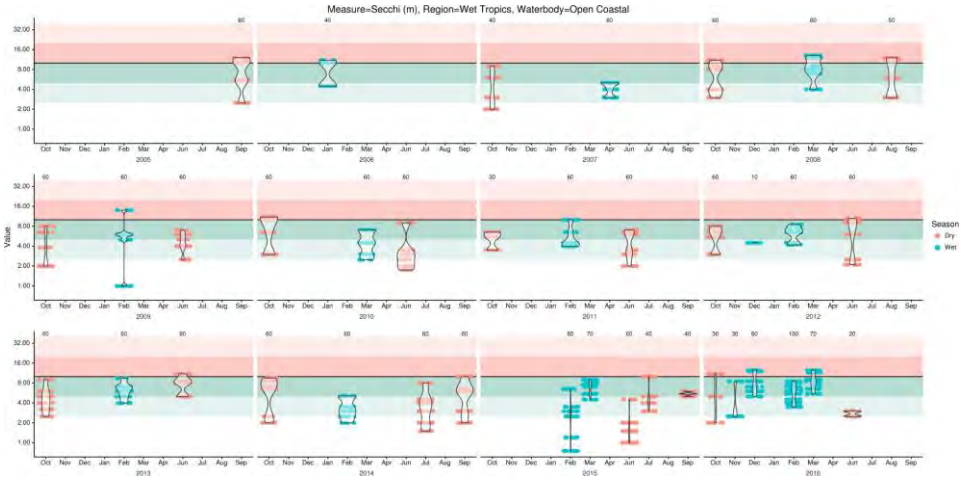


b) Satellite

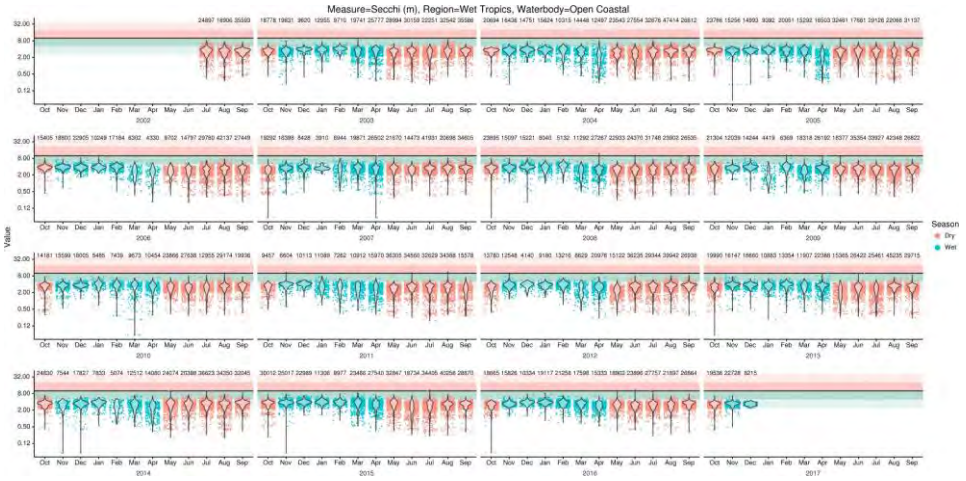


c) eReefs

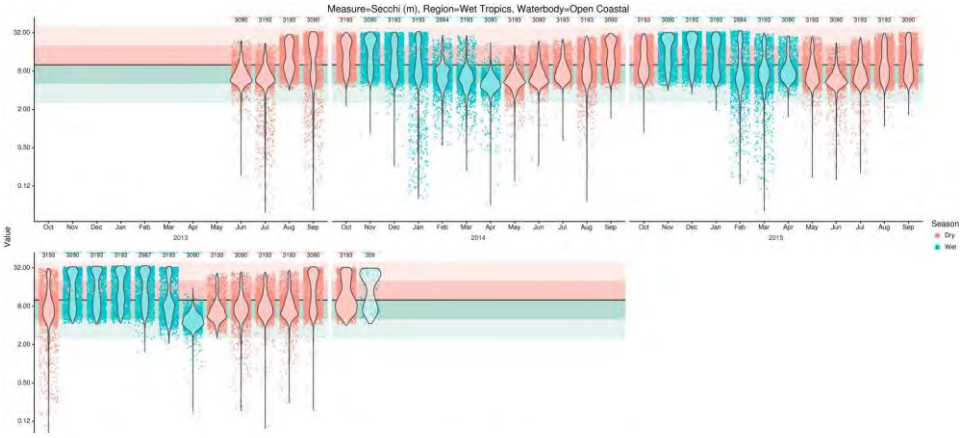


**Figure 17: Observed (logarithmic axis with violin plot overlay) Secchi depth data for the Wet Tropics Open Coastal Zone from a) AIMS insitu, b) Satellite and c) eReefs. Observations grouped into months are ordered over time and colored conditional on season as Wet (blue symbols) and Dry (red symbols). Sample sizes represented as numbers above violins and horizontal black dashed line denotes threshold value. Red and green background shading indicates the range (10% shade: x4,/4; 30% shade: x2,/2) above and below threshold respectively.**

a) AIMS insitu

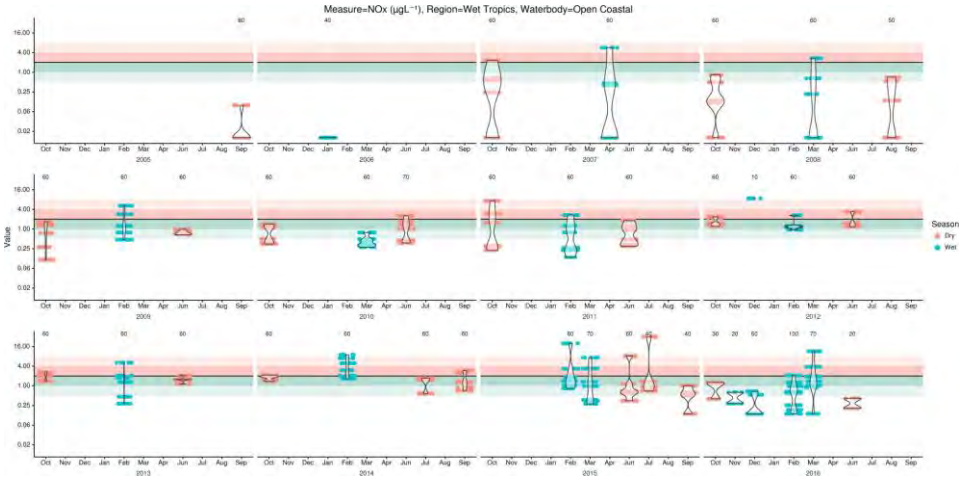


b) eReefs

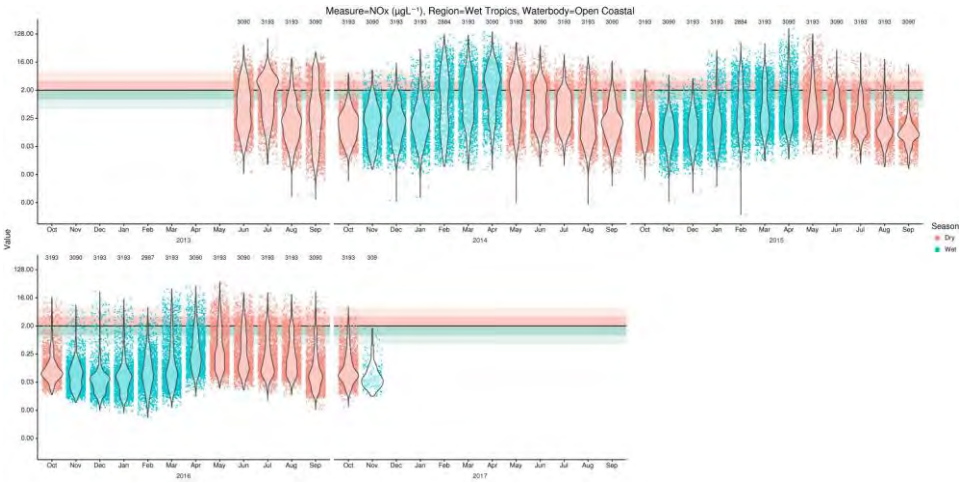


c) eReefs926

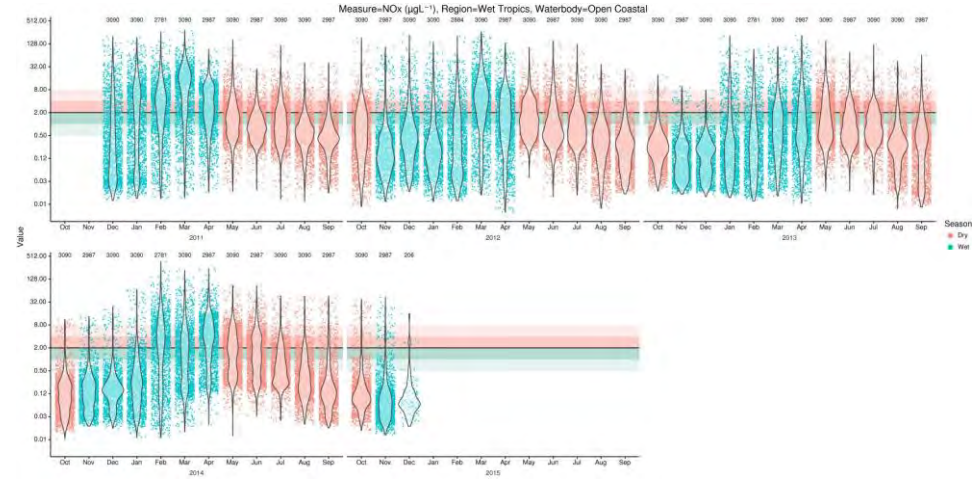


**Figure 18: Observed (logarithmic axis with violin plot overlay) NOx data for the Wet Tropics Open Coastal Zone from a) AIMS insitu, b) eReefs c) eReefs926. Observations grouped into months are ordered over time and colored conditional on season as Wet (blue symbols) and Dry (red symbols). Sample sizes represented as numbers above violins and horizontal black dashed line denotes threshold value. Red and green background shading indicates the range (10% shade: x4,/4; 30% shade: x2,/2) above and below threshold respectively**

## 2.4 Spatial data

Figures 19 – 25 explore the spatio-temporal patterns in observed data from a finer spatial perspective (again focussing on just the Wet Tropics Open Coastal and Dry Tropics Midshelf Zones). Importantly, the colour scales have been mapped to a constant value range for each source for a given Measure. Colour scales have been mapped to a constant value range for each source for a given Measure, the lower and upper bounds of which are based on the minimum and maximum data range for the Measure within the Region/Water body combination across all years. The scale is a viridis (colour blind safe) colour mapping.

These figures also highlight the disparity in resolution between the different data sources. The AIMS insitu data is spatially very sparse[3]. The Satellite data has the most extensive spatial resolution and notwithstanding the many gaps due to various optical interferences (such as cloud cover), also has the greatest temporal coverage[4]. For the selected Zones and span of water years, there is little evidence of a major latitudinal gradient in Satellite Chlorophyll-a with most of any change (if any) occurring across the shelf. Indeed, Satellite parameters are relatively constant over space and time for the Dry Tropics Midshelf Zone (see Figs. 22–24b). Moreover, the spatial patterns of Satellite derived Chlorophyll-a and TSS appear relatively invariant between years (see Figs.19–24b).

The eReefs and eReefs926 do show some variability in spatial and temporal Chlorophyll-a and Secchi depth (see Figs. 19c-d,20c-d,22c-d and 24c-d), yet relatively little for TSS and NOx (at least for Dry Tropics Midshelf). Whilst this apparent lack of variability is largely an artefact of the colour scale mapping, the values of these Measures are constantly substantially below the threshold value and thus invariant on the scale considered appropriate for comparison against the associated thresholds.

[3] the AIMS FLNTU logger data is even more sparse and thus is not shown.
[4] The remote sensing Satellite data span a temporal range of 2002 through to 2017, although only the range 2010-2016 is displayed

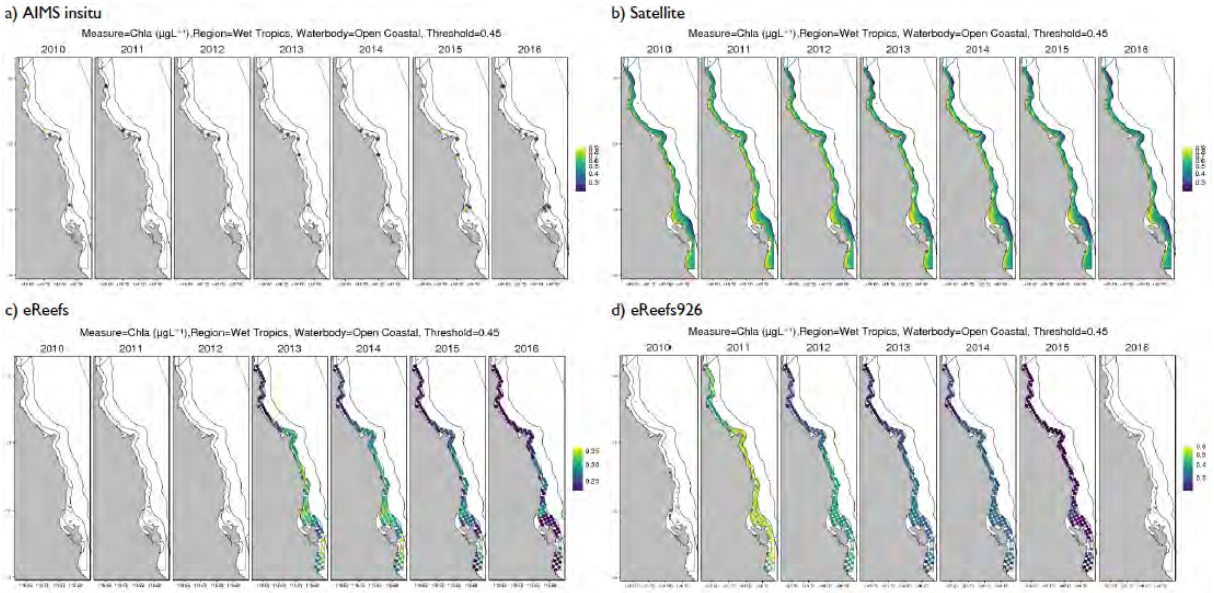


**Figure 19: Spatial distribution of observed a) AIMS insitu, b) Satellite, c) eReefs and d) eReefs926 Chlorophyll-a (2009–2016) for the Wet Tropics Open Coastal Zone.**

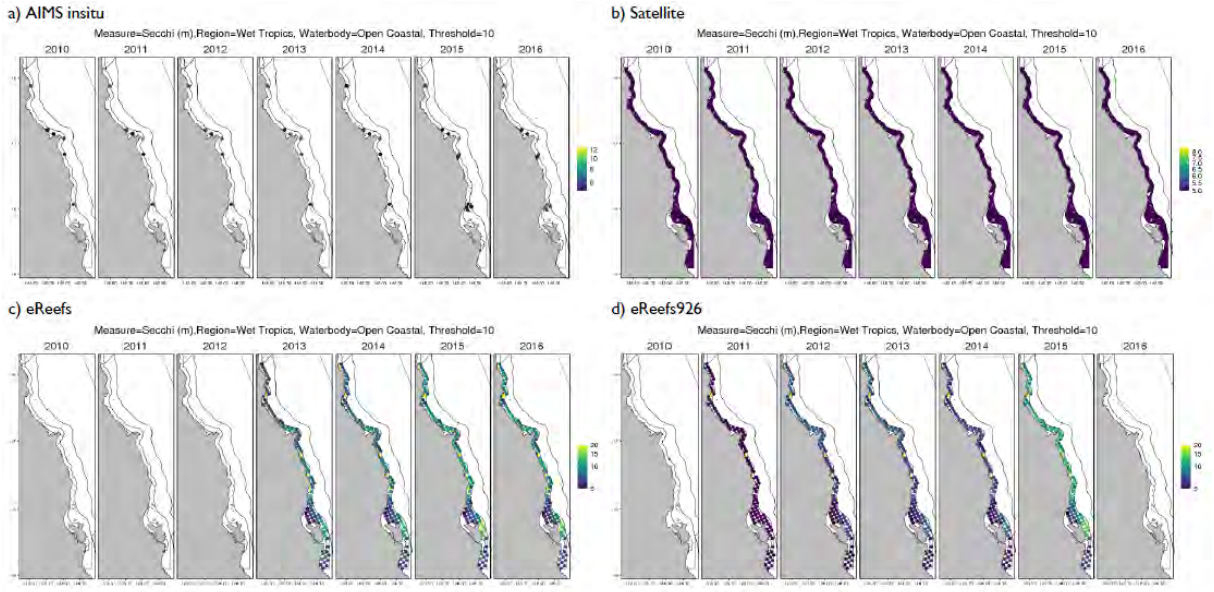


**Figure 20: Spatial distribution of observed a) AIMS insitu, b) Satellite, c) eReefs and d) eReefs926 Secchi depth (2009–2016) for the Wet Tropics Open Coastal Zone.**

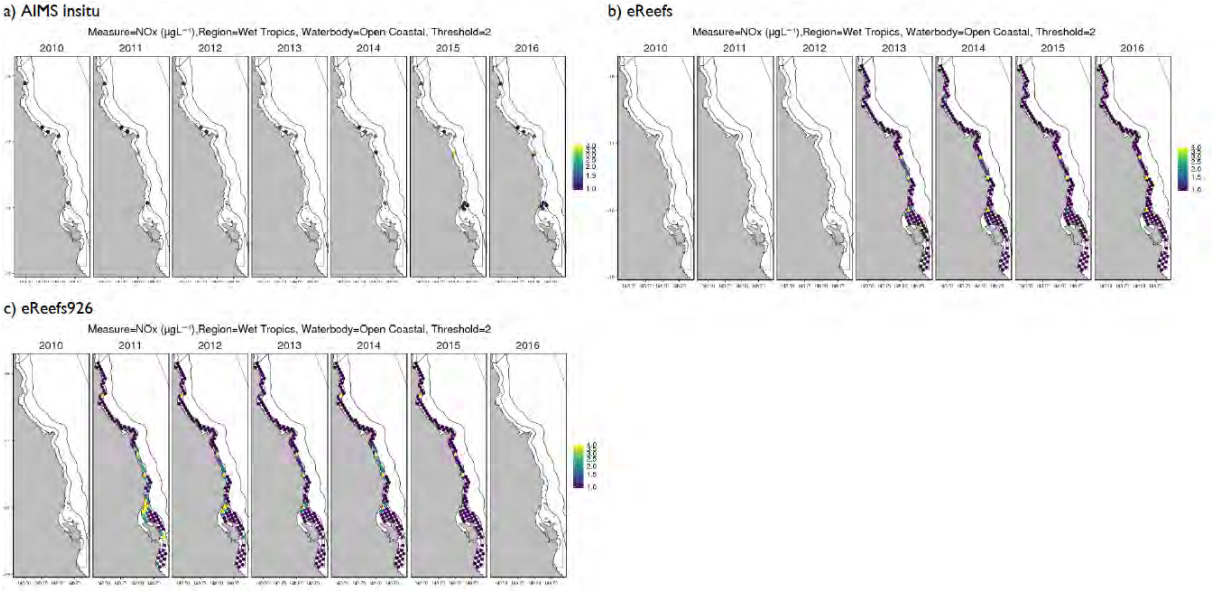


**Figure 21: Spatial distribution of observed a) AIMS insitu, b) eReefs and c) eReefs926 NOx (2009–2016) for the Wet Tropics Open Coastal Zone.**

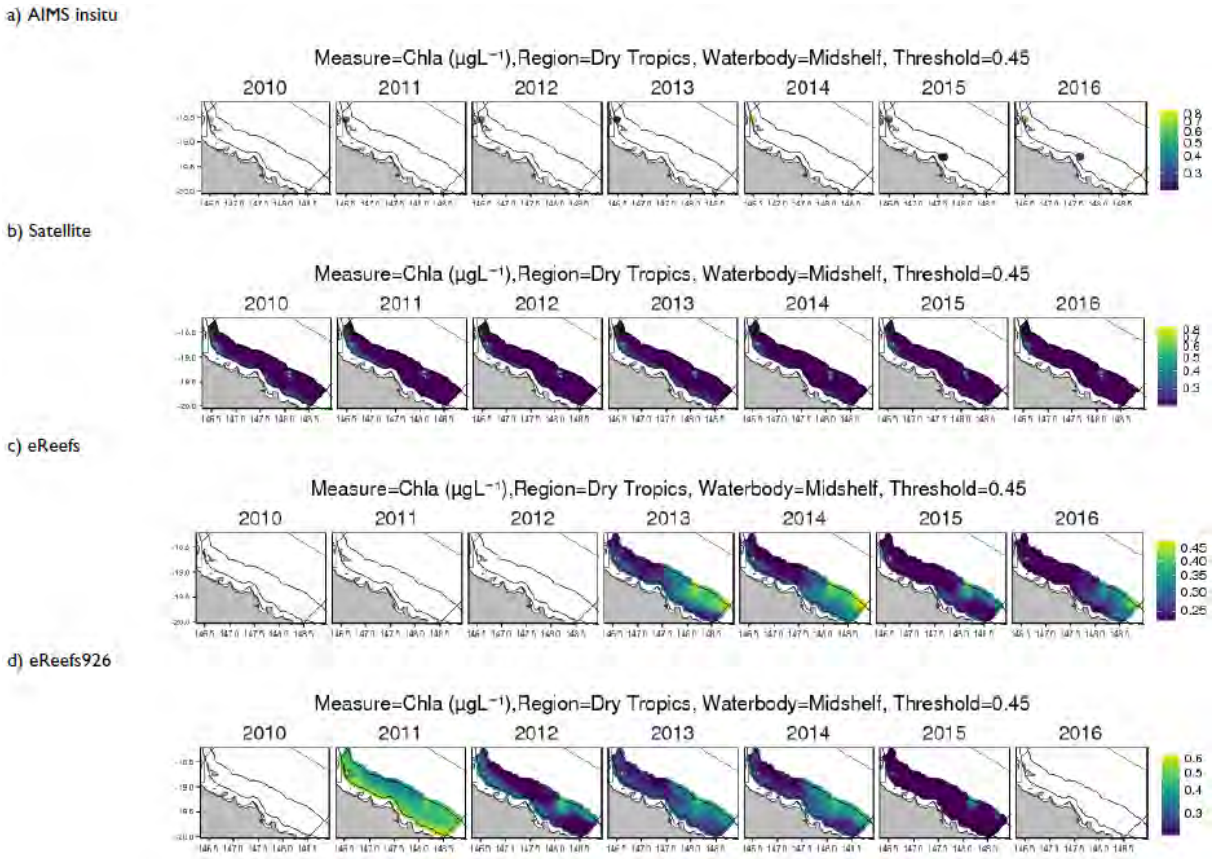


**Figure 22: Spatial distribution of observed a) AIMS insitu, b) Satellite, c) eReefs and d) eReefs926 Chlorophyll-a (2009–2016) for the Dry Tropics Midshelf Zone.**

a) AIMS insitu

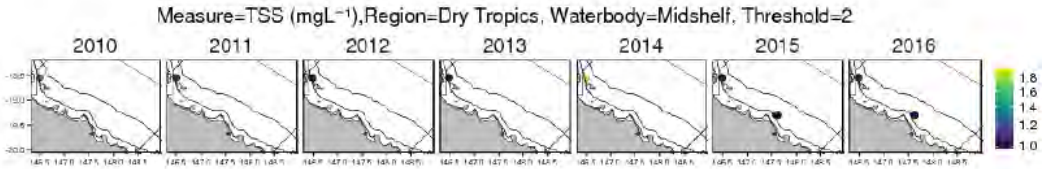


b) Satellite

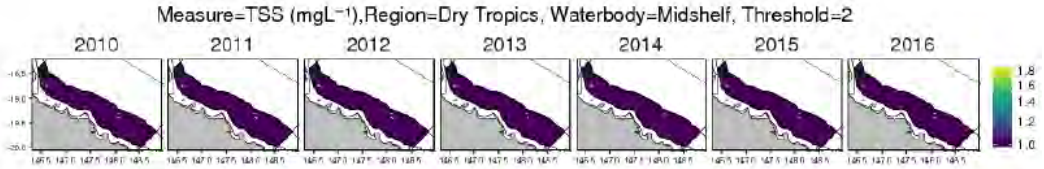


c) eReefs

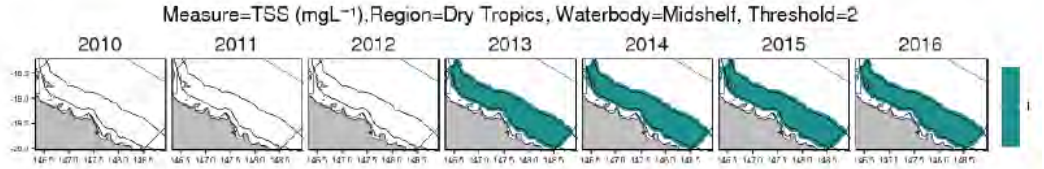


d) eReefs926

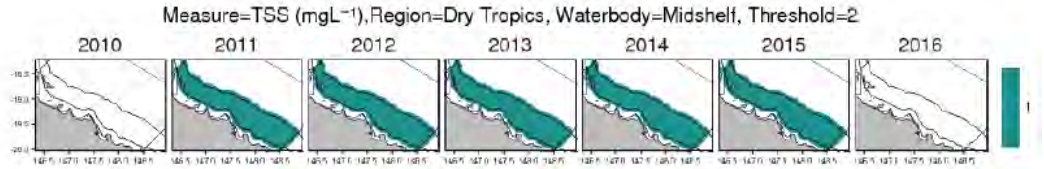


**Figure 23: Spatial distribution of observed a) AIMS insitu, b) Satellite, c) eReefs and d) eReefs926 TSS (2009–2016) for the Dry Tropics Midshelf Zone.**

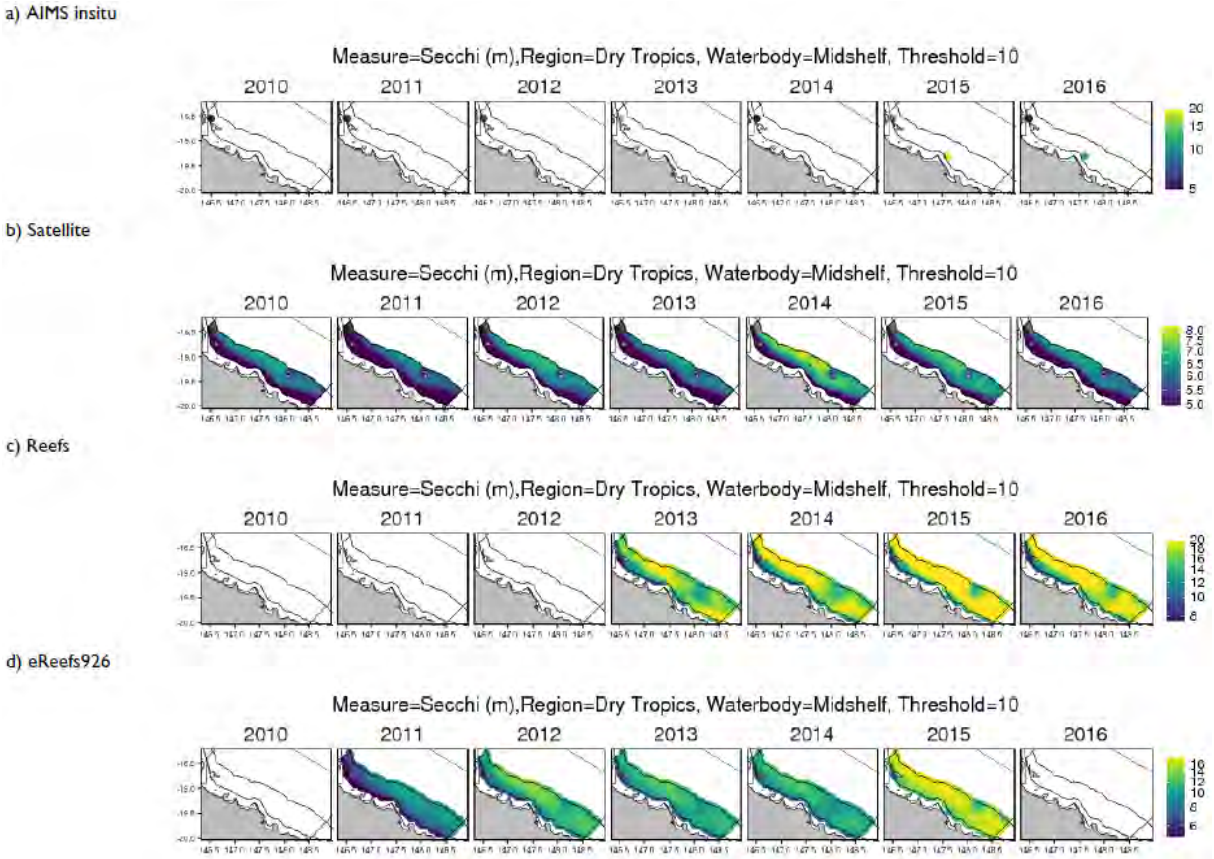


**Figure 24: Spatial distribution of observed a) AIMS insitu, b) Satellite, c) eReefs and d) eReefs926 Secchi depth (2009–2016) for the Dry Tropics Midshelf Zone.**

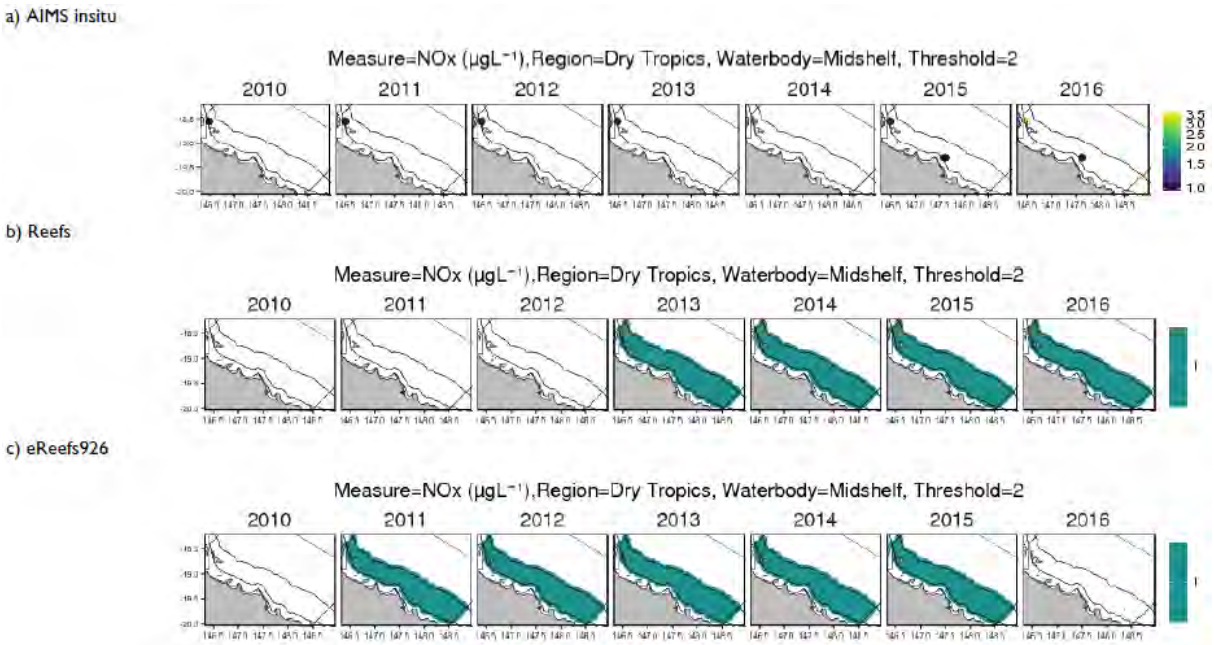


**Figure 25: Spatial distribution of observed a) AIMS insitu, b) eReefs and c) eReefs926 NOx (2009–2016) for the Dry Tropics Midshelf Zone.**

## 2.5 Comparison of data sources

Ensuring that the data underpinning the metric calculations are fit-for-purpose is a critical part of the process, especially if multiple data sources for a specific indicator are to be aggregated as part of these calculations. For example, successful aggregation of Chlorophyll-a as modelled by the eReefs BGC with Chlorophyll-a as extracted from satellite reflectance data (optical properties) will largely depend on the underlying compatibility of these two sources. Moreover, further combining with far more sparse and irregular sources (such as AIMS insitu Chlorophyll-a samples) relies on general patterns of spatial and temporal autocorrelation being present across the more dense data sources so as to facilitate a contagious projection of sparse data across the denser layers.

Based on substantial inconsistencies in the magnitude and variation of the observations between sources (AIMS insitu, Satellite and eReefs models), we recommend not to aggregate across the streams of data. Although it might be possible to normalize each source such that they do all have the same basic characteristics prior to aggregation[5], all the various approaches to achieve normalization rely on the availability of independent estimates of either data reliability, accuracy or biases present in each source. Unfortunately, such information is not available.

Instead of aggregating the sources together, the preferred approach is to assimilate satellite reflectance information into the eReefs BGC model and to rely on in situ measurements for verification of the model performance. It is worthwhile noting that there is no single point of truth as the sparse in situ sampling does not account for the dynamic nature of the receiving environment, both temporally and spatially. It is however possible to compare different measurement methods at a high level.

The five different sources (Satellite, eReefs, eReefs926, AIMS Insitu and AIMS FLNTU loggers) were all collected at different spatio-temporal resolutions. Specifically:

- the Satellite data are collected on a 1km grid on a daily basis, however there are many gaps in the time series of each cell due to cloud cover and other issues that affect the reliability of observations.
- the eReefs data are modelled and projected on to a 4km grid on a daily basis without any time series gaps between 2013 and 2016
- the eReefs926 data are modelled and projected on to a 4km grid on a daily basis without any time series gaps between 2011 and 2014
- the AIMS Insitu samples are collected from specific sampling sites (28-32 throughout the GBR) and on an infrequent basis (approx. 3-4 times per year although more frequently in later years). Furthermore, apart from relatively recently, the majority of samples were collected in the dry season and thus these samples could be biased towards long term water quality trends rather than short-term pulses.
- the AIMS FLNTU logger data are deployed at a subset (16) of the AIMS Insitu sampling locations and record measurements every 10 minutes (although there are frequent gaps due to instrument failure).

[5] indeed this is one of the functions of indexing metrics (see section 3)

The AIMS in situ sampling locations are strategically positioned so as to generally represent transects away from major rivers discharging into the GBR. As such, they likely represent biased estimates of the water parameters of the surrounding water bodies. Nevertheless, the observed data are direct measurements of a range of parameters considered to be important measures of water quality and are therefore considered to be relatively accurate estimates of the true state - albeit for a potentially narrow (and biased) spatio-temporal window. By contrast, the Satellite data represent indirect proxies for some of these parameters (Chlorophyll-a, Total Suspended Solids and Secchi Depth) and similarly, the eReefs data are indirect modelled estimates simulated from a deterministic manifestation of a conceptual model. Hence, to gauge the accuracy of the Satellite and eReefs data (and thus inform qualitative confidence), time series and spatial patterns in the Satellite and eReefs observations were compared to the AIMS in situ observations.

The disparate spatio-temporal resolutions of the data sources present substantial challenges for extracting comparable data. For example, the proximity of AIMS Insitu samples to reefs and the spatial resolution (1km or 4km grid) frequently results in an inability to obtain matching spatial location for all three sources[6]. Furthermore, gaps in the Satellite time series frequently prevent matching Satellite data to the same day as AIMS Insitu sampling. Compounding these issues is the added inherent complications and added noise associated with the inability to control exactly when sampling occurs in throughout dynamic environments. For example, Insitu samples are collected when (date as well as time of day) based largely on logistics and availability of acceptable Satellite data are determined by when the satellite passes over the GBR as whether the data are of sufficient quality[7].

The degree to which the discrete AIMS In situ samples reflect space and time around the actual sampling sites/times is largely unknown. That is, it is not clear how broadly representative the direct observations are. Consequently, it is difficult to estimate how broadly to filter the Satellite and eReefs data in space and time around the AIMS In situ sampling events in order to generate comparable data. The 'best' breadth is likely to be a compromise between data availability (time limited for Satellite and space limited for eReefs) and data equivalence (the degree to which samples from different sources are considered to represent the same spatio-temporal unit).

Figures 26 and 27 illustrate the spatial distribution of Satellite and eReefs grid cell centroid locations relative to the AIMS In situ sampling locations. The different colour spokes denote distance categories (red: <1km, olive: <2km, aqua: <3km and purple: <4km) from the AIMS In situ data. The approach we took was to extract all observations within a specific series of spatio-temporal windows or neighbourhoods from which we could calculate a range of association and correspondence (such as RMSE and $R_2$) metrics (see Tables 10, 11, 12 & 13). Tables 11, 12 and 13 document the top 5 ranked (according to RMSE, MAE and MAPE respectively) spatio-temporal lag associations between Satellite/eReefs data and AIMS In situ data.

[6] Satellite data and eReefs models are of limited value in shallow water
[7] Effected by light levels, viewing angle, cloud cover etc.

**Table 9: Association and correspondence metrics between Satellite/eReefs observations ($\hat{\theta}_i$) and AIMS Niskin observations ($\theta_i$). Similar calculations can be performed on model residuals.**

| Metric | Description | Formulation |
|---|---|---|
| RMSE | Root Mean Square Error - is a measure of accuracy | $RMSE(\hat{\theta}) = \sqrt{\frac{1}{n}\sum_{i=1}^{n}(\hat{\theta}_i - \theta_i)^2}$ |
| MAE | Mean Absolute Error - is a measure of accuracy | $MAE(\hat{\theta}) = \frac{1}{n}\sum_{i=1}^{n}\lvert(\hat{\theta}_i - \theta_i)\rvert$ |
| MAPE | Mean Absolute Percentage Error - is a measure of accuracy expressed as a percentage of AIMS insitu samples | $MAPE(\hat{\theta}) = \frac{100}{n}\sum_{i=1}^{n}\frac{\hat{\theta}_i - \theta_i}{\theta_i}$ |

Whilst it is well established that water quality parameters can be highly varied over time and space, even approximate degrees of spatio-temporal autocorrelation for these parameters remain largely unknown. Nevertheless, we might expect that observations from different sources collected at similar locations and at similar times should be more similar to one another than they are to more distal observations. Furthermore, whilst the absolute values derived from different sources might not be exactly the same, we should expect a reasonable degree of correlation between the sources. Given these two positions (that observations should be autocorrelated and that different sources should be correlated), we should expect that the degree of correlation between the different sources for a given measure should be strongest for observation pairs closer together in space and time.

Tables 11 – 13 tabulate the association and correspondence metrics between the AIMS insitu samples and either the Satellite or eReefs data for each Measure. Irrespective of the association metric (RMSE, MAE or MAPE), closest associations with AIMS insitu observations tend to occur at shorter spatial distances for eReefs data than Satellite data, yet the opposite is apparent for temporal lags. We might have expected that associations would be strongest proximal (in both time and space) to the AIMS insitu samples and associations to weaken in some sort of multidimentional decaying pattern with increasing separation. Such a pattern would permit relatively straight forward integration of the AIMS insitu observational data into the Satellite or eReefs layers[8]. However this is not the case and thus it is very difficult to formulate an integration routine that does more than just update a very limited number of points in space and time.

The other rationale for exploring the spatio-temporal associations between AIMS insitu data and Satellite/eReefs data is to be able to determine the optimal temporal lag and spatial distance for making comparisons of trends. Given that AIMS insitu data are in some respects considered the more accurate (albeit limited in the degree to which they more broadly represent space and time around the samples), a comparison of the general temporal trends of each source should give some idea of the relative accuracy of the sources of indirect measurements (Satellite and eReefs). Figures. 28 – 31 illustrate the temporal patterns of Chlorophyll-a, TSS, Secchi depth and NOx for each source (AIMS in situ, AIMS FLNTU, Satellite, eReefs and eReefs926) for each of the AIMS in situ sampling locations. The background fills of the site titles are coloured according to water body (Red: Enclosed

[8] Having a robust and consistent pattern of spatial and temporal autocorrelation would allow us to model the expected value of AIMS insitu data at unobserved locations.

Coastal, Green: Open Coastal, Blue: Midshelf).

All sources of data are typically most variable at Enclosed Coastal sites and substantially less variable at Midshelf sites. Moreover, the alignment of trends also appears to be substantially better at Midshore sites. Enclosed Coastal and Open Coastal sites are closer to the coasts and in particular, closer to major sources of discharge (as intended by the AIMS Water Quality MMP) whereby water conditions are subject to more extreme fluctuations that result in conditions varying rapidly in time and space. Moreover, these sites are likely to be in shallower water or water whose depth is relatively heterogeneous. As a result, data pooled within a 5km radius might represent a substantially different body of water than that represented by the AIMS insitu point sources. By contrast, the conditions represented within a 5km radius at Midshelf sites are likely to be more homogeneous and thereby resulting in a fairer comparison. Notwithstanding the disparity in fairness between different water bodies as a result of how well the various sources represent spatial and temporal envelopes, it is unlikely that either the eReefs 4km models or Satellite data are going to provide accurate estimates for Enclosed Coastal water bodies.

**Table 10: Top five ranked AIMS Niskin vs Satellite/eReefs observation association metrics (RMSE: root mean square error, MAE: mean absolute error, MAPE: mean percent error, Value: regression slope, residual.RMSE: residual root mean square error, residual.MAE: residual mean absolute error, R2.marginal: $R^2$ marginalized over sites, R2.conditional: $R^2$ conditional on sites) per Measure per source (Satellite, eReefs) for spatial/temporal lags. Rows ranked and filtered based on RMSE. Dist and Lag represent spatial (km) and temporal (days) lags.**

| Source | Measure | Dist | Lag | RMSE | MAE | MAPE | Value | Std.Error | DF | t.value | p.value | residual.RMSE | residual.MAE | R2.marginal | R2.conditional |
|---|---|---|---|---|---|---|---|---|---|---|---|---|---|---|---|
| Satellite | chl | 8.00 | 6.00 | 0.33 | 0.22 | 0.69 | 0.42 | 0.04 | 566.00 | 11.43 | 0.00 | 0.22 | 0.14 | 0.10 | 0.66 |
| Satellite | chl | 9.00 | 6.00 | 0.33 | 0.22 | 0.69 | 0.42 | 0.04 | 566.00 | 11.37 | 0.00 | 0.22 | 0.14 | 0.09 | 0.67 |
| Satellite | chl | 6.00 | 6.00 | 0.33 | 0.22 | 0.69 | 0.43 | 0.04 | 566.00 | 11.54 | 0.00 | 0.22 | 0.14 | 0.10 | 0.65 |
| Satellite | chl | 10.00 | 6.00 | 0.33 | 0.22 | 0.69 | 0.42 | 0.04 | 566.00 | 11.30 | 0.00 | 0.22 | 0.13 | 0.09 | 0.67 |
| Satellite | chl | 11.00 | 6.00 | 0.33 | 0.22 | 0.69 | 0.42 | 0.04 | 566.00 | 11.27 | 0.00 | 0.22 | 0.13 | 0.09 | 0.67 |
| eReefs | chl | 1.00 | 5.00 | 0.34 | 0.24 | 0.44 | 0.13 | 0.03 | 96.00 | 3.67 | 0.00 | 0.10 | 0.08 | 0.08 | 0.48 |
| eReefs | chl | 1.00 | 4.00 | 0.34 | 0.24 | 0.44 | 0.14 | 0.04 | 96.00 | 3.85 | 0.00 | 0.10 | 0.08 | 0.09 | 0.48 |
| eReefs | chl | 1.00 | 6.00 | 0.34 | 0.24 | 0.45 | 0.12 | 0.03 | 96.00 | 3.63 | 0.00 | 0.09 | 0.08 | 0.08 | 0.49 |
| eReefs | chl | 1.00 | 3.00 | 0.34 | 0.24 | 0.45 | 0.16 | 0.04 | 96.00 | 3.76 | 0.00 | 0.12 | 0.09 | 0.09 | 0.42 |
| eReefs | chl | 1.00 | 7.00 | 0.34 | 0.24 | 0.45 | 0.11 | 0.03 | 96.00 | 3.46 | 0.00 | 0.09 | 0.07 | 0.07 | 0.50 |
| Satellite | nap | 4.00 | 1.00 | 1.65 | 0.90 | 1.02 | 0.48 | 0.03 | 432.00 | 16.60 | 0.00 | 1.15 | 0.54 | 0.40 | 0.45 |
| Satellite | nap | 1.00 | 1.00 | 1.66 | 0.87 | 1.08 | 0.54 | 0.04 | 358.00 | 14.58 | 0.00 | 1.30 | 0.57 | 0.38 | 0.45 |
| Satellite | nap | 4.00 | 0.00 | 1.67 | 0.87 | 1.21 | 0.51 | 0.04 | 225.00 | 13.99 | 0.00 | 1.17 | 0.52 | 0.45 | 0.49 |
| Satellite | nap | 3.00 | 1.00 | 1.70 | 0.91 | 0.97 | 0.47 | 0.03 | 427.00 | 15.41 | 0.00 | 1.19 | 0.55 | 0.37 | 0.43 |
| Satellite | nap | 3.00 | 0.00 | 1.73 | 0.90 | 1.11 | 0.54 | 0.04 | 214.00 | 13.28 | 0.00 | 1.23 | 0.57 | 0.43 | 0.53 |
| eReefs | nap | 5.00 | 3.00 | 2.07 | 1.18 | 0.73 | 0.12 | 0.02 | 239.00 | 6.20 | 0.00 | 0.57 | 0.38 | 0.13 | 0.16 |
| eReefs | nap | 5.00 | 4.00 | 2.07 | 1.17 | 0.73 | 0.11 | 0.02 | 239.00 | 5.51 | 0.00 | 0.56 | 0.39 | 0.11 | 0.16 |
| eReefs | nap | 4.00 | 3.00 | 2.08 | 1.17 | 0.70 | 0.11 | 0.02 | 239.00 | 5.78 | 0.00 | 0.53 | 0.37 | 0.12 | 0.18 |
| eReefs | nap | 4.00 | 4.00 | 2.08 | 1.16 | 0.70 | 0.09 | 0.02 | 239.00 | 5.03 | 0.00 | 0.54 | 0.39 | 0.09 | 0.16 |
| eReefs | nap | 5.00 | 2.00 | 2.08 | 1.18 | 0.74 | 0.12 | 0.02 | 239.00 | 6.00 | 0.00 | 0.57 | 0.39 | 0.13 | 0.16 |
| Satellite | sd | 5.00 | 2.00 | 4.47 | 3.38 | 0.44 | 0.11 | 0.01 | 463.00 | 11.77 | 0.00 | 0.55 | 0.42 | 0.24 | 0.54 |
| Satellite | sd | 4.00 | 2.00 | 4.48 | 3.38 | 0.44 | 0.11 | 0.01 | 462.00 | 11.71 | 0.00 | 0.56 | 0.42 | 0.24 | 0.52 |
| Satellite | sd | 3.00 | 2.00 | 4.48 | 3.39 | 0.44 | 0.12 | 0.01 | 455.00 | 11.73 | 0.00 | 0.57 | 0.42 | 0.25 | 0.51 |
| Satellite | sd | 11.00 | 2.00 | 4.48 | 3.37 | 0.44 | 0.11 | 0.01 | 470.00 | 11.65 | 0.00 | 0.53 | 0.41 | 0.20 | 0.61 |
| Satellite | sd | 12.00 | 2.00 | 4.48 | 3.37 | 0.44 | 0.11 | 0.01 | 470.00 | 11.65 | 0.00 | 0.53 | 0.41 | 0.20 | 0.61 |
| eReefs | sd | 4.00 | 1.00 | 13.13 | 11.31 | 2.37 | 1.23 | 0.12 | 196.00 | 10.39 | 0.00 | 6.47 | 4.92 | 0.35 | 0.37 |
| eReefs | sd | 4.00 | 2.00 | 13.29 | 11.68 | 2.49 | 1.14 | 0.11 | 196.00 | 9.89 | 0.00 | 6.10 | 4.75 | 0.34 | 0.37 |
| eReefs | sd | 5.00 | 1.00 | 13.46 | 11.62 | 2.36 | 1.29 | 0.12 | 185.00 | 10.81 | 0.00 | 6.61 | 5.12 | 0.38 | 0.39 |
| eReefs | sd | 6.00 | 1.00 | 13.53 | 11.69 | 2.37 | 1.30 | 0.13 | 185.00 | 10.40 | 0.00 | 6.43 | 4.96 | 0.38 | 0.41 |
| eReefs | sd | 5.00 | 2.00 | 13.66 | 12.02 | 2.48 | 1.18 | 0.12 | 185.00 | 10.20 | 0.00 | 6.30 | 5.02 | 0.36 | 0.37 |

**Table 11: Top five ranked AIMS Niskin vs Satellite/eReefs observation association metrics (RMSE: root mean square error, MAE: mean absolute error, MAPE: mean percent error, Value: regression slope, residual.RMSE: residual root mean square error, residual.MAE: residual mean absolute error, R2.marginal: $R^2$ marginalized over sites, R2.conditional: $R^2$ conditional on sites) per Measure per source (Satellite, eReefs) for spatial/temporal lags. Rows ranked and filtered based on MAE. Dist and Lag represent spatial (km) and temporal (days) lags.**

| Source | Measure | Dist | Lag | RMSE | MAE | MAPE | Value | Std.Error | DF | t.value | p.value | residual.RMSE | residual.MAE | R2.marginal | R2.conditional |
|---|---|---|---|---|---|---|---|---|---|---|---|---|---|---|---|
| Satellite | chl | 10.00 | 0.00 | 0.38 | 0.21 | 0.64 | 0.82 | 0.08 | 253.00 | 9.99 | 0.00 | 0.33 | 0.17 | 0.27 | 0.37 |
| Satellite | chl | 11.00 | 0.00 | 0.38 | 0.21 | 0.65 | 0.81 | 0.08 | 254.00 | 9.89 | 0.00 | 0.33 | 0.17 | 0.26 | 0.38 |
| Satellite | chl | 12.00 | 0.00 | 0.38 | 0.21 | 0.65 | 0.81 | 0.08 | 254.00 | 9.89 | 0.00 | 0.33 | 0.17 | 0.26 | 0.38 |
| Satellite | chl | 4.00 | 0.00 | 0.38 | 0.21 | 0.65 | 0.91 | 0.08 | 226.00 | 10.82 | 0.00 | 0.33 | 0.17 | 0.32 | 0.44 |
| Satellite | chl | 9.00 | 0.00 | 0.39 | 0.21 | 0.64 | 0.84 | 0.09 | 250.00 | 9.86 | 0.00 | 0.35 | 0.17 | 0.27 | 0.36 |
| eReefs | chl | 3.00 | 5.00 | 0.34 | 0.23 | 0.43 | 0.14 | 0.02 | 221.00 | 6.09 | 0.00 | 0.09 | 0.08 | 0.11 | 0.46 |
| eReefs | chl | 3.00 | 6.00 | 0.34 | 0.23 | 0.43 | 0.13 | 0.02 | 221.00 | 6.09 | 0.00 | 0.09 | 0.07 | 0.11 | 0.46 |
| eReefs | chl | 3.00 | 4.00 | 0.34 | 0.23 | 0.43 | 0.14 | 0.02 | 221.00 | 6.09 | 0.00 | 0.10 | 0.08 | 0.11 | 0.45 |
| eReefs | chl | 3.00 | 7.00 | 0.35 | 0.23 | 0.43 | 0.12 | 0.02 | 221.00 | 5.88 | 0.00 | 0.09 | 0.07 | 0.10 | 0.46 |
| eReefs | chl | 4.00 | 5.00 | 0.34 | 0.23 | 0.43 | 0.13 | 0.02 | 239.00 | 5.98 | 0.00 | 0.09 | 0.07 | 0.10 | 0.46 |
| Satellite | nap | 4.00 | 0.00 | 1.67 | 0.87 | 1.21 | 0.51 | 0.04 | 225.00 | 13.99 | 0.00 | 1.17 | 0.52 | 0.45 | 0.49 |
| Satellite | nap | 1.00 | 1.00 | 1.66 | 0.87 | 1.08 | 0.54 | 0.04 | 358.00 | 14.58 | 0.00 | 1.30 | 0.57 | 0.38 | 0.45 |
| Satellite | nap | 4.00 | 1.00 | 1.65 | 0.90 | 1.02 | 0.48 | 0.03 | 432.00 | 16.60 | 0.00 | 1.15 | 0.54 | 0.40 | 0.45 |
| Satellite | nap | 3.00 | 0.00 | 1.73 | 0.90 | 1.11 | 0.54 | 0.04 | 214.00 | 13.28 | 0.00 | 1.23 | 0.57 | 0.43 | 0.53 |
| Satellite | nap | 3.00 | 1.00 | 1.70 | 0.91 | 0.97 | 0.47 | 0.03 | 427.00 | 15.41 | 0.00 | 1.19 | 0.55 | 0.37 | 0.43 |
| eReefs | nap | 4.00 | 4.00 | 2.08 | 1.16 | 0.70 | 0.09 | 0.02 | 239.00 | 5.03 | 0.00 | 0.54 | 0.39 | 0.09 | 0.16 |
| eReefs | nap | 4.00 | 3.00 | 2.08 | 1.17 | 0.70 | 0.11 | 0.02 | 239.00 | 5.78 | 0.00 | 0.53 | 0.37 | 0.12 | 0.18 |
| eReefs | nap | 4.00 | 2.00 | 2.09 | 1.17 | 0.72 | 0.11 | 0.02 | 239.00 | 5.52 | 0.00 | 0.55 | 0.38 | 0.11 | 0.18 |
| eReefs | nap | 5.00 | 4.00 | 2.07 | 1.17 | 0.73 | 0.11 | 0.02 | 239.00 | 5.51 | 0.00 | 0.56 | 0.39 | 0.11 | 0.16 |
| eReefs | nap | 5.00 | 3.00 | 2.07 | 1.18 | 0.73 | 0.12 | 0.02 | 239.00 | 6.20 | 0.00 | 0.57 | 0.38 | 0.13 | 0.16 |
| Satellite | sd | 11.00 | 2.00 | 4.48 | 3.37 | 0.44 | 0.11 | 0.01 | 470.00 | 11.65 | 0.00 | 0.53 | 0.41 | 0.20 | 0.61 |
| Satellite | sd | 12.00 | 2.00 | 4.48 | 3.37 | 0.44 | 0.11 | 0.01 | 470.00 | 11.65 | 0.00 | 0.53 | 0.41 | 0.20 | 0.61 |
| Satellite | sd | 10.00 | 2.00 | 4.48 | 3.37 | 0.44 | 0.11 | 0.01 | 470.00 | 11.67 | 0.00 | 0.53 | 0.41 | 0.20 | 0.61 |
| Satellite | sd | 4.00 | 2.00 | 4.48 | 3.38 | 0.44 | 0.11 | 0.01 | 462.00 | 11.71 | 0.00 | 0.56 | 0.42 | 0.24 | 0.52 |
| Satellite | sd | 9.00 | 2.00 | 4.49 | 3.38 | 0.44 | 0.11 | 0.01 | 468.00 | 11.89 | 0.00 | 0.53 | 0.41 | 0.22 | 0.60 |
| eReefs | sd | 4.00 | 1.00 | 13.13 | 11.31 | 2.37 | 1.23 | 0.12 | 196.00 | 10.39 | 0.00 | 6.47 | 4.92 | 0.35 | 0.37 |
| eReefs | sd | 1.00 | 1.00 | 14.04 | 11.52 | 2.73 | 1.10 | 0.29 | 85.00 | 3.86 | 0.00 | 7.61 | 5.43 | 0.15 | 0.22 |
| eReefs | sd | 1.00 | 2.00 | 13.71 | 11.58 | 2.79 | 1.12 | 0.26 | 85.00 | 4.31 | 0.00 | 6.87 | 5.36 | 0.18 | 0.26 |
| eReefs | sd | 5.00 | 1.00 | 13.46 | 11.62 | 2.36 | 1.29 | 0.12 | 185.00 | 10.81 | 0.00 | 6.61 | 5.12 | 0.38 | 0.39 |
| eReefs | sd | 4.00 | 2.00 | 13.29 | 11.68 | 2.49 | 1.14 | 0.11 | 196.00 | 9.89 | 0.00 | 6.10 | 4.75 | 0.34 | 0.37 |

**Table 12: Top five ranked AIMS Niskin vs Satellite/eReefs observation association metrics (RMSE: root mean square error, MAE: mean absolute error, MAPE: mean percent error, Value: regression slope, residual.RMSE: residual root mean square error, residual.MAE: residual mean absolute error, R2.marginal: $R^2$ marginalized over sites, R2.conditional: $R^2$ conditional on sites) per Measure per source (Satellite, eReefs) for spatial/temporal lags. Rows ranked and filtered based on MAPE. Dist and Lag represent spatial (km) and temporal (days) lags.**

| Source | Measure | Dist | Lag | RMSE | MAE | MAPE | Value | Std.Error | DF | t.value | p.value | residual.RMSE | residual.MAE | R2.marginal | R2.conditional |
|---|---|---|---|---|---|---|---|---|---|---|---|---|---|---|---|
| Satellite | chl | 4.00 | 2.00 | 0.37 | 0.21 | 0.62 | 0.64 | 0.05 | 508.00 | 12.12 | 0.00 | 0.30 | 0.15 | 0.18 | 0.48 |
| Satellite | chl | 3.00 | 2.00 | 0.37 | 0.21 | 0.63 | 0.67 | 0.05 | 501.00 | 12.20 | 0.00 | 0.30 | 0.15 | 0.19 | 0.46 |
| Satellite | chl | 2.00 | 2.00 | 0.35 | 0.21 | 0.63 | 0.63 | 0.05 | 492.00 | 12.64 | 0.00 | 0.27 | 0.15 | 0.19 | 0.54 |
| Satellite | chl | 8.00 | 0.00 | 0.41 | 0.21 | 0.64 | 0.87 | 0.09 | 248.00 | 9.86 | 0.00 | 0.36 | 0.17 | 0.27 | 0.34 |
| Satellite | chl | 10.00 | 0.00 | 0.38 | 0.21 | 0.64 | 0.82 | 0.08 | 253.00 | 9.99 | 0.00 | 0.33 | 0.17 | 0.27 | 0.37 |
| eReefs | chl | 3.00 | 6.00 | 0.34 | 0.23 | 0.43 | 0.13 | 0.02 | 221.00 | 6.09 | 0.00 | 0.09 | 0.07 | 0.11 | 0.46 |
| eReefs | chl | 4.00 | 6.00 | 0.34 | 0.23 | 0.43 | 0.12 | 0.02 | 239.00 | 6.03 | 0.00 | 0.09 | 0.07 | 0.10 | 0.47 |
| eReefs | chl | 3.00 | 5.00 | 0.34 | 0.23 | 0.43 | 0.14 | 0.02 | 221.00 | 6.09 | 0.00 | 0.09 | 0.08 | 0.11 | 0.46 |
| eReefs | chl | 2.00 | 6.00 | 0.35 | 0.23 | 0.43 | 0.13 | 0.02 | 195.00 | 5.72 | 0.00 | 0.09 | 0.07 | 0.11 | 0.45 |
| eReefs | chl | 3.00 | 7.00 | 0.35 | 0.23 | 0.43 | 0.12 | 0.02 | 221.00 | 5.88 | 0.00 | 0.09 | 0.07 | 0.10 | 0.46 |
| Satellite | nap | 3.00 | 2.00 | 1.76 | 0.95 | 0.90 | 0.35 | 0.02 | 500.00 | 15.62 | 0.00 | 0.94 | 0.50 | 0.31 | 0.50 |
| Satellite | nap | 2.00 | 2.00 | 1.81 | 0.96 | 0.91 | 0.35 | 0.02 | 491.00 | 14.78 | 0.00 | 0.97 | 0.50 | 0.27 | 0.52 |
| Satellite | nap | 7.00 | 2.00 | 1.88 | 1.00 | 0.93 | 0.34 | 0.02 | 514.00 | 13.50 | 0.00 | 1.04 | 0.54 | 0.22 | 0.52 |
| Satellite | nap | 8.00 | 2.00 | 1.88 | 1.01 | 0.93 | 0.33 | 0.02 | 514.00 | 13.35 | 0.00 | 1.03 | 0.54 | 0.21 | 0.54 |
| Satellite | nap | 9.00 | 2.00 | 1.88 | 1.01 | 0.93 | 0.33 | 0.02 | 514.00 | 13.43 | 0.00 | 1.01 | 0.53 | 0.20 | 0.56 |
| eReefs | nap | 1.00 | 4.00 | 2.34 | 1.36 | 0.68 | 0.10 | 0.03 | 96.00 | 3.12 | 0.00 | 0.76 | 0.50 | 0.08 | 0.08 |
| eReefs | nap | 1.00 | 3.00 | 2.37 | 1.37 | 0.68 | 0.12 | 0.04 | 96.00 | 3.11 | 0.00 | 0.87 | 0.51 | 0.08 | 0.08 |
| eReefs | nap | 11.00 | 4.00 | 2.57 | 1.28 | 0.69 | 0.07 | 0.02 | 246.00 | 4.48 | 0.00 | 0.55 | 0.39 | 0.07 | 0.17 |
| eReefs | nap | 12.00 | 4.00 | 2.57 | 1.28 | 0.69 | 0.07 | 0.02 | 246.00 | 4.49 | 0.00 | 0.55 | 0.39 | 0.07 | 0.17 |
| eReefs | nap | 10.00 | 4.00 | 2.57 | 1.28 | 0.69 | 0.07 | 0.02 | 246.00 | 4.45 | 0.00 | 0.56 | 0.39 | 0.07 | 0.16 |
| Satellite | sd | 6.00 | 0.00 | 4.64 | 3.50 | 0.43 | 0.16 | 0.02 | 217.00 | 10.16 | 0.00 | 0.74 | 0.54 | 0.34 | 0.42 |
| Satellite | sd | 4.00 | 0.00 | 4.73 | 3.59 | 0.43 | 0.16 | 0.01 | 207.00 | 11.42 | 0.00 | 0.70 | 0.54 | 0.40 | 0.45 |
| Satellite | sd | 7.00 | 0.00 | 4.63 | 3.51 | 0.43 | 0.15 | 0.02 | 224.00 | 10.00 | 0.00 | 0.73 | 0.55 | 0.33 | 0.41 |
| Satellite | sd | 10.00 | 0.00 | 4.62 | 3.50 | 0.43 | 0.15 | 0.02 | 231.00 | 9.27 | 0.00 | 0.75 | 0.57 | 0.29 | 0.38 |
| Satellite | sd | 5.00 | 0.00 | 4.70 | 3.56 | 0.43 | 0.16 | 0.01 | 211.00 | 11.05 | 0.00 | 0.70 | 0.53 | 0.38 | 0.44 |
| eReefs | sd | 5.00 | 1.00 | 13.46 | 11.62 | 2.36 | 1.29 | 0.12 | 185.00 | 10.81 | 0.00 | 6.61 | 5.12 | 0.38 | 0.39 |
| eReefs | sd | 4.00 | 1.00 | 13.13 | 11.31 | 2.37 | 1.23 | 0.12 | 196.00 | 10.39 | 0.00 | 6.47 | 4.92 | 0.35 | 0.37 |
| eReefs | sd | 6.00 | 1.00 | 13.53 | 11.69 | 2.37 | 1.30 | 0.13 | 185.00 | 10.40 | 0.00 | 6.43 | 4.96 | 0.38 | 0.41 |
| eReefs | sd | 8.00 | 1.00 | 13.91 | 12.00 | 2.38 | 1.38 | 0.13 | 185.00 | 10.31 | 0.00 | 6.39 | 4.97 | 0.40 | 0.45 |
| eReefs | sd | 7.00 | 1.00 | 13.75 | 11.88 | 2.39 | 1.33 | 0.13 | 185.00 | 10.30 | 0.00 | 6.45 | 4.98 | 0.38 | 0.42 |

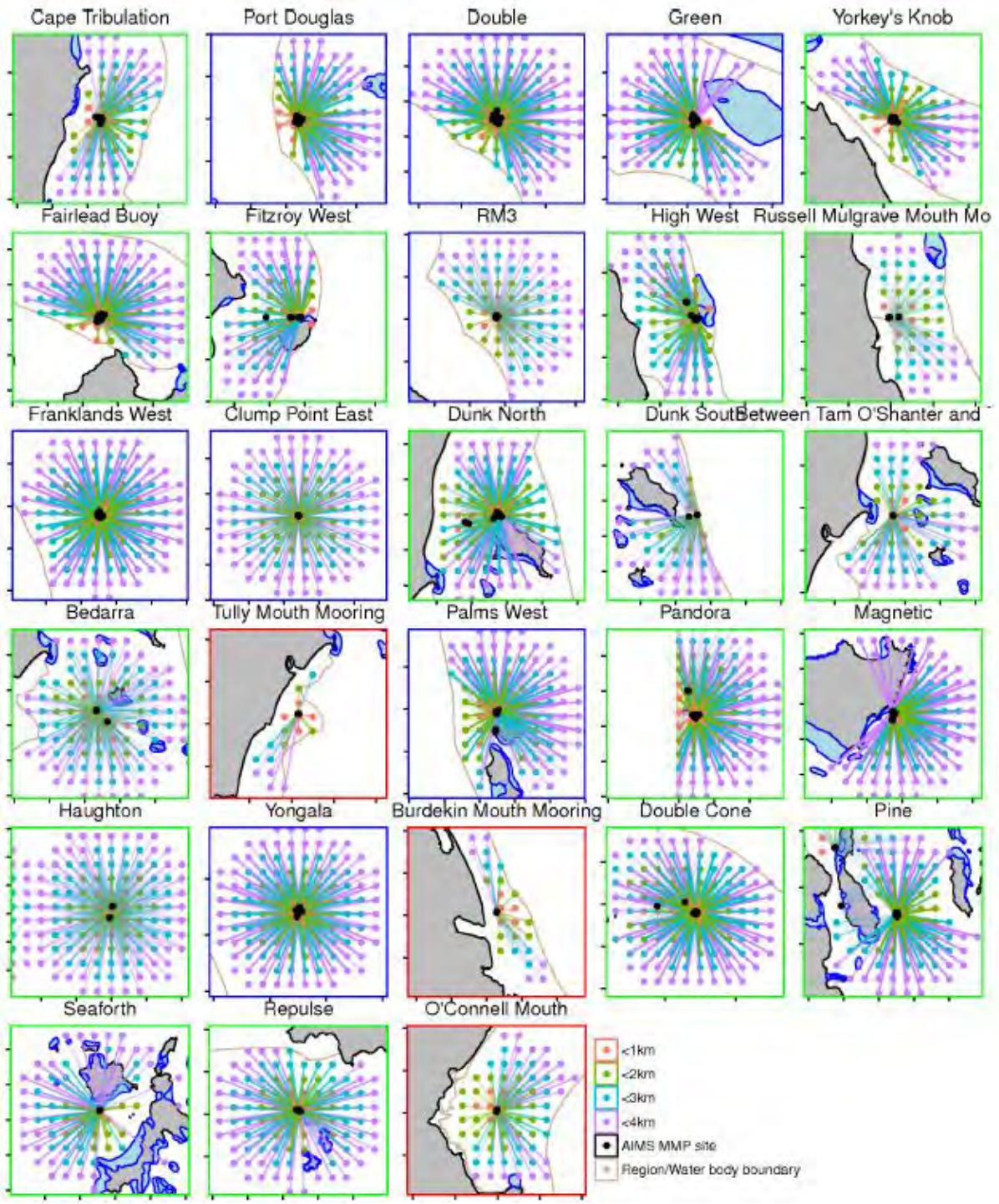


**Figure 26: Location of Satellite cells within 5km of AIMS niskin samples. Panel borders represent water bodies (Red: Enclosed Coastal, Green: Open Coastal, Blue: Midshelf).**

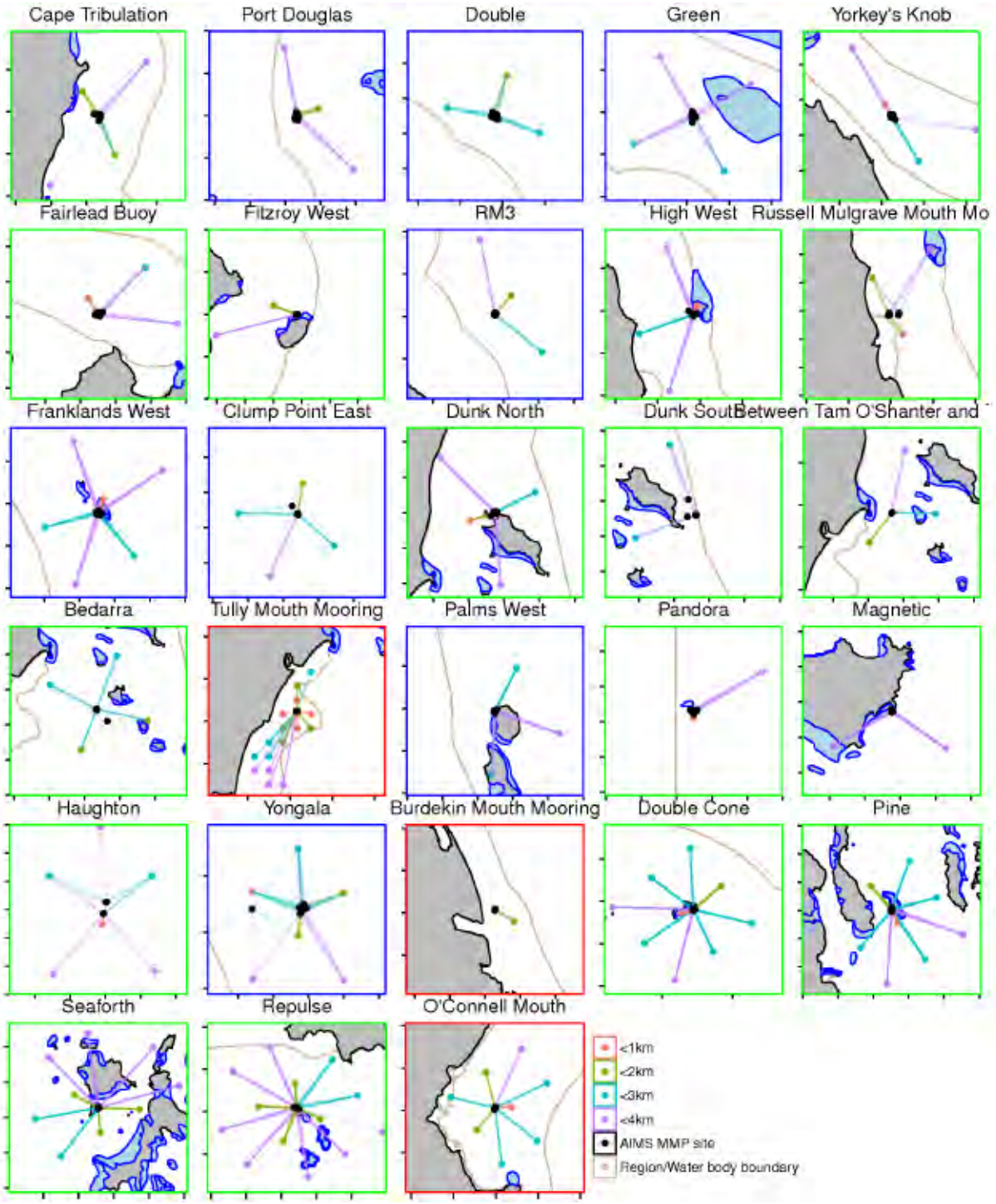


**Figure 27: Location of eReefs cells within 5km of AIMS niskin samples. Panel borders represent water bodies (Red: Enclosed Coastal, Green: Open Coastal, Blue: Midshelf).**

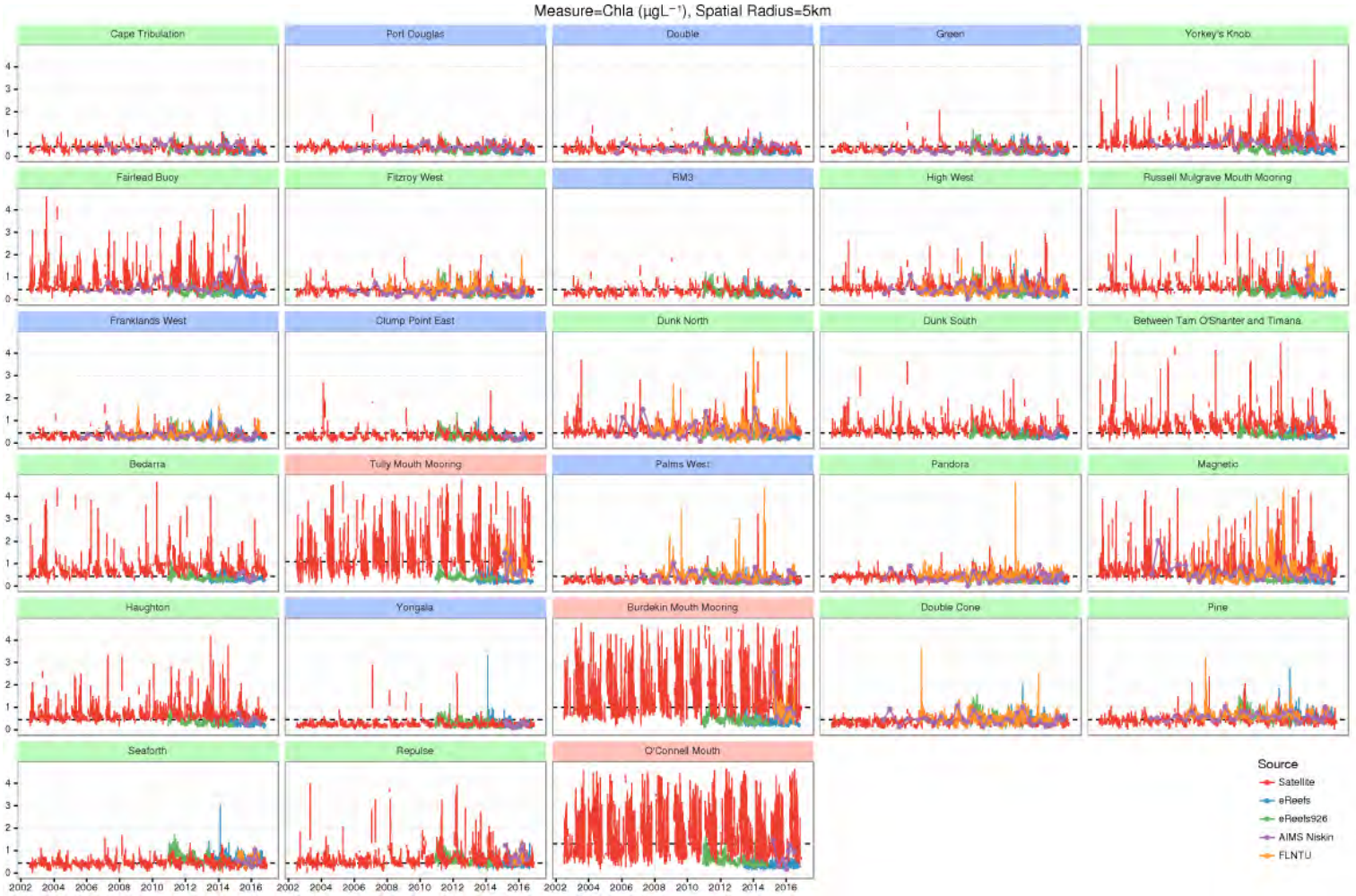


**Figure 28: Temporal patterns in Chlorophyll-a within 5km of each AIMS MMP sampling site for eReefs, Satellite and AIMS insitu and FLNTU logger sources. Horizontal dashed line represents the guideline value. Title backgrounds represent water bodies (Red: Figure 29.Enclosed Coastal, Green: Open Coastal, Blue: Midshelf).**

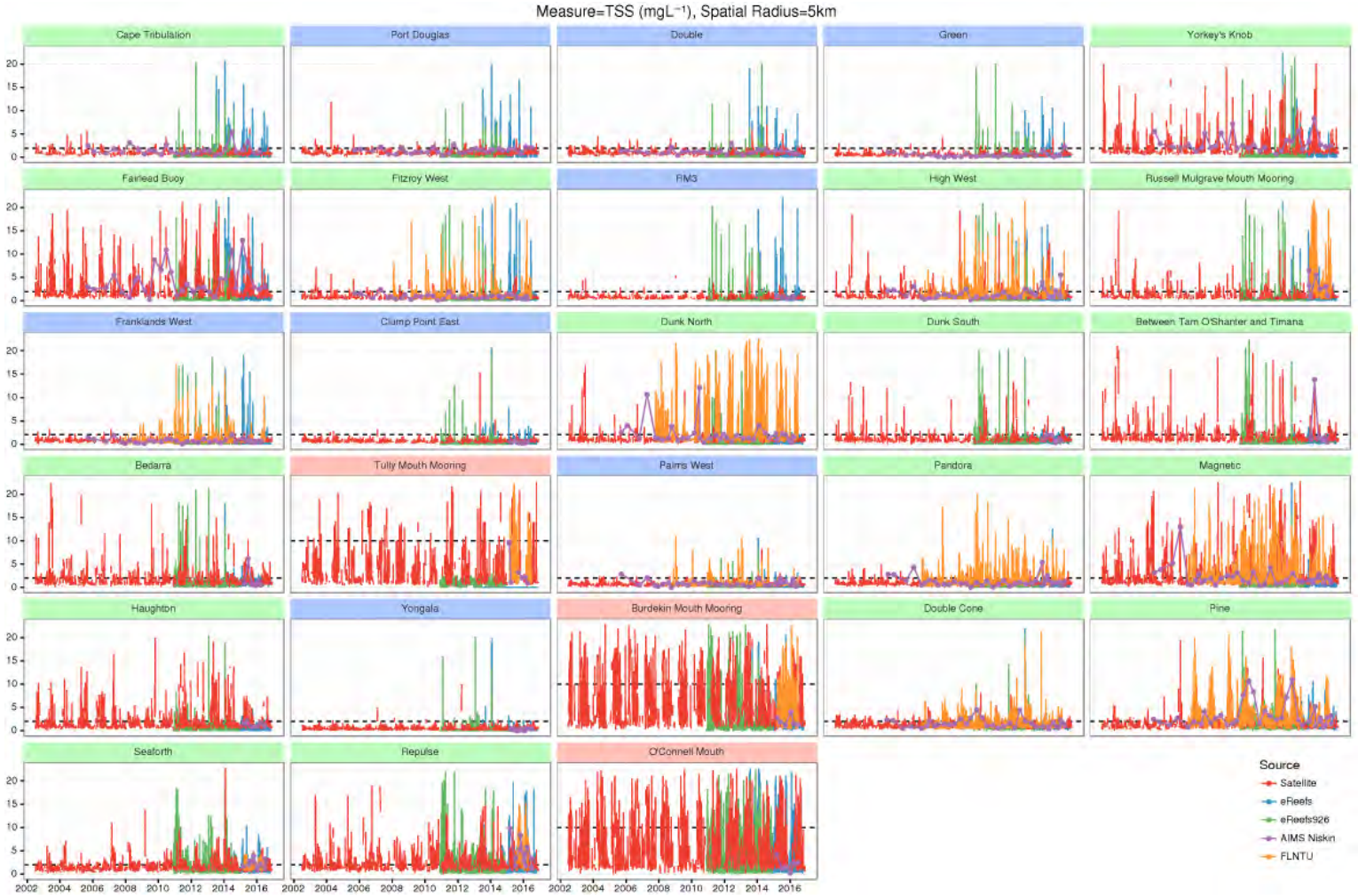


**Figure 29: Temporal patterns in TSS within 5km of each AIMS MMP sampling site for eReefs, Satellite and AIMS insitu and FLNTU logger sources. Horizontal dashed line represents the guideline value. Title backgrounds represent water bodies (Red: Enclosed Coastal, Green: Open Coastal, Blue: Midshelf).**

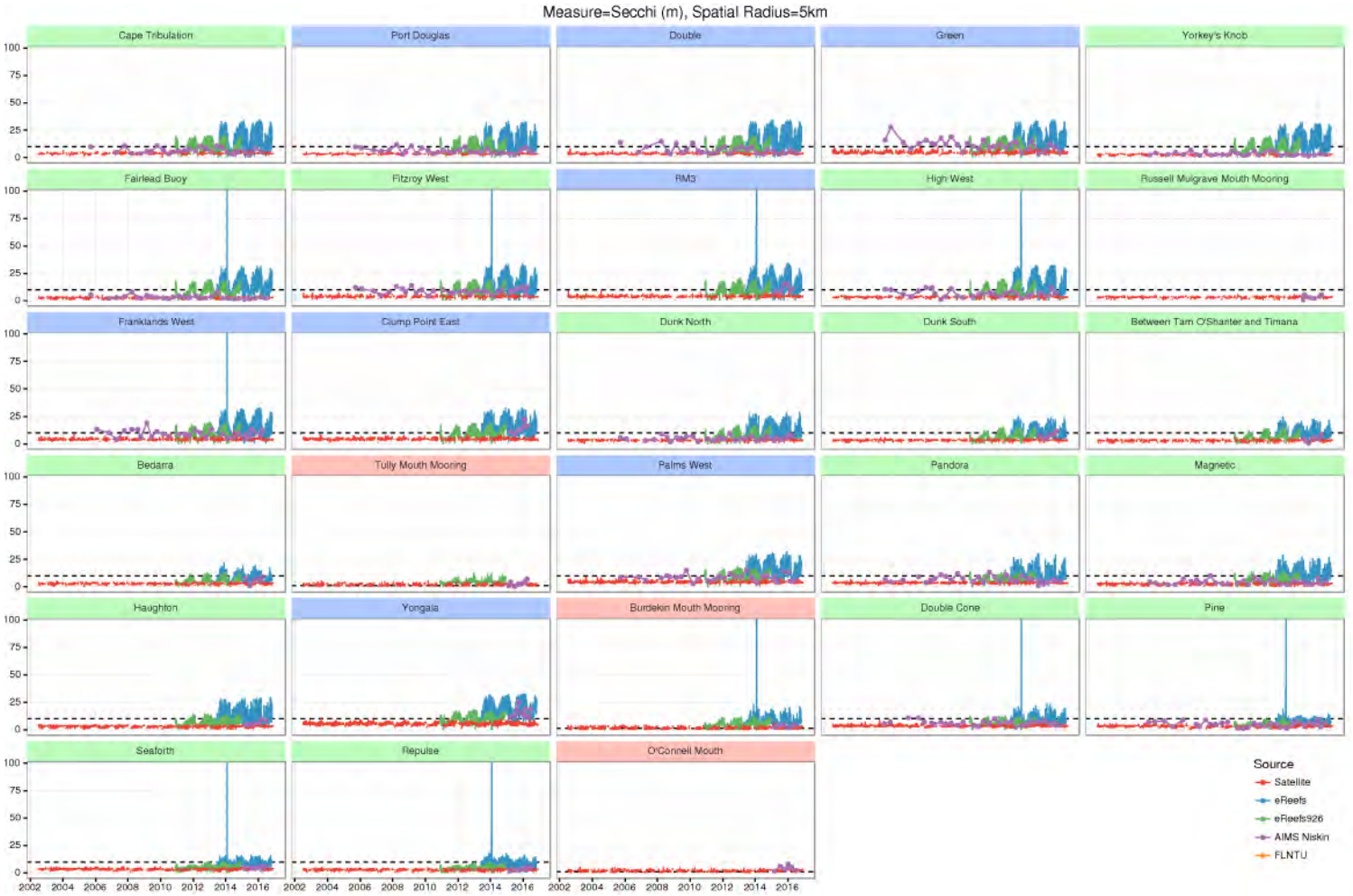


**Figure 30: Temporal patterns in Secchi Depth within 5km of each AIMS MMP sampling site for eReefs, Satellite and AIMS insitu and FLNTU logger sources. Horizontal dashed line represents the guideline value. Title backgrounds represent water bodies (Red: Enclosed Coastal, Green: Open Coastal, Blue: Midshelf).**

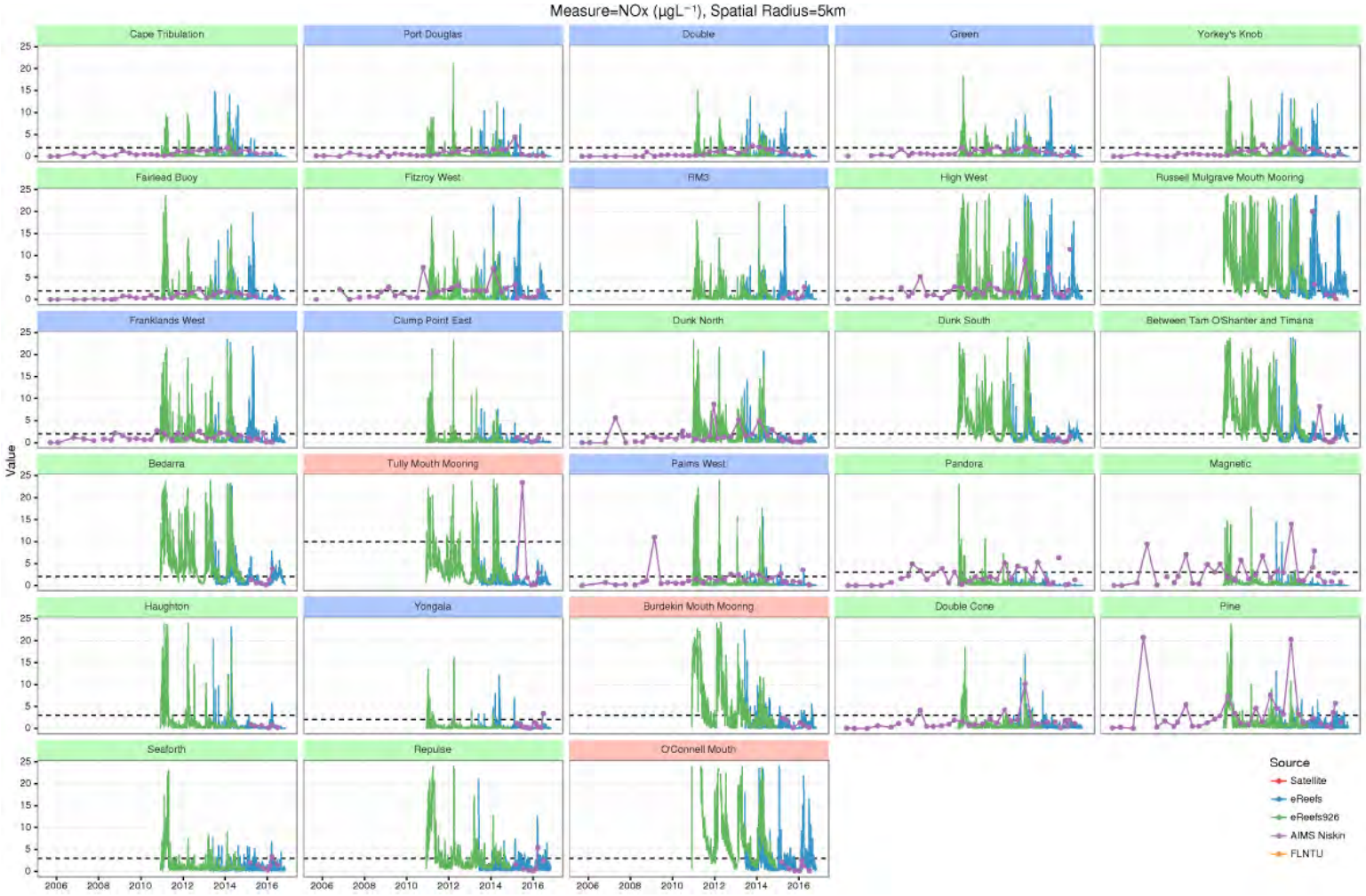


**Figure 31: Temporal patterns in NOx within 5km of each AIMS MMP sampling site for eReefs, Satellite and AIMS insitu and FLNTU logger sources. Horizontal dashed line represents the guideline value. Title backgrounds represent water bodies (Red: Enclosed Coastal, Green: Open Coastal, Blue: Midshelf).**

# 3.0 INDEX METRICS

## 3.1 Theoretical Framework

Each individual indicator (or sub-indicator) addresses a different aspect of the state of an ecosystem. Hence, even a modest number of (sub) indicators will yield multiple perspectives on ecosystem health. Capturing the essence of the ecosystem health or an indicator thereof, necessitates integrating (aggregating) each of these perspectives together into a single *index*. There are numerous methods that have been applied to index aggregation, the most popular of which are itemized by Fox (2013) and described and evaluated in the context of water quality indices by either Walsh and Wheeler (2012) (from the perspective of cost benefit analyses) or Whittaker et al. (2012).

### *3.1.1 Multivariate health indicators*

Motivated by the need to integrate multiple disparately scaled ecological variables together in the absence of any normalizing information (such as benchmarks, guidelines or thresholds, see Section 3.1.2), a variety of predominantly multivariate analyses have been used in the generation of ecosystem health indices. However, Whittaker et al. (2012) cautioned that since the incorporated weights are all exclusively informed by the statistical properties of the constituent indicator data, if these statistical properties did not coincide with expert knowledge of the relative importance of the indicators, then the resulting indices are likely to be poor.

As an alternative, Whittaker et al. (2012) suggest the Malmquist index. The computational details of the Marlmquist index are rather complex and since this method does not appear to have been adopted by any report cards, we will restrict our description to just a brief overview. Whittaker et al. (2012)'s proposed version of the Malmquist index calculates pairwise ratios of indicator distances from a multivariate benchmark curve. The benchmark curve (a form of indifference curve), is a multivariate curve defined by the lower boundary of a convex hull of all indicator values and is thus derived entirely from the observed data. Using simulated data with manufactured statistical complications (heterogeneity and temporal autocorrelation), Whittaker et al. (2012) demonstrated that the Malmquist index out performs indices based on principal components analysis and suggested other statistical methods would have similar shortcomings.

### *3.1.2 Thresholds*

The absolute value of an indicator is rarely a meaningful assessment of ecosystem health assessments. Nor are the statistical properties of a time series necessarily a good basis for normalizing indicators or representing the objectives. What constitutes a 'good' or 'poor' level is likely to vary according to indicator, the ecosystem (e.g. freshwater, estuarine or marine) as well as the geographical and temporal (e.g. pre-industrial or current, seasonal) context. Another way to normalize the location (centre) of indicators (if not the scale as well) that incorporates both knowledge about the ecological basis of the indicator and the objectives that they address is to express the indicators relative to *benchmarks*.

Benchmarks are typically either reference or baseline conditions (sites or historic data representing relatively low disturbance 'healthy' conditions), threshold values (ecotoxicology

tolerances representing the cusp of 'unhealthy conditions) or guideline values (derived from either historical quantiles or ecotoxicology). Thresholds and guideline values are typically peer reviewed and ecologically meaningful, yet their specificity varies from local to regional, national or international standards.

Whilst a 'distance to benchmark' approach does provide some level of standardization (Connolly et al., 2013), to be useful, not only should there be some form of homogenization in what the benchmark condition represents, the polarity of the distance should be well understood (Hijuelos and Reed, 2013) and the magnitude of the distance should be commensurate with position along a disturbance gradient. That is, there should be some consistency in what it means to be above or below a benchmark, and indeed what it means to be a certain distance from a benchmark. Ideally, benchmarks should also be locally relevant (Connolly et al., 2013) and consider seasonal variability (Coates et al., 2007; Hallett et al., 2012). Indeed, in a review of the methodologies used to set benchmarks, (Borja et al., 2012) demonstrated the importance of setting appropriate benchmarks from which to assess ecosystem quality by directly linking the inability of indices to detect impacts in ecosystems to inappropriate reference conditions.

It is also important that benchmarks align with objectives in order to ensure indicators are appropriate. For example, if an objective is to maintain sustainable stocks of a particular species of fish, a benchmark that reflect either historical numbers or the numbers present at low pressure sites do not necessarily represent the level of sustainability.

Ecological monitors have long recognized the need to express ecosystem ratings as standardized scores and in terms that are more accessible to policy makers and the general public. Whilst initial applications focused on normalizing observed measures against subjective rating curves to yield dimensionless index values on the scale of [0,1] that could be readily combined into a single understandable score or rating (e.g. Miller et al., 1986), more recent studies have explored formulations that compare observed measures to baseline, reference, objectives or guideline values (collectively, benchmarks) values (e.g. CCME, 2001; Hurley et al., 2012; Jones et al., 2013).

Connolly et al. (2013) reviewed the use of report cards for monitoring ecosystem health and tabulated the general properties of a range of methods employed across a many different monitoring programs. Rather than duplicate that information here, the current intention is to provide more specific details about the algorithms used across those programs.

### *3.1.3 Unifying indices*

The Canadian Council of Ministers of the Environment Water Quality Index (CCME WQI; CCME, 2001) incorporates comparisons to baseline based on *scope* (proportion of indicators that have one or more failures to meet objectives), *frequency* (proportion of all comparisons failing to meet objectives) and *amplitude* (the normalized degree to which failed comparisons exceed objectives).

$$F_1 = 100.\left(\frac{Number\ of\ failed\ indicators}{Total\ number\ of\ indicators}\right)$$

$$F_2 = 100.\left(\frac{Number\ of\ failed\ comparisons}{Total\ number\ of\ comparisons}\right)$$

$$F_3 = \frac{100.E}{1+E}; \qquad E = \frac{\sum_{i=1}^{n} e_i}{n}; \qquad e_i = z_i.\left[\left(\frac{x_i}{benchmark_i}\right)^{\lambda_i} - 1\right]$$

$$z_i = \begin{cases} 1 & \text{if ith comparison fails} \\ 0 & \text{otherwise} \end{cases}; \qquad \lambda_1 = \begin{cases} 1 & \text{If} < benchmark_i = \text{fail} \\ -1 & \text{If} > benchmark_i = \text{fail} \end{cases}$$

$$CCMEWQI = 100 - \left(\frac{\sqrt{F_1^2 + F_2^2 + F_3^2}}{1.732}\right)$$

where *n* is the number of comparisons.

Whilst the CCME WQI might serve its purpose in the context to which it is applied, it is unlikely to be a useful metric for any indices involving remote sensing data or indeed any situation with a reasonable large amount of data or indicators. One-third of the weighting of the metric is calculated on the proportion of indicators that failed. The more observations are collected, the more likely at least one of them will exceed the benchmark. Hence, this one-third will quickly approach a constant of 1 thereby reducing overall sensitivity. In addition, the one-third of the method that weighting on amplitude only does so with respect to failure - there is no degree of how well the data recedes the benchmark. Finally, unifying indices have very limited scope for propagating any uncertainty. Consequently, this metric of index computation will not be explored in this project.

Rather than calculate the proportion of all comparisons failing to meet objectives across all indicators (as in the *frequency* component of the CCME WQI), we could perform the calculation separately for each variable (measure). Whilst this formulation (**Exceedance**), is characterised by the same limitations as the above *frequency* component, since it is calculated separately for each variable, when aggregated together to form an overall indicator, there is greater potential for improved resolution and granularity.

### *3.1.4 Hierarchical indices*

The CCME WQI unifies all indicators into a single index as part of the calculations. However, most other indices involve aggregating across a sets of individual indicator scores. There are numerous ways to formulate indicator scores based on deviations from a benchmark (see Table 14). Importantly, these scores are typically calculated at the level of the observations. Most of the index formulations are relatively robust to outliers (since the scores are either on a scale that reduces the magnitude of outliers or are capped to a range) and thus aggregating together indices is likely to be more robust than calculating indices from aggregated raw data. An exception to this might be in situations where benchmarks are defined in the context of a specific spatial or temporal aggregation (such as annual mean or median value).

The Binary method expresses a comparison to benchmark values on a binary compliance scale (1: complies with benchmark, 0: fails to comply) and whilst simple to perform and

understand, this method results in indices that have the potential to be either under or overly sensitive (depending on how far observed values typically are from the benchmark). For example, at one extreme (when values are close to benchmark), slight changes yield dramatic fluctuations in scores. However, when values are substantially above or below the benchmark, even modest improvements or deterioration will be undetected. This rapid 'switching' behaviour is depicted by the stepped response curve.

Note, when aggregated via means, the Binary method is identical to the Exceedance method, except that uncertainty propagation is slightly more straight forward via the Binary method.

In the State of the Great Lakes Report (EPA/EC, 1995), greater granularity is achieved via a panel of experts who classify each of six health indicators (aquatic community health, human health, habitat, contaminants, nutrients and economy) into four categories: poor, mixed/deteriorating, mixed/improving, good/restored. Similar expert rating or multi-category exceedance grading systems are employed in other report cards (e.g. Tamar estuary Report Card; Attard et al., 2012) and whilst probably reasonably accurate, they are nonetheless highly dependent on the ongoing availability of a reasonably stable panel of independent experts.

The Benchmark and Worst Case Scenario method (see Table 14) employed by the Fitzroy Basin Report Card (Jones et al., 2013) reflects the degree of failure by scaling the difference between the observed values and benchmarks (20*th* or 80*th* percentile of long term data for values above and below the benchmark respectively) to the Worst Case Scenario values (10*th* or 90*th* percentiles respectively). The associated response curve demonstrates a linear decline in Score with increasing distance from the benchmark. The Modified Amplitude method calculates the distance to benchmark on a logarithmic (base 2) scale. The base 2 logarithm represents ratios on a symmetric scale such that value that are twice and half the benchmark yield scores of the same magnitude (yet apposing signs), and has some inbuilt capacity to accommodate skewed data.

The Modified Amplitude response curve illustrates how this method can be simultaneously relatively insensitive to slight fluctuations around the benchmark as well as sensitive to changes further away from the benchmark. Contrastingly, the Logistic Amplitude method operates on a logit scale such that it is very sensitive to slight fluctuations close to the benchmark and becomes progressively less sensitive with increasing distance. This method is also automatically scaled to the range [0,1]. The steepness of the Logistic Amplitude response can also be controlled by a tuning parameter ($T$).

Water Quality indices (which are standardized measures of condition) are typically expressed relative to a guideline, threshold (see Table A1) or benchmark. Of the numerous calculation methods available, those that take into account the distance from the threshold (i.e. incorporate *difference-to-reference*) rather than simply an indication of whether or not a threshold value has been exceeded are likely to retain more information as well as being less sensitive to small changes in condition close to the threshold.

The challenging aspect of distance (or amplitude) based index methodologies is that determination what constitutes a large deviation from a benchmark depends on the scale of the measure. For example, a deviation of 10 units might be considered relatively large of turbidity (NTU) or salinity (ppt), yet might be considered only minor for the Chlorophyll-a ($\_g/L$).

In order to combine a range of such metrics together into a meaningful index, the individual scores must be expressed on a common scale. Whilst this is automatically the case for Binary compliance, it is not necessarily the case for distance based indices.

Table 14 describes and compares the formulations and response curves of the Binary compliance method as well as a number of amplitude (distance based) indexing methods.

The Modified Amplitude and Logistic Modified Amplitude are both based on a base 2 logarithm of the ratio of observed values to the associated be benchmark (see Table 14). This scale ensures that distances to the benchmark are symmetric (in that a doubling and halving equate to the same magnitude - yet apposing sign). Furthermore, the logarithmic transformation does provide some inbuilt capacity to accommodate log-normality (a common property of measured values).

By altering the sign of the exponent, the Modified Amplitude methods can facilitate stressors and responses for which a failure to comply with a benchmark would be either above or below the benchmark (e.g. NTU vs Secchi depth). Further modifications can be applied to accommodate measures in which the benchmark represents the ideal and deviations either above or below represent increasingly poorer conditions (e.g. pH and dissolved oxygen).

The raw Modified Amplitude scores are relatively insensitive to small fluctuations around a benchmarks and sensitivity increases exponentially with increasing distance to the benchmark. The resulting scores can take any value in the real line $[-\infty,\infty]$ and hence are not bounded[9]. There are two broad approaches to scaling (see Table 14):

- Capping and scaling: The log2 scale can be capped to a range representing either a constant extent of change (e.g. twice and half the benchmark - a cap factor of 2) or else use historical quantiles (10th and 90th percentiles) to define the upper and lower bounds to which to cap the scale. Note historical quantiles are unavailable for the current application[10]. Thereafter, either can be scaled to the range [0,1] via a simple formula (see Table 14 III.Scaled).
- Logistic Modified Amplitude: By expressing the scores on a logistic scale, the range of scores can be automatically scaled to range [0,1]. Moreover, this method allows the shape of the response curve to be customized for purpose. For example, the relative sensitivity to changes close or far from the benchmarks can be altered by a tuning parameter.

Rather than aggregating across sites before calculating indices, we would suggest that indices should be calculated at the site level. This is particularly important when different

[9] Unbounded indices are difficult to aggregate, since items that have very large magnitude scores will have more influence on the aggregation than those items with scores of smaller magnitude. Furthermore, unbounded scores are difficult to convert into alphanumeric Grades. Consequently, the Scores need to be scaled before they can be converted to alphabetical grading scale.
[10] The use of historical quantiles makes the explicit assumption that the domain of expectations (from very good to very poor) is encapsulated within the historical data. For the eReefs model data, only three years of historical data are available. This is unlikely to be sufficient to represent the full spread of what we should consider our expectations - particularly when we acknowledge that the eReefs model data do not extend back as far as the 2010-2011 floods during which water quality conditions might be expected to be lower than the years to follow.

measures are measured at different sites. Spatial variability can be addressed via the use of a bootstrapping routine (see below).

**Table 13: Formulations and example response curves for a variety of indicator scoring methods that compare observed values ($x_i$) to associated benchmark, thresholds or references values ($B\_i$ and dashed line). The Scaled Modified Amplitude Method can be viewed as three Steps: I. Initial Score generation, II. Score capping (two alternatives are provided) and III. Scaling to the range [0,1]. A schematic within the table illustrates the different combination of Modified Amplitude forumations. The first of the alternative capping formulations simply caps the Scores to set values (on a $log_2$ scale), whereas the second formulation (Quantile based, where Q1 and Q2 are quantiles) allows thresholds quantiles to be used for capping purposes. Dotted lines represent capping boundaries. In the Logistic Scaled Amplitude method, T is a tuning parameter that controls the logistic rate (steepness at the inflection point). For the purpose of example, the benchmark was set to 50.**

| Method | Formulation | Response curve |
|---|---|---|
| Binary compliance | $Score_i = \begin{cases} 1 & \text{if } x_i \le B_i \\ 0 & \text{if } x_i \text{ else} \end{cases}$ | 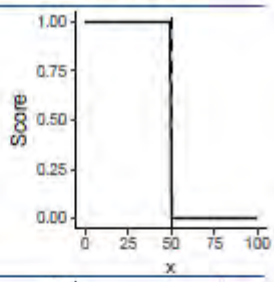 |
| Benchmark and WCS | $Score_i = \begin{cases} 100 & \text{if } x_i \le B_i \\ 0 & \text{if } x_i \ge WCS_i \\ \left\|1.0 - \left\|\frac{x_i - B_i}{WCS_i - B_i}\right\|\right\|.100 & \text{else} \end{cases}$ | 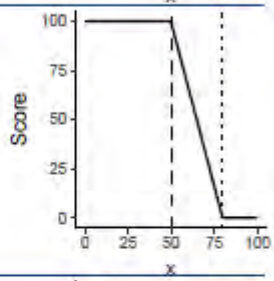 |
| Amplitude | $Score_i = \begin{cases} (\frac{x_i}{B_i})^{-1} & \text{if} > B_i = \text{fail} \\ (\frac{x_i}{B_i})^{1} & \text{if} < B_i = \text{fail} \end{cases}$ <br> $Score_i = \frac{100 \times Score_i}{1 + Score_i}$ | 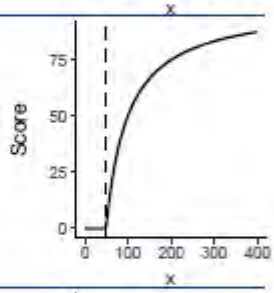 |
| Modified Amplitude | I. Raw (MAMP) <br> $Score_i = \begin{cases} log_2(\frac{x_i}{B_i})^{-1} & \text{if} > B_i = \text{fail} \\ log_2(\frac{x_i}{B_i})^{1} & \text{if} < B_i = \text{fail} \end{cases}$ | 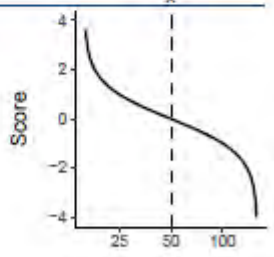 |
| | IIa. Fixed caps (Fold=2: [0.5,2]) (Fold=4: [0.25,4]) <br> $Score_i = \begin{cases} log_2(1/2) & \text{if } Score_i < -1 \\ log_2(2/1) & \text{if } Score_i > 1 \\ Score_i & otherwise \end{cases}$ | 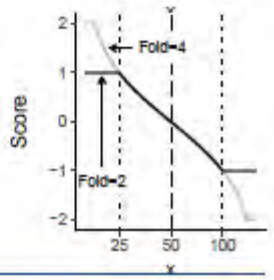  |

| Method | Formulation | Response curve |
|---|---|---|
| | IIb. Quantile/extremes based caps ([15,170]) $Score_i = \begin{cases} log_2(\frac{Q1}{B_i})^{-1} & \text{if } x_i < Q1 \\ log_2(\frac{Q2}{B_i})^{-1} & \text{if } x_i > Q2 \\ Score_i & otherwise \end{cases}$ | 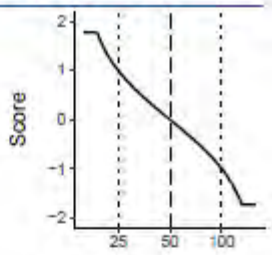  |
| | III. Scaled ([0,1]) $Score_i = \frac{Score_i - min(Score_i)}{max(Score_i) - min(Score_i)}$ | 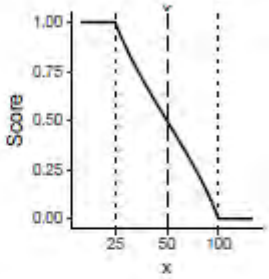  |
| | I. → MAMP<br>IIa. → fMAMP<br>IIb. → III. → fsAMP<br>III. → sMAMP | |
| Logistic Scaled Modified Amplitude | Raw $Score_i = \begin{cases} log_2(\frac{x_i}{B_i})^{-1} & \text{if} > B_i = \text{fail} \\ log_2(\frac{x_i}{B_i})^{1} & \text{if} < B_i = \text{fail} \end{cases}$ $Score_i = \frac{1}{1+e^{S core_i - T}}$ | |
| Logistic | Raw $Score_i = \begin{cases} \frac{1}{1+e^{T(x_i/B_i)}} & \text{if} > B_i = \text{fail} \\ \frac{1}{1+e^{-T(x_i/B_i)}} & \text{if} < B_i = \text{fail} \end{cases}$ | 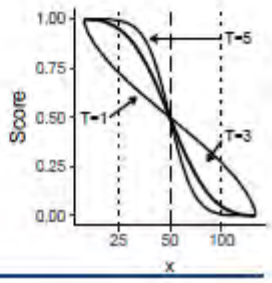  |

We would recommend that measurements collected throughout the reporting year be aggregated together into a single annual value. This is primarily because most water quality thresholds pertain specifically to annual averages rather than single time samples. Although it is possible to incorporate uncertainty due to temporal variability, the low sparse temporal frequency of sample collection is likely to yield uncertainty characteristics that will swamp the more interesting spatial sources of uncertainty.

Alternatively, if we relax the application of thresholds to individual observations, annual indices can be generated by aggregating observations level indices. When doing so, the Binary

Compliance formulation aggregated via means will yield identical outcomes to the Exceedance formulation.

A useful metric for comparing the sensitivity of one indexing method over another is to take some representative longitudinal data and calculate indices based on the actual data as well as data that introduces progressively more noise.

Whilst the state of the water (or other environmental condition) might be of interest in its own right, it might also be of interest from the perspective of the ecosystem supported by the water. For example, turbidity might be considered to provide important insights into the light availability within the ecosystem. As such, the variability in light availability (turbidity) might be a more influential ecological driver/pressure than the exact light level within any given time frame. Furthermore, sustained conditions might be more influential than rapidly fluctuating conditions. For example, two time windows could experience the same turbidity average and variance, yet these summaries could manifest from very different fluctuation patterns (one experiencing rapid fluctuations, and the other experiencing sustained periods of contrasting conditions).

One index that captures the pattern of fluctuations could be based on a metric that expresses the number of consecutive days in which a threshold has been exceeded as a proportion of number of days in the time window (e.g. 365 days).

$$Score_i = 1 - (\frac{n_i}{N_i})$$

where $n_i$ is the maximum number of consecutive time units in which $x_i > B_i$ and $N_i$ is the number of time units in the $i_{th}$ spatio-temporal window.

Unfortunately, such a formulation imposes some relatively difficult requirements on the data. Firstly, the time series within each window must be complete (no gaps), otherwise it is difficult to asses $N_i$. This requirement limits its use to only the eReefs modelled data as the Satellite data, AIMS insitu and AIMS FLNTU data have substantial time gaps. Secondly, as the formulation is based on summing up exceedances, it is likely to be as susceptible to the recognised insensitivities associated with binary compliance. Indeed, these sensitivities may well be further amplified. Furthermore, it is not responsive to the magnitude of exceedance. The next section will explore the performance of the following index formulations:

Binary compliance (Binary)

- Exceedance - proportion of observations exceeding the threshold (on large datasets, this will converge with Binary compliance (Exceed)
- Maximum duration of exceedance (Max_Duration)
- Modified Amplitude (MAMP)
- Fixed Modified Amplitude (fMAMP)
- Fixed Scaled (x2,1/2) Modified Amplitude (fsMAMP)
- Fixed Scaled (x4,1/4) Modified Amplitude (fsMAMP4)

## 3.2 Index sensitivity

The sensitivity of a metric can be gauged by either:

- Quantitative exploration of the relationships between the metric and gradients of the underlying conditions that the metric should respond to. This approach requires very well defined gradients as well as a clear understanding and measures of what constitutes a relationship. By optimizing the metric(s) to these gradients, this approach has the potential to bias outcomes towards these gradients at the expense of generality to other gradients.
- Have experts (or end users) qualitatively gauge the outcomes of different metrics against expected trends and patterns. That is, do the outcomes align with end user expectations? Although this approach is equally subjective and potentially biased as the quantitative exploration, it does not necessitate formulating statistical cutoffs and associated artefacts.
- Explore the behaviour and characteristics of the metric when calculated on data simulated to represent a range of scenarios (altering location and spread). Whilst this approach will not necessarily select the 'best' metric, it does permit identification of the limitations and assumptions associated with different metrics.

The above approaches are not mutually exclusive. The current project will explicitly explore sensitivity via a simulation approach, yet will also encourage feedback as to whether final outcomes align with expectations. It should be noted that the current project is limited in sources of data and measured properties. A metric is purely a re-expression of data in order to enhance or highlight a signal. If the underlying data do not contain the expected signal, a signal will likewise be absent from any metrics.

To explore the performance and sensitivity of the various index computations for a range of data scenarios, data were simulated from Gamma distributions varying in mean (relative to a threshold) and variance and sample size. The Gamma distribution is parameterized by two shape parameters that can be expressed in terms of mean and variance ($Gamma(\frac{\mu^2}{\sigma^2}, \frac{\mu}{\sigma^2})$).

For each threshold value (GL = 0.1,0.2,0.5,1,1,10,100) and sample size (R=10,100,1000), a set of 28 data scenarios where simulated (see Table 15 so as to represent a full spectrum of possible sampling outcomes. For each threshold/sample size and set combination, indices were calculated and aggregated for the simulated data. The extremes of these combinations are presented in Figures 32, 35 and 36, a more extensive set of Figures are in https://eatlas.org.au/nesp-twq-3/3-2-5-analysis-catalogue. For the set of simulations, the smaller the threshold, the more variable the samples relative to the threshold. Within each threshold, the set of 28 scenarios thereby represent combinations of varying mean and relative variability.

**Table 14: Index performance and sensitivity data scenarios. Data in each group are drawn from Gamma distributions whose parameterizations are based on a mean and variance. In each case the mean is some multiple of the threshold (GL) value. Multiples of threshold that are less than 1 result in data with greatest density below the threshold value.**

**Lower variances result in less varied data.**

| Grp | Mean | SD | Grp | Mean | SD | Grp | Mean | SD | Grp | Mean | SD |
|---|---|---|---|---|---|---|---|---|---|---|---|
| 1 | $\mu = 0.2GL$ | $\sigma^2 = 0.1$ | 9 | $\mu = 0.75GL$ | $\sigma^2 = 0.1$ | 17 | $\mu = 1.5GL$ | $\sigma^2 = 0.1$ | 25 | $\mu = 4GL$ | $\sigma^2 = 0.1$ |
| 2 | $\mu = 0.2GL$ | $\sigma^2 = 0.2$ | 10 | $\mu = 0.75GL$ | $\sigma^2 = 0.2$ | 18 | $\mu = 1.5GL$ | $\sigma^2 = 0.2$ | 26 | $\mu = 4GL$ | $\sigma^2 = 0.2$ |
| 3 | $\mu = 0.2GL$ | $\sigma^2 = 0.3$ | 11 | $\mu = 0.75GL$ | $\sigma^2 = 0.3$ | 19 | $\mu = 1.5GL$ | $\sigma^2 = 0.3$ | 27 | $\mu = 4GL$ | $\sigma^2 = 0.3$ |
| 4 | $\mu = 0.2GL$ | $\sigma^2 = 0.5$ | 12 | $\mu = 0.75GL$ | $\sigma^2 = 0.5$ | 20 | $\mu = 1.5GL$ | $\sigma^2 = 0.5$ | 28 | $\mu = 4GL$ | $\sigma^2 = 0.5$ |
| 5 | $\mu = 0.5GL$ | $\sigma^2 = 0.1$ | 13 | $\mu = 1GL$ | $\sigma^2 = 0.1$ | 21 | $\mu = 2GL$ | $\sigma^2 = 0.1$ | | | |
| 6 | $\mu = 0.5GL$ | $\sigma^2 = 0.2$ | 14 | $\mu = 1GL$ | $\sigma^2 = 0.2$ | 22 | $\mu = 2GL$ | $\sigma^2 = 0.2$ | | | |
| 7 | $\mu = 0.5GL$ | $\sigma^2 = 0.3$ | 15 | $\mu = 1GL$ | $\sigma^2 = 0.3$ | 23 | $\mu = 2GL$ | $\sigma^2 = 0.3$ | | | |
| 8 | $\mu = 0.5GL$ | $\sigma^2 = 0.5$ | 16 | $\mu = 1GL$ | $\sigma^2 = 0.5$ | 24 | $\mu = 2GL$ | $\sigma^2 = 0.5$ | | | |

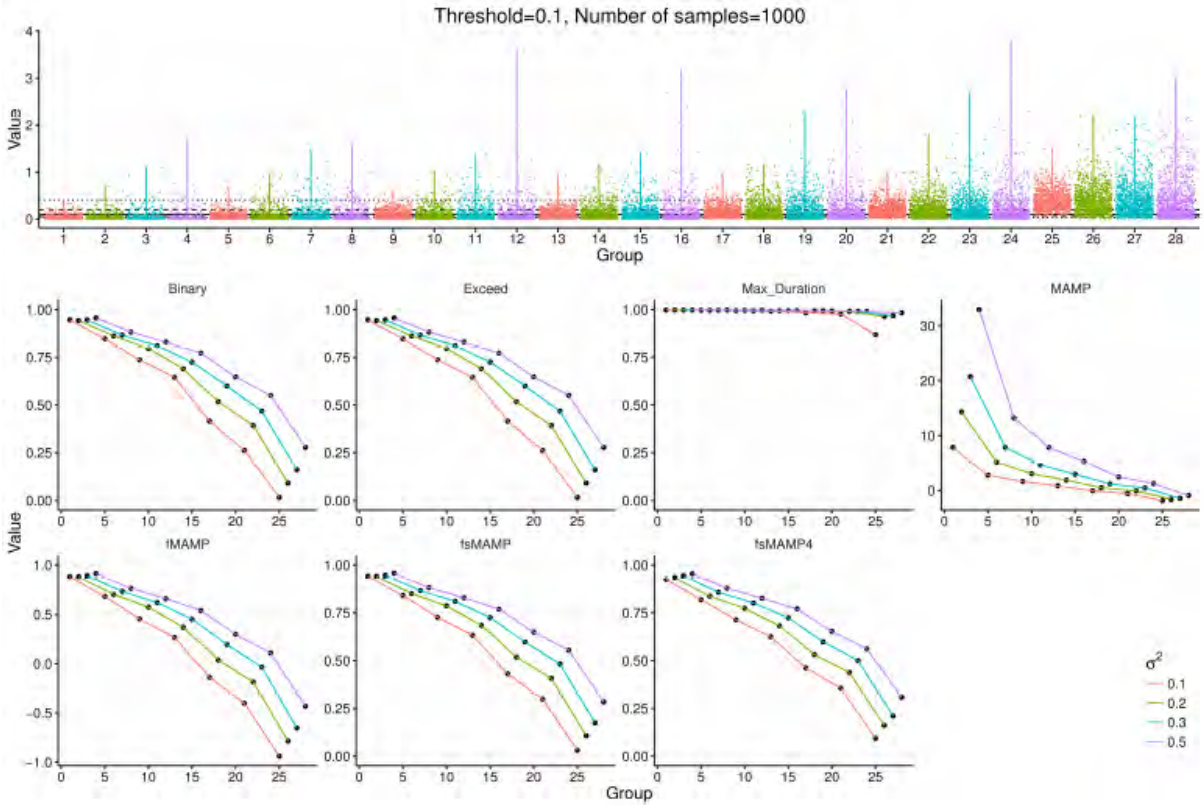


**Figure 32: Simulated data and associated indices for threshold of 0.1 and very large sample sizes (R=1000). Samples represent high variability relative to threshold.**

As expected, indices decline with increasing values relative to the threshold (as would be the case for Chl-a or TSS) with a generally linear response being the attribute sought in our specific context. Testing the responses of indices to various combinations allowed the identification of the most appropriate and robust index calculation method.

When the number of samples and the relative sample variability is very large (e.g. Figure 32), with the exception of the maximum duration of exceedance and the uncapped and unscaled modified amplitude (MAMP) methods, the different index calculation methods behave very similarly. However, as the variability of the samples declines relative to the threshold (e.g. compare Figures 32, 33 and 34), such that observations are predominantly within twice/half the threshold value, and data is predominantly distributed between the threshold value binary

or frequency of exceedance methods both increasingly become simultaneously overly and under sensitive. The response curve of these metrics becomes less linear, whereas the linearity of the other metrics is maintained for a greater span of observation means. This is further exacerbated by small sample sizes (see Figure 36).

Over all of the scenarios, the fsMAMP4 (Modified Amplitude capped at four times/quarter of threshold values) appears to be as linear or more linear than the fsMAMP (Modified Amplitude capped at twice/half), particularly as relative variability declines. However, the cost of this extended range of sensitivity, is that it is predominantly more sensitive at the extremes and less so (at least compared to fsMAMP) towards the mid-region (corresponding to values close to the threshold). Arguably, it is more desirable for an index to be most sensitive around the threshold (unless there is substantial uncertainty about the threshold value) and become progressively less sensitive at increasing distance from the threshold - the binary and exceedance metrics are the extreme cases of this.

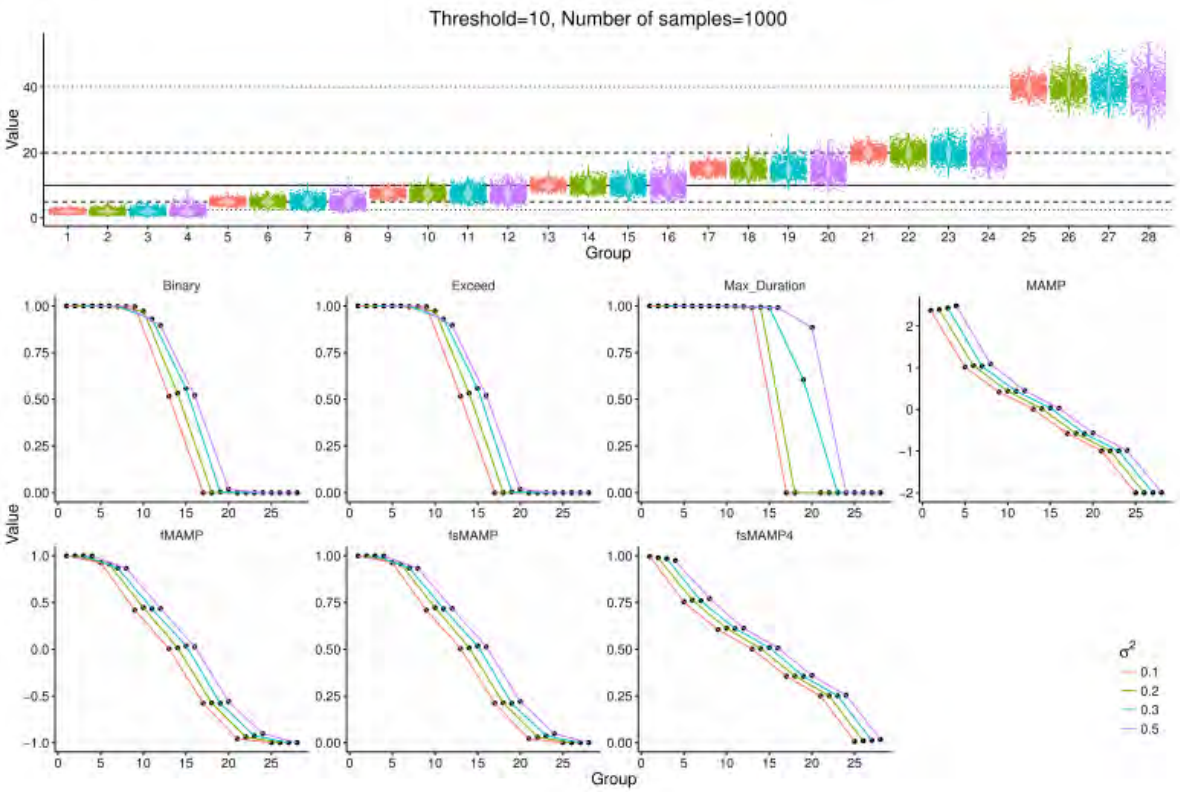


**Figure 33: Simulated data and associated indices for threshold of 10 and very large sample sizes (R=1000).**

The fixed capped modified amplitude (fsMAMP) index was considered the 'best' compromise between consistent sensitivity throughout the range of scenarios and the nature of data presented in exploratory data analyses (see Section 2). It should be noted that it is possible to modify the fsMAMP index metric to facilitate caps based on historical, biological or ecological parameters. It is also possible to define these parameters (an upper and lower capping) at any spatial/temporal/measure level so as to potentially build indices that are optimized for each measure. Such an exercise requires extensive expert knowledge to define and justify each of the parameters and is beyond the scope of the current project.

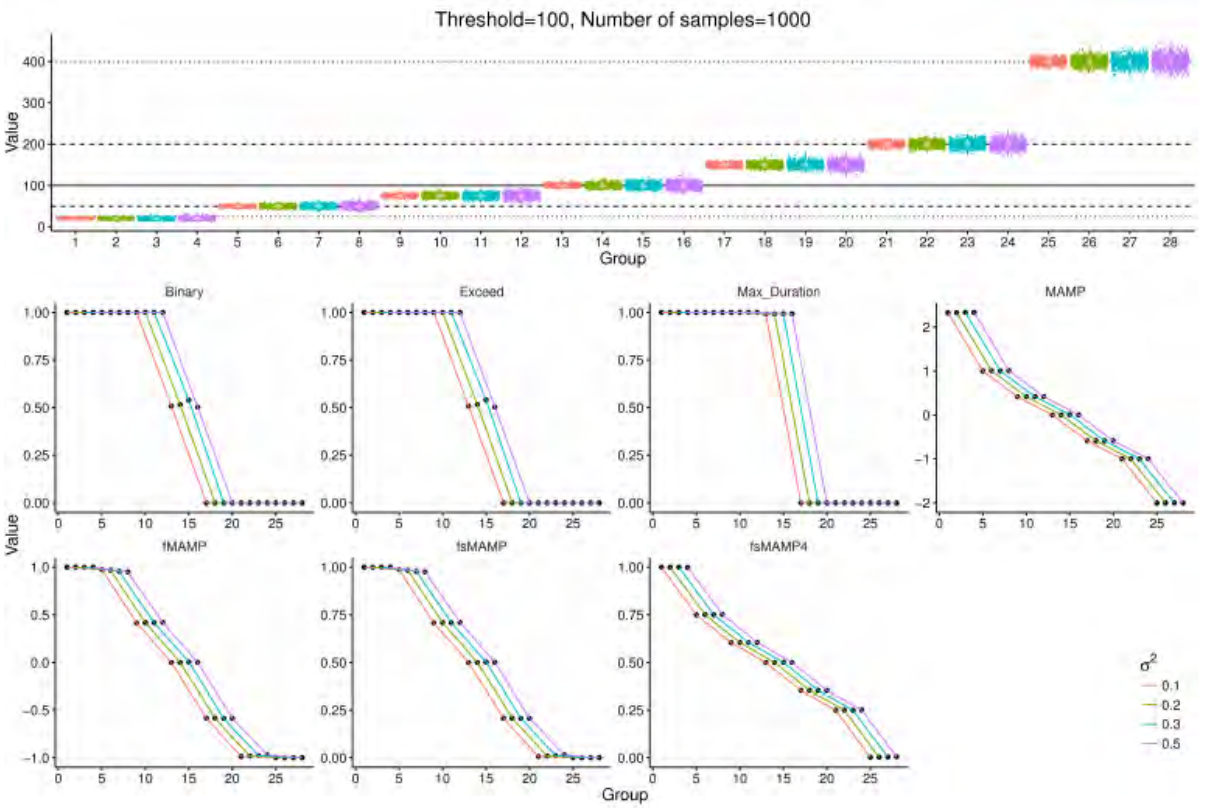


**Figure 34: Simulated data and associated indices for threshold of 100 and very large sample sizes (R=1000).**

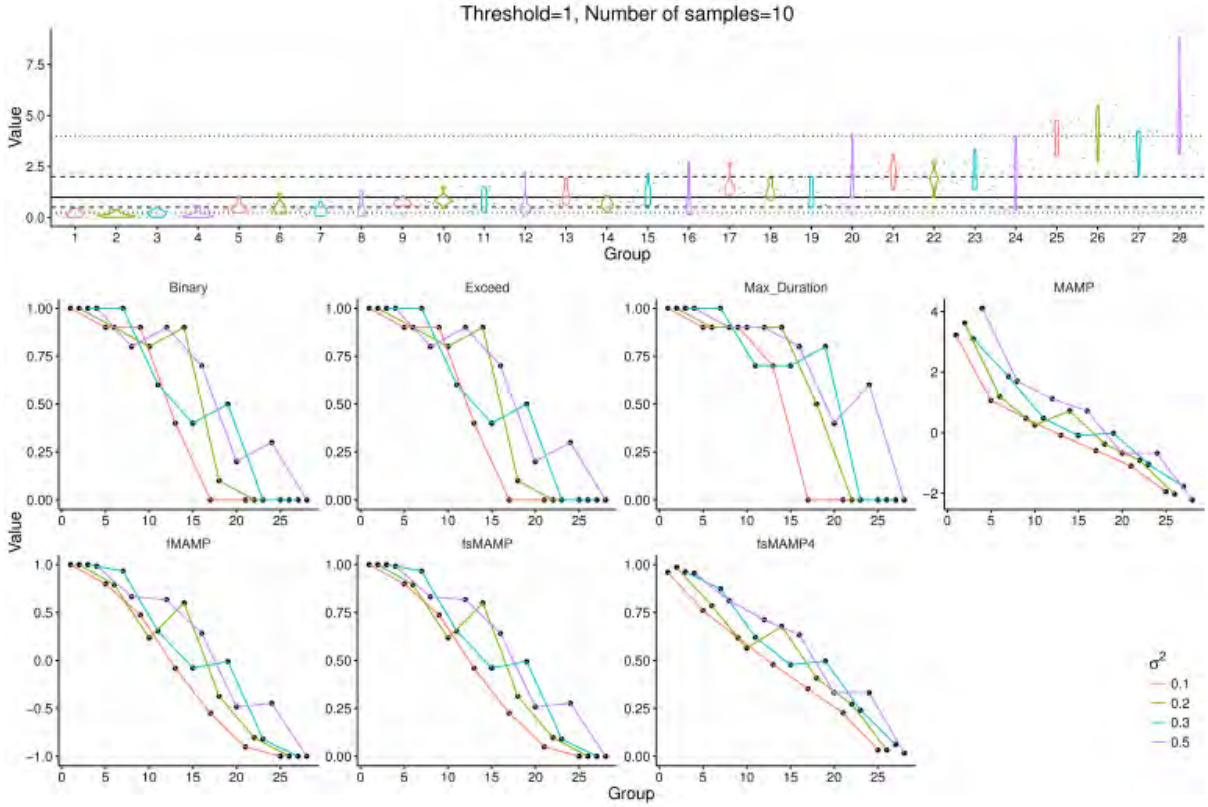


**Figure 35: Simulated data and associated indices for threshold of 1 and large sample sizes (R=100).**

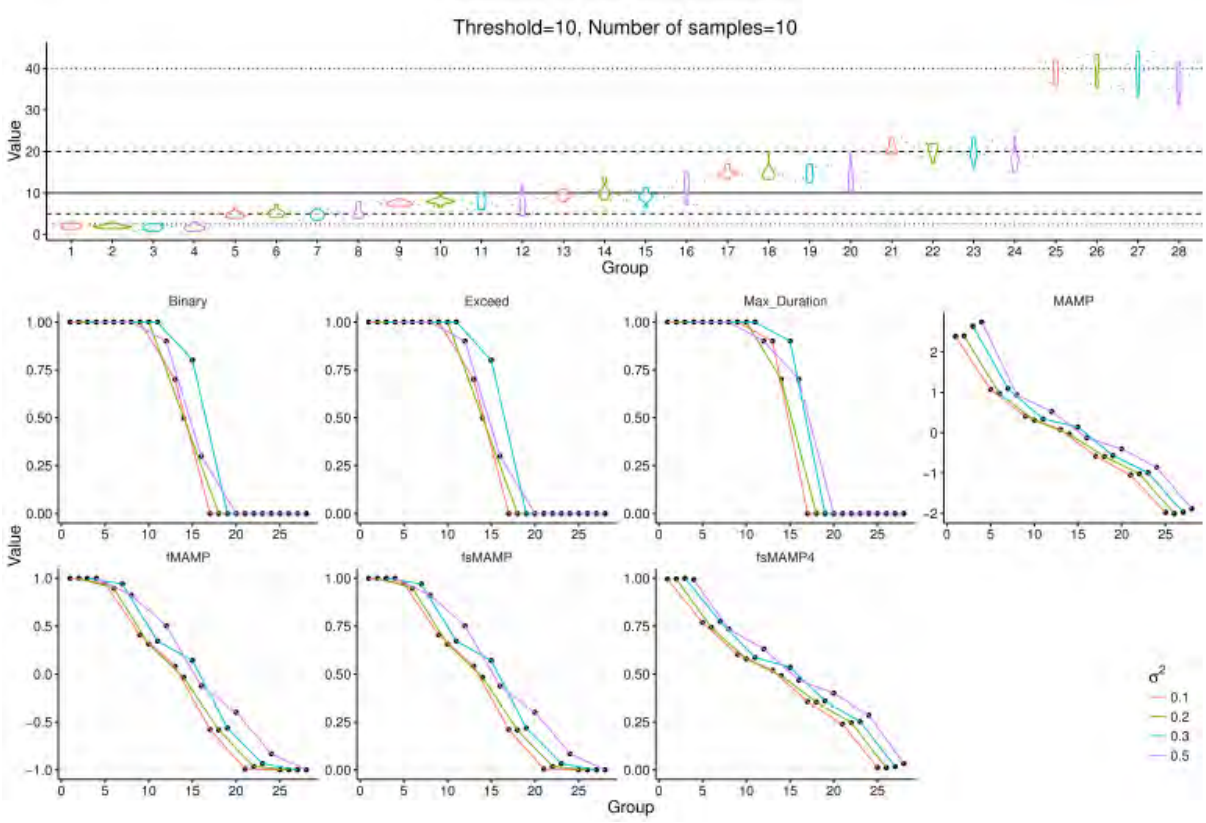


**Figure 36: Simulated data and associated indices for threshold of 10 and small sample sizes (R=10).**

### *3.2.1 Summary of simulation index sensitivity exploration*

- Indices decline with increasing values relative to the thresholds (and for a given variability)
- Indices increase with increasing variability (since in Gamma distributions, this results in more values towards lower end)
- when R is very large, the different indicators behave similarly (except Max_Duration and MAMP)
- MAMP is more susceptible to outliers
- fsMAMP4 (as an example of increasing the capping range from 1/2 and x2) is more sensitive at the extremes and less discerning closer to the threshold
- fsMAMP (with capes fixed at the range of 1/2 and x2) appears to be a good compromise between under and over sensitivity across the range of simulated scenarios.

## 3.3 Index explorations

Before data can be combined and aggregated across the various Sources (AIMS insitu, AIMS FLNTU, Satellite, eReefs and eReefs926) and Measures (Chlorophyll, TSS, Secchi depth and NOx), it is important that we evaluate the likely usefulness of each Source/Measure combination. For example, a Measure or Source that does not vary in both time and space is not considered very informative parameter.

Although an exploration of the patterns of spatial and temporal variation of the raw data does offer some insights into the usefulness of a parameter, it is variation in relation to expectations

(thresholds) that are likely to be of greatest utility. For example, a parameter might vary substantially in time and or space and yet always be well above (or below) the threshold. In this situation (despite the apparent variability), with respect to the expectation domain, there is very little (if any) variability and thus the realised utility of the parameter is low (or else the threshold is inappropriate for the particular measure to which it is being applied).

Different parameters are measured on different scales or else have different natural background levels. Since variability (for example variance) is dependent on scale, parameters measured in larger units will typically exhibit more variability in absolute terms. Hence, in order to compare the relative utility of different parameters, it is necessary to either express variation relative to scale (such as coefficient of variation) or standardize the parameters. The scaled hierarchical index formations of Section 4.1.4 (such as Binary, fsMAMP, fsMAMP4 and logistic MAMP) are all a form of standardization which yield scores on scales that are all bound [0,1].

The following three subsections will provide information to assist in the selection of:

- which Index formulation to adopt
- which Sources of data to use
- which Measures to include

### *3.3.1 Indices*

Theoretical sensitivity investigation suggested that the fixed capped (half/twice threshold) Modified Amplitude (fsMAMP) is likely to be the best compromise between under and over sensitivity given the patterns of variance observed across and between the various Sources (AIMS insitu, AIMS FLNTU, Satellite, eReefs and eReefs926) and Measures (Chlorophyll, TSS, Secchi depth and NOx). The alternate approach is to explore and compare the patterns of the various index formulations in the context of both the raw collected data and expert expectations. Broadly speaking, we might expect that many water Quality parameters improve across the shelf with increasing distance from coastline. We might also expect some latitudinal patterns in which water quality generally improves along a south-north gradient with interruptions coinciding with outflow of major rivers.

To explore how the raw data are transformed into the various indices, it is useful to pair up 'before' and 'after' figures. Again, for the sake of brevity, we will focus on the same data that featured in Figure 9 (Chlorophyll-a from Wet Tropics, Open Coastal). Figures 37 – 41 illustrate the associations between the site means (subfigure a) and three of the major index candidates (b: Binary, c: fsMAMP and d: fsMAMP4) for each of the Sources of data (AIMS insitu, AIMS FLNTU, Satellite, eReefs and eReefs926). In these figures, purple and blue lines represent annual means and within year Generalized Additive Model (Wood, 2006) respectively and help highlight inter- and intra-annual variation[11].

Similar figures for the other Measures (Total Suspended Solids, Secchi Depth and NOx) for the Dry Tropics Midshelf zone are presented in https://eatlas.org.au/nesp-twq-3/3-2-5-analysis-catalogue.

[11] GAMs not performed for AIMS in situ data due to a lack of data over which to estimate splines

Inter and Intra annual variation is greatest in the Binary index method for each data Source[12]. Whilst this method does illustrate sensitivity, the values of the index do not contain any context about the magnitude of values relative to the threshold. That is, it is not possible to distinguish situations in which all observations are just under (or over) the threshold from when they are substantially under (or over) the threshold. In this way, the index has the potential to be under-sensitive to magnitude, yet very sensitive to change around the threshold. For each of the Sources (except AIMS insitu for which data are too sparse), the relative magnitude of fluctuations in the Binary index (subfigure b) appears to be substantially greater than the relative magnitude of fluctuation in the observed data (subfigure a). These patterns of relative variability might imply that the Binary index is over-sensitive.

By contrast, the fsMAMP4 (capped at four times and one-forth threshold, subfigures d) could be interpreted as under-sensitive - particularly for the Satellite data (which has highly variable observations). The fsMAMP (twice/half threshold) appears to in between these two extremes and thus could be considered a reasonable compromise between over and under sensitivity.

Spatial representations for Wet Tropics Open Coastal Chlorophyll-a (figs. 42 – 45) and Dry Tropics Midshelf Chlorophyll-a (figs. 46 – 50) offer similar assessments - that fsMAMP provides a reasonable compromise between the potentially under and over sensitive fsMAMP4 and Binary formulations. Similar representations for Total Suspended Solids, Secchi Depth and NOx are presented in https://eatlas.org.au/nesp-twq-3/3-2-5-analysis-catalogue.

Time series of annually aggregated observations and associated annually aggregated indices (figs. 51 – 55) provide simplified representations of the overall spatio-temporal patterns. As with the temporal and spatial representations, the fsMAMP index consistently manifests between the Binary and fsMAMP4 formulations.

[12] this pattern also persists across all Zones (Region/Water body) and Measures - although other Measures and Zones not provided here to reduce space.

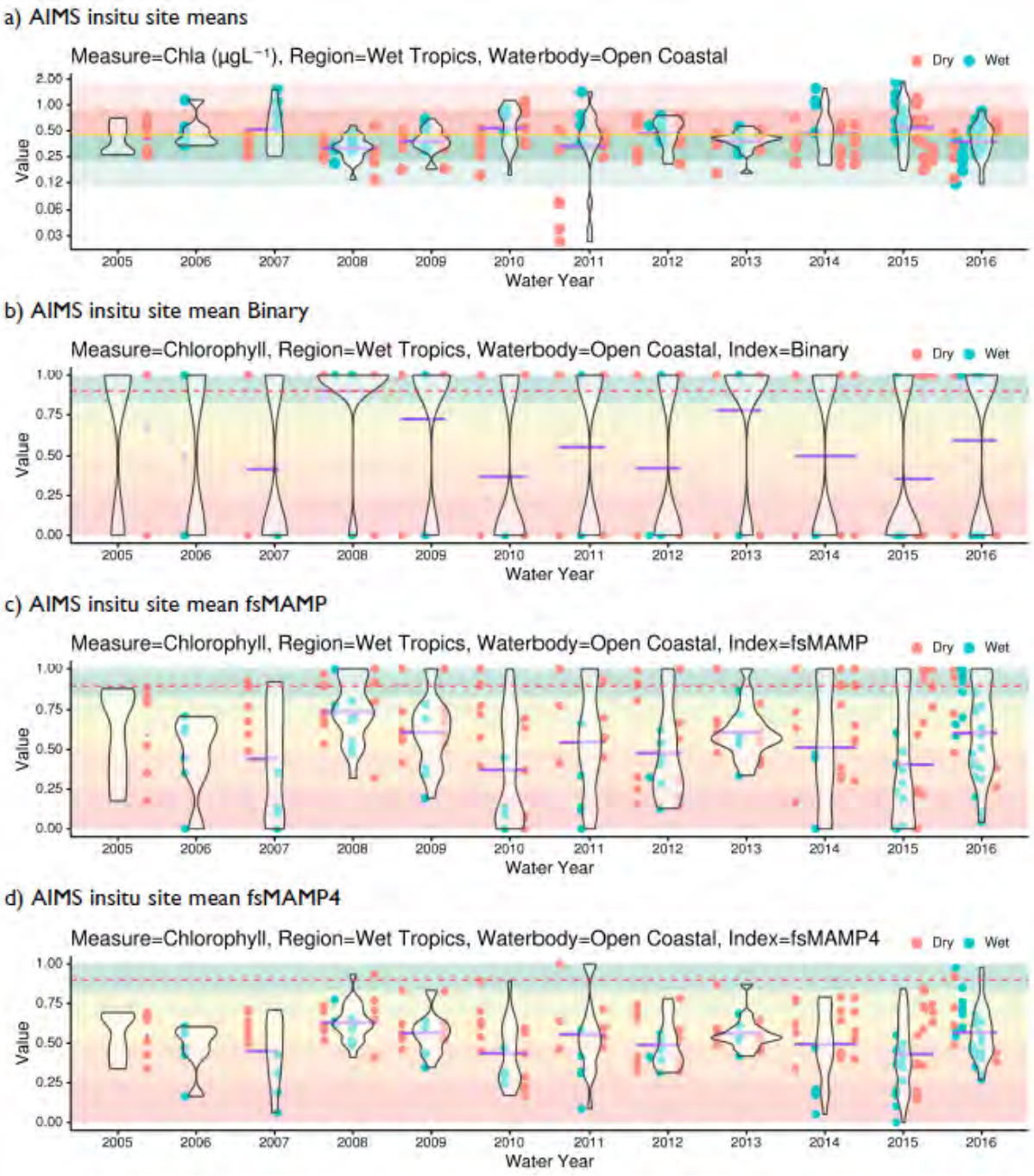


**Figure 37: Temporal distribution of AIMS insitu Chlorophyll-a a) samples and associated b) Binary, c) fsMAMP and d) fsMAMP4 index formulations for the Wet Tropics Open Coastal zone. Red and Blue symbols represent samples collected in Dry and Wet seasons respectively. Green and red shaded banding on a) respectively represent half and twice threshold value (50% shading) and one-forth and four times threshold value (30% shading). Traffic-light banding on b-d) indicates simple 5-level colour scheme. Purple lines represent annual means.**

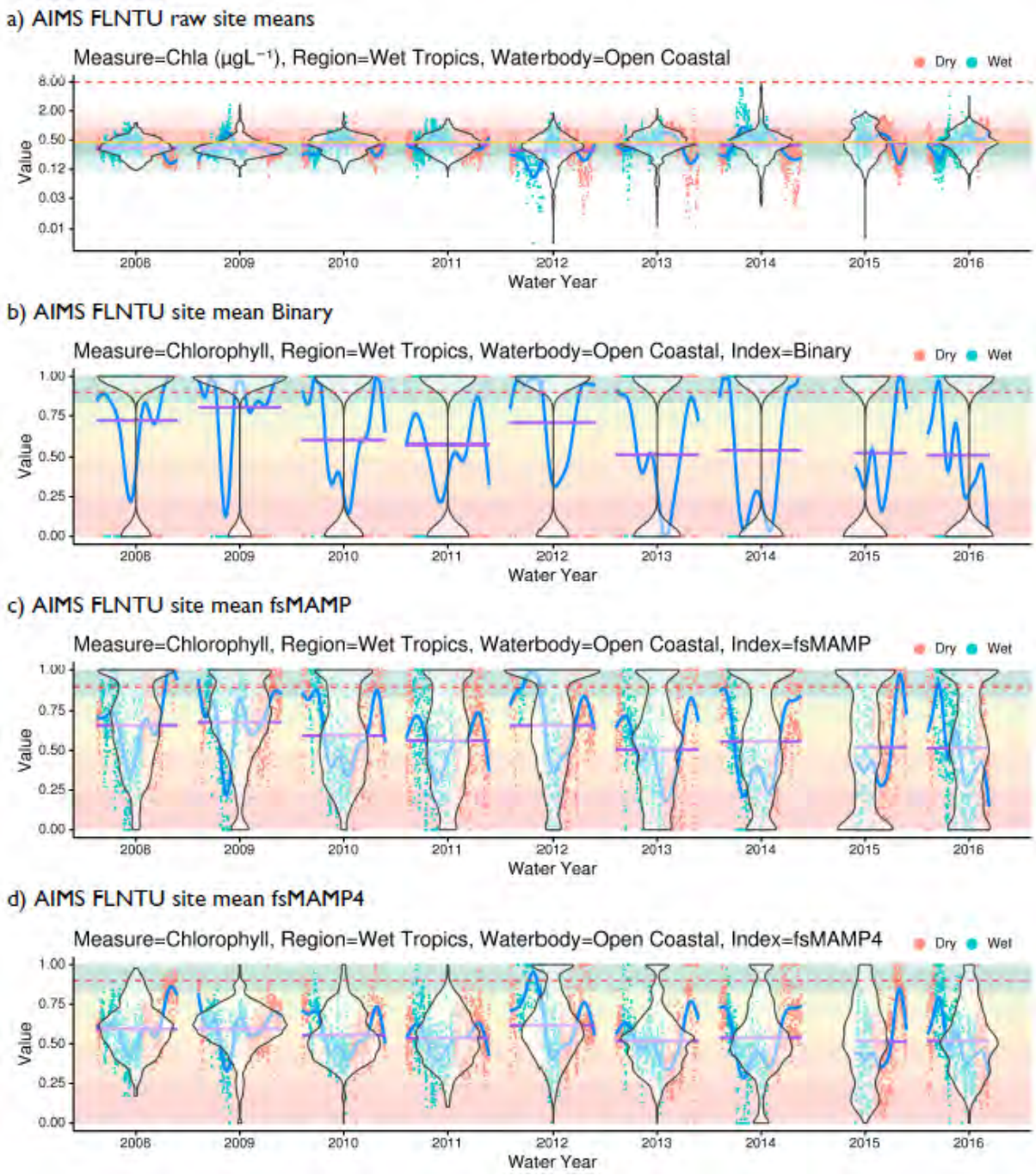


**Figure 38: Temporal distribution of AIMS FLNTU Chlorophyll-a a) samples and associated b) Binary, c) fsMAMP and d) fsMAMP4 index formulations for the Wet Tropics Open Coastal zone. Red and Blue symbols represent samples collected in Dry and Wet seasons respectively. Green and red shaded banding on a) respectively represent half and twice threshold value (50% shading) and one-forth and four times threshold value (30% shading). Traffic-light banding on b-d) indicates simple 5-level color scheme. Purple lines represent annual means.**

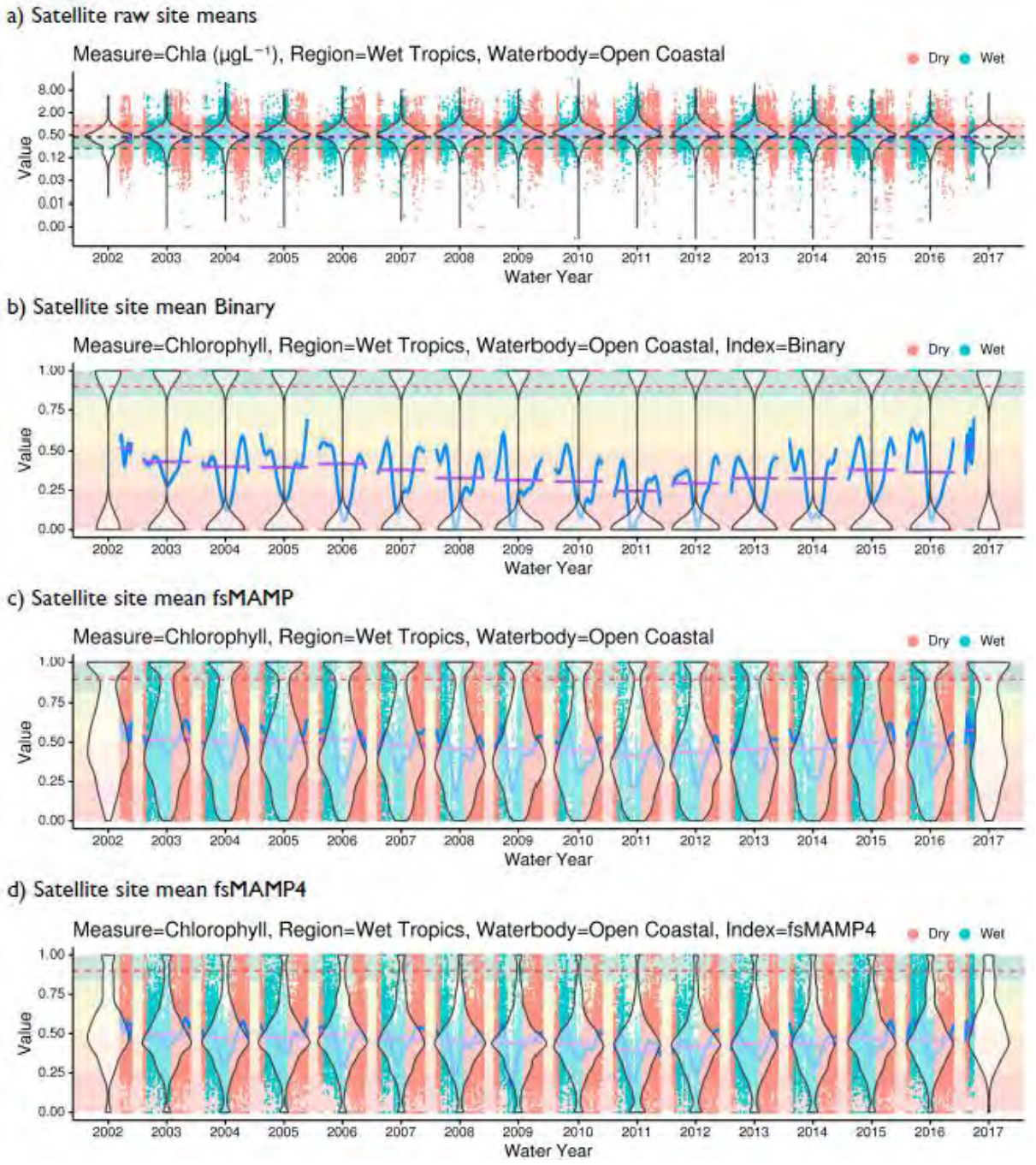


**Figure 39: Temporal distribution of Satellite Chlorophyll-a a) samples and associated b) Binary, c) fsMAMP and d) fsMAMP4 index formulations for the Wet Tropics Open Coastal zone. Red and Blue symbols represent samples collected in Dry and Wet seasons respectively. Green and red shaded banding on a) respectively represent half and twice threshold value (50% shading) and one-forth and four times threshold value (30% shading). Traffic-light banding on b-d) indicates simple 5-level color scheme. Purple lines represent annual means.**

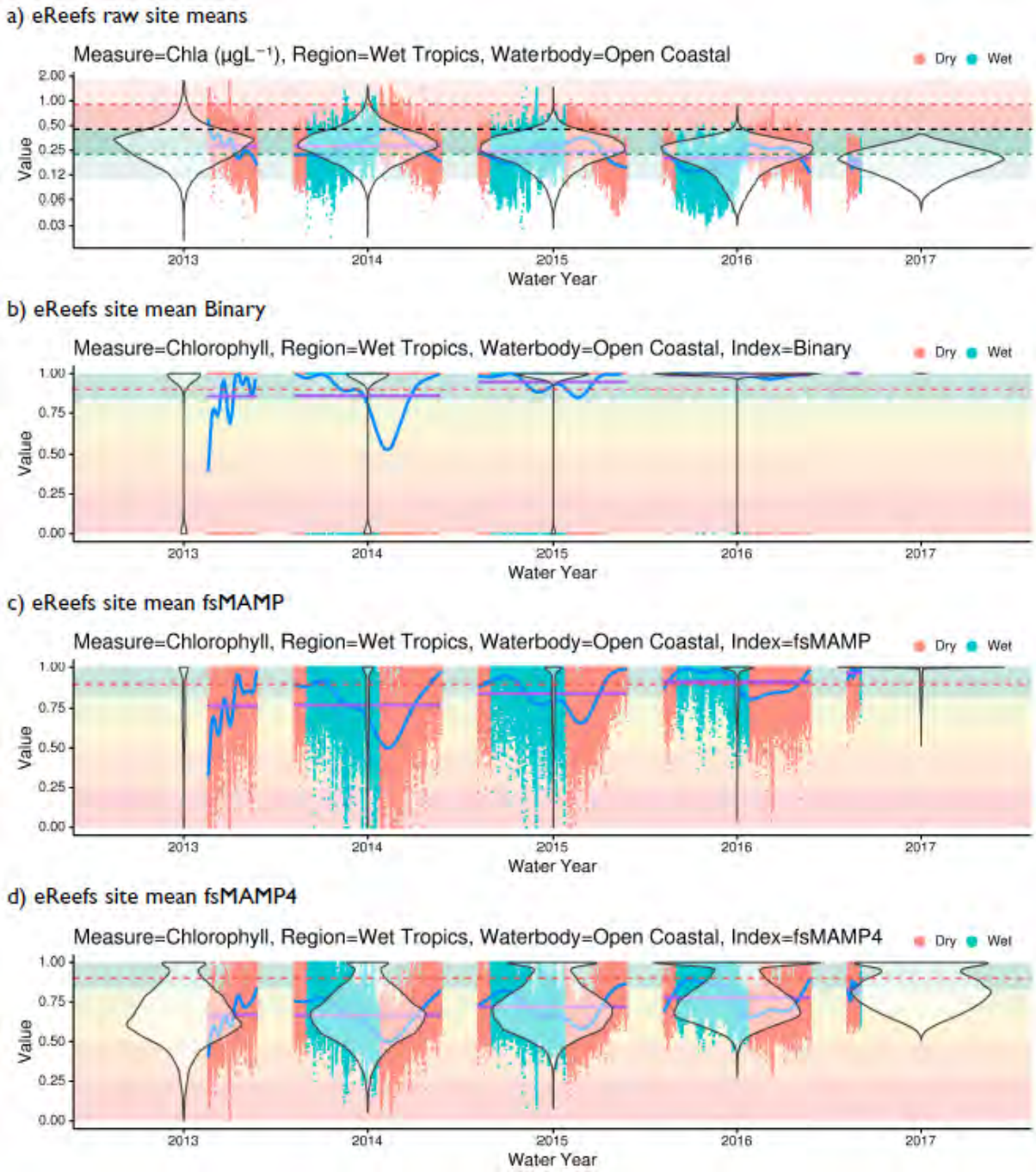


**Figure 40: Temporal distribution of eReefs Chlorophyll-a a) samples and associated b) Binary, c) fsMAMP and d) fsMAMP4 index formulations for the Wet Tropics Open Coastal zone. Red and Blue symbols represent samples collected in Dry and Wet seasons respectively. Green and red shaded banding on a) respectively represent half and twice threshold value (50% shading) and one-forth and four times threshold value (30% shading). Traffic-light banding on b-d) indicates simple 5-level color scheme. Purple lines represent annual means.**

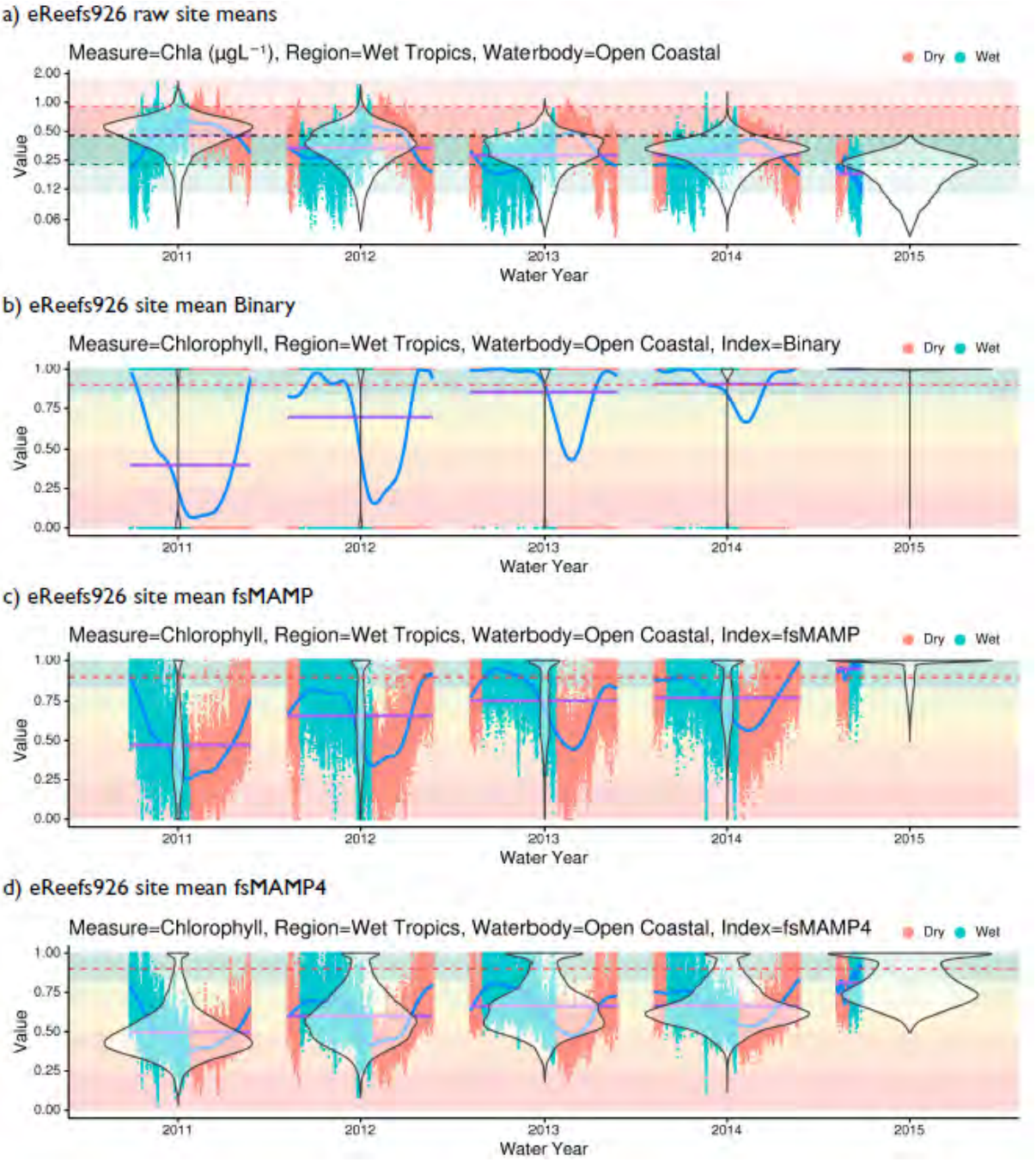


**Figure 41: Temporal distribution of eReefs926 Chlorophyll-a a) samples and associated b) Binary, c) fsMAMP and d) fsMAMP4 index formulations for the Wet Tropics Open Coastal zone. Red and Blue symbols represent samples collected in Dry and Wet seasons respectively. Green and red shaded banding on a) respectively represent half and twice threshold value (50% shading) and one-forth and four times threshold value (30% shading). Traffic-light banding on b-d) indicates simple 5-level color scheme. Purple lines represent annual means.**

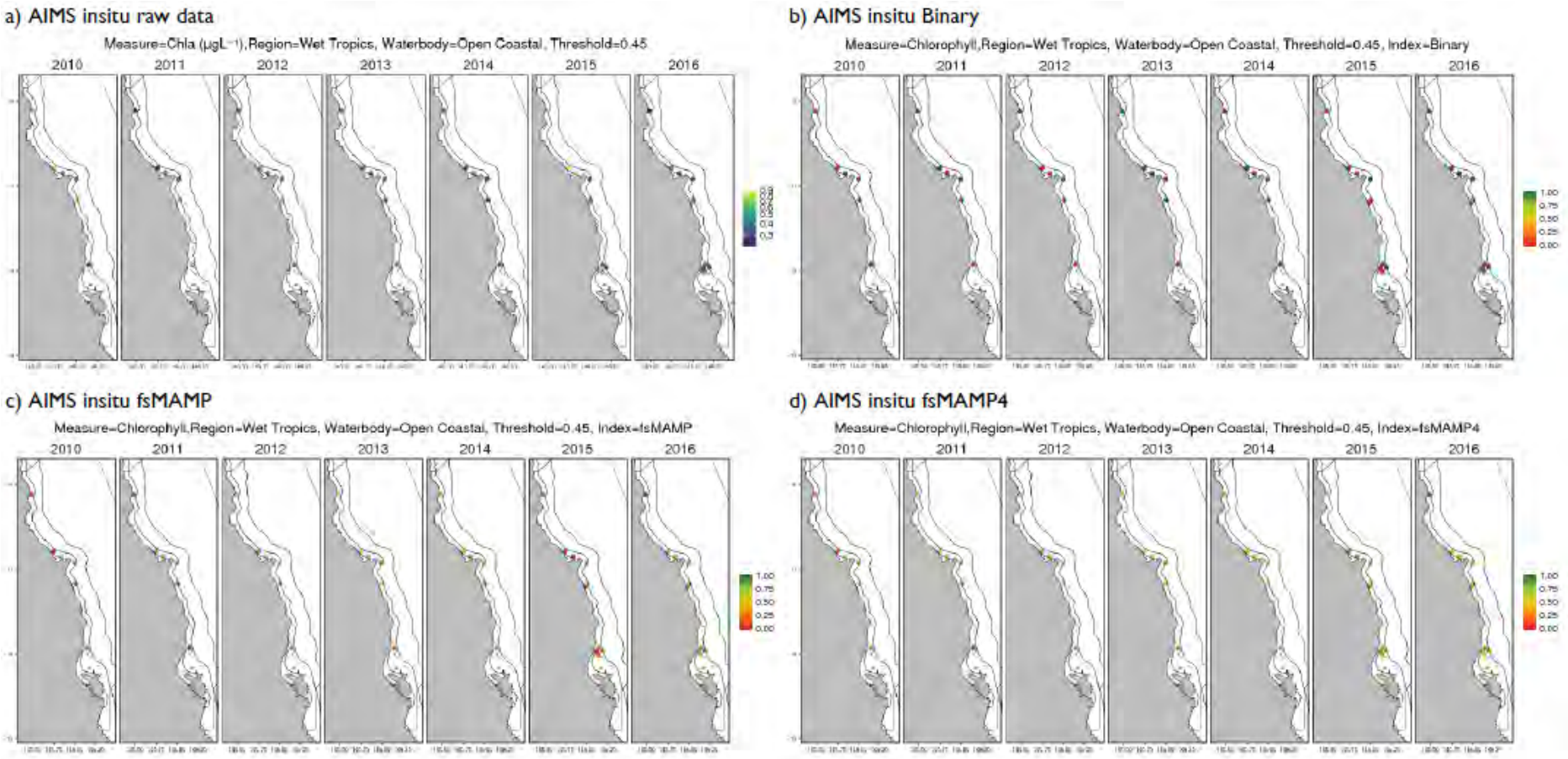


**Figure 42: Spatial distribution of AIMS in situ Chlorophyll-a a) samples and associated b) Binary, c) fsMAMP and d) fsMAMP4 index formulations for the Wet Tropics Open Coastal zone. Color bars scaled to half (green) and twice (red) threshold value for raw data and 1 (green) and 0 (red) for Binary, fsMAMP and fsMAMP4.**

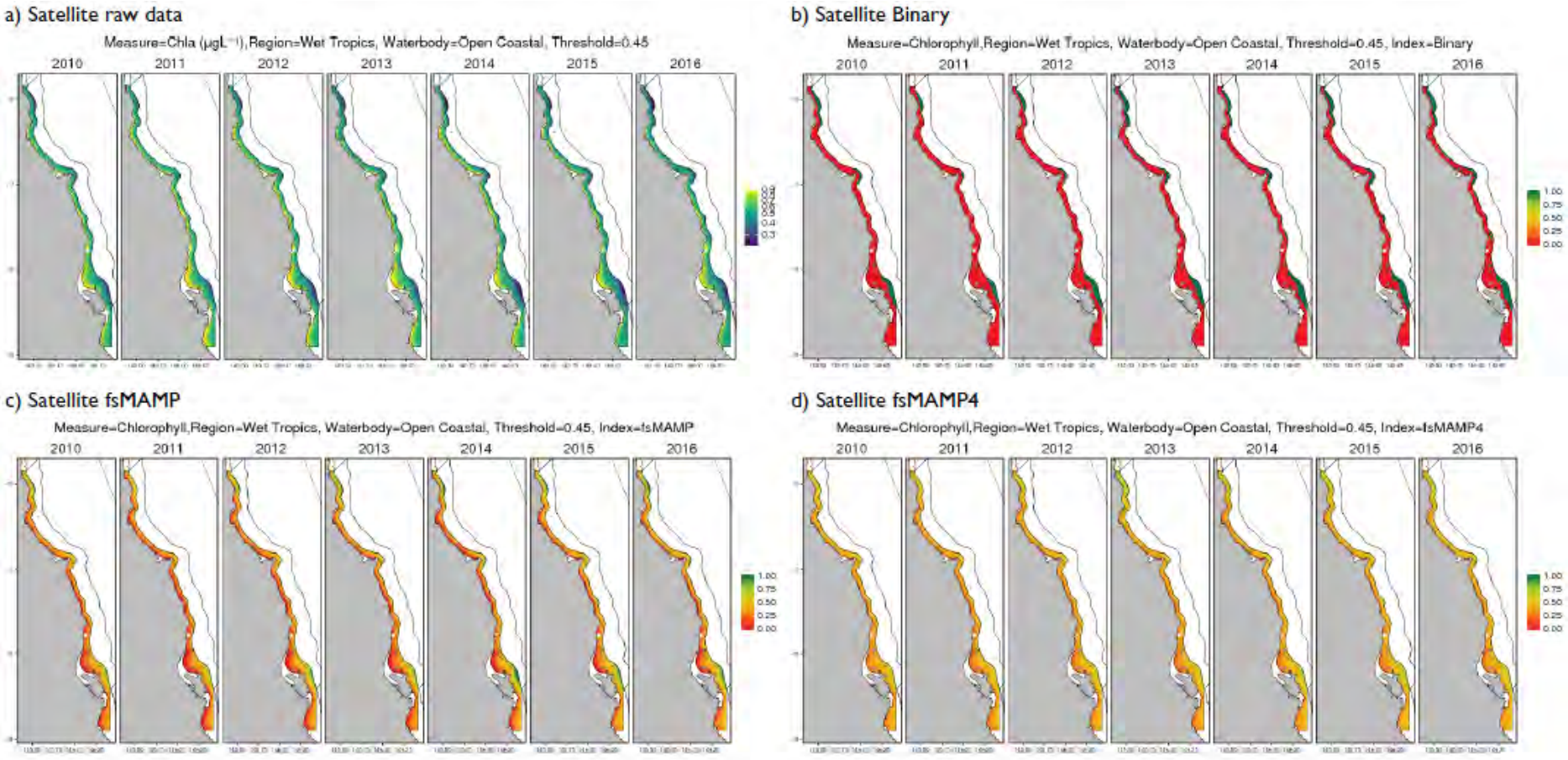


**Figure 43: Spatial distribution of Satellite Chlorophyll-a a) samples and associated b) Binary, c) fsMAMP and d) fsMAMP4 index formulations for the Wet Tropics Open Coastal zone. Color bars scaled to half (green) and twice (red) threshold value for raw data and 1 (green) and 0 (red) for Binary, fsMAMP and fsMAMP4.**

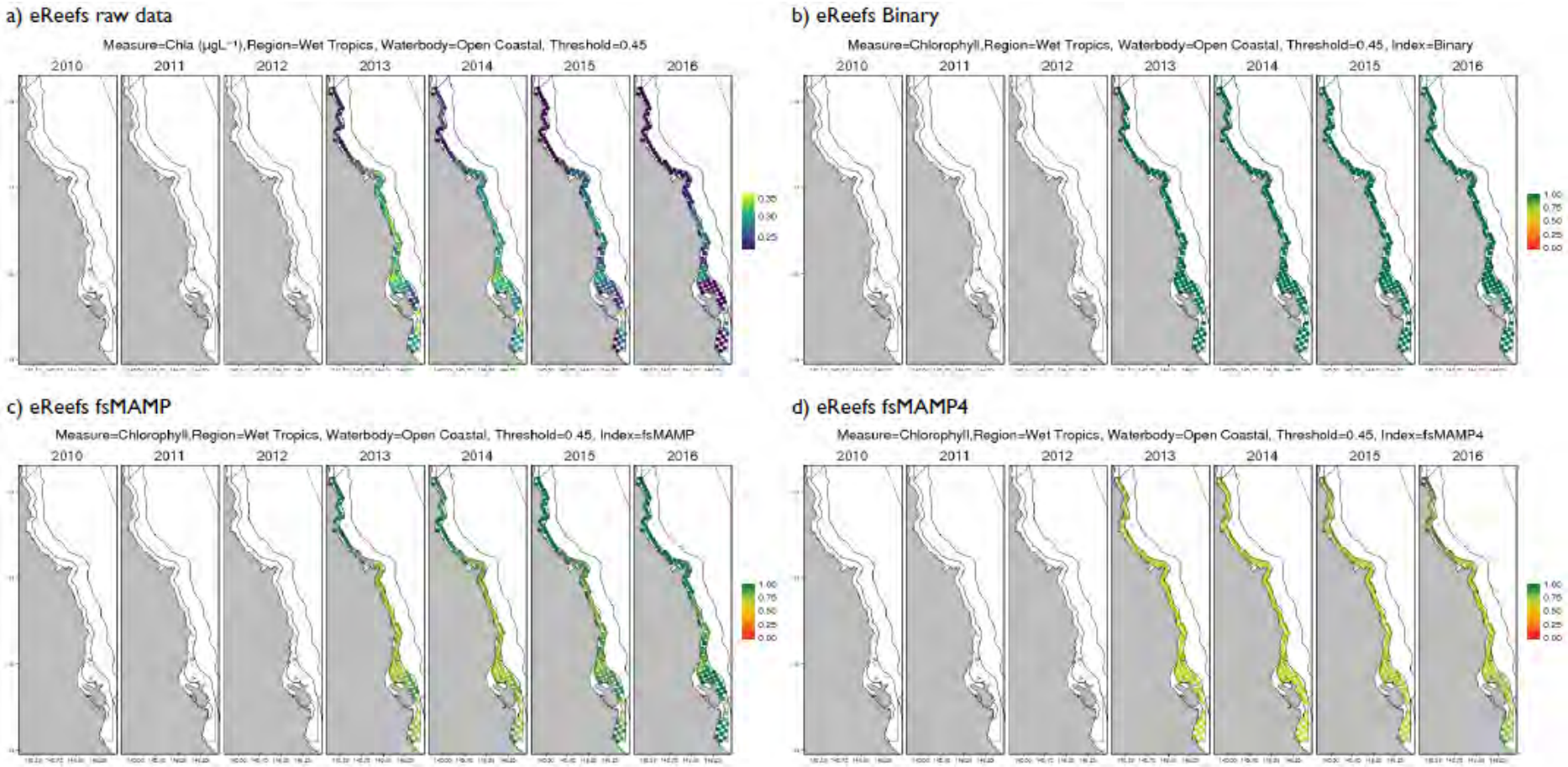


**Figure 44: Spatial distribution of eReefs Chlorophyll-a a) samples and associated b) Binary, c) fsMAMP and d) fsMAMP4 index formulations for the Wet Tropics Open Coastal zone. Color bars scaled to half (green) and twice (red) threshold value for raw data and 1 (green) and 0 (red) for Binary, fsMAMP and fsMAMP4.**

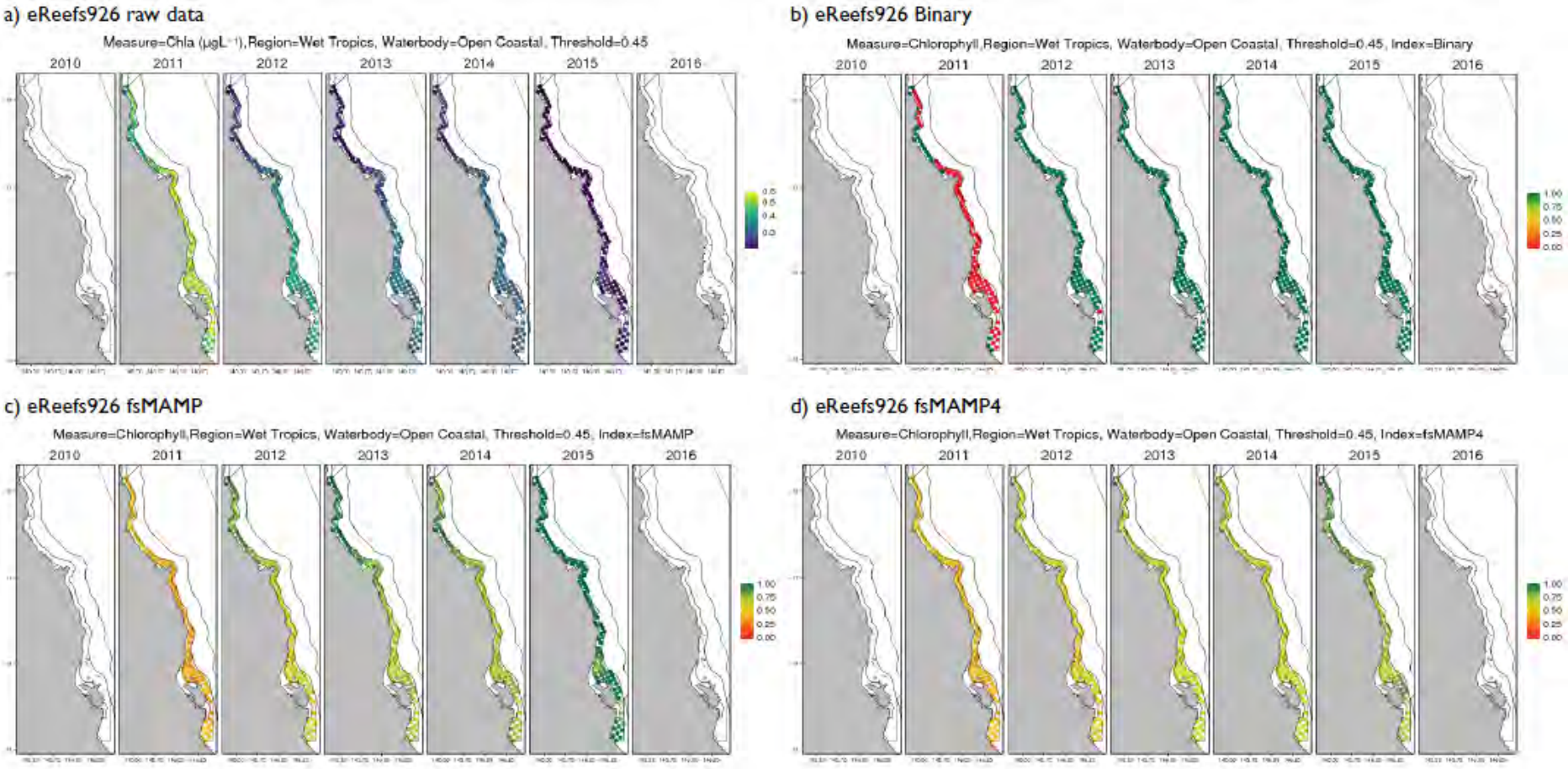


**Figure 45: Spatial distribution of eReefs926 Chlorophyll-a a) samples and associated b) Binary, c) fsMAMP and d) fsMAMP4 index formulations for the Wet Tropics Open Coastal zone. Color bars scaled to half (green) and twice (red) threshold value for raw data and 1 (green) and 0 (red) for Binary, fsMAMP and fsMAMP4.**

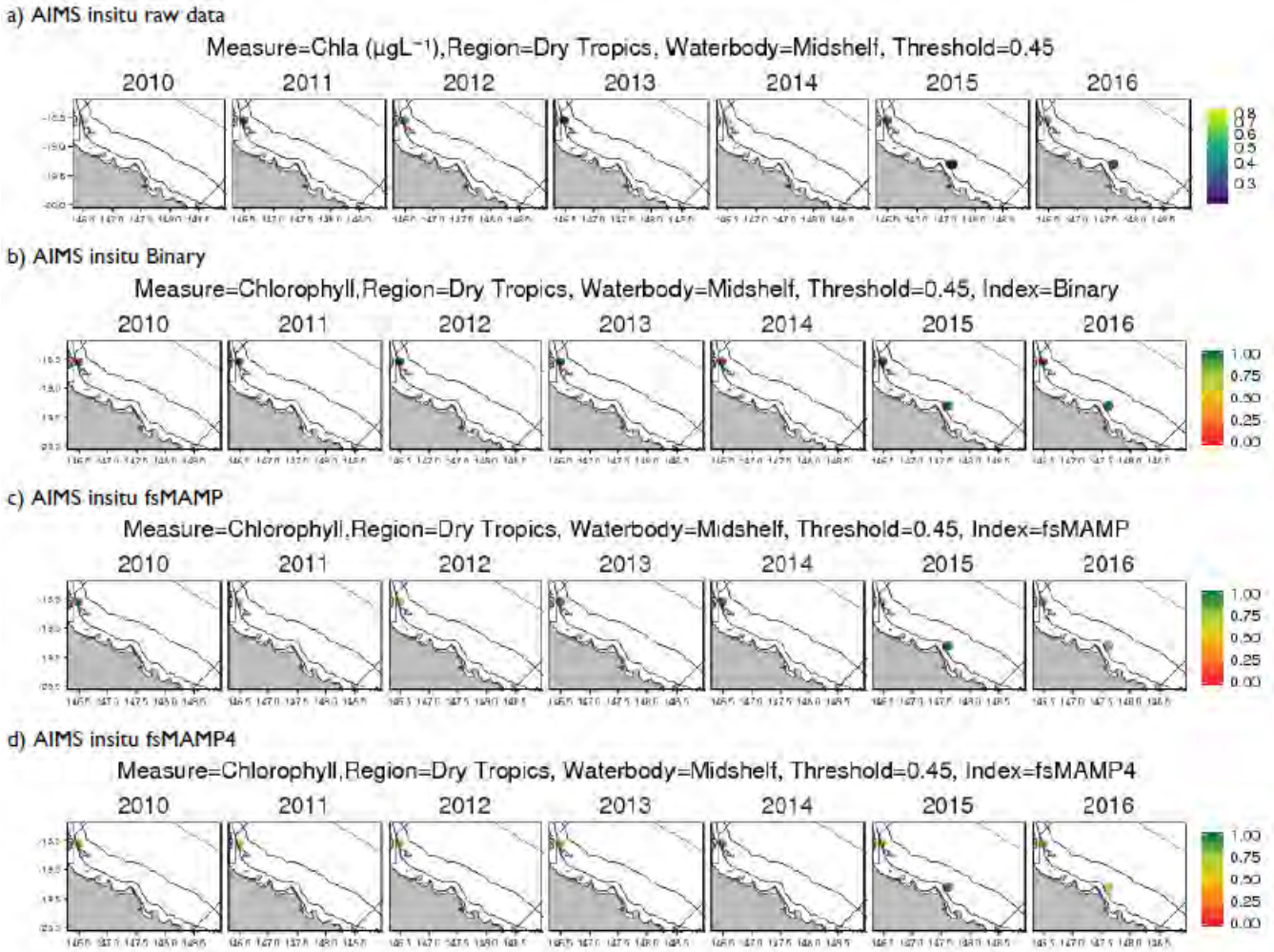


**Figure 46: Spatial distribution of AIMS insitu Chlorophyll-a a) samples and associated b) Binary, c) fsMAMP and d) fsMAMP4 index formulations for the Dry Tropics Midshelf zone. Color bars scaled to half (green) and twice (red) threshold value for raw data and 1 (green) and 0 (red) for Binary, fsMAMP and fsMAMP4.**

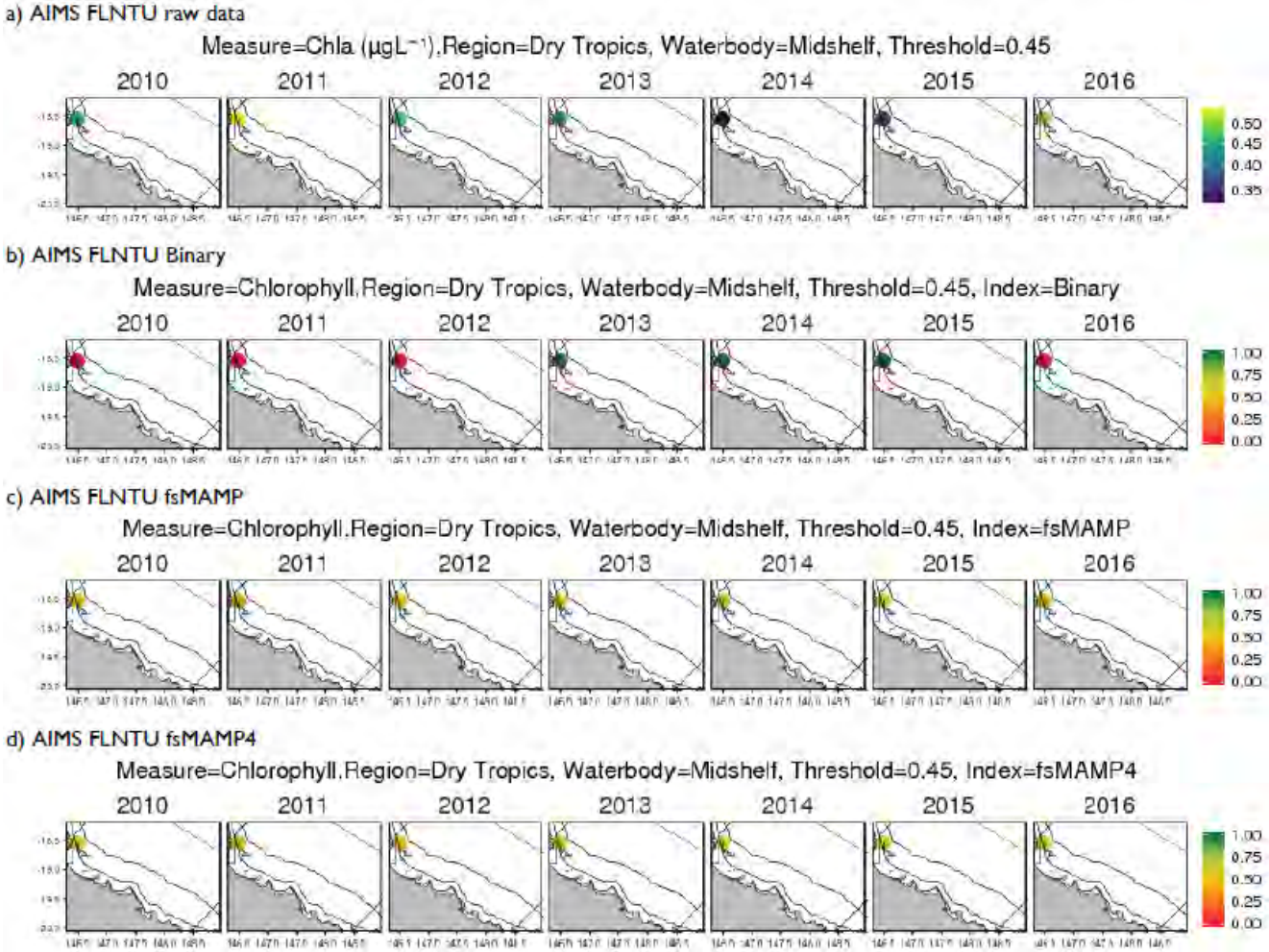


**Figure 47: Spatial distribution of AIMS FLNTU Chlorophyll-a a) samples and associated b) Binary, c) fsMAMP and d) fsMAMP4 index formulations for the Dry Tropics Midshelf zone. Color bars scaled to half (green) and twice (red) threshold value for raw data and 1 (green) and 0 (red) for Binary, fsMAMP and fsMAMP4.**

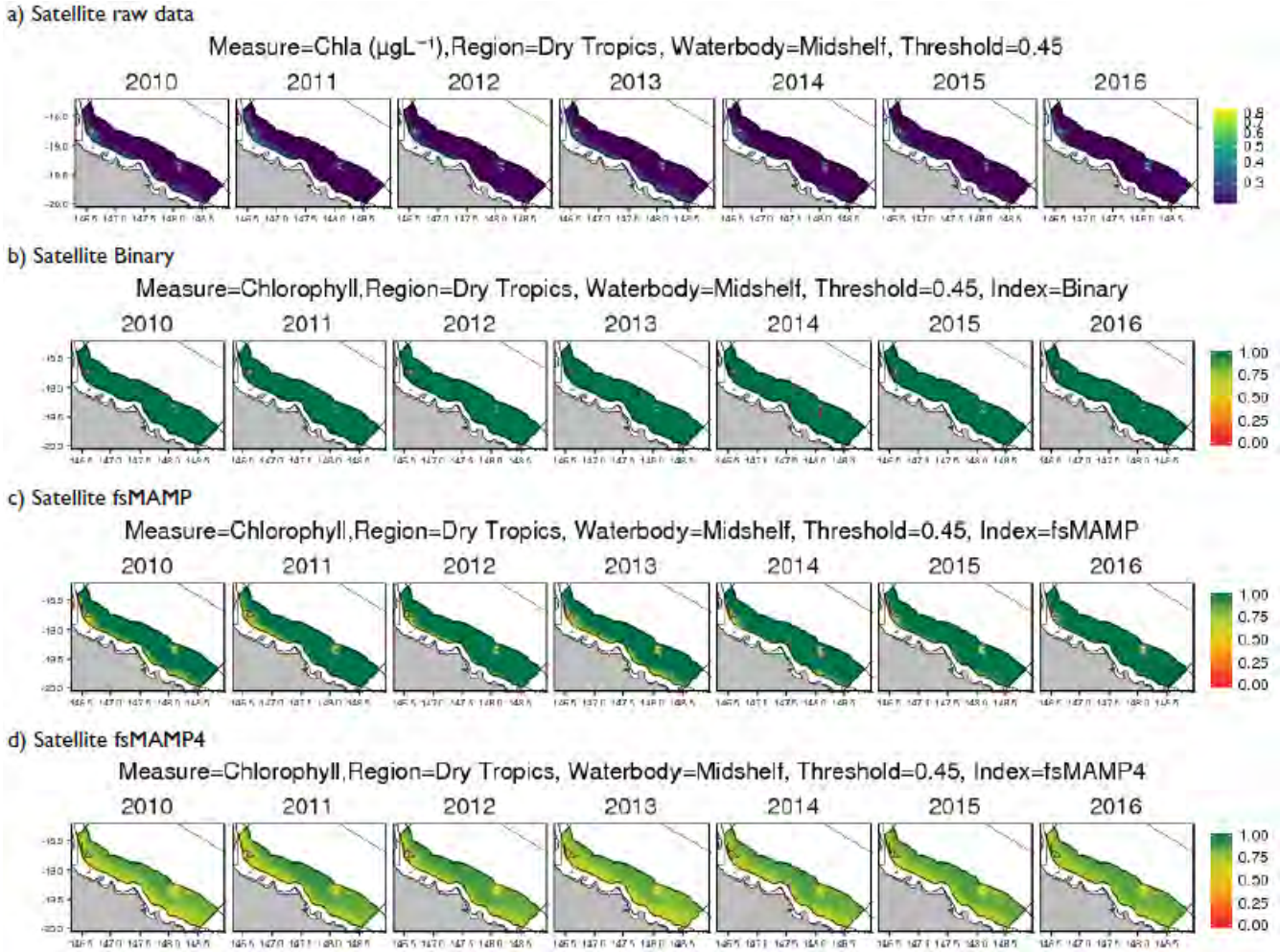


**Figure 48: Spatial distribution of Satellite Chlorophyll-a a) samples and associated b) Binary, c) fsMAMP and d) fsMAMP4 index formulations for the Dry Tropics Midshelf zone. Color bars scaled to half (green) and twice (red) threshold value for raw data and 1 (green) and 0 (red) for Binary, fsMAMP and fsMAMP4.**

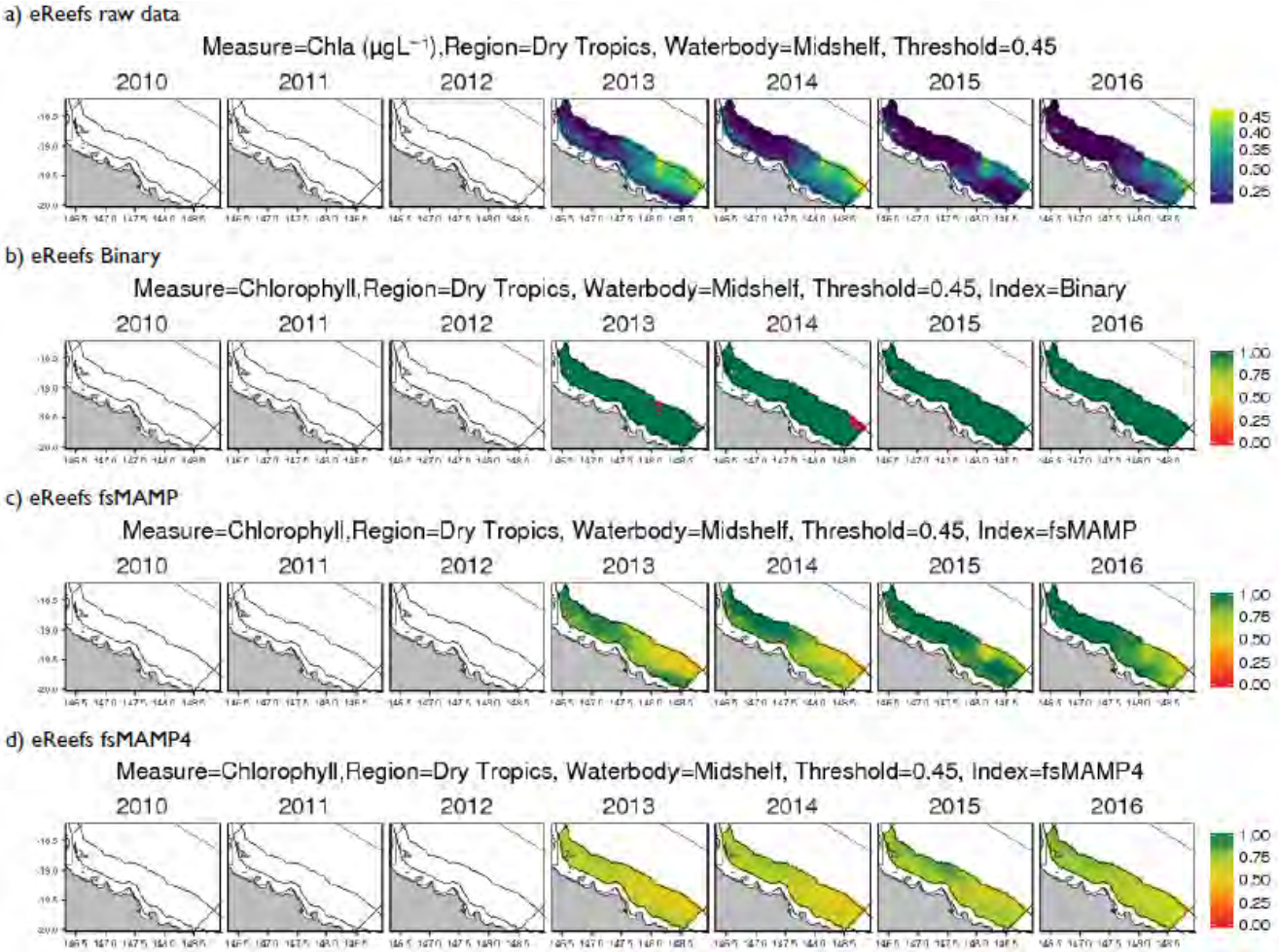


**Figure 49: Spatial distribution of eReefs Chlorophyll-a a) samples and associated b) Binary, c) fsMAMP and d) fsMAMP4 index formulations for the Dry Tropics Midshelf zone. Color bars scaled to half (green) and twice (red) threshold value for raw data and 1 (green) and 0 (red) for Binary, fsMAMP and fsMAMP4.**

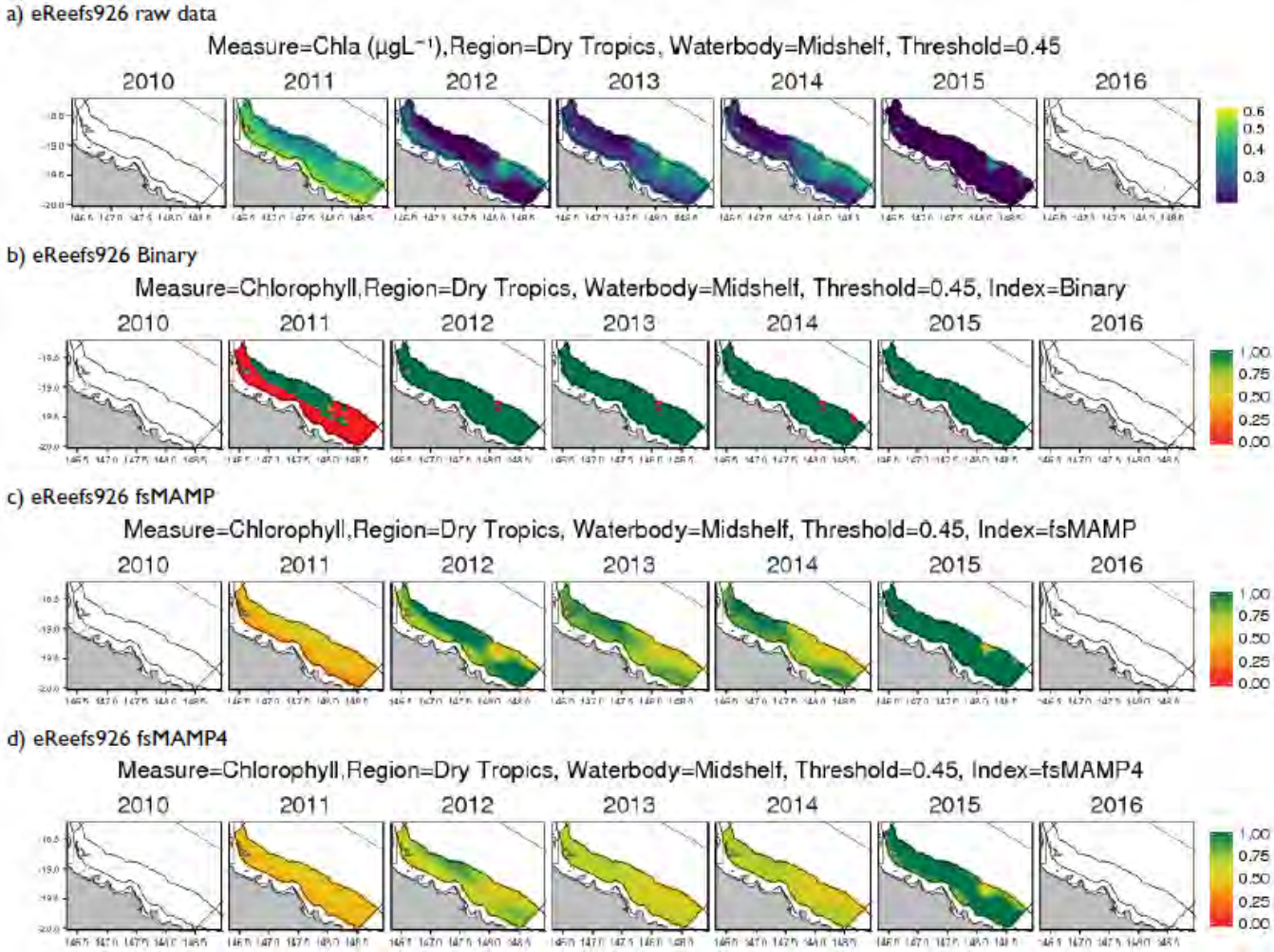


**Figure 50: Spatial distribution of eReefs926 Chlorophyll-a a) samples and associated b) Binary, c) fsMAMP and d) fsMAMP4 index formulations for the Dry Tropics Midshelf zone. Color bars scaled to half (green) and twice (red) threshold value for raw data and 1 (green) and 0 (red) for Binary, fsMAMP and fsMAMP4.**

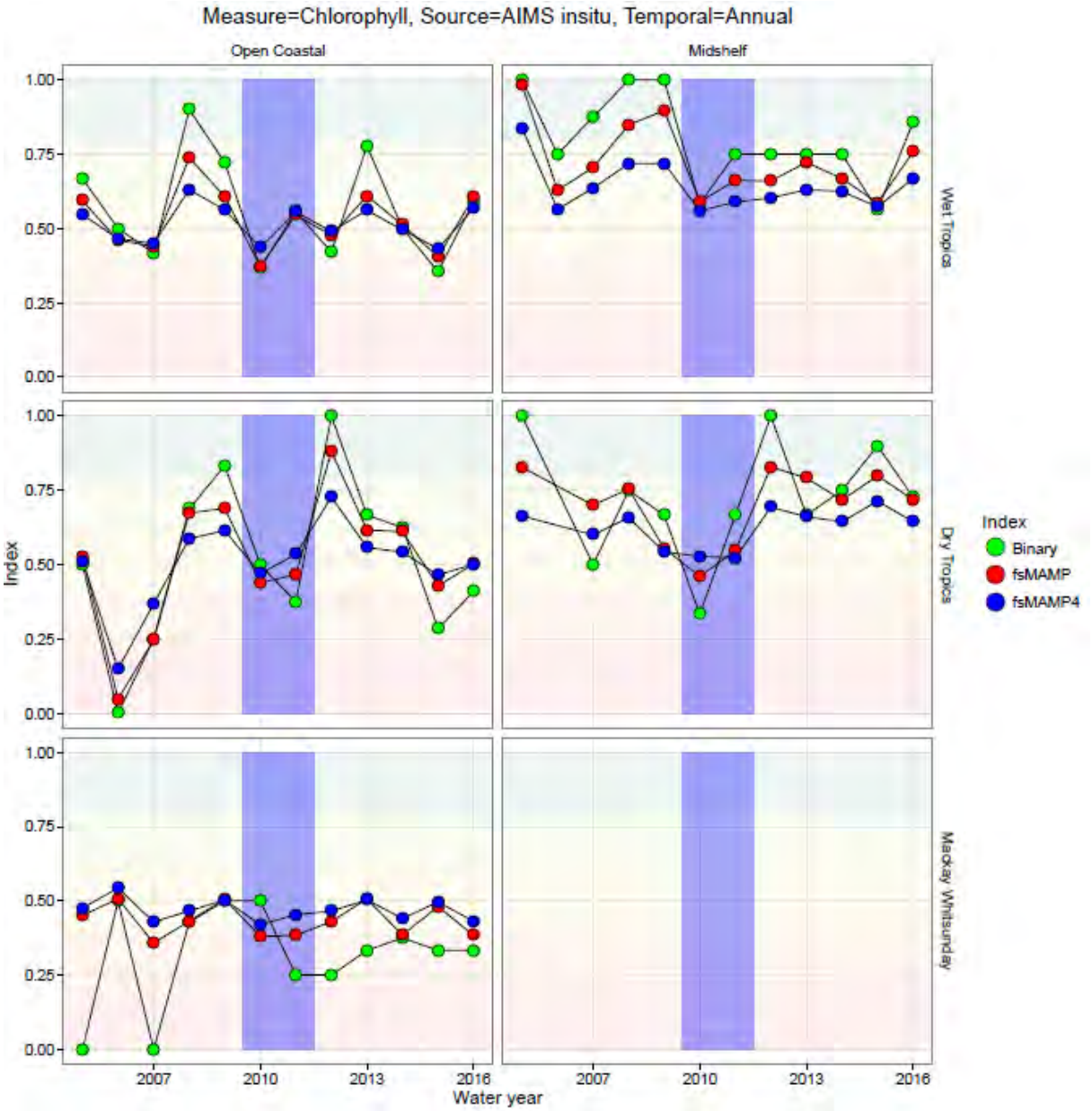


**Figure 51: Time series of annually aggregated Binary, fsMAMP and fsMAMP4 index formulations for AIMS insitu Chlorophyll-a across each of the Regions and Water bodies. The blue vertical bar spans from mid 2009 to mid 2011.**

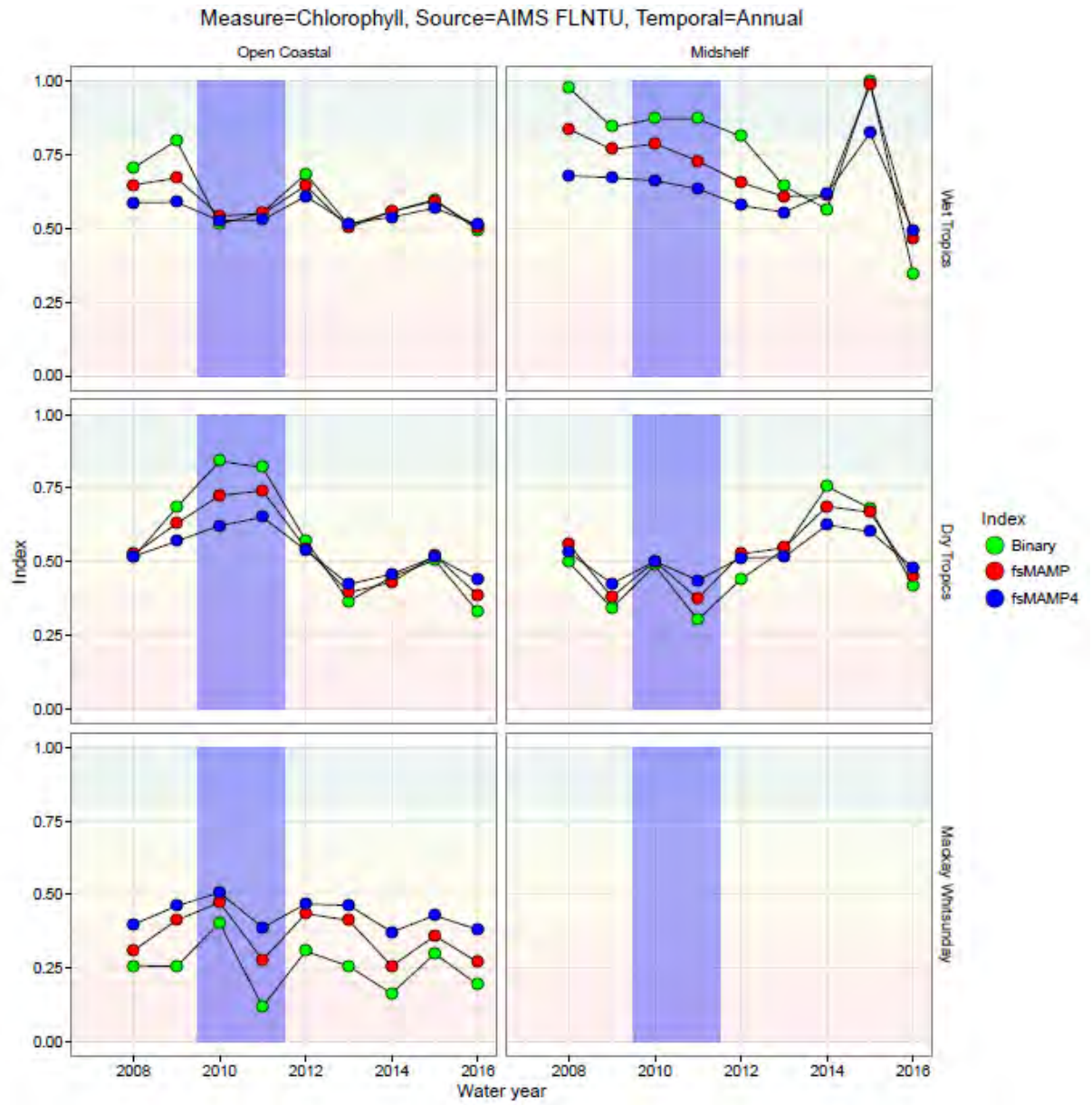


**Figure 52: Time series of annually aggregated Binary, fsMAMP and fsMAMP4 index formulations for AIMS FLNTU Chlorophyll-a across each of the Regions and Water bodies. The blue vertical bar spans from mid 2009 to mid 2011.**

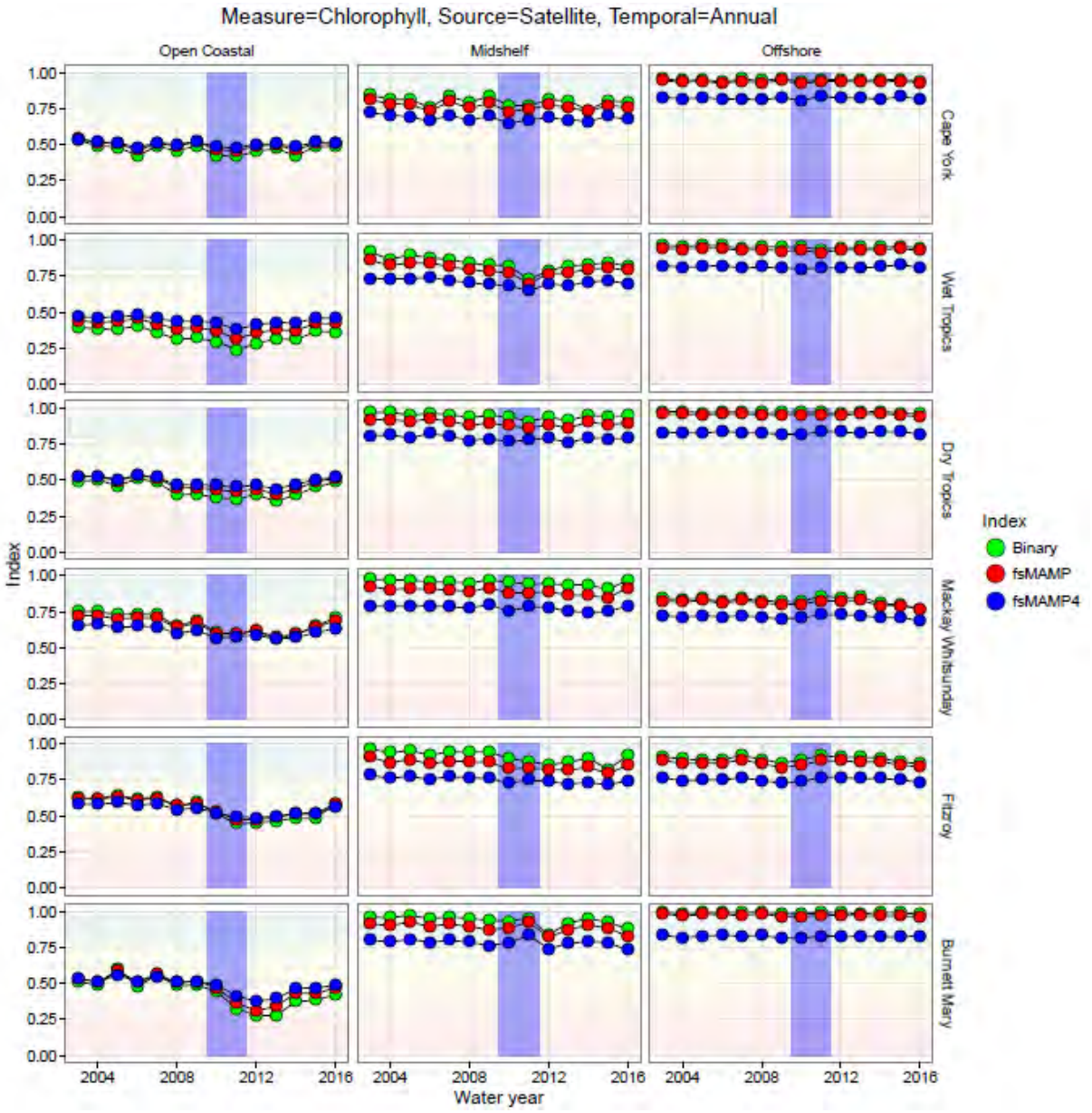


**Figure 53: Time series of annually aggregated Binary, fsMAMP and fsMAMP4 index formulations for Satellite Chlorophyll-a across each of the Regions and Water bodies. The blue vertical bar spans from mid 2009 to mid 2011.**

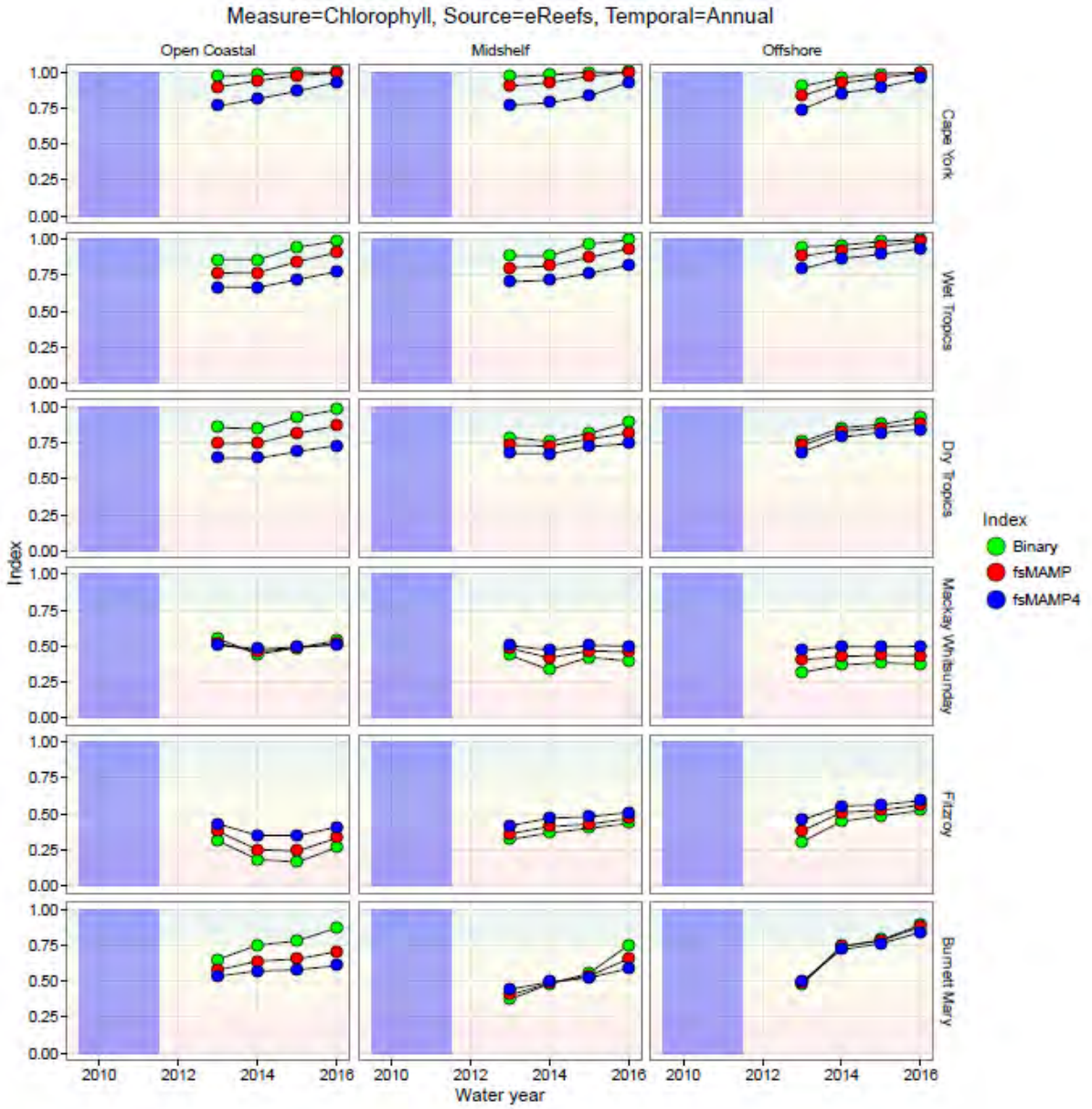


**Figure 54: Time series of annually aggregated Binary, fsMAMP and fsMAMP4 index formulations for eReefs Chlorophyll-a across each of the Regions and Water bodies. The blue vertical bar spans from mid 2009 to mid 2011.**

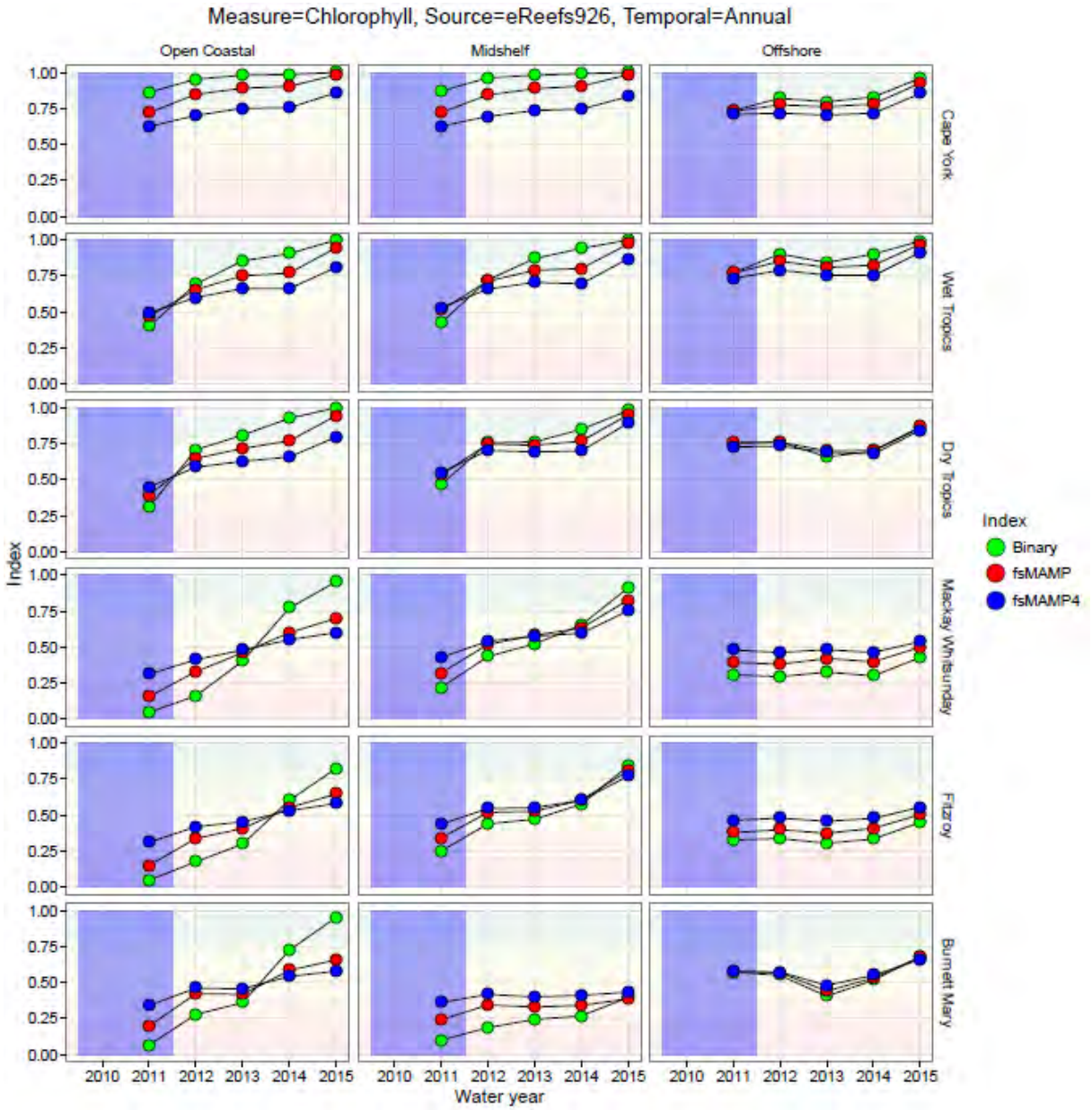


**Figure 55: Time series of annually aggregated Binary, fsMAMP and fsMAMP4 index formulations for eReefs926 Chlorophyll-a across each of the Regions and Water bodies. The blue vertical bar spans from mid 2009 to mid 2011.**

### *3.3.2 Sources*

Typically, the major aspects of a property like water quality are not directly measurable. Properties such as productivity, water clarity, nutrients, pesticides etc encapsulate a set of underlying conditions and yet themselves are not directly measurable. Directly measurable properties (such as Chlorophyll-a, total suspended solids etc) thus act as proxies for the broader properties. As directly measurable entities, many of these measures have long monitoring histories and there is at least some understanding of the ecological role of these measures.

A major advantage of remote sensing and modelling products in the context of environmental monitoring is that they provide substantially greater spatial and temporal coverage. However, the majority of the parameters yielded from these tools are algorithmic approximations of

traditional measures. Consequently, in the context of water quality, they produce proxies of proxies.

The current project has access to a variety of sources of water quality monitoring data (see Section 2) ranging from sparse, yet rigorous direct in situ measurements (AIMS insitu) and temporally rich, spatially sparse AIMS FLNTU logger data through to spatio-temporally extensive, yet patchy Satellite data and spatio-temporally extensive eReefs modelled data, with or without assimilation of remotely sensed surface reflectance. These different sources of data are likely to provide estimates of the parameters that differ in both statistical location (such as mean) as well as scale (variability).

Whilst it is beyond the scope of the current project to undertake a full evaluation of the accuracy, robustness and reliability of each of these sources, the indexed data allow us to explore and compare the spatio-temporal patterns of each data source. In particular, we can focus on sensitivity as suggested by variability in spatio-temporal patterns of indices of each data source and whether these patterns are consistent with expert expectations.

It is reasonable to expect that since the AIMS insitu data are the most direct measures, they would be the most accurate of all the sources, however it is also likely that these observations only represent conditions over a very restricted space and time. They are predominantly the limited spatial coverage of the AIMS insitu data that limits its utility as input into a water quality metric for the entire Great Barrier Reef.

A motivating inspiration for this project was the perceived lack of sensitivity of the water quality metric when based solely on the Satellite data source. It was hoped that the introduction of eReefs modelled data would result in a metric that yields patterns that are more consistent with expectations based on historical observations, empirical evidence and experience in the field.

Figures 56 – 59 contrast the broad spatial and temporal patterns in aggregated fsMAMP Chlorophyll-a, TSS, Secchi depth and NOx indices. Within a zone (Region/Water body), the Satellite data (Remote sensing) are substantially less varied than the other sources. Obvious deviations in trajectory are only really apparent for the Open Coastal areas (although not for Cape York). Moreover, while the Satellite indices are suggestive of a cross-shelf (West to East) increase in water quality, this mainly occurs between Open Coastal and Midshelf and there is little (if any) consistent South-North water quality increase.

The AIMS insitu data result in the most sensitive metrics. However, the temporal deviances in data (and thus indices) could be exaggerated by the proximal location of AIMS insitu sites relative to sources of major river discharge. Thus, this sensitivity could be artificially inflated and is unlikely to be unrepresentative. In particular, these absolute state and temporal trends in these data are likely to be mainly representative of water conditions close to major sources of discharge. Moreover, the AIMS insitu data are restricted to just a subset (5/18) of the zones of interest.

Surprisingly, there is relatively little correspondence in trajectories between AIMS insitu and AIMS FLNTU logger data. These differences could be due either to differences in sampling designs (AIMS insitu have additional sites and thus represent a different spatial domains, AIMS

FLNTU have substantially greater temporal coverage and thus are potentially more representative over time) and could also reflect direct (AIMS insitu) vs indirect (AIMS FLNTU) nature of the measurements. Either way, it is not recommended to use either of these sources as a primary data source on which to construct GBR wide Water Quality metrics.

The broad spatial pattern of both eReefs and eReefs926 appear to follow the overall expectations of South - North and West - East gradients[13], with Chlorophyll-a typically increasing from S to N and W to E - more so for eReefs926 than eReefs. Unfortunately it is difficult to assess the sensitivity of temporal patterns in eReefs and eReefs926 data sources due to their relatively short availability windows. In particular, it is inconvenient that neither eReefs source extend back to the 2010–2011 wet years to provide some form of qualitative calibration.

The data assimilation of remotely sensed surface reflectance into the eReefs model has resulted in some relatively large changes for each of Chlorophyll-a, Secchi depth and NOx and evaluating the causes of these differences is beyond the scope of the current study.

[13] less obvious for TSS and NOx

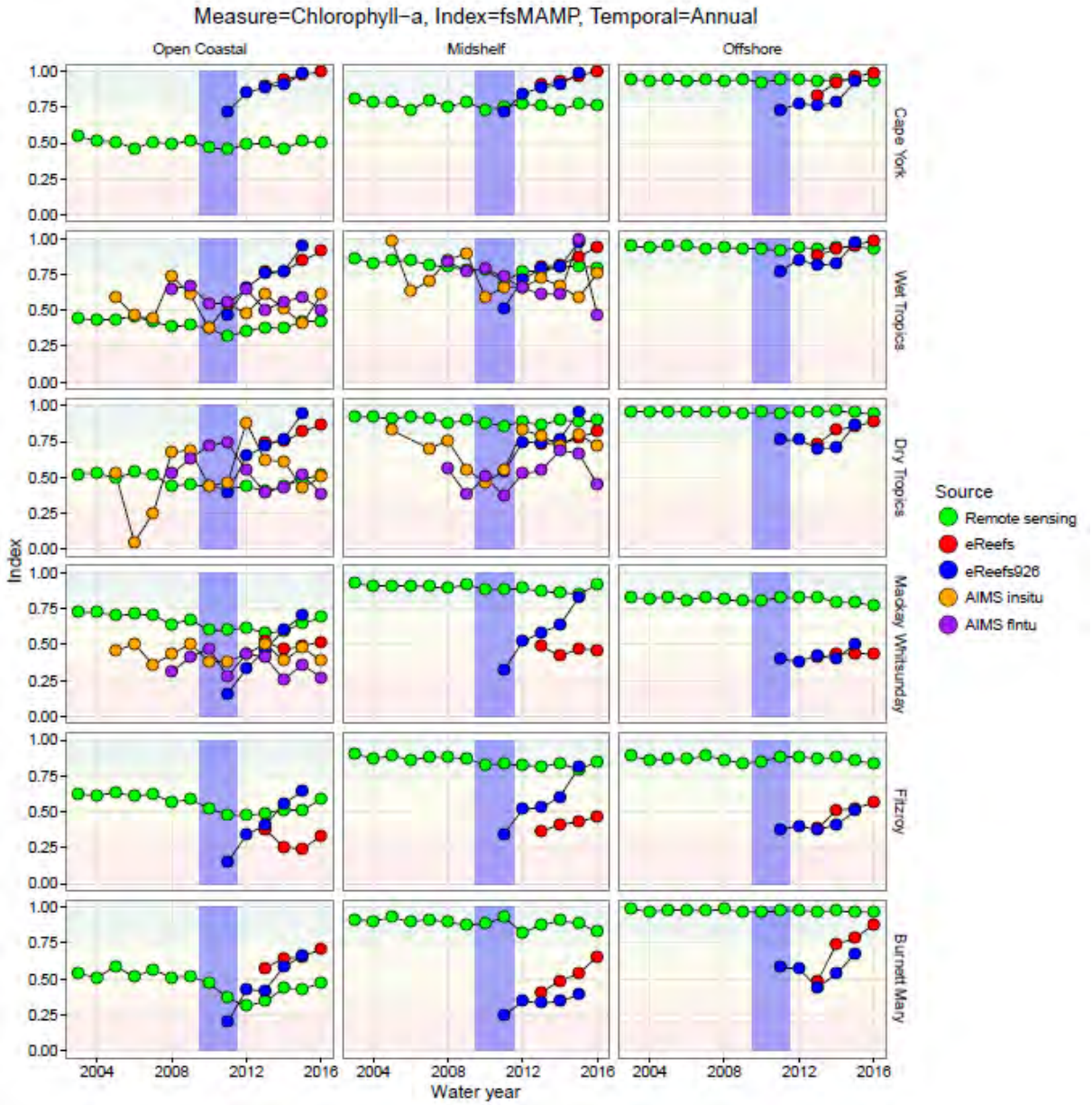


**Figure 56: Time series of fsMAMP Chlorophyll-a index scores by zone for each data source. The blue vertical bar spans from mid 2009 to mid 2011.**

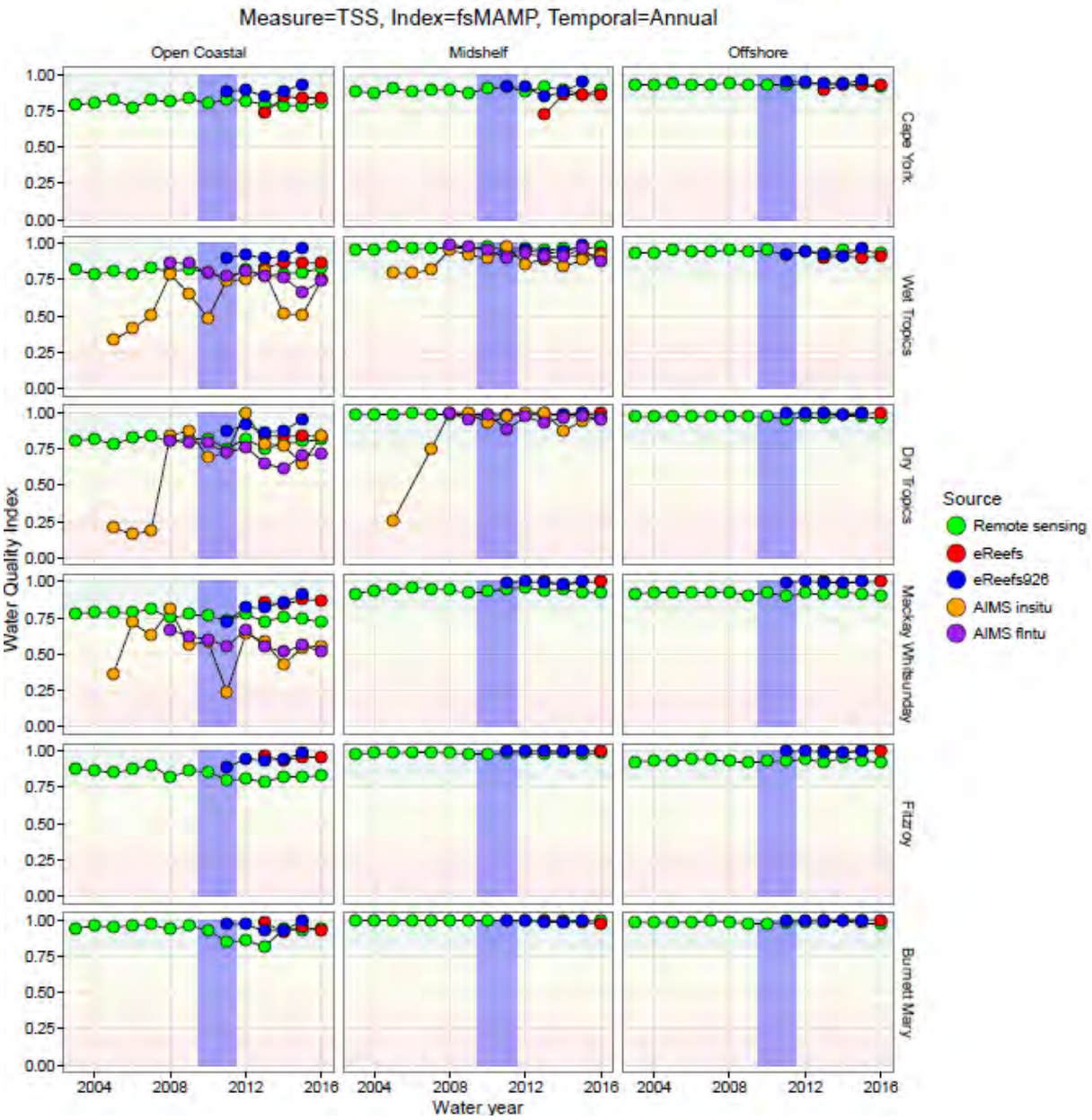


**Figure 57: Time series of fsMAMP TSS index scores by zone for each data source. The blue vertical bar spans from mid 2009 to mid 2011.**

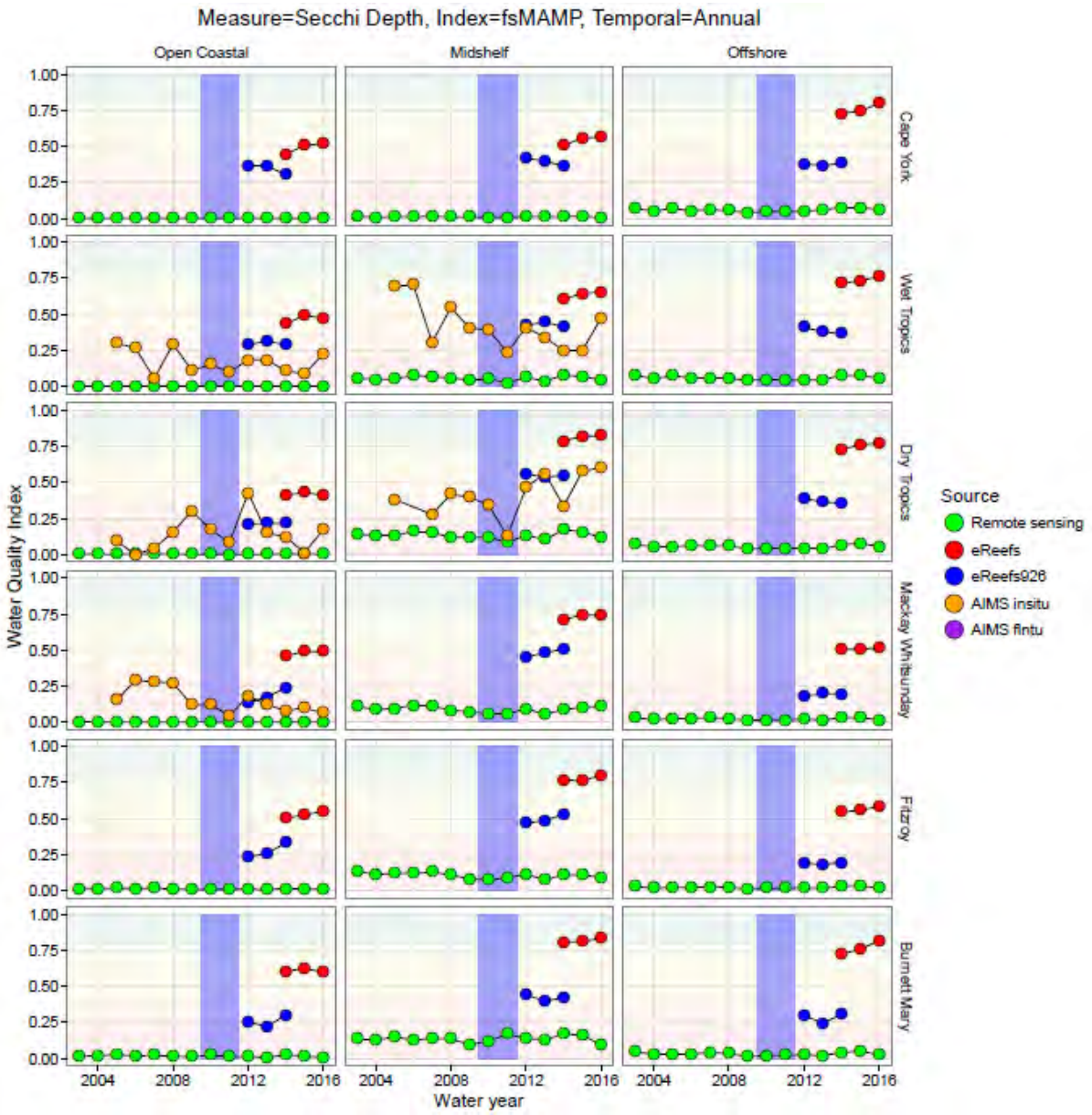


**Figure 58: Time series of fsMAMP Secchi depth index scores by zone for each data source. The blue vertical bar spans from mid 2009 to mid 2011.**

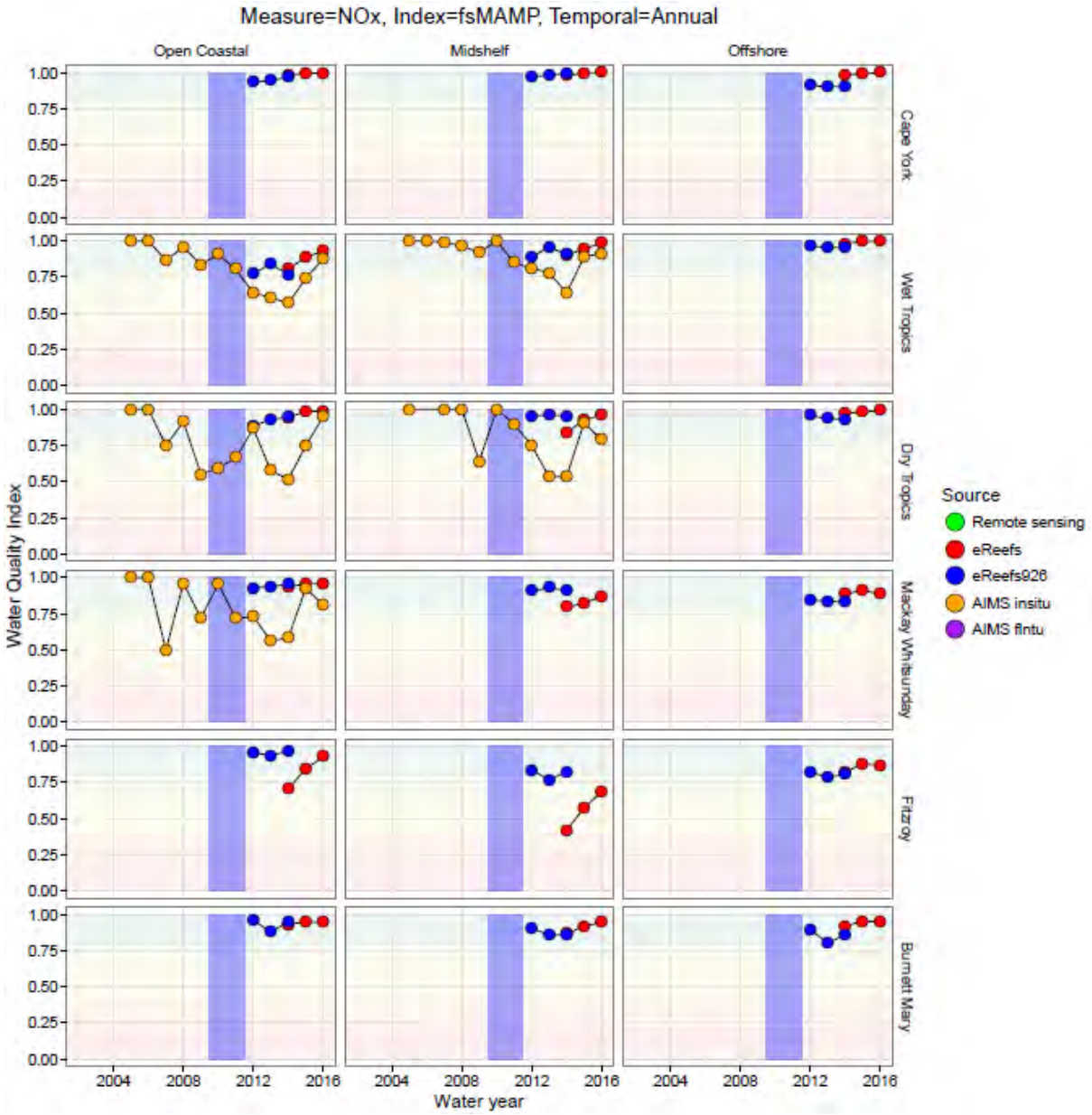


**Figure 59: Time series of fsMAMP NOx index scores by zone for each data source. The blue vertical bar spans from mid 2009 to mid 2011.**

### *3.3.3 Exploration of measures*

A Water Quality Index should attempt to reflect multiple properties of the underlying water bodies. For example, Water Quality could be characterized by combinations of Productivity, Water clarity, Nutrients, Toxicants etc. In turn, each of the above Sub-indicators, can be characterized by actual measureable properties (such as Chlorophyll-a, Total Suspended Solids, Total Nitrogen etc).

Typically, a Water Quality index is limited to what measureable properties are available and have appropriate guidelines (thresholds). The spatial extent of the current application of Water Quality metrics limits the Measures to Chlorophyll-a, Total Suspended Solids, Secchi Depth and NOx (Nitrite + Nitrate). Temporal series of the individual Measures for each Zone (based on fsMAMP of eReefs data) are presented in Figure 60.

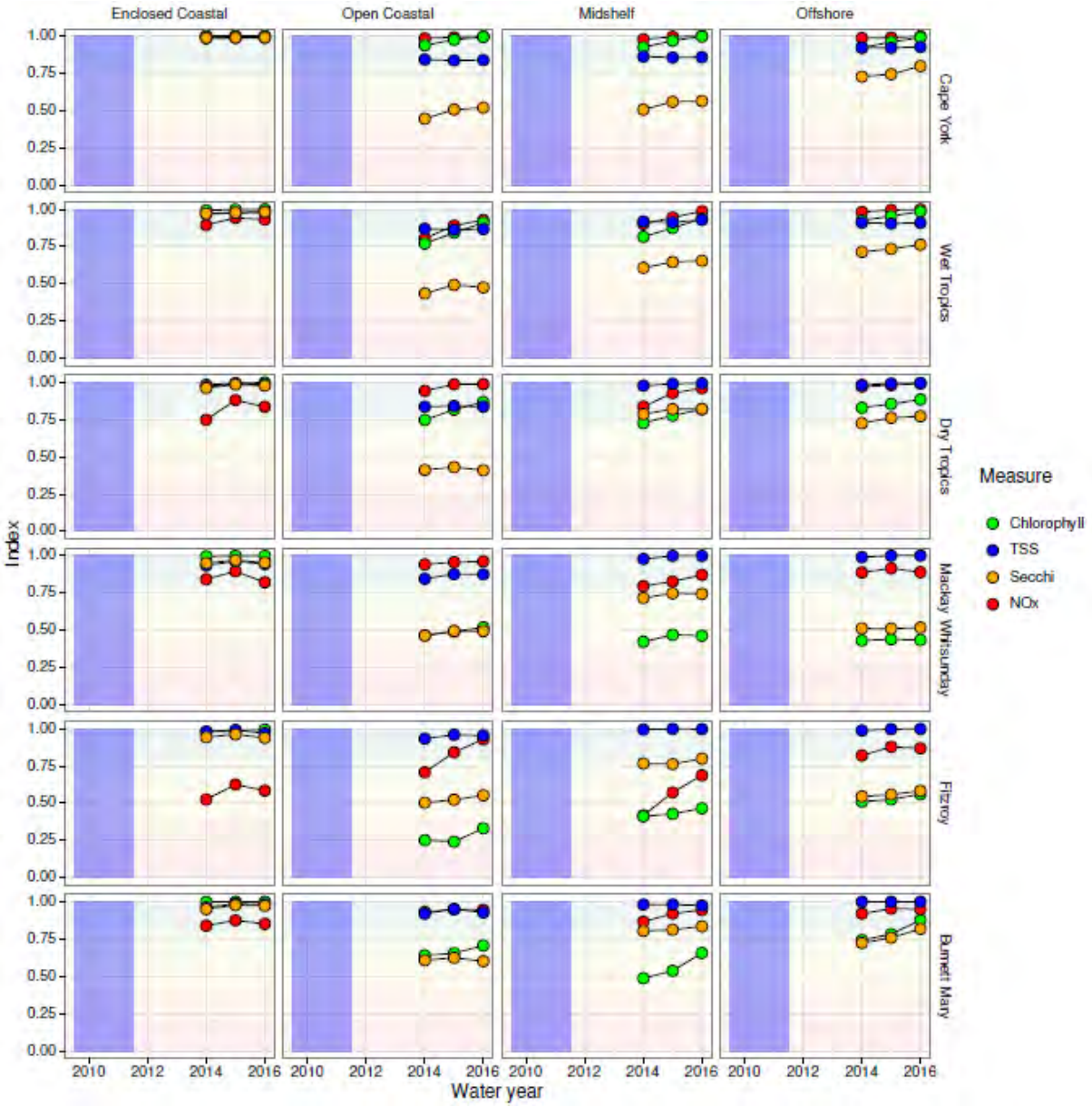


**Figure 60: Time series of eReefs fsMAMP index scores by zone. The blue vertical bar spans from mid 2009 to mid 2011.**

These four Measures can be placed in an aggregation hierarchy such as depicted in Table 16.

**Table 15: Hierarchical association between Measures, Sub-indicators and Indicators.**

| Measure | Sub-indicator | Indicator |
|---|---|---|
| Chlorophyll-a | Productivity | Water Quality |
| Total Suspended Solids | Water Clarity | Water Quality |
| Secchi Depth | Water Clarity | Water Quality |
| NOx | Nutrients | Water Quality |

Nevertheless, the reliability and utility of each of these Measures are not necessarily equal. A number of candidate Measure combinations[14] are considered (see below). The contributions of each Measure to the corresponding Water Quality Indicator Scores (based on the hierarchy presented in Table 16) are:

- Chlorophyll-a (1/3), TSS (1/2 _ 1/3 = 1/6), SD (1/2 _ 1/3 = 1/6) and NOx (1/3)
- Chlorophyll-a (1/2), TSS (1/2 _ 1/2 = 1/4), SD (1/2 _ 1/2 = 1/4)
- Chlorophyll-a (1/2), SD (1/2)
- Chlorophyll-a (1/2), TSS (1/2)

For each candidate, eReefs data with fsMAMP formulations are presented (see Figure 61). Water Quality Indicator Scores based on candidate combinations that include either all of Chl, TSS, SD and NOx or just Chl and TSS are considered very similar. Generally, Water Quality Indicator Scores are substantially lowered by the inclusion of Secchi Depth, the severity of which depends on the degree of dilution by other Measures.

Questions have been raised about the reliability and accuracy of the Satellite TSS (non-algal particles) as well as the eReefs TSS and NOx data or else their suitability as good indicators. In particularly, eReefs TSS in Midshelf and Offshore is consistently well below the associated threshold values - so much so that the indices are virtually invariant over space and time.

[14] These effectively act as weights

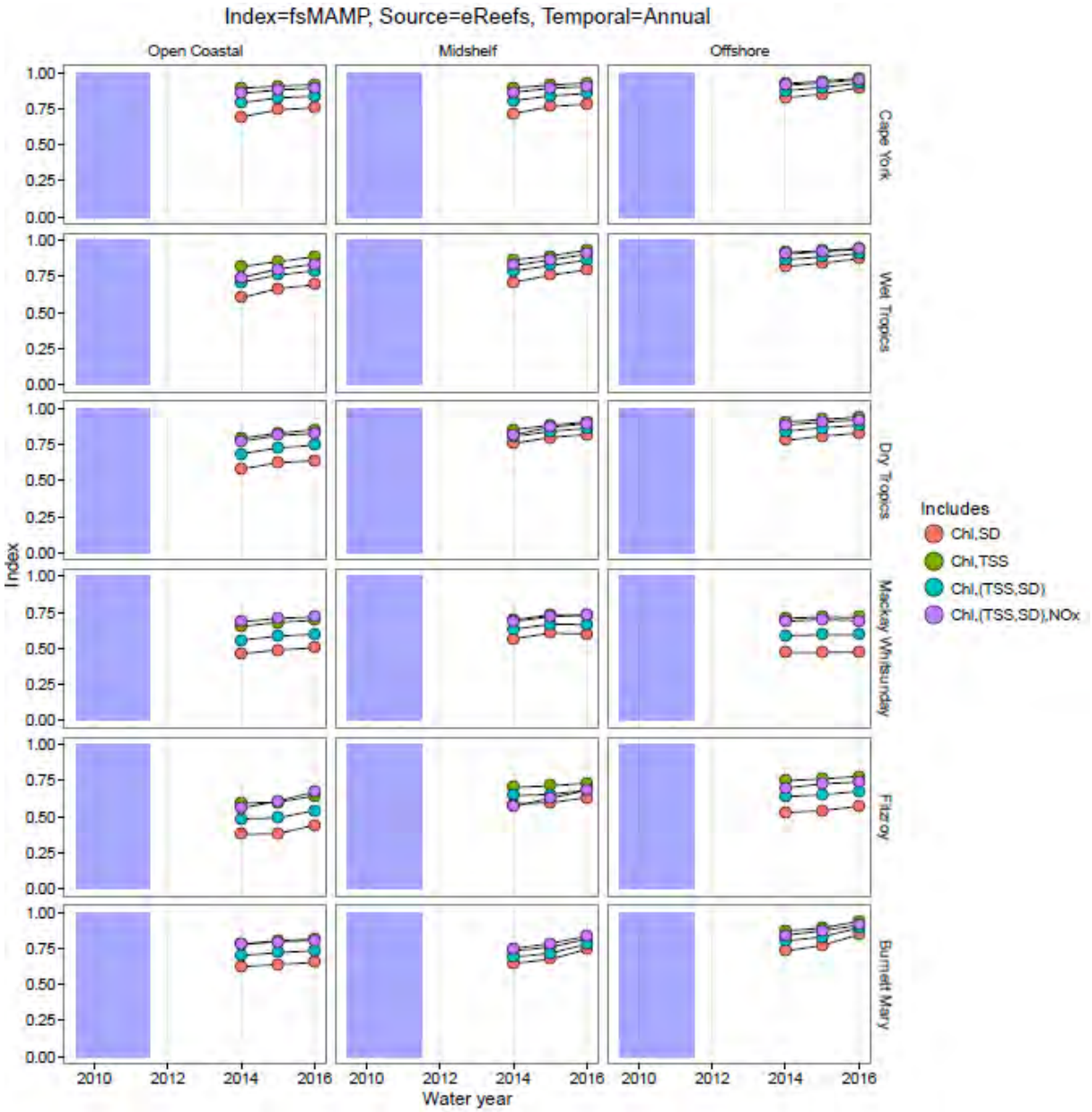


**Figure 61: Time series of eReefs fsMAMP Measure Index Scores by zone. The blue vertical bar spans from mid 2009 to mid 2011.**

### *3.3.4 Measures/Site*

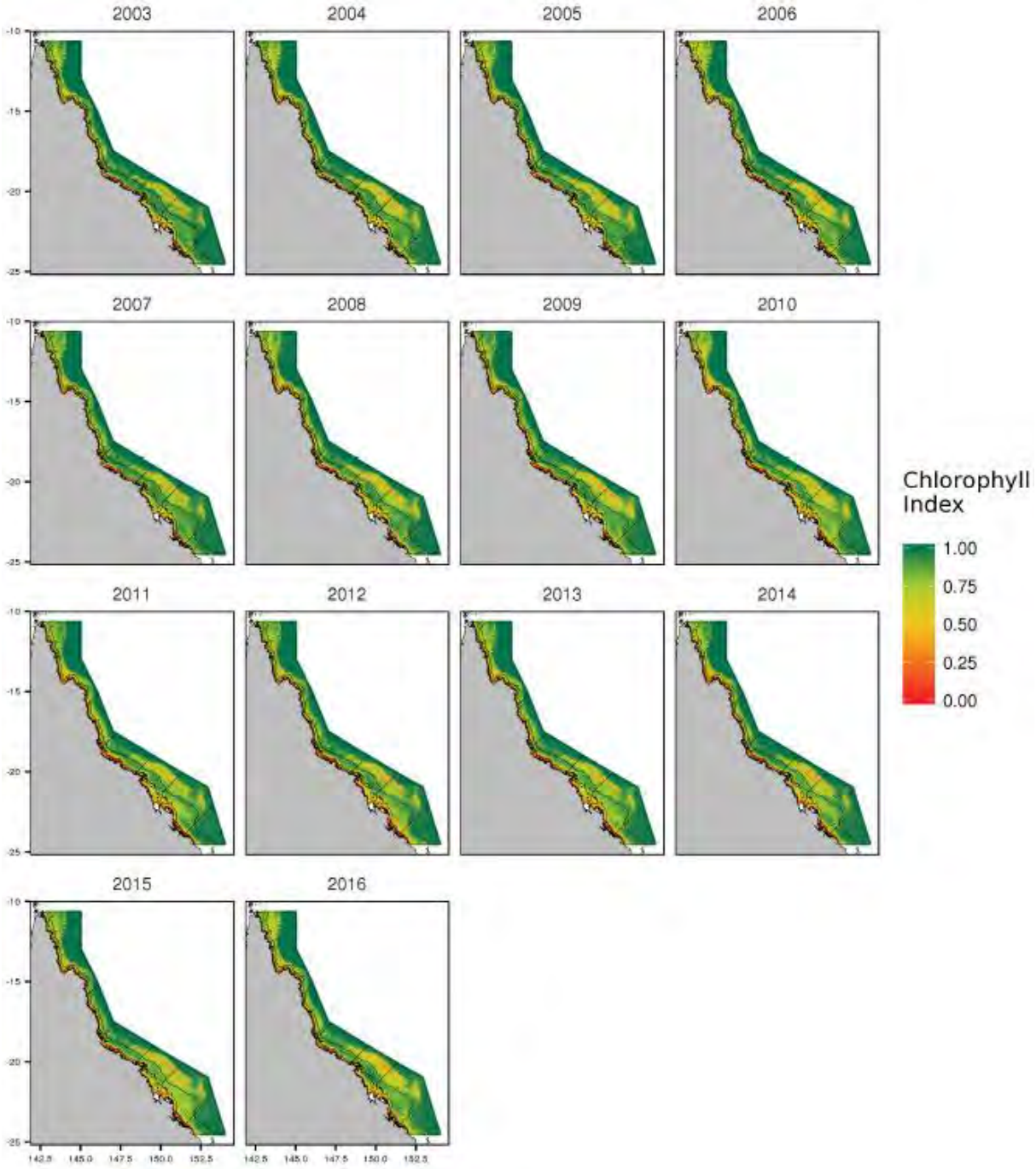


**Figure 62: Spatio-temporal Satellite fsMAMP Chlorophyll-a index scores.**

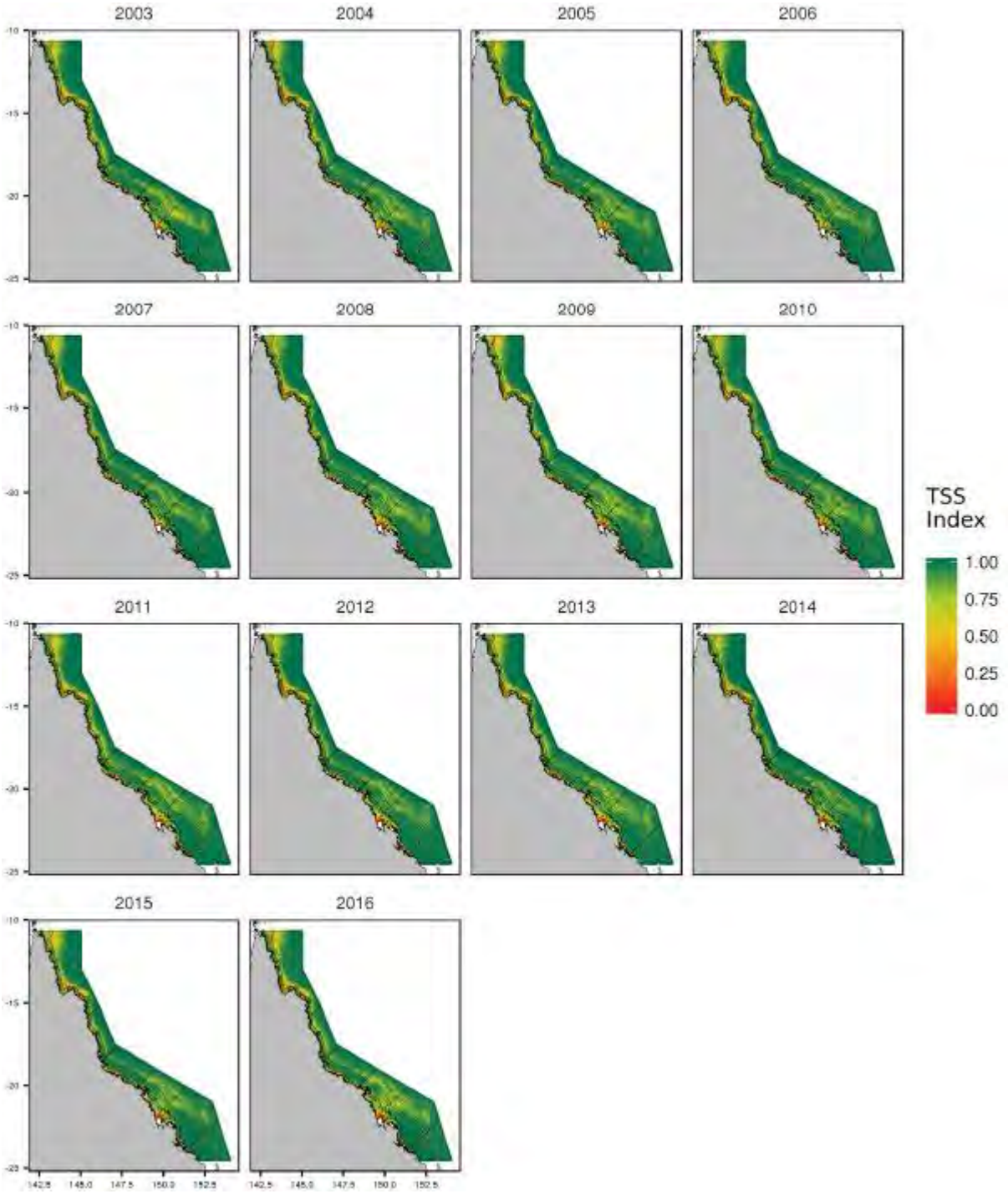


**Figure 63: Spatio-temporal Satellite fsMAMP TSS index scores.**

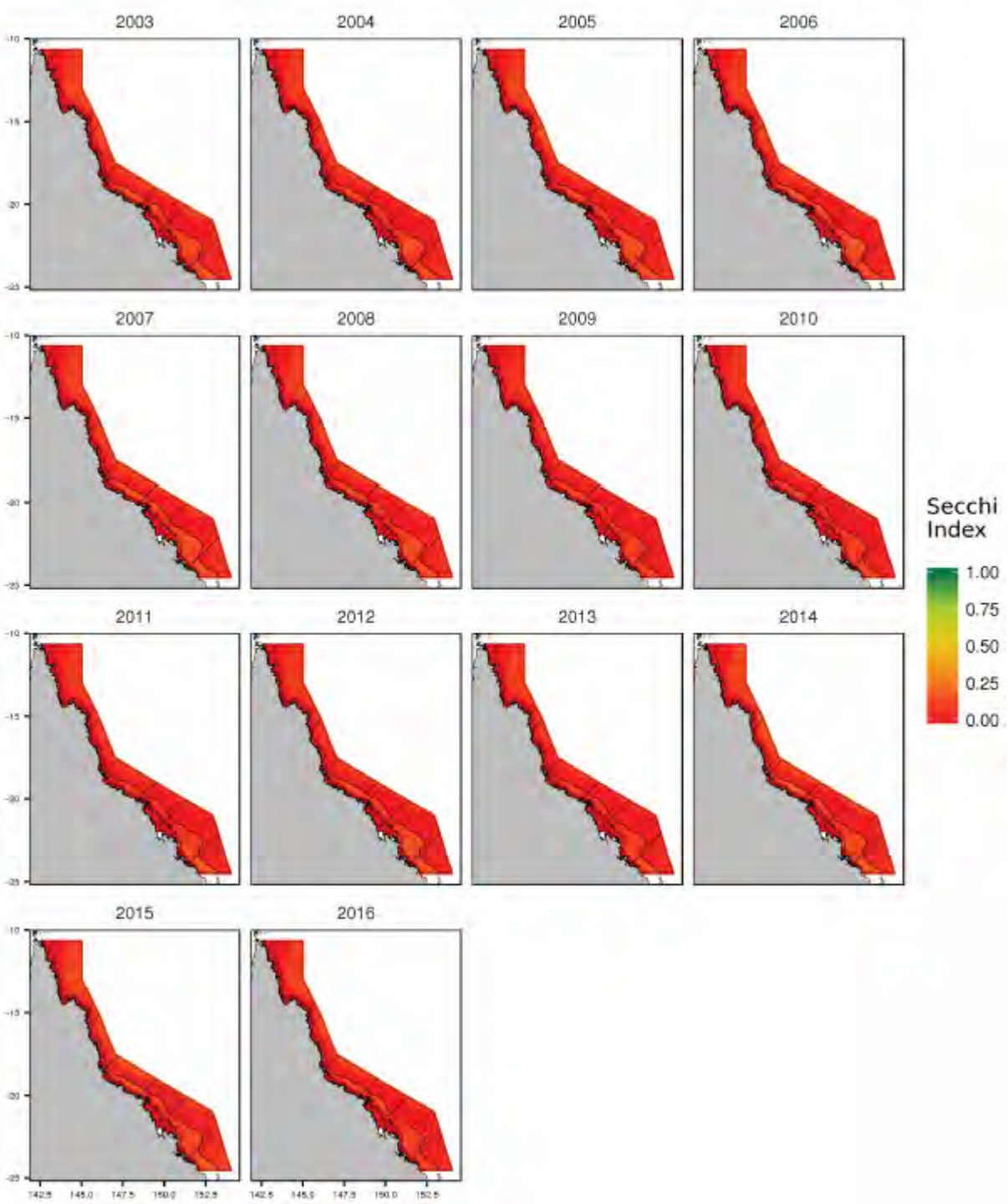


**Figure 64: Spatio-temporal Satellite fsMAMP Secchi depth index scores.**

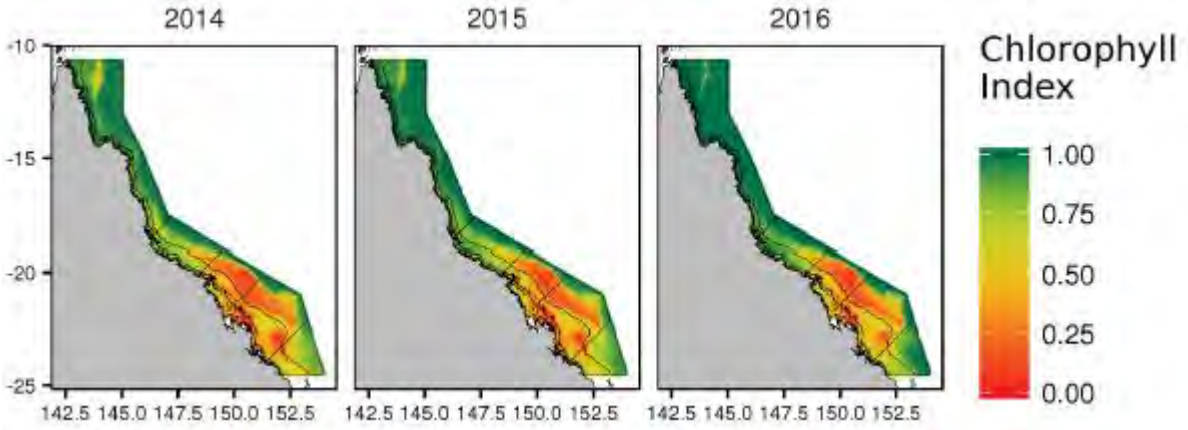


**Figure 65: Spatio-temporal eReefs fsMAMP Chlorophyll-a index scores.**

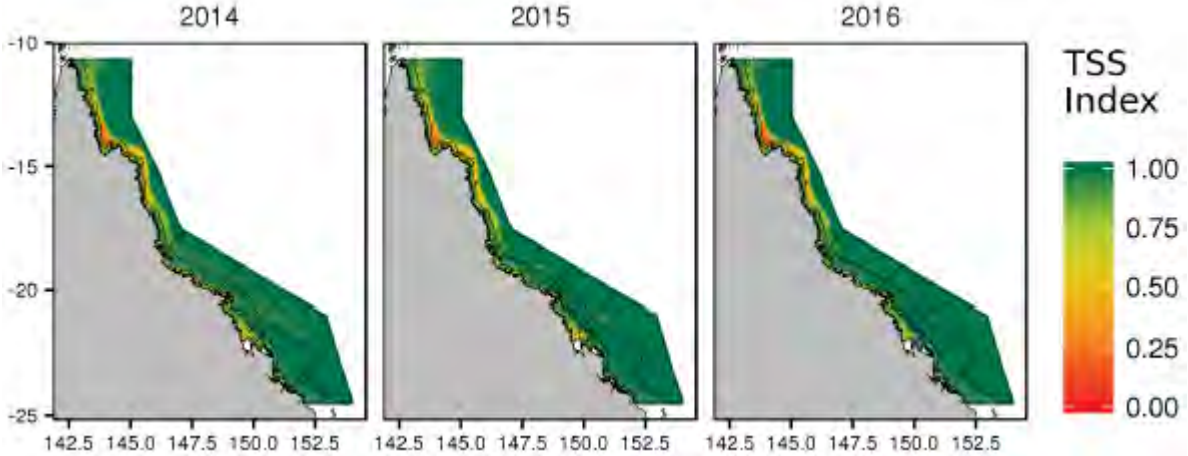


**Figure 66: Spatio-temporal eReefs fsMAMP TSS index scores.**

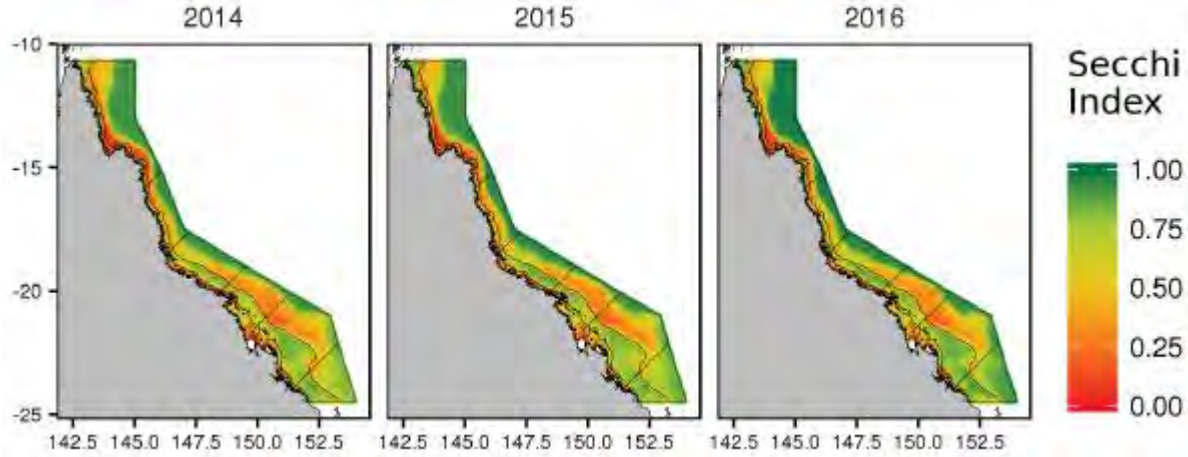


**Figure 67: Spatio-temporal eReefs fsMAMP Secchi depth index scores.**

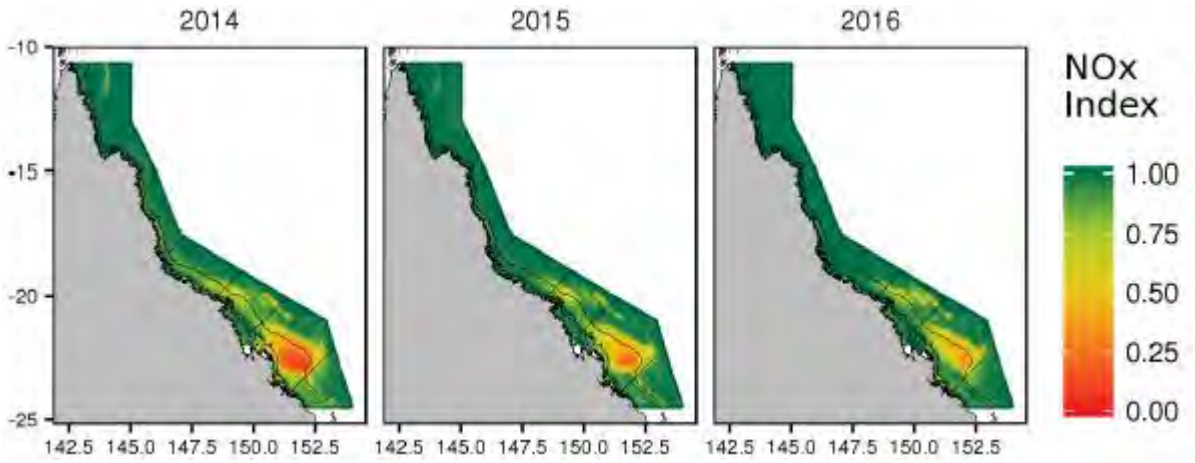


**Figure 68: Spatio-temporal eReefs fsMAMP NOx index scores.**

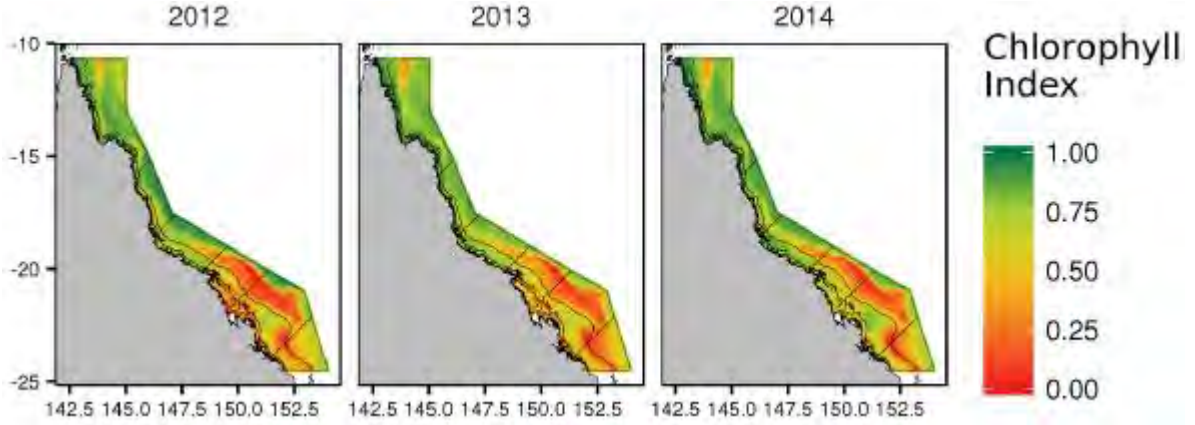


**Figure 69: Spatio-temporal eReefs926 fsMAMP Chlorophyll-a index scores.**

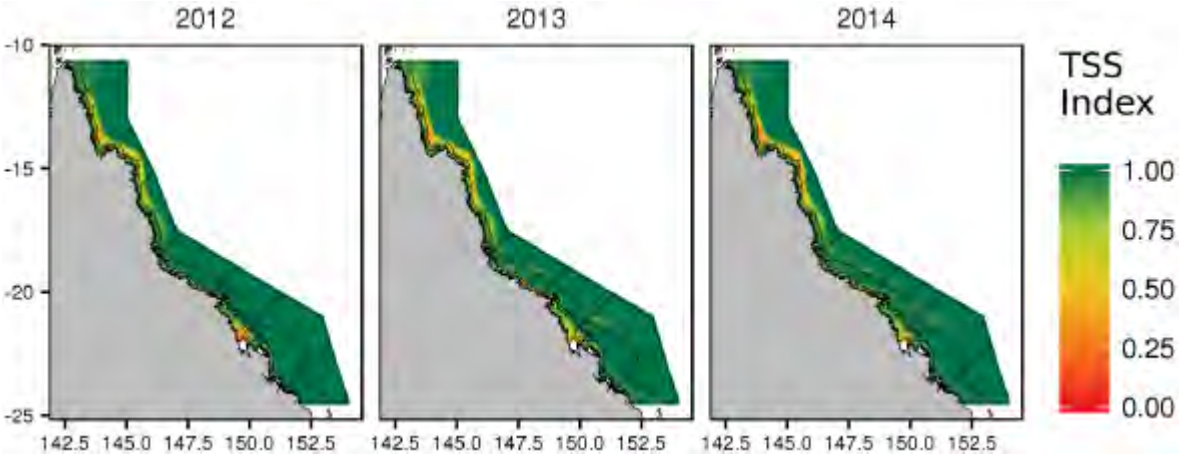


**Figure 70: Spatio-temporal eReefs926 fsMAMP TSS index scores.**

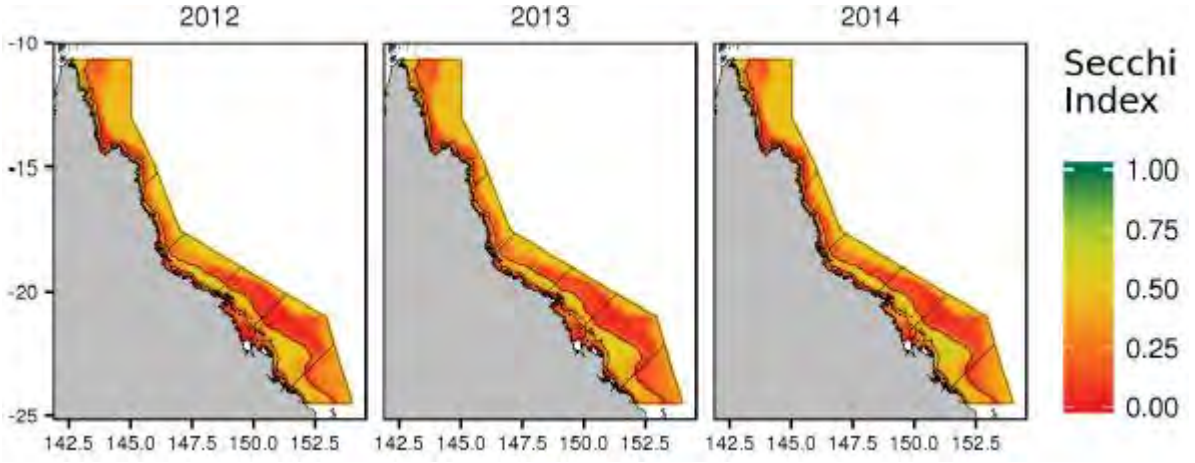


**Figure 71: Spatio-temporal eReefs926 fsMAMP Secchi depth index scores.**

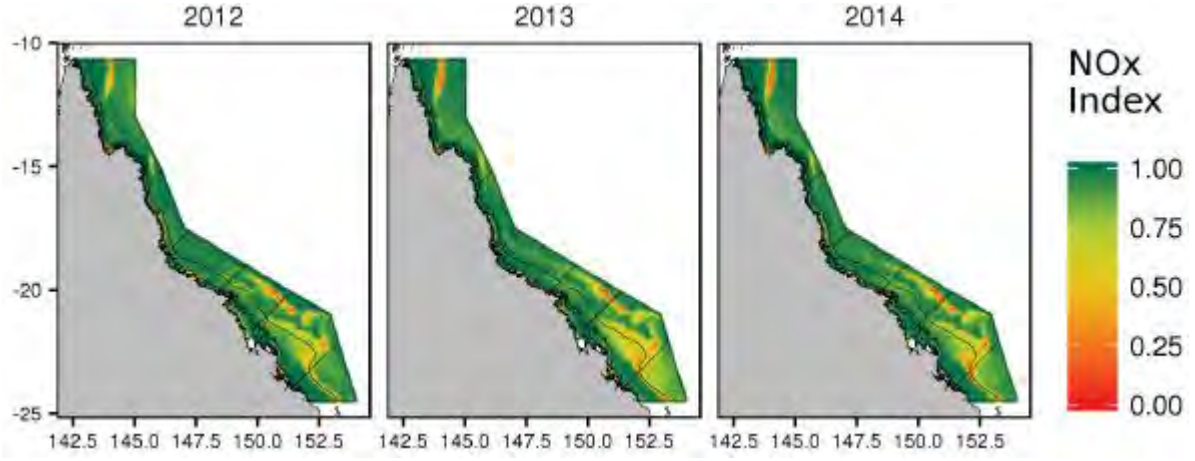


**Figure 72: Spatio-temporal eReefs926 fsMAMP NOx index scores.**

## 3.4 Summary of recommendations

- Whilst demonstrably more sensitive than either the Satellite or eReefs (with and without assimilation), the AIMS in situ data are likely to be spatially biased (predominantly reflecting conditions relatively close to major discharge sources) and lack the spatial and temporal coverage to provide representative metrics for entire GBR.
- Although the Satellite data shows some spatial variability (except for Secchi depth), temporal variability is very subtle.
- Assuming the eReefs assimilated modelled data encapsulates both deterministic expectations (models) and some form of observable realisations of state, these data should provide a solid basis on which to build water quality report card metrics.
- eReefs TSS and NOx both appear to be very low (particularly in Midshelf and Offshore) compared to the associated thresholds thereby resulting in highly insensitive indices.
- In the short-term, water quality metrics should comprise only eReefs Chlorophyll-a and Secchi depth.

# 4.0 HIERARCHICAL AGGREGATIONS

## 4.1 Theoretical Framework

To facilitate the integration of additional input Measures into the report card scores (such as additional Physical or Chemical), or even additional Sub-indicators (such as sediment metals, aquaculture yields etc), we can defined a hierarchical structure in which Measures (such as Chlorpohyll-a, NOx, sediment aluminum and yield etc) are nested within appropriate Sub-indicators. In turn, these Sub-indicators are nested within Indicators.

By progressively abstracting away the details of the Measures and Sub-indicators, a more focused narrative can be formulated around each level of the hierarchy. For example, when discussing the current state (and trend in state) of the Water Quality Indicator, rather than needing to discuss each individual constituent of Water Quality, high-level Grades are available on which to base high-level interpretations. More detailed explorations are thence revealed as required by exploring the Grades at progressively finer scales of the hierarchy. Moreover, the hierarchical structure offers great redundancy and thus flexibility to add, remove and exchange individual measures.

Similar arguments can be made for a spatial hierarchy in which Sites are nested within Zones which in turn are nested within the Whole GBR. The purpose of aggregation is to combine together multiple items of data. For Nesp 3.2.5, the report card is informed by a triple hierarchical data structure in which Daily observations are nested within Seasonal and Annual aggregates, Measures are nested within Sub-indicators which are nested in Indicators and Sites are nested within Zones (see Figure 73).

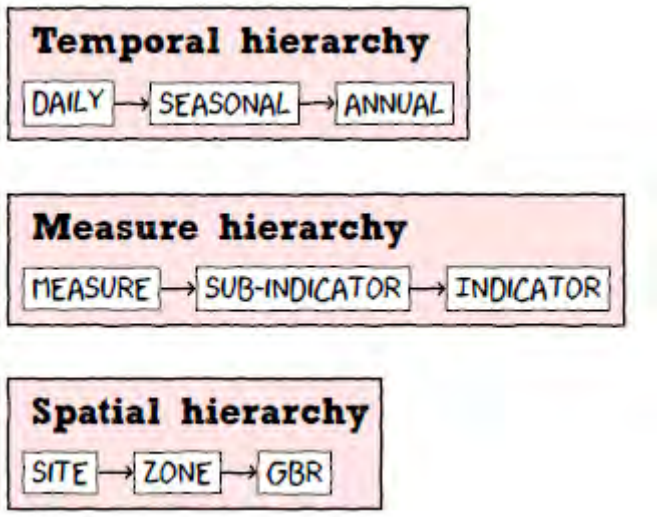


**Figure 73: Temporal, measure and spatial aggregation hierarchy.**

Although the triple hierarchy (temporal, Spatial and Measurement), does offer substantial redundancy and power advantages, it also introduces the complexity of how to combine the hierarchies into a single hierarchical aggregation schedule. Table 17 (a fabricated example), illustrates this complexity for aggregating across Spatial and Measure scales when data availability differs. This simple example demonstrates how different aggregation schedules can result in different Zone Indicator scores:

- calculating Zone 1 Indicator Score as the average of the Site level Water Quality Scores prioritizes that the Zone 1 Indicator Score should reflect the average of the Water Quality Indicator Scores for the Site. This routine will bias the resulting Zone 1 Water Quality Indicator Score towards Sub-indicators represented in more Sites. The current MMP sampling design is unbalanced (some Zones have more Sites than others and not all Measures are observed in all Sites), and there is no guarantee that the design will be maintained over time. If for example, Chemical Measures were not available for certain Zones, then the Whole GBR Water Quality Indicator Score will be biased towards Water Clarity Sub-indicators.
- calculating Zone 1 Water Quality Indicator Score as the average of the Zone 1 level Sub-indicator Scores prioritizes equal contributions of Sub-indicators to the Indicator Score at the expense of being able to relate Zone 1 Scores to the corresponding Site Scores.

The above becomes even more complex when the temporal dimension is include:

**Table 16: Fabricated illustration of the discrepancies between total means (i.e. Zone 1 Indicator Score) generated from row means (Site Sub-indicator Scores) and column means (Zone 1 Sub-indicator Scores).**

| | Sub-Indicators | | |
|---|---|---|---|
| Site | Water Clarity | Nutrients | Indicator |
| 1 | 5 | 2 | 3.50 |
| 2 | 6 | | 6.00 |
| 3 | 6 | 4 | 5.00 |
| Zone 1 | 5.67 | 3.00 | X |

If X (mean) is calculated from the three row means = 4.83
If X (mean) is calculated from the two column means = 4.33

An additional complication is how the different hierarchies integrate together. Specifically, what level of data should be aggregated first and at what point do the aggregations of one hierarchy feed into other hierarchies. For example, should observations first be aggregated from Daily to Seasonal or Annual, then aggregated from Site level to Zone level and then finally aggregated from Measure to Indicator? Some possible configurations are presented in Figure 74.

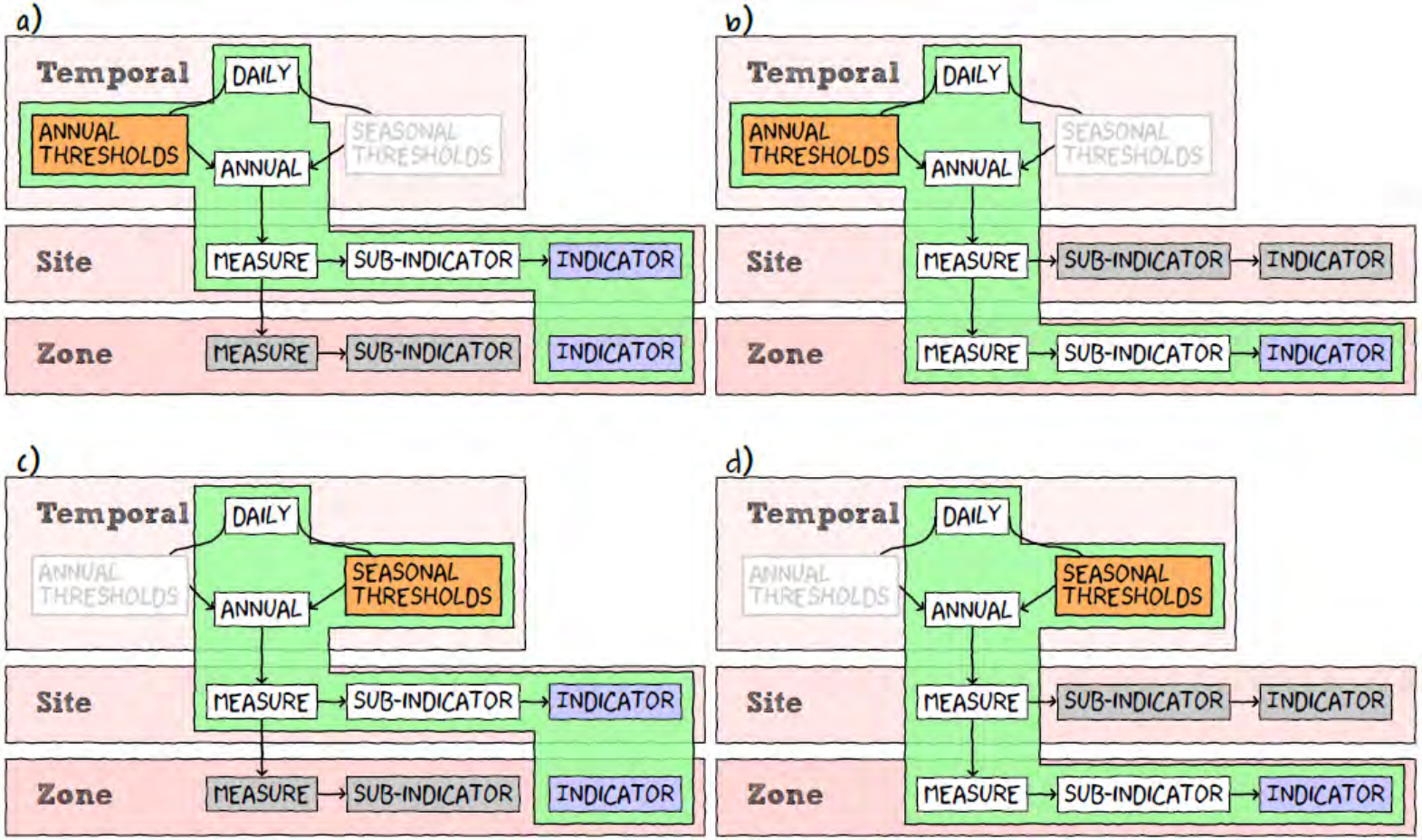


**Figure 74: Schematic illustrating four possible aggregation routines through the combination of Temporal (Daily, Seasonal and Annual), Spatial (Site, Zone) and Measure (Measure, Sub-indicator, Indicator) nodes of the triple hierarchical aggregation routine associated with the GBR Report Card. Aggregation directions between nodes are signified by arrows and the main aggregation pathway through the routines is illustrated by the green polygon.**

To maximize information retention throughout a series of aggregations, it is preferable to aggregate distributions rather than single properties of those distributions (such as means). The simplest way to perform a hierarchy of aggregations is to interactively calculate the means (or median) of items (means of means etc). At each successive aggregation level only very basic distributional summaries (such as the mean and perhaps standard deviation) are retained, the bulk of upstream information is lost. Alternatively, more complex methods that involve combining data or probability distributions can be effective at aggregating data in a way that propagates rich distributional properties throughout a series of aggregations.

Importantly, if the purpose of aggregation is purely to establish a new point estimate of the combined items, a large variety of methods essentially yield the same outcomes. On the other hand, if the purpose of aggregation is also to propagate a measure of uncertainty or confidence in the point estimate through multiple hierarchical levels of aggregation (as is the case here), then the different methodologies offer differing degrees of flexibility and suitability.

Hierarchical aggregations are essentially a series of steps that sequentially combine distributions (which progressively become more data rich). The resulting distribution formed at each step should thereby reflect the general conditions typified by its parent distributions and by extension, each of the distributions higher up the hierarchy.

Numerous characteristics can be estimated from a distribution including the location (such as mean and median) and scale (such as variance and range). For the current project, the mean and variance were considered the most appropriate[15] distributional descriptions and from these estimates Grades and measures of confidence can be respectively derived. Hence the numerical summaries (mean and variance) at any stage of the hierarchical aggregation are a by-product rather than the sole property of propagation.

### *4.1.1 Bootstrap aggregation*

Although some of the items to be aggregated together might initially comprise only a few values (or even a single value), it is useful to conceptualize them as continuous distributions. For example, when aggregating multiple *Measures* (such as all Water Quality Chemicals) together to generate a (*Site* level) *Sub-indicator* average, each *Measure* in each *Site* can be considered a distribution comprising the single Score for that *Measure*. Aggregation then involves combining together the multiple distributions into a single amalgam (by adding the distributions together, see Figure 75). Similarly, when aggregating at the *Indicator* level across *Site* to generate *Zone* summaries for each *Indicator*, *Site* distributions are respectively added together to yield a single distribution per *Zone*.

[15] The aggregations typically involve some Measures with a small number of unique observations (and thus indices) and thus means and variances provide greater sensitivity than medians and ranges. Moreover, the indexing stage effectively removes outliers and standardizes the scale range thereby reducing the need for robust estimators.

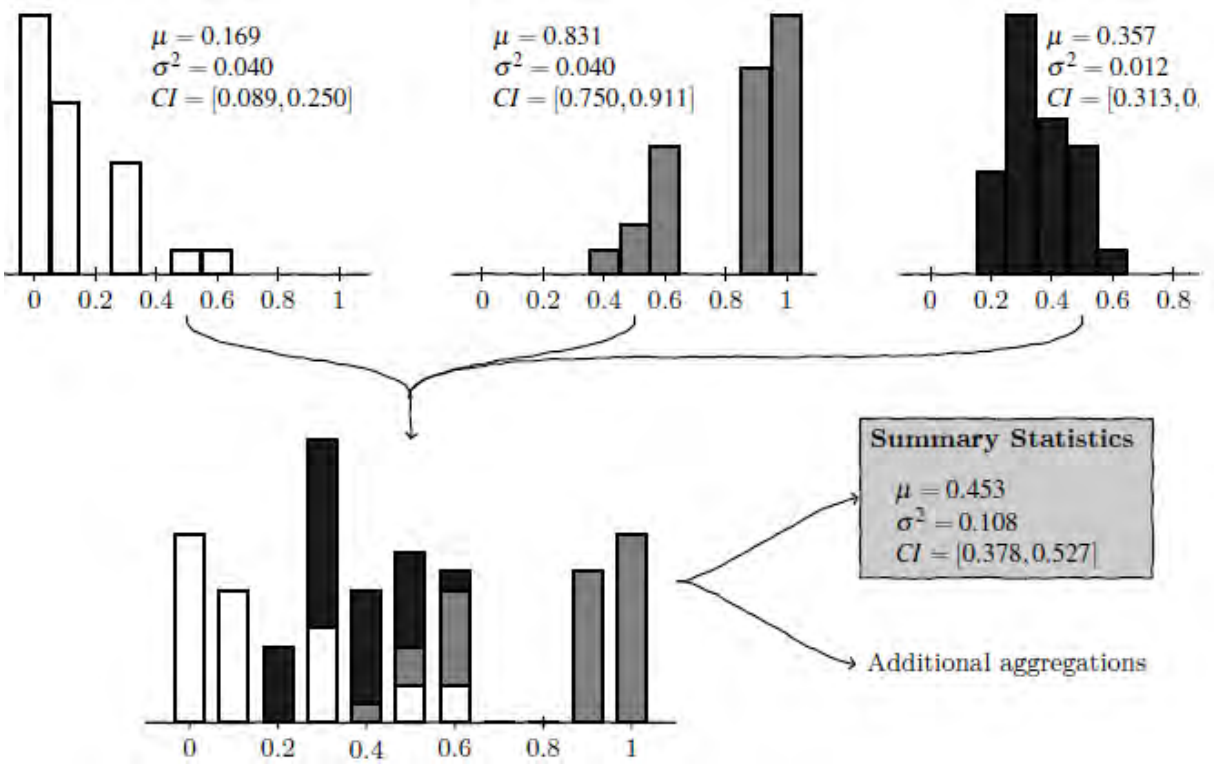


**Figure 75: Illustration of Bootstrapped aggregation of three distributions. Simple summary statistics (mean, variance and 95% confidence interval presented for each distribution).**

If the distributions being aggregated are all proportional distributions (e.g. density distributions), adding them altogether is trivially simple. However, if, rather than actual distributions, the items to be aggregated are actually just small collections of values (as is the case for many of the discrete Measures here) or even large, yet unequally populous collections of values (as could be the case for Continuous Flow Monitoring with missing or suspect observations), then simply aggregating the distributions together will result in amalgams that are weighted according to the size of the collections (larger collections will have more influence). For example, if we were aggregating together three *Zones* (to yield Whole GBR estimates), one of which comprised twice as many Sites, simple aggregation of distributions would result in a distribution that was more highly influenced by the Zone with the more *Sites*. Similarly, when aggregating from the level of Sub-indicator to the level of Indicator, the resulting Indicator would be biased towards the Sub-indicator with the most Measures. Whilst this may well be a useful property (e.g. stratified aggregation), it may also be undesirable.

Bootstrapping is a simulation process that involves repeated sampling (in this case with replacement) of a sample set with the aim of generating a bootstrap sample from a distribution. This bootstrap sample can be used to estimate the underlying probability distribution function that generated the data as well as any other summary statistics. Importantly, bootstrapping provides a way to generate distributions that are proportional and thus unweighted by the original sample sizes thereby facilitating un-weighted aggregation[16]. Bootstrapped distributions can be aggregated (added together) to yield accumulated child distributions that retain the combined properties of both parents (see Figure 75). As a stochastic process, repeated

[16] technically, all equally weighted rather than un-weighted.

calculations will yield slightly different outcomes. Nevertheless, the more bootstrap samples are collected, the greater the bootstrap distributions will reflect the underlying Score distribution and provided the number of drawn samples is sufficiently large (e.g. 10,000 resamples), repeated outcomes will converge.

To reiterate, the advantage of bootstrapping data before concatenating (or averaging) versus simply concatenating data from multiple sources together, is to ensure that source data are all of exactly the same sample size (so as to not weight more heavily towards the more populous source(s)[17]). Bootstrapping also provides a mechanism for propagating all distribution information throughout an aggregation hierarchy and ensures that estimates of variance derived from child distributions are on a consistent scale[18]. The latter point is absolutely critical if variance is going to be used to inform a Confidence Rating system and confidence intervals.

Minimum operator procedures are supported by filtering on the lowest performed indicator prior to bootstrapping. Importantly, the bootstrapping routine simply provides a mechanism to collate all sources together to yield a super distribution. Thereafter, the joint distribution can be summarized in what ever manner is deemed appropriate (arithmetic, geometric, harmonic means, medians, variance, range, quantiles etc). Moreover, different levels of the aggregation can be summarized with different statistics if appropriate.

### *4.1.2 Beta approximation*

Whilst the bootstrap aggregation approach described above does offer a robust way to combine data across scales and sources, for large data sets, it does impose large computational and storage burdens. For such cases (large data such as remote sensing), index distributions can be approximated by beta distributions. The beta distribution is defined on the interval [0,1] and is parameterized by two positive shape parameters ($\alpha, \beta$) according to the following:

$$f(x;\ \alpha, \beta) = \frac{\Gamma(\alpha + \beta)}{\Gamma(\alpha)\Gamma(\beta)} x^{\alpha-1}(1-x)^{\beta-1}$$

A beta function can manifest as many different shapes and as all of these are described by just two shape parameters. Therefore, rather than store all the bootstrapped values for each distribution, we can alternatively approximate each distribution by a beta and store only the defining shape parameters of each distribution. When combining, rather than randomly sample 10,000 stored values of each distribution, we simple resample 10,000 random draws from each beta distribution[19]. The combined distribution can then be approximated by a beta distribution and so on.

### *4.1.3 Weights*

Standard bootstrapping yields equally weighted distributions, however, specific weighting schemes can also be easily applied by bootstrapping in proportion to the weights. For example, to weight one parent twice as high as another, simply collect twice as many re-samples from the first distribution. To ensure that all resulting distributions have the same size (by default

[17] Such weightings should be handled in other ways if at all.
[18] Variance is inversely proportional to sample size.
[19] Unfortunately there is no closed-form general formula for the sum of multiple independent beta distributions.

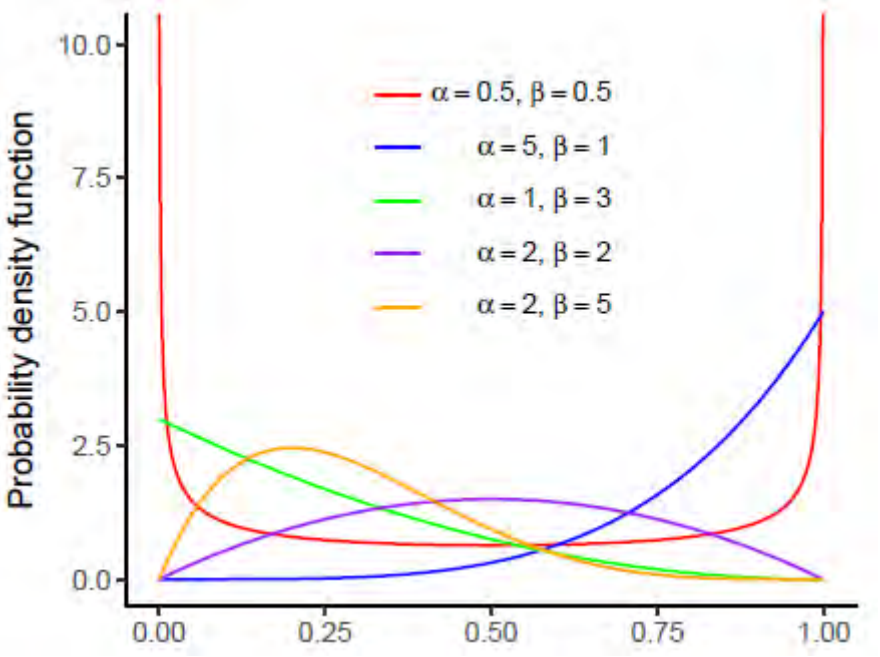


**Figure 76:** Beta probability densities

10,000 items), the number of bootstrap samples collected ($n$) from each of the ($p$) parent distributions ($i$), given the weights ($w_i$) is calculated as:

$$n_i = (S/p).w_i$$

where $S$ is the target size (10,000) and : indicates the ceiling. Qualitative data (such as ratings) can also be incorporated by enumerating the categories before bootstrapping.

In addition to allowing expert driven weights that govern the contribution of different items during aggregations, it is possible to weight according to relative spatial areas during spatial aggregations. Currently, all Sites are equally weighted when aggregating to Zone level and all Zones equal when aggregating to Whole of GBR level. That means that small Zones have an equal contribution as large Zones despite representing a smaller fraction of the water body. Area based weights could be applied such that Sites and Zones contribute in proportion to relative areas.

Weights are defined by a user editable configuration file that is similar in structure to the Water Quality thresholds file.

### *4.1.4 Expert interventions*

The ability for experts and Report Card managers to intervene (exclude or overwrite) Scores/Grades at any Spatial/Measure scale is essential to maintain the quality of a Report Card in the event of unrepresentative or suspect data. The current system is able to support expert interventions in the form of exclusions and overwrites. For example, after reviewing the QAQC, an expert can elect to exclude one or more Measures (or Subindicators etc) from one

or more spatial scales. Such interventions are specified via a user editable configuration files[20] (csv) that is similar in structure to the Water Quality thresholds file.

The essential component of this configuration file is that it allows a user to specify what Data are to be excluded or replaced. These can be at any of the levels of the Measure hierarchy (Measures, Sub-indications and Indicators) and any level of the Spatial hierarchy (Sites, Zones and Whole GBR). Settings pertaining to levels further along the aggregation hierarchies have precedence. For example, if Chemicals are excluded (or overridden) in a particular Zone, then all Chemical Measures within all Sites will be excluded irrespective of what the settings are for any specific Measure/Site.

### *4.1.5 Scores and Grades*

The double hierarchy Bootstrap aggregation described above, yields **Score** distributions for each Measure-level/Spatial-level combination. The location and scale of each distribution can thus be described by its mean and variance. Mean **Scores** are then converted into a simple five-point alphanumeric **Grade** scale (and associated colours) using a conversion (see Figure 77).

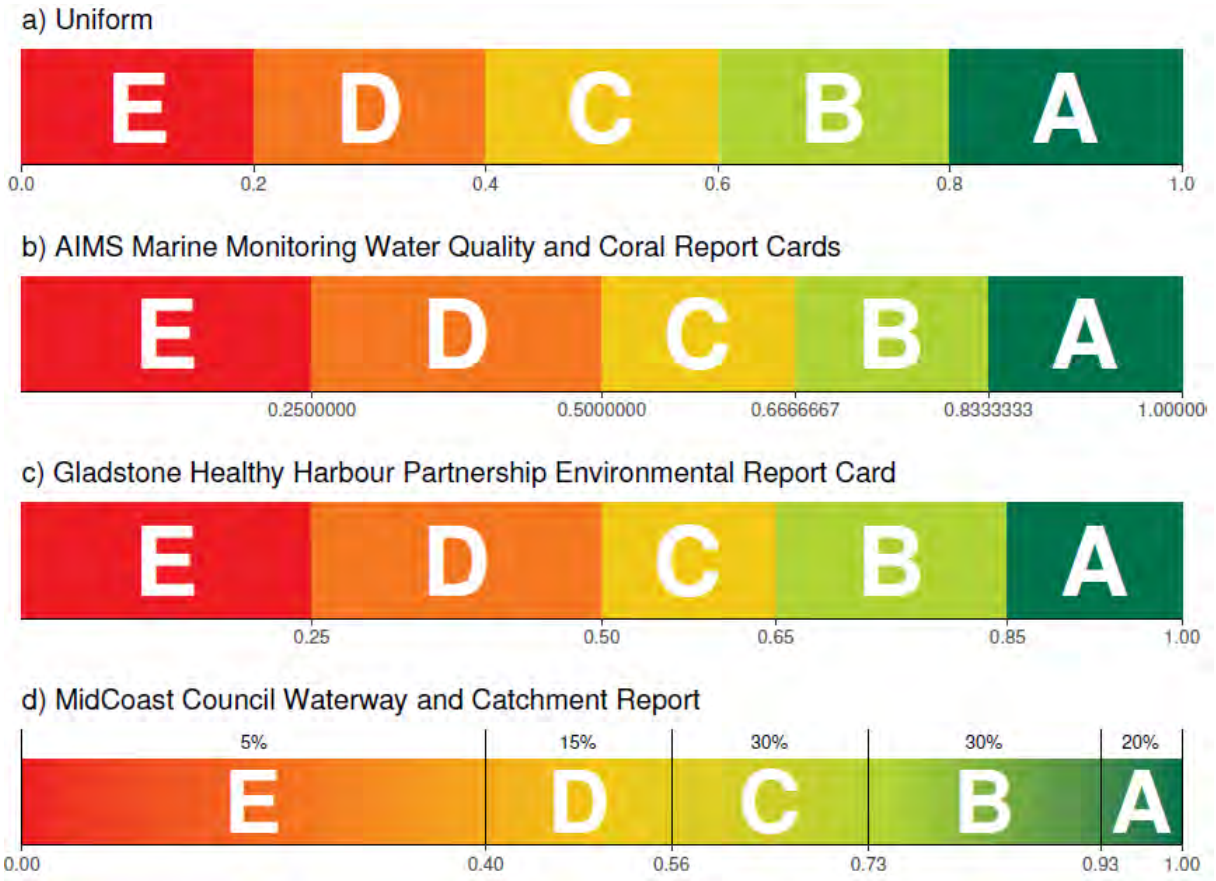


**Figure 77: Score to grade conversions. In each case, the scale along the base defines the grade boundaries.**

[20] Since aggregation occurs across two hierarchies (the Measure hierarchy and the Spatial hierarchy - see Figures 73 and 74), two configuration files are necessary.

The conversions adopted by the AIMS inshore water quality Marine Monitoring Program (MMP Lønborg et al., 2016) and the Gladstone Healthy Harbour Partnership (Gladstone Healthy Harbour Partnership, 2016) both define two levels (Poor and Very Poor) under the Threshold values and three above (Satisfactory, Good and Very Good). The threshold is purposely placed at the boundary of two grades so as to ease the distinction between 'pass' and 'fail'. The major difference between these two charts is that whereas the AIMS MMP report card conversion partitions the three better than threshold categories, the Gladstone Healthy Harbour Partnership report card conversion employs simpler boundary cutoffs around the 'B' grade (although this does result in arbitrarily unequal category sizes.

By contrast, the MidCoast Council (formally Great Lakes Council) Waterway and Catchment Report (MidCoast Council, 2016) uses grade boundaries based on historical score distribution quantiles associated with definitions of what proportion of total observations (sites) are considered 'Excellent' (A), 'Good' (B), 'Fair' (C), 'Poor' (D) and 'Very Poor' (Fig. 77d). For example, the 'Very Poor' grade was defined as the worst 5% of sites across the entire State of New South Wales and the lowest 5% of sites has a maximum score of 0.4. This approach recognizes the non-linear spread of scores resulting from their particular metrics and attempts to ensure that grades are intuitively interpretable (A grade of A means the site is in Excellent condition). Nevertheless, it does necessitate historical data and as well as a very specific and agreed upon set of a priori condition definitions.

In each of the above approaches, grade boundaries are usually determined to some extent by expert panel to ensure that the range of indices represented by each grade classification is congruent with community interpretation of a letter grade report cards. It is far less clear how estimates of uncertainty can be incorporated into such a grading scheme in a manner that will be intuitive to non-technical audiences. That said, statistical uncertainty is just one of many sources of un- certainty that should be captured into a confidence or certainty rating. Hence any expectations of presenting uncertainty in a quantitative manner may well be unrealistic anyway.

In the absence of expert opinion, we have elected to adopt a very simple score-grade conversion in which the score range is simply partitioned into five equal grades (Fig. 77a).

### *4.1.6 Certainty rating*

Incorporating an estimate of scale (variance) into a certainty or confidence rating necessitates re-scaling the estimates into a standard scale. In particular, whereas a scale parameter of high magnitude indicates lower degrees of certainty, for a certainty rating to be useful for end users, larger numbers should probably represent higher degrees of certainty. Thus, the scaling process should also reverse the scale. Furthermore, variance is dependent on the magnitude of the values.

In order to re-scale a scale estimate into a certainty rating, it is necessary to establish the range of values possible for the scale estimate. Whilst the minimum is simple enough (it will typically be 0), determining the maximum is a little more challenging depending on the aggregation algorithm (bootstrapping, Bayesian Network etc). One of the advantages in utilizing proportional distributions (such as is the case for a Bayesian Network or a re-sampled bootstrap distribution) is that the scale parameter for the single worst case scenario can be

devised (once the worst case scenario has been determined) independent of sample sizes or weightings. In most situations this is going to be when the distribution comprises equal mass at (and only at) each of the two extremes (for example, values of just 0 and 1).

The measure of confidence rating discussed above is purely an objective metric derived from the variance in the aggregation hierarchy. It is completely naive to issues such as missing data, outliers and Limit of Detection issues - the influences of which on a confidence rating are necessarily subjective. A full Confidence Rating would combine these objective variance component with additional subjective considerations such as climatic and disturbance information, and the perceived influence of missing, Limit of Detection and outlying data. Hence, the statistical scaled statistical variance would form just one component in the Confidence Rating system.

The bootstrap aggregation method provides a mechanism for estimating variance from which to build such an expert considered Confidence Rating system.

Table 18 presents the Water Quality Indicator Scores and associated Grades for each Zone based on three of the grade control chart types described in Figure 77 for the eReefs data indexed using the fsMAMP formulation. Whilst there is some agreement between the different grade types, in general, the Uniform type yields higher grades than either MMP or GHHP.

**Table 17: Score and associated Grades based on three different grade control charts (Uniform, MMP and GHHP) for eReefs data indexed via fsMAMP and aggregated to Zone/Indicator level.**

| Region | Water Body | Water Year | Score | Grade (MMP) | Grade (Uniform) | Grade (GHHP) |
|---|---|---|---|---|---|---|
| Cape York | Open Coastal | 2014 | 0.692 | B | B | B |
| Cape York | Open Coastal | 2015 | 0.741 | B | B | B |
| Cape York | Open Coastal | 2016 | 0.757 | B | B | B |
| Cape York | Midshelf | 2014 | 0.716 | B | B | B |
| Cape York | Midshelf | 2015 | 0.764 | B | B | B |
| Cape York | Midshelf | 2016 | 0.781 | B | B | B |
| Cape York | Offshore | 2014 | 0.825 | B | A | B |
| Cape York | Offshore | 2015 | 0.852 | A | A | A |
| Cape York | Offshore | 2016 | 0.895 | A | A | A |
| Wet Tropics | Open Coastal | 2014 | 0.602 | C | B | C |
| Wet Tropics | Open Coastal | 2015 | 0.668 | B | B | B |
| Wet Tropics | Open Coastal | 2016 | 0.692 | B | B | B |
| Wet Tropics | Midshelf | 2014 | 0.711 | B | B | B |
| Wet Tropics | Midshelf | 2015 | 0.760 | B | B | B |
| Wet Tropics | Midshelf | 2016 | 0.796 | B | B | B |
| Wet Tropics | Offshore | 2014 | 0.819 | B | A | B |
| Wet Tropics | Offshore | 2015 | 0.844 | A | A | B |
| Wet Tropics | Offshore | 2016 | 0.873 | A | A | A |
| Dry Tropics | Open Coastal | 2014 | 0.580 | C | C | C |
| Dry Tropics | Open Coastal | 2015 | 0.624 | C | B | C |
| Dry Tropics | Open Coastal | 2016 | 0.639 | C | B | C |
| Dry Tropics | Midshelf | 2014 | 0.758 | B | B | B |
| Dry Tropics | Midshelf | 2015 | 0.799 | B | B | B |

..continued from previous page

| Region | Water Body | Water Year | Score | Grade (MMP) | Grade (Uniform) | Grade (GHHP) |
|---|---|---|---|---|---|---|
| Dry Tropics | Midshelf | 2016 | 0.821 | B | A | B |
| Dry Tropics | Offshore | 2014 | 0.778 | B | B | B |
| Dry Tropics | Offshore | 2015 | 0.809 | B | A | B |
| Dry Tropics | Offshore | 2016 | 0.829 | B | A | B |
| Mackay Whitsunday | Open Coastal | 2014 | 0.464 | D | C | D |
| Mackay Whitsunday | Open Coastal | 2015 | 0.491 | D | C | D |
| Mackay Whitsunday | Open Coastal | 2016 | 0.505 | C | C | C |
| Mackay Whitsunday | Midshelf | 2014 | 0.568 | C | C | C |
| Mackay Whitsunday | Midshelf | 2015 | 0.607 | C | B | C |
| Mackay Whitsunday | Midshelf | 2016 | 0.602 | C | B | C |
| Mackay Whitsunday | Offshore | 2014 | 0.470 | D | C | D |
| Mackay Whitsunday | Offshore | 2015 | 0.474 | D | C | D |
| Mackay Whitsunday | Offshore | 2016 | 0.475 | D | C | D |
| Fitzroy | Open Coastal | 2014 | 0.377 | D | D | D |
| Fitzroy | Open Coastal | 2015 | 0.382 | D | D | D |
| Fitzroy | Open Coastal | 2016 | 0.442 | D | C | D |
| Fitzroy | Midshelf | 2014 | 0.589 | C | C | C |
| Fitzroy | Midshelf | 2015 | 0.595 | C | C | C |
| Fitzroy | Midshelf | 2016 | 0.631 | C | B | C |
| Fitzroy | Offshore | 2014 | 0.528 | C | C | C |
| Fitzroy | Offshore | 2015 | 0.541 | C | C | C |
| Fitzroy | Offshore | 2016 | 0.571 | C | C | C |
| Burnett Mary | Open Coastal | 2014 | 0.624 | C | B | C |
| Burnett Mary | Open Coastal | 2015 | 0.639 | C | B | C |
| Burnett Mary | Open Coastal | 2016 | 0.653 | C | B | B |
| Burnett Mary | Midshelf | 2014 | 0.646 | C | B | C |
| Burnett Mary | Midshelf | 2015 | 0.675 | B | B | B |
| Burnett Mary | Midshelf | 2016 | 0.745 | B | B | B |
| Burnett Mary | Offshore | 2014 | 0.733 | B | B | B |
| Burnett Mary | Offshore | 2015 | 0.771 | B | B | B |
| Burnett Mary | Offshore | 2016 | 0.848 | A | A | B |

### *4.1.7 Confidence intervals*

Confidence intervals (CI) represent the intervals in which we have a certain degree of confidence (e.g. 95%) that repeated estimates will fall. Hence the 95% CI of the mean is the range defined by the quantiles representing 95% of repeated estimates of the mean.

To calculate 95% confidence intervals for bootstrap aggregated distributions (e.g. Wet Tropics Open Coastal/Chlorophyll-a distribution), we repeatedly[21] draw a single sample from each of the constituent distributions (e.g. a single value from the Wet Tropics Open Coastal Chlorophyll-a, Chlorophyll-a and NOx distributions) and from each set of draws, calculate the

[21] The more repeated draws the closer the distribution of means will converge. For the current project, the number of repeated draws is 10,000.

weighted[22] mean of the values. The 95% CI is thus calculated as the quantiles (p=0.025 and p=0.975) of the means.

Confidence intervals are used to represent uncertainty in estimations. For example, 95% confidence intervals associated with an estimated mean roughly express a range of values over which we have the nominated degree of confidence that the true value is likely to lie[23].

Uncertainty arises from multiple sources. Firstly, it arises from the accuracies of the measured data and secondly, from the imprecisions introduced by the statistical methodologies for processing and summarizing the dat. Hence encapsulating and communicating full uncertainty requires information about both of these sources of uncertainty.

Estimates (such as sample means) are typically calculated from very small (yet ideally representative) samples drawn from a much larger population. In such cases, the statistically derived confidence intervals are used to provide an indication of the range of estimates in which we are confident the true value is likely to lie. That is, they depict the statistical uncertainty that arises from the need to estimate parameters from small amounts of the total possible spatial/temporal domain.

If measurement uncertainty is also known, then it is possible to incorporate and propagate this through the aggregation schedule so as to yield total uncertainty. Measurement uncertainty is very typically very difficult to obtain. Nevertheless, it is usually assumed to be relatively small compared to the statistical uncertainty. However, in the case of the Satellite and eReefs data, we have a virtual saturation of sample data. That is, with respect to the spatial and temporal extent of the data, we essentially have the entire population. Consequently, the statistical uncertainty is virtually zero. We are not estimating a mean, we are calculating the mean. Hence measurement uncertainty is of elevated importance. Unfortunately, we do not have any information about the measurement uncertainty at a spatial and temporal scale appropriate. As a result, we have elected not to represent uncertainty (as it would only be based on statistical uncertainty which would give the misleading impression of extremely low levels of uncertainty).

[22] Weights according to the weights defined for that level of the aggregation hierarchy
[23] From a frequentist perspective, 95% confidence intervals technically indicate that 95% of intervals of the calculated extent will contain the true mean

## 4.2 Summary of adopted methodologies

The aggregation schedule can be summarized as:

**A. Calculation of Zone level Score and Grades**

1. Collect raw data (= *Measures*) at each fixed monitoring *Site* and compare individual observations to associated *Threshold*
2. Create **indexed** data as an expression of degree of difference with associated *Threshold* values (**fixed capped scaled modified amplitude method**) to yield a *Score* for each *Measure* per sampling location (e.g. *Site*) (applies to *Measures* in all *Indicators*, Water Quality).
3. Apply any expert opinion interventions (if appropriate - not employed in the current version).
4. Combine *Measure* Scores into *Site*-level *Sub-indicator* Scores by **averaging** taking into account any weightings, i.e. aggregate into observation-level Sub-indicator Scores. This step involves **Bootstrapping** each input to distributions of 10,000 re-samples (or fewer if weighted), combining distributions and finally Bootstrapping again into a single 10,000 size distribution.
5. Combine *Sub-indicator Scores* into *Site*-level *Indicator Scores* by **averaging** (bootstrapping), i.e. aggregate into *Site*-level *Indicator Scores*.
6. Convert *Scores* into coloured *Grades* (A-E) for visual presentation in report card using a **Uniform** control chart

**B. Calculation of Zone level Grades**

1. Aggregate *Site*-level *Measure* Scores from step A.4 into *Zone*-level *Measure Scores* by **averaging** (bootstrapping incorporating any weights)
2. Aggregate *Zone*-level *Sub-indicator Scores* into *Zone*-level *Indicator Scores* by **averaging** (bootstrapping incorporating any weights)
3. Convert *Scores* into coloured *Grades* (A-E) for visual presentation in report card using a **Uniform** control chart

**C. Calculation of Whole GBR Grades**

1. Establish spatial weights as proportional Open Coastal Zone geographic areas
2. Aggregate Open Coastal *Zone*-level *Measure Scores* from step B.1 into Open Coastal *GBR*-level *Sub-indicator Scores* by **averaging** (bootstrapping incorporating spatial weights)
3. Aggregate Open Coastal *GBR*-level *Sub-indicator Scores* into Open Coastal *GBR*-level *Indicator Scores* by **averaging** (bootstrapping)
4. Convert *Scores* into coloured *Grades* (A-E) for visual presentation in report card using a **Uniform** control chart

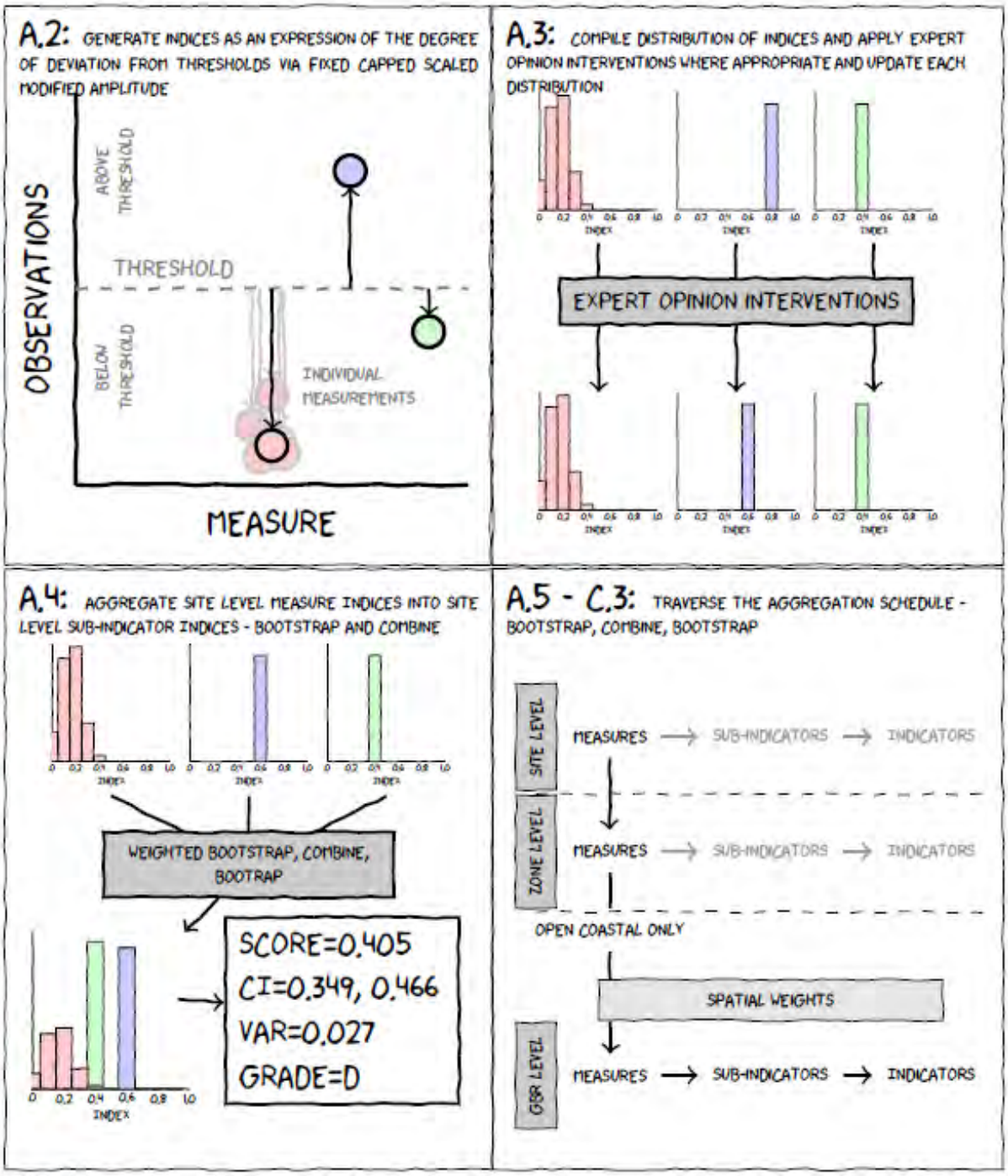


**Figure 78: Schematic illustrating the major steps of the GBR Water Quality Report Card. In this fabricated example, there are three Measures (Red, Green and Blue). Each of the Blue and Green Measures are represented by a single discrete observation, whereas the Red Measure is represented by a large collection of observations. Expert option (top right panel) intervened to lower the blue Measure distribution from observed values at 0.8 to 0.6. Bootstrap aggregations (bottom left panel) are used to combine data together proportionally. Aggregation follows a specific pathway through the aggregation hierarchy depicted in the bottom right panel. Great Barrier Reef (GBR) level aggregations utilize Open Coastal data only and aggregations are weighted according to proportional geographic areas of the Zones.**

## 4.3 Aggregation summaries

The ISP have indicated that the Water Quality metric should be based purely on eReefs fsMAMP indexed Chlorophyll-a and Secchi Depth and that the conversion of scores to grades should follow a uniform control chart. Consequently, this section will only present graphical summaries for these metric determinants.

### *4.3.1 Site/Measure level*

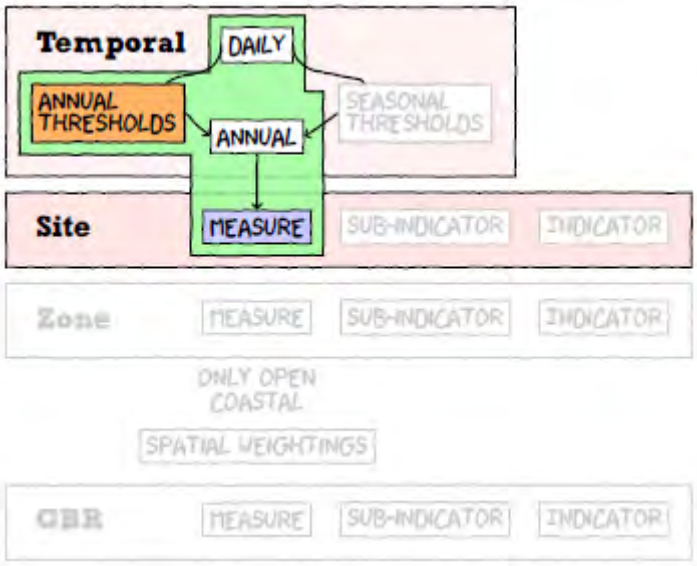


#### *4.3.1.1 Site level maps*

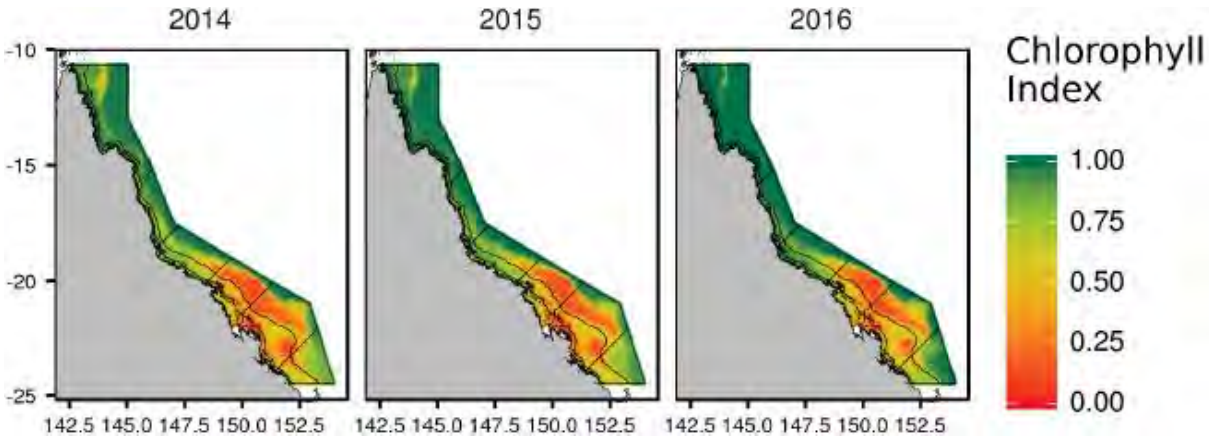


**Figure 79: Spatio-temporal patterns in eReefs fsMAMP Chlorophyll-a index grades (Uniform grade type conversion applied).**

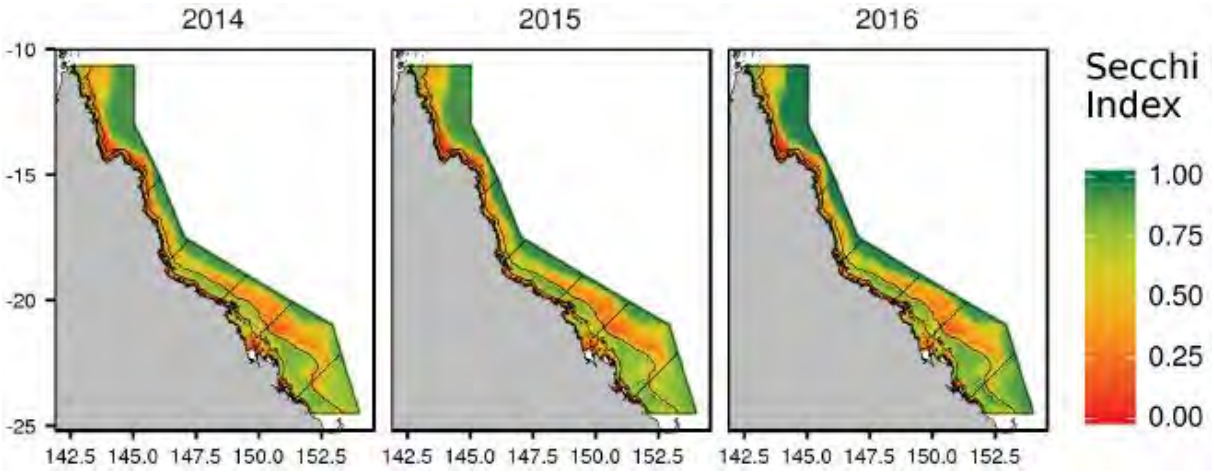


**Figure 80: Spatio-temporal patterns in eReefs fsMAMP Secchi Depth index grades (Uniform grade type conversion applied).**

### *4.3.2 Site/Subindicator level*

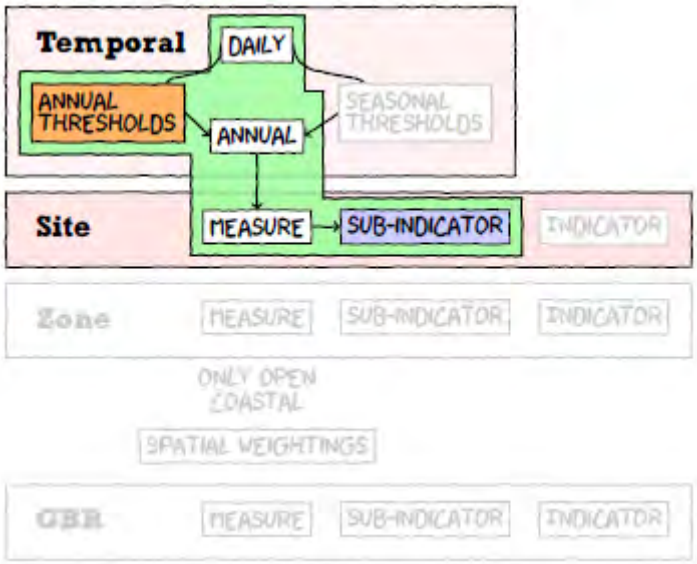


### *4.3.2.1 Site level maps*

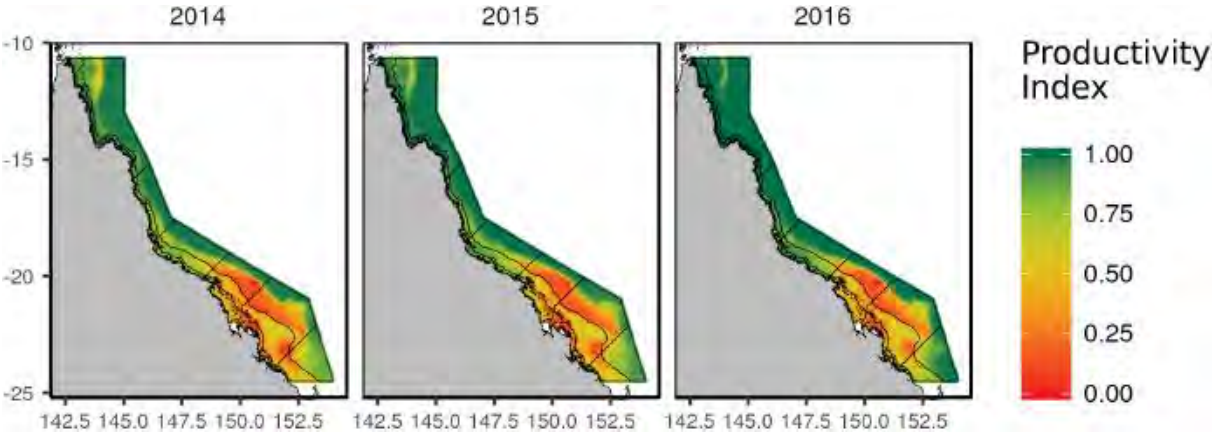


**Figure 81: Spatio-temporal patterns in eReefs fsMAMP Productivity index grades (Uniform grade type conversion applied).**

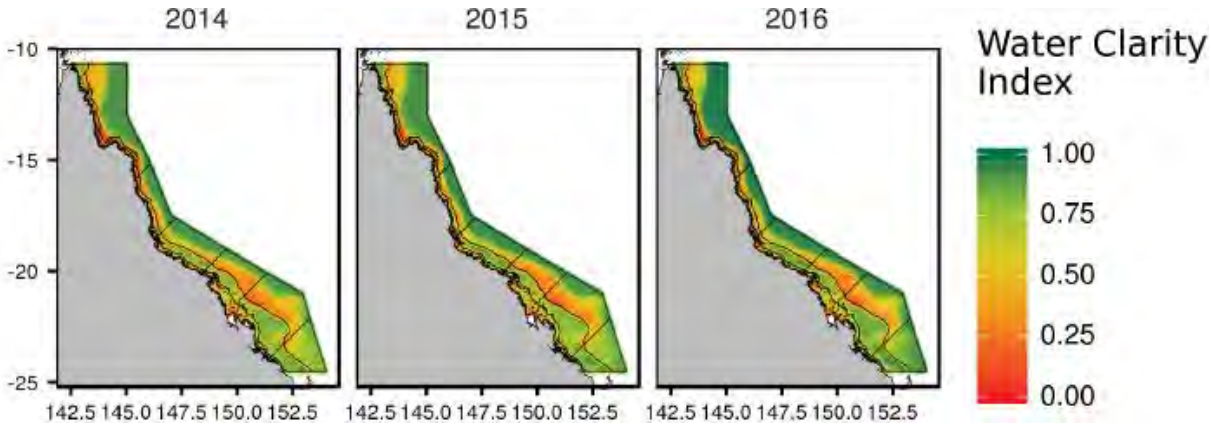


**Figure 82: Spatio-temporal patterns in eReefs fsMAMP Water Clarity index grades (Uniform grade type conversion applied).**

### *4.3.3 Site/Indicator level*

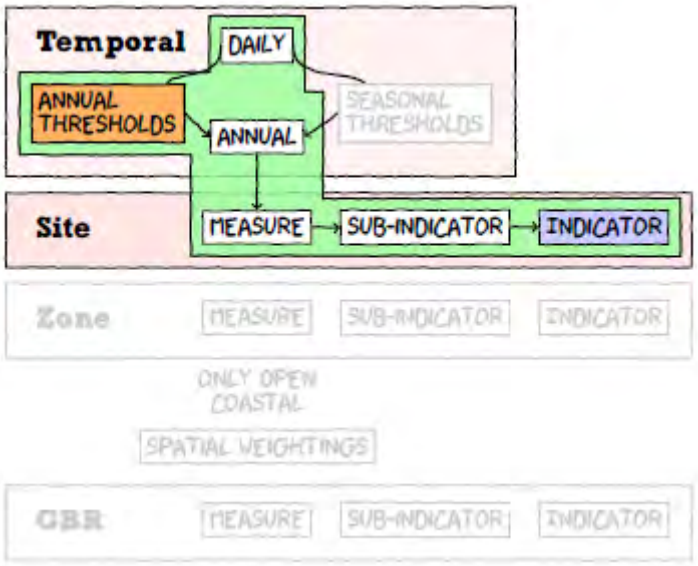


### *4.3.3.1 Site level maps*

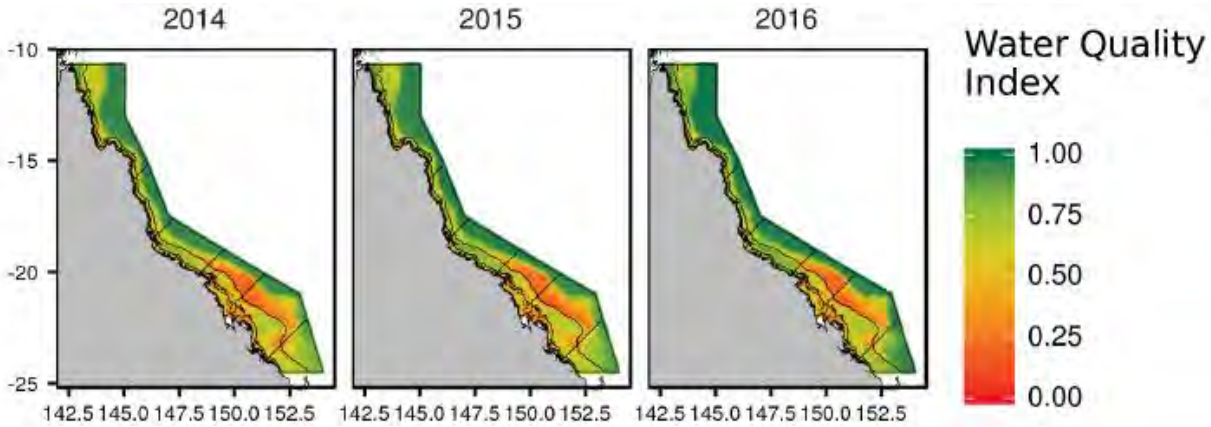


**Figure 83: Spatio-temporal patterns in eReefs fsMAMP Water Quality index grades (Uniform grade type conversion applied).**

### 4.3.4 Zone/Measure level

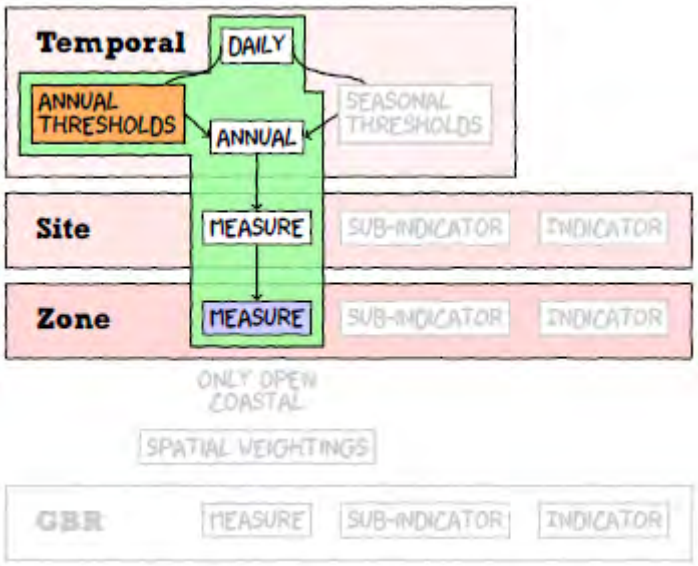

### 4.3.4.1 Simple time series

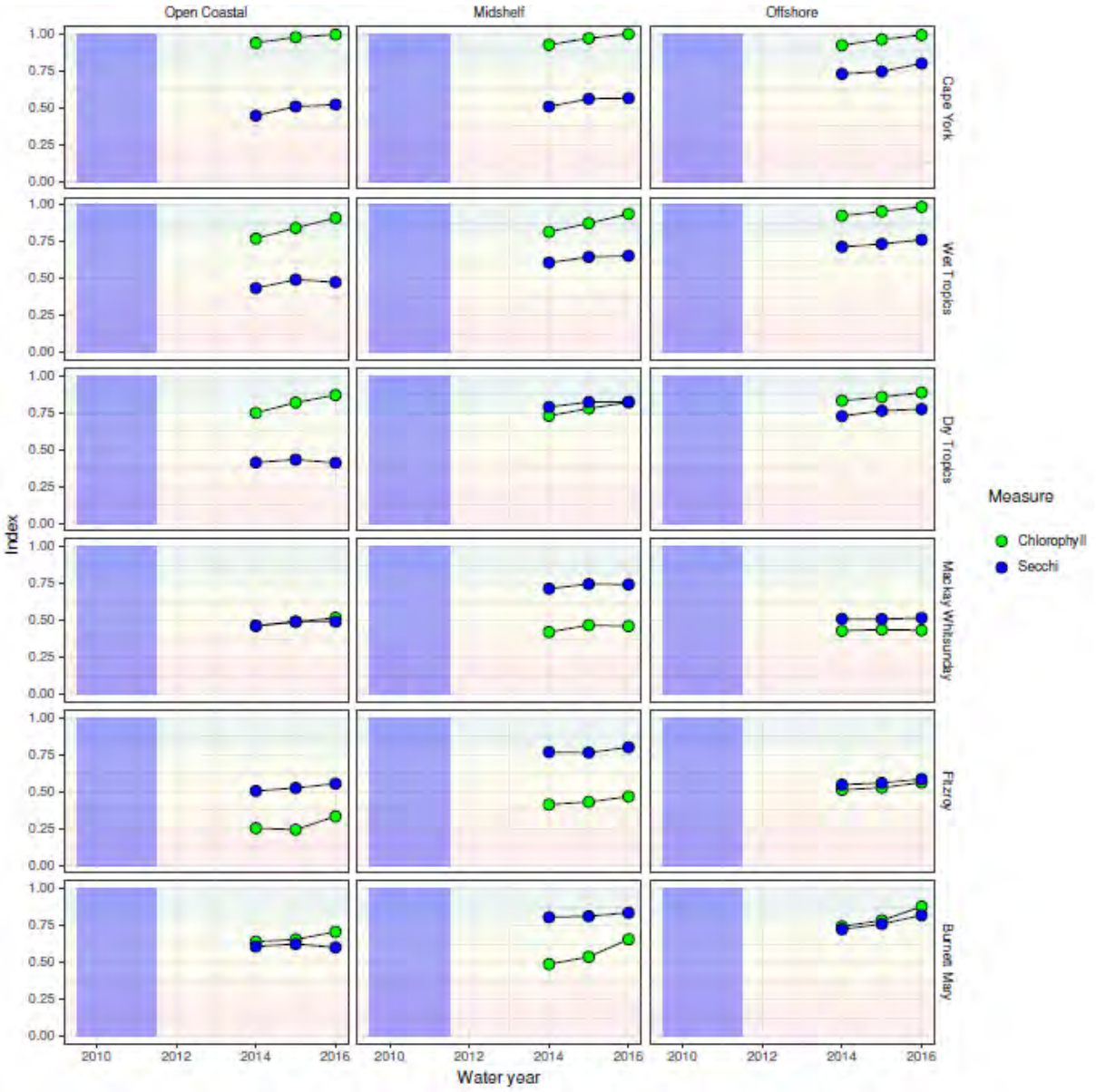


**Figure 84: Time series of fsMAMP measures (Chlorophyll-a and Secchi Depth) index scores by zone. The blue vertical bar spans from mid 2009 to mid 2011. Faint coloured horizontal bands represent Uniform grade ranges.**

### 4.3.4.2 Flat map

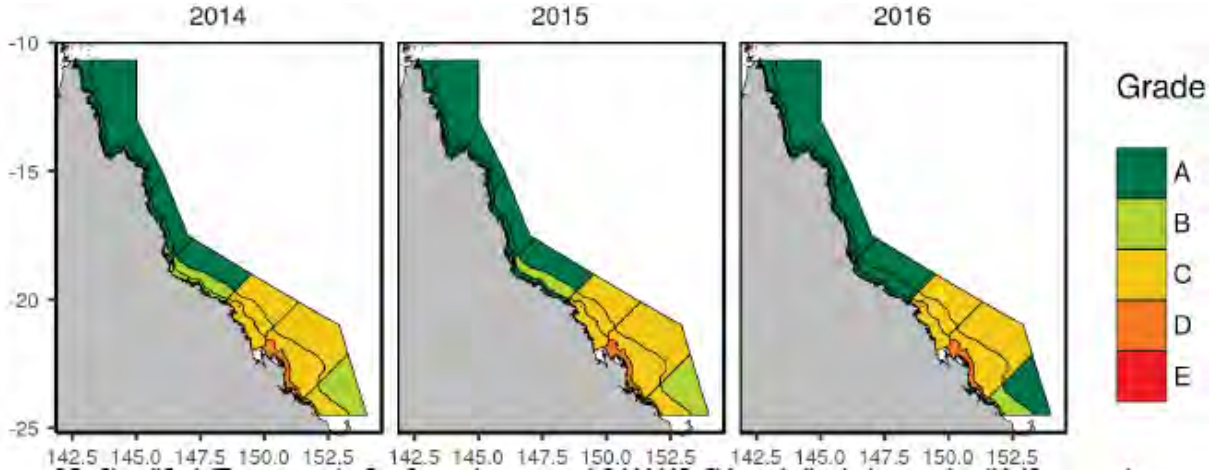


**Figure 85: Simplified (Zone mean) eReefs spatio-temporal fsMAMP Chlorophyll-a index grades (Uniform grade type Conversion applied).**

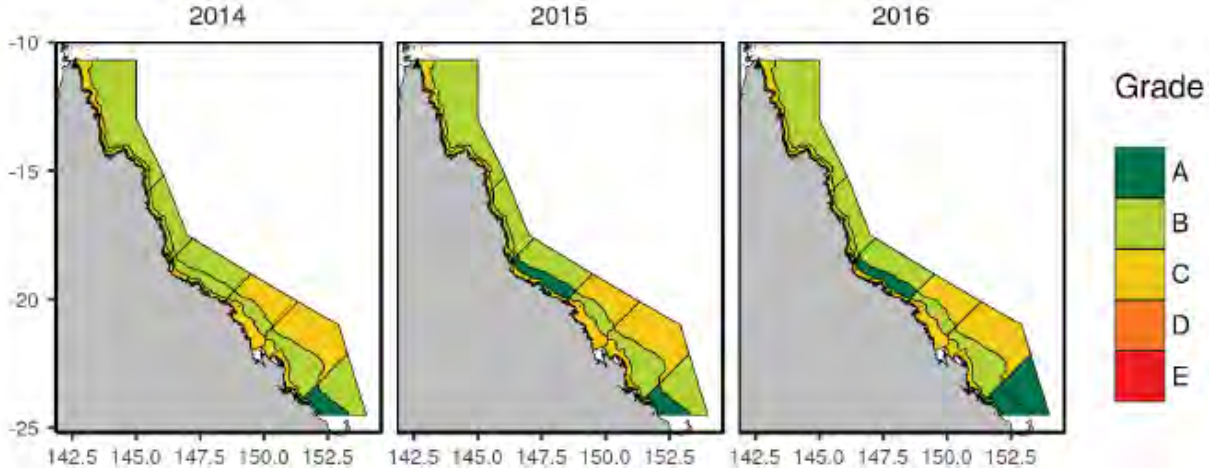


**Figure 86: Simplified (Zone mean) eReefs spatio-temporal fsMAMP Secchi Depth index grades (Uniform grade type conversion applied).**

### *4.3.4.3 Mosaic plots*


**Figure 87: Simplified (Zone mean) eReefs spatio-temporal fsMAMP Chlorophyll-a index grades (Uniform grade type conversion applied).**

### 4.3.5 Zone/Subindicator level

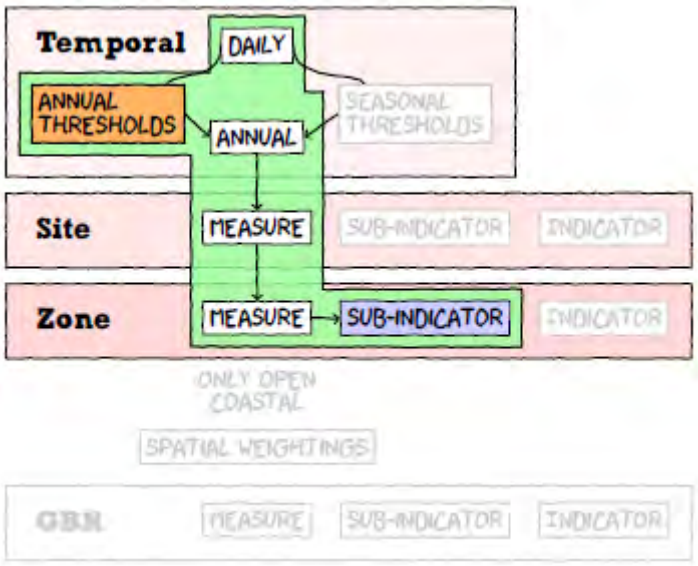

### *4.3.5.1 Simple time series*

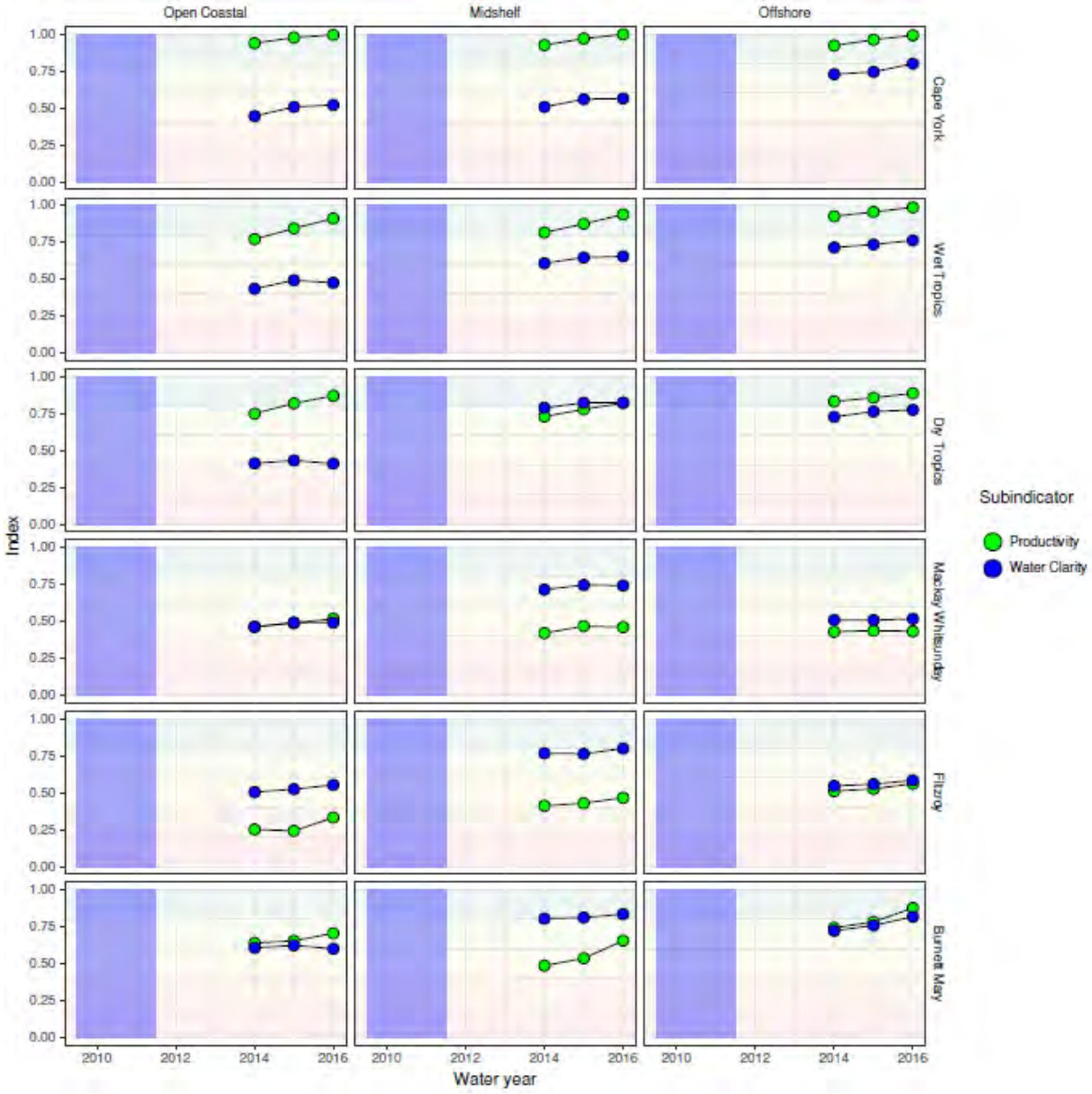


**Figure 88: Time series of fsMAMP Productivity and Water Clarity index scores by zone. The blue vertical bar spans from mid 2009 to mid 2011. Faint coloured horizontal bands represent Uniform grade ranges.**

### 4.3.5.2 Flat map

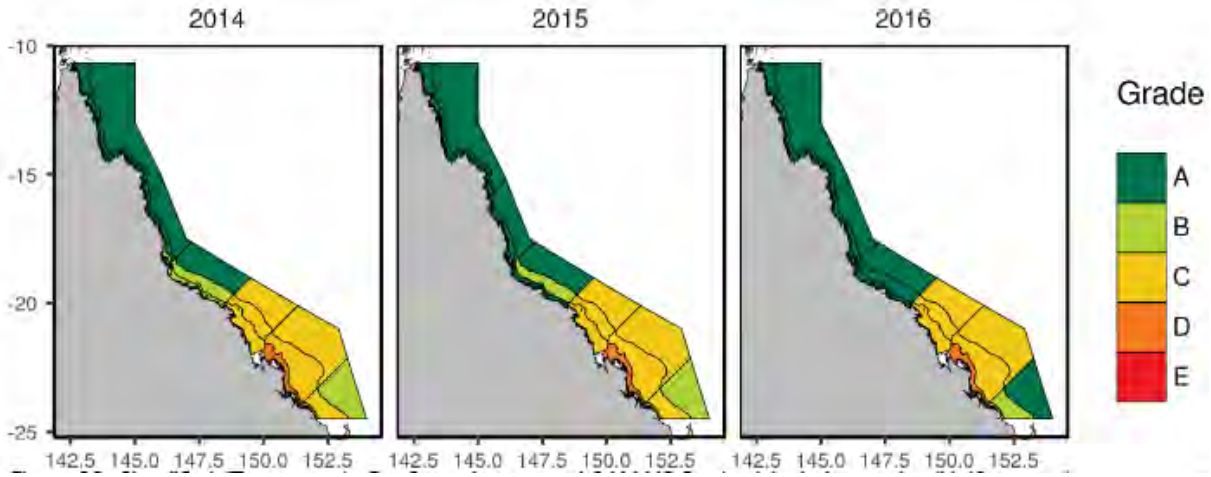


**Figure 89: Simplified (Zone mean) eReefs spatio-temporal fsMAMP Productivity index grades (Uniform grade type conversion applied).**

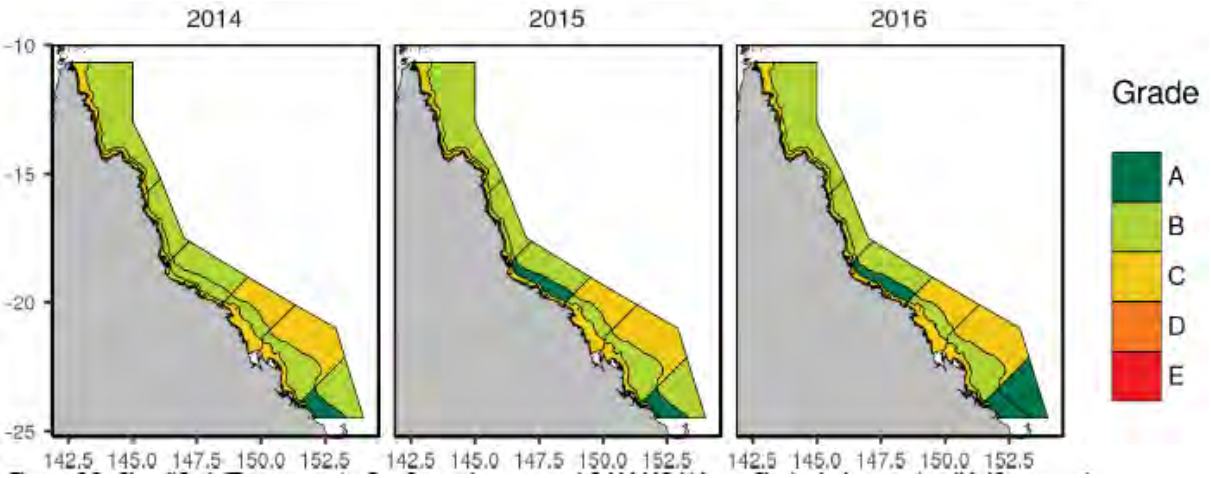


**Figure 90: Simplified (Zone mean) eReefs spatio-temporal fsMAMP Water Clarity index grades (Uniform grade type Conversion applied).**

### 4.3.5.3 Mosaic plots

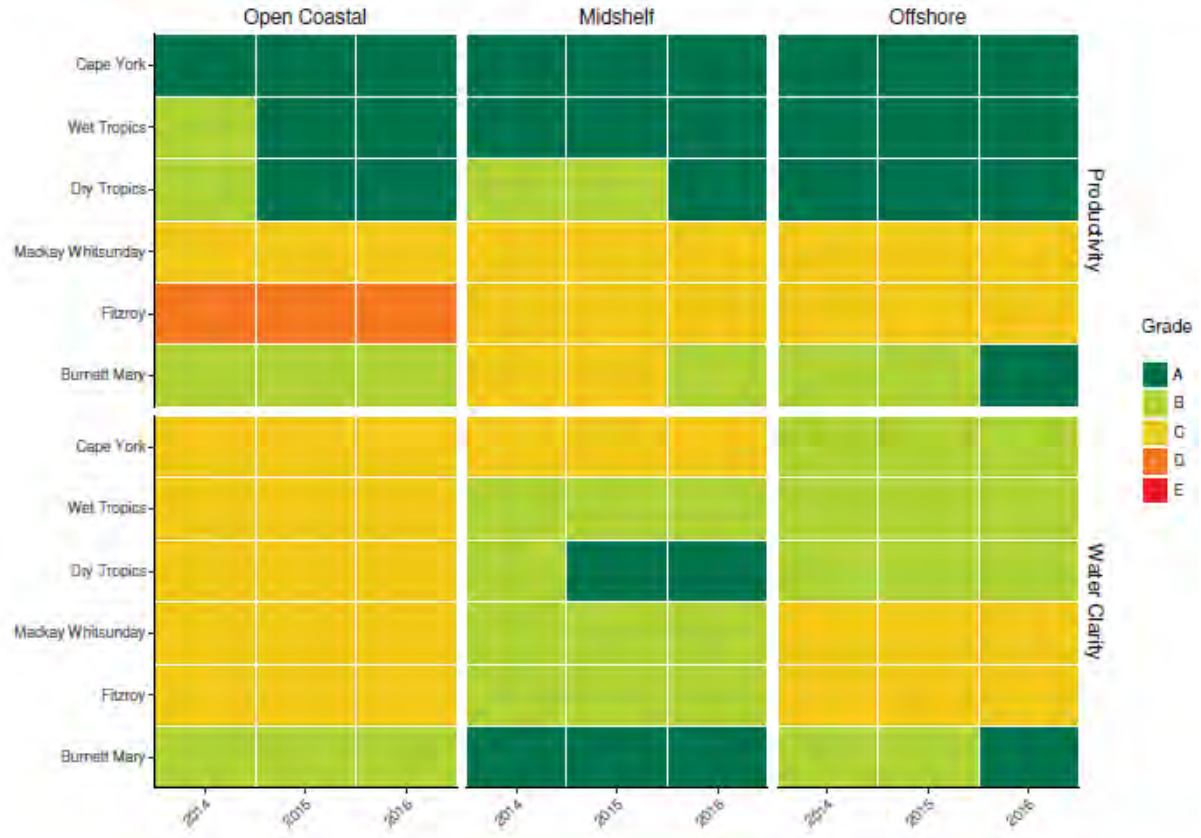


**Figure 91: Simplified (Zone mean) eReefs spatio-temporal fsMAMP Subindicator index grades (Uniform grade type Conversion applied).**

### 4.3.6 Zone/Indicator level

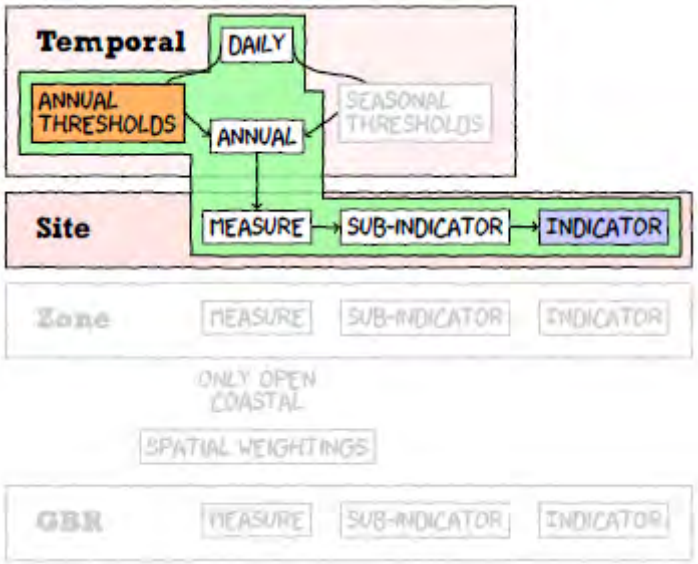

### 4.3.6.1 Simple time series

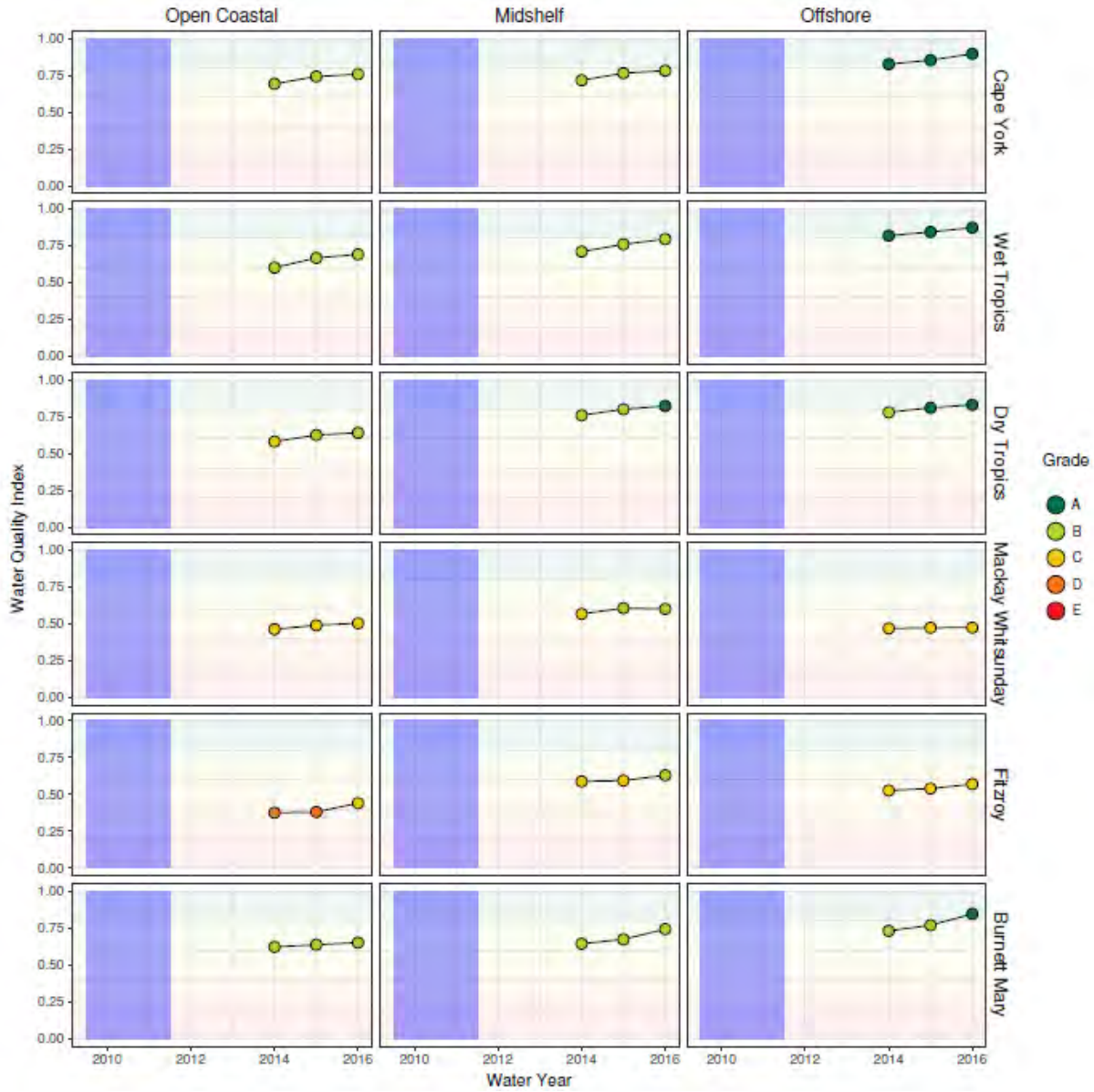


**Figure 92: Time series of fsMAMP Water Quality index scores by zone. The blue vertical bar spans from mid 2009 to mid 2011. Faint coloured horizontal bands represent Uniform grade ranges.**

### *4.3.6.2 Flat map*

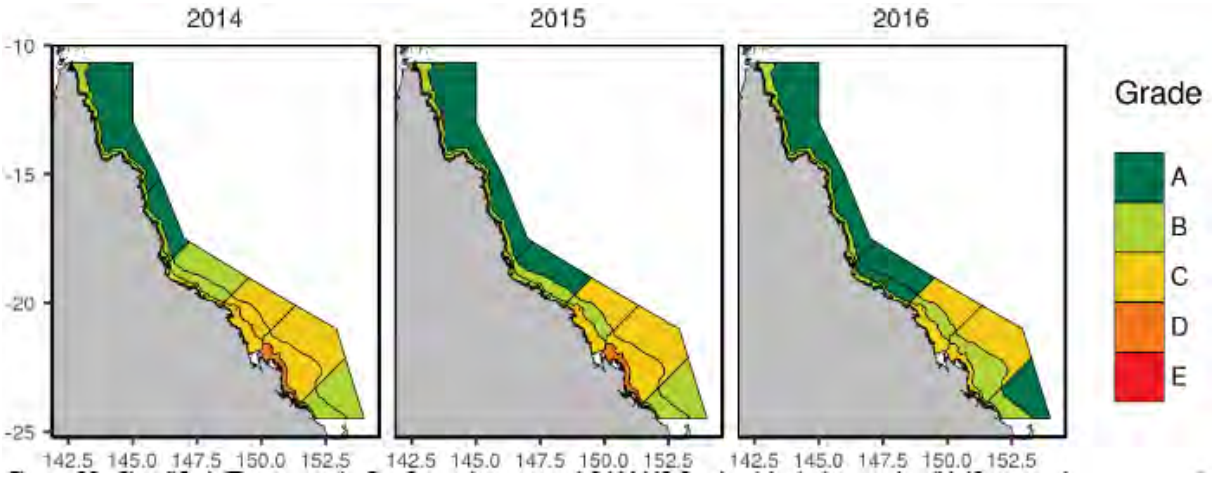


**Figure 93: Simplified (Zone mean) eReefs spatio-temporal fsMAMP Productivity index grades (Uniform grade type conversion applied).**

### *4.3.6.3 Mosaic plots*

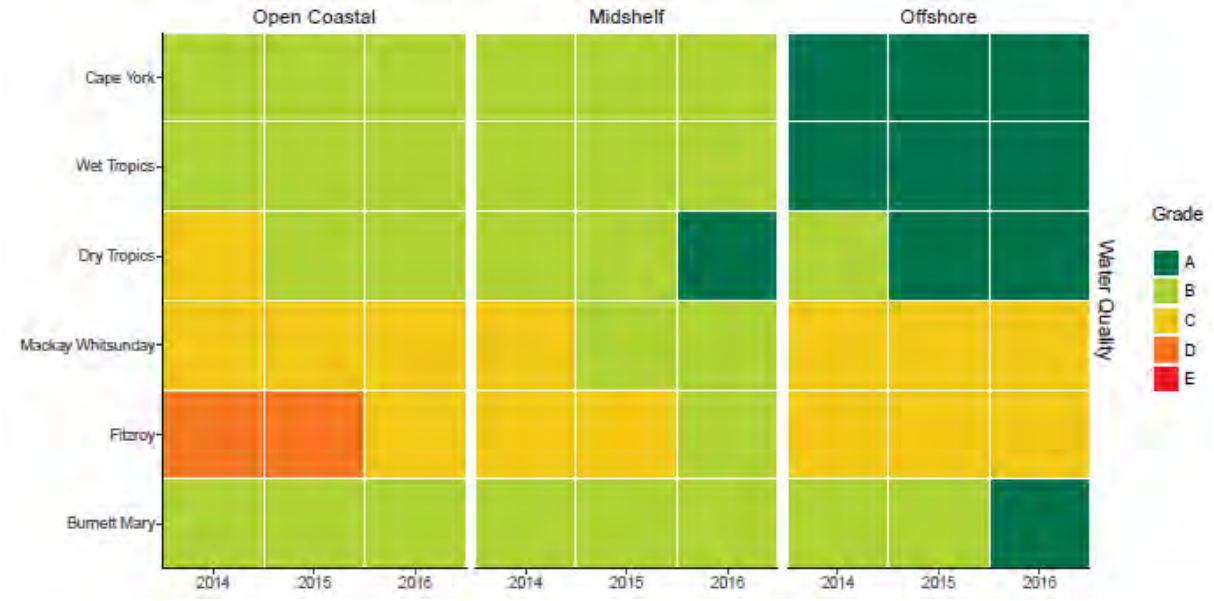


**Figure 94: Simplified (Zone mean) eReefs spatio-temporal fsMAMP indicator index grades (Uniform grade type conversion applied).**

## 4.4 Aggregations to water body level

### 4.4.1 Water body/Measure level

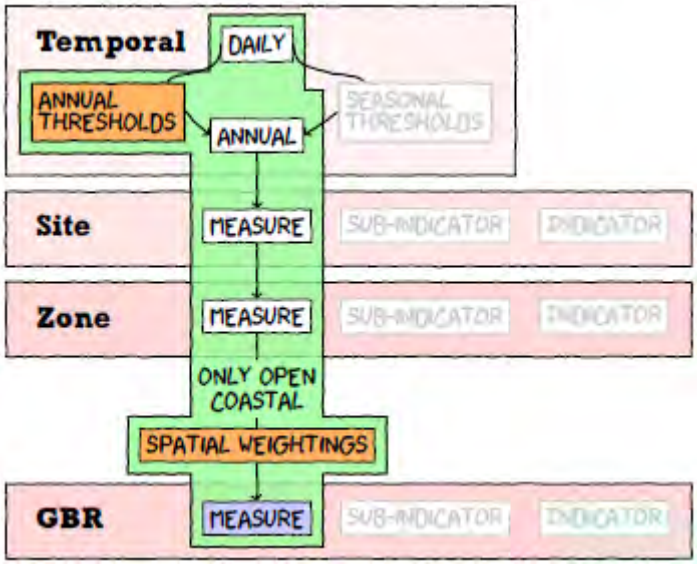


#### 4.4.1.1 Simple time series

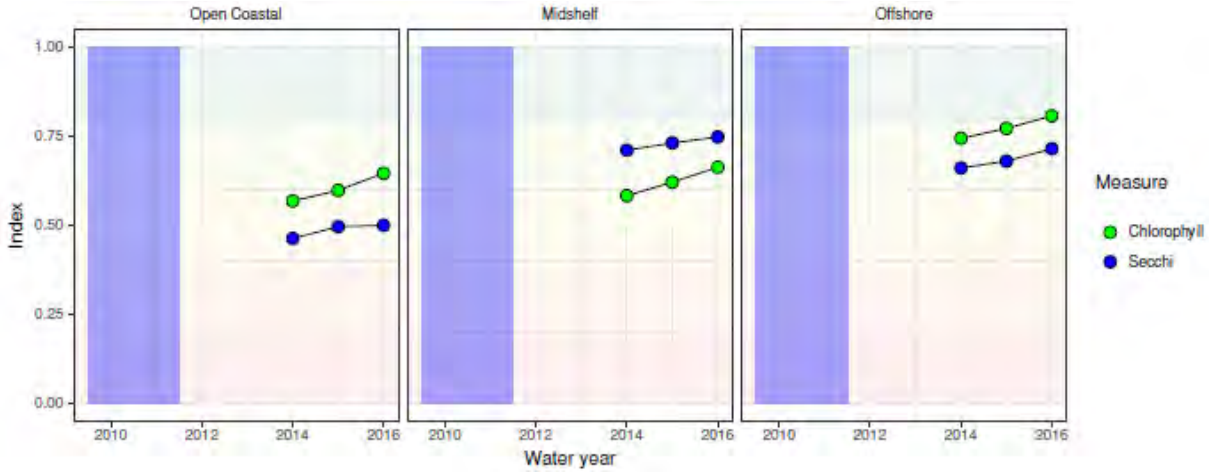


**Figure 95: Time series of fsMAMP Measure index scores by water body (aggregated over management region weighted by area). The blue vertical bar spans from mid 2009 to mid 2011. Faint coloured horizontal bands represent Uniform grade ranges.**

#### 4.4.1.2 Mosaic plots

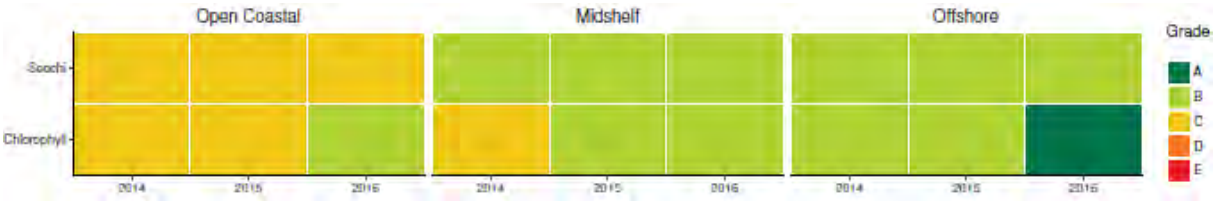


**Figure 96: Simplified (Zone mean) eReefs spatio-temporal fsMAMP Measurement index grades (Uniform grade type conversion applied).**

### 4.4.2 Water body/Subinidicator level

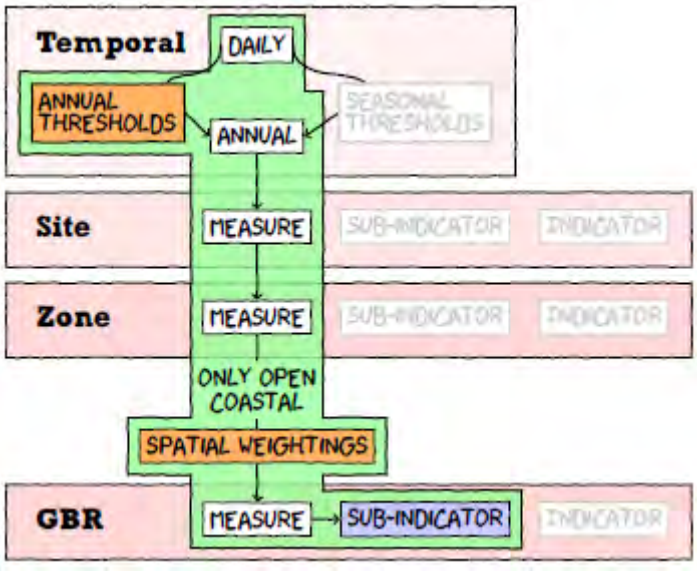


#### 4.4.2.1 Simple time series

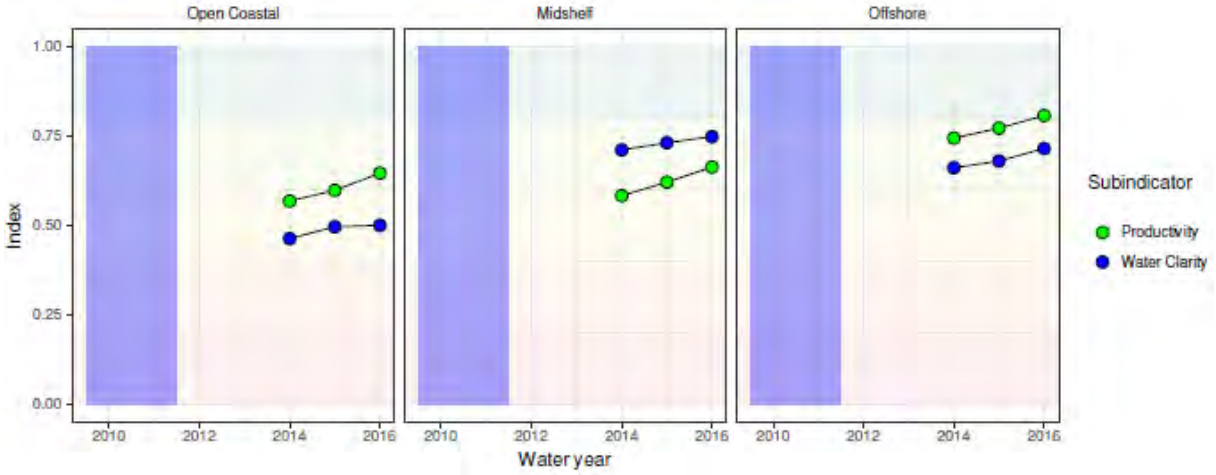


**Figure 97: Time series of fsMAMP Subindicator index scores by water body (aggregated over management region weighted by area). The blue vertical bar spans from mid 2009 to mid 2011. Faint coloured horizontal bands represent Uniform grade ranges.**

#### 4.4.2.2 Mosaic plots

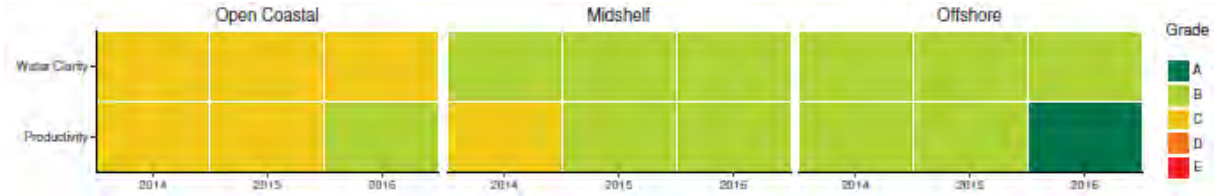


**Figure 98: Simplified (Zone mean) eReefs spatio-temporal fsMAMP Subindicator index grades (Uniform grade type conversion applied).**

### 4.4.3 Water body/Indicator level

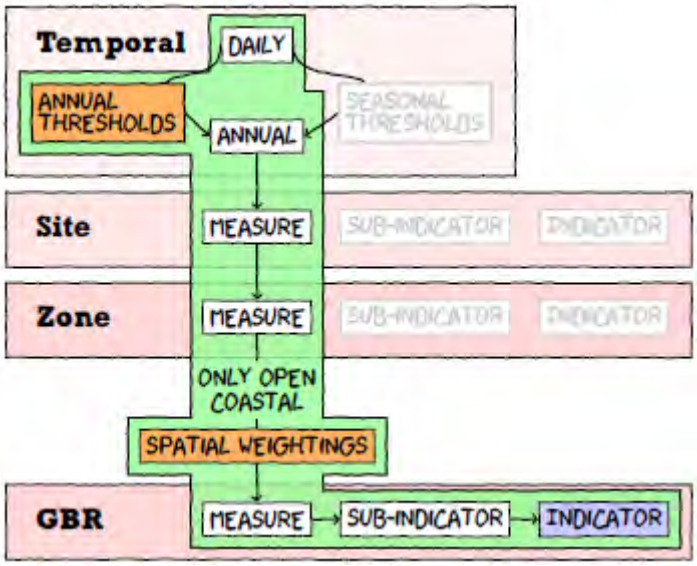


### 4.4.3.1 Simple time series

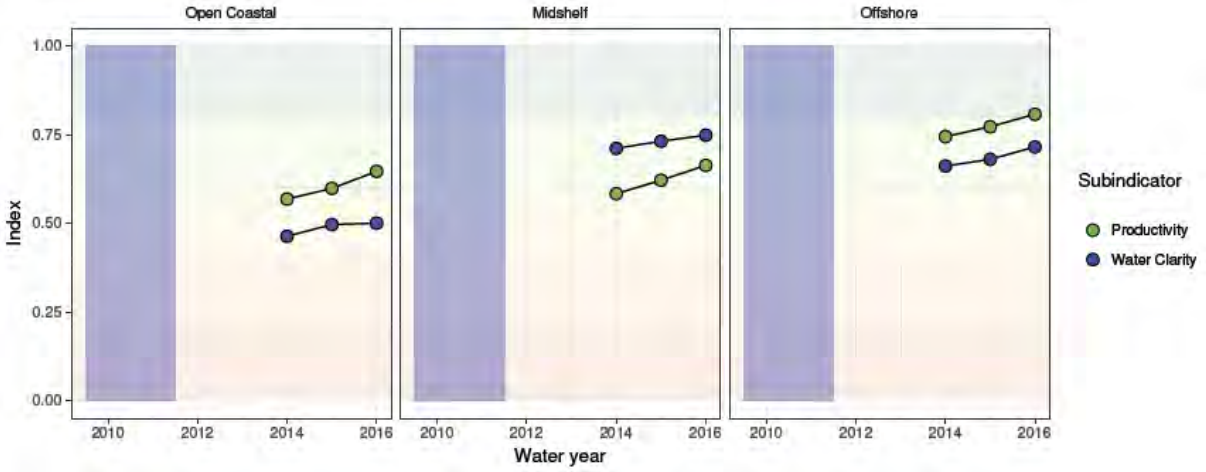


**Figure 99: Time series of fsMAMP Indicator index scores by water body (aggregated over management region weighted by area). The blue vertical bar spans from mid 2009 to mid 2011. Faint colored horizontal bands represent Uniform grade ranges.**

### 4.4.3.2 Mosaic plots

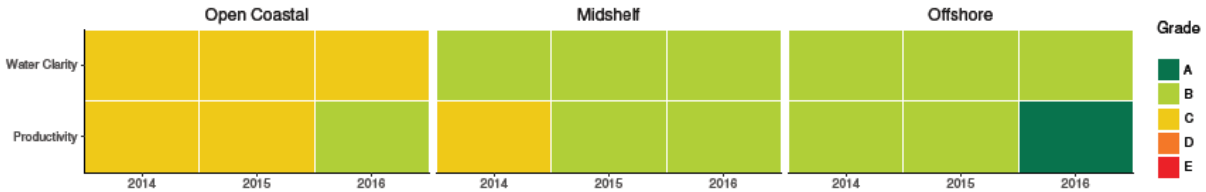


**Figure 100: Simplified (Zone mean) eReefs spatio-temporal fsMAMP Indicator index grades (Uniform grade type conversion applied).**

## 4.5 Aggregations to GBR level

### *4.5.1 GBR/Measure level*

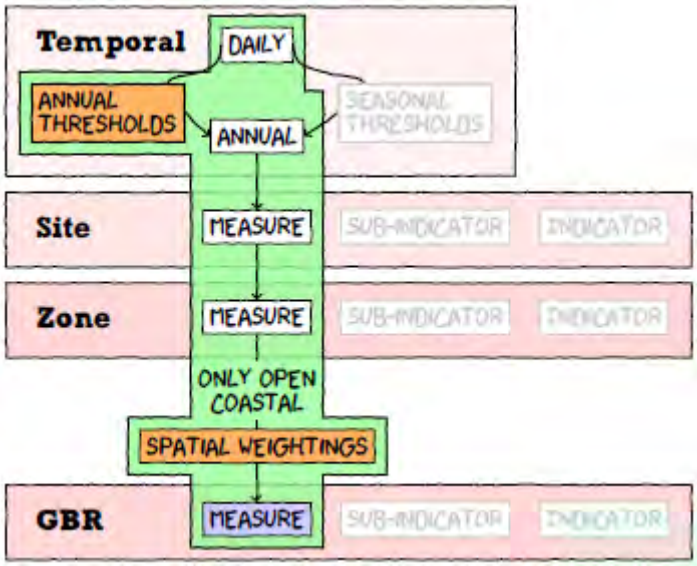

### 4.5.1.1 Simple time series

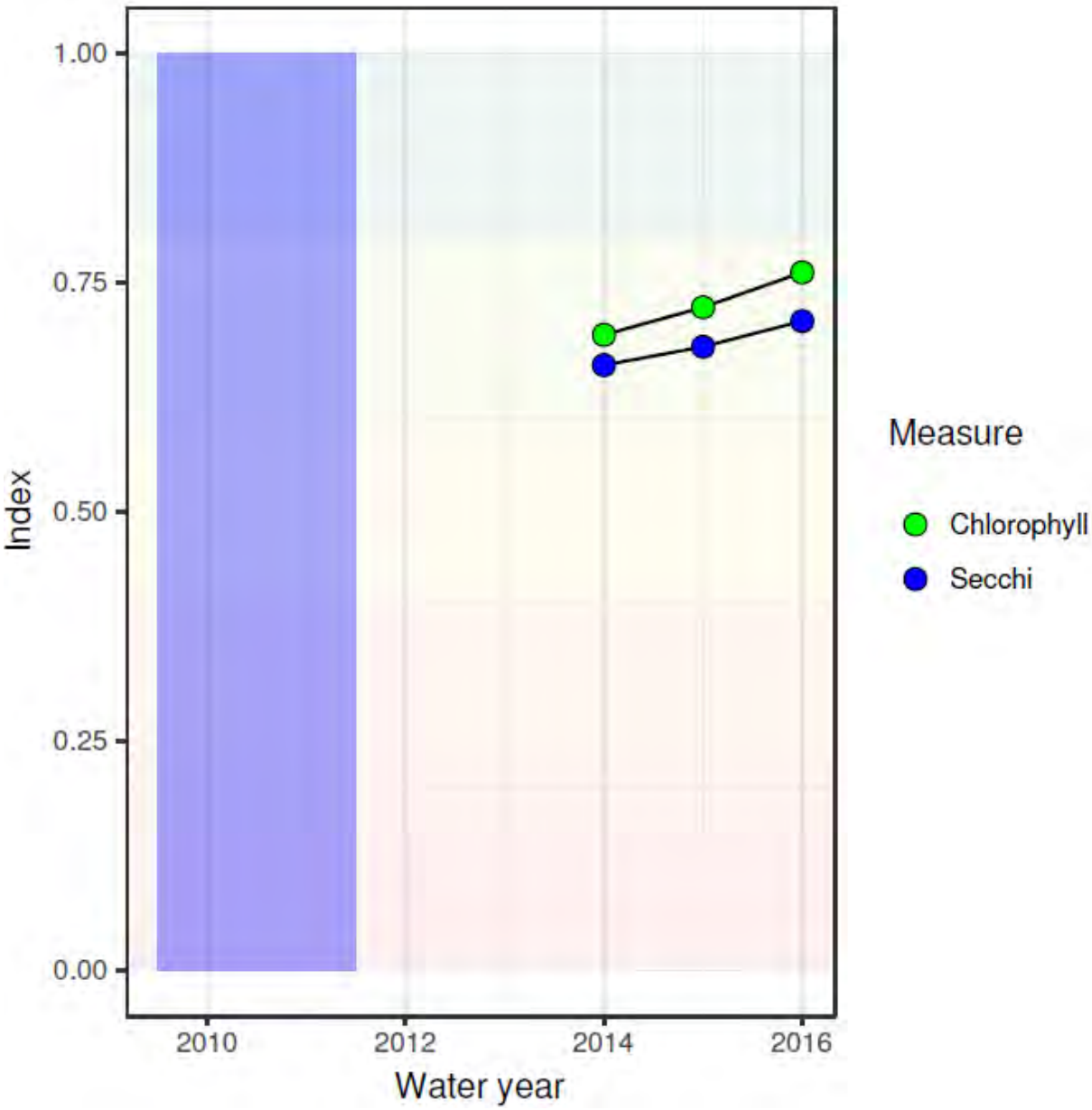


**Figure 101: Time series of fsMAMP Measure index scores by GBR (aggregated over management region weighted by area). The blue vertical bar spans from mid 2009 to mid 2011. Faint coloured horizontal bands represent Uniform grade ranges.**

### 4.5.1.2 Mosaic plots

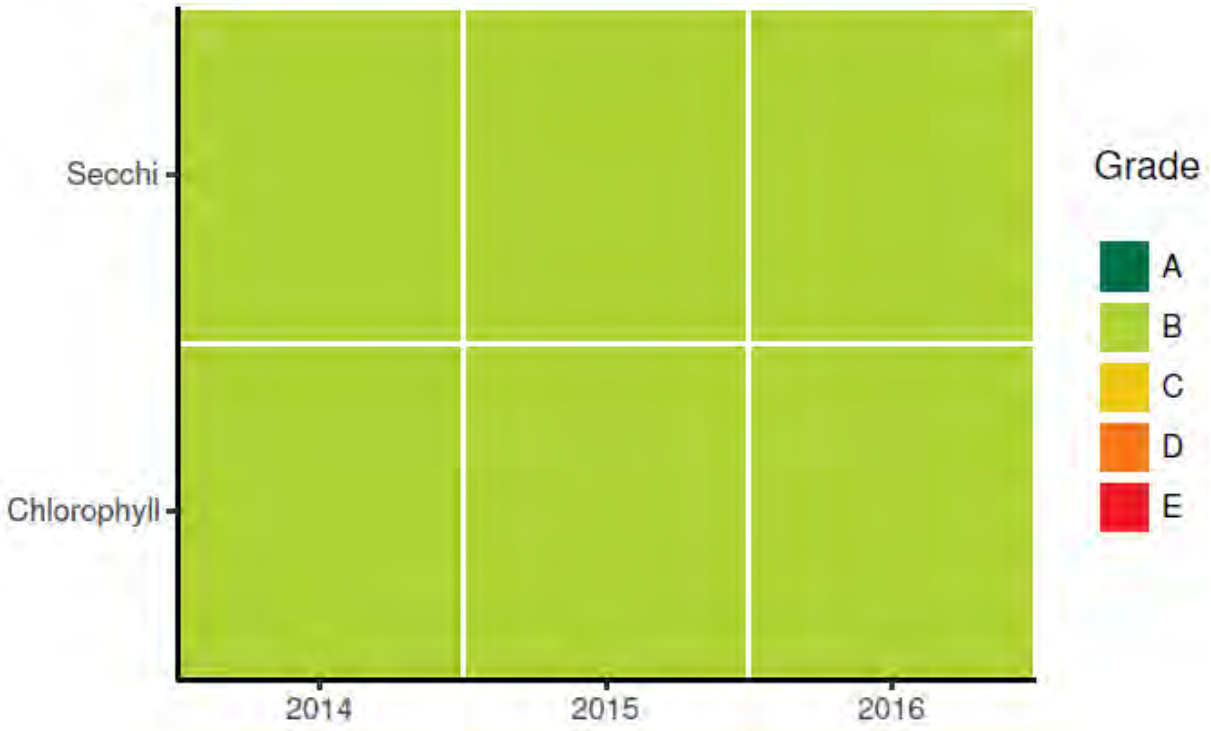


**Figure 102: Simplified (Zone mean) eReefs spatio-temporal fsMAMP Measurement index grades (Uniform grade type conversion applied).**

### 4.5.2 GBR/Subindicator level

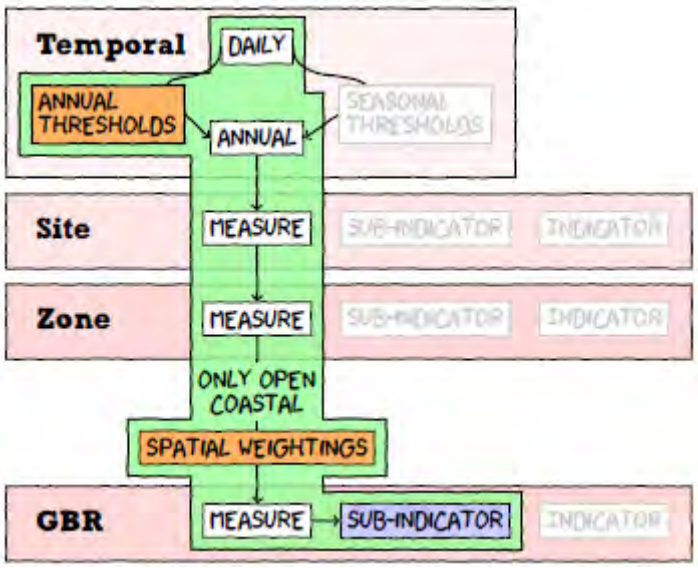

### 4.5.2.1 Simple time series

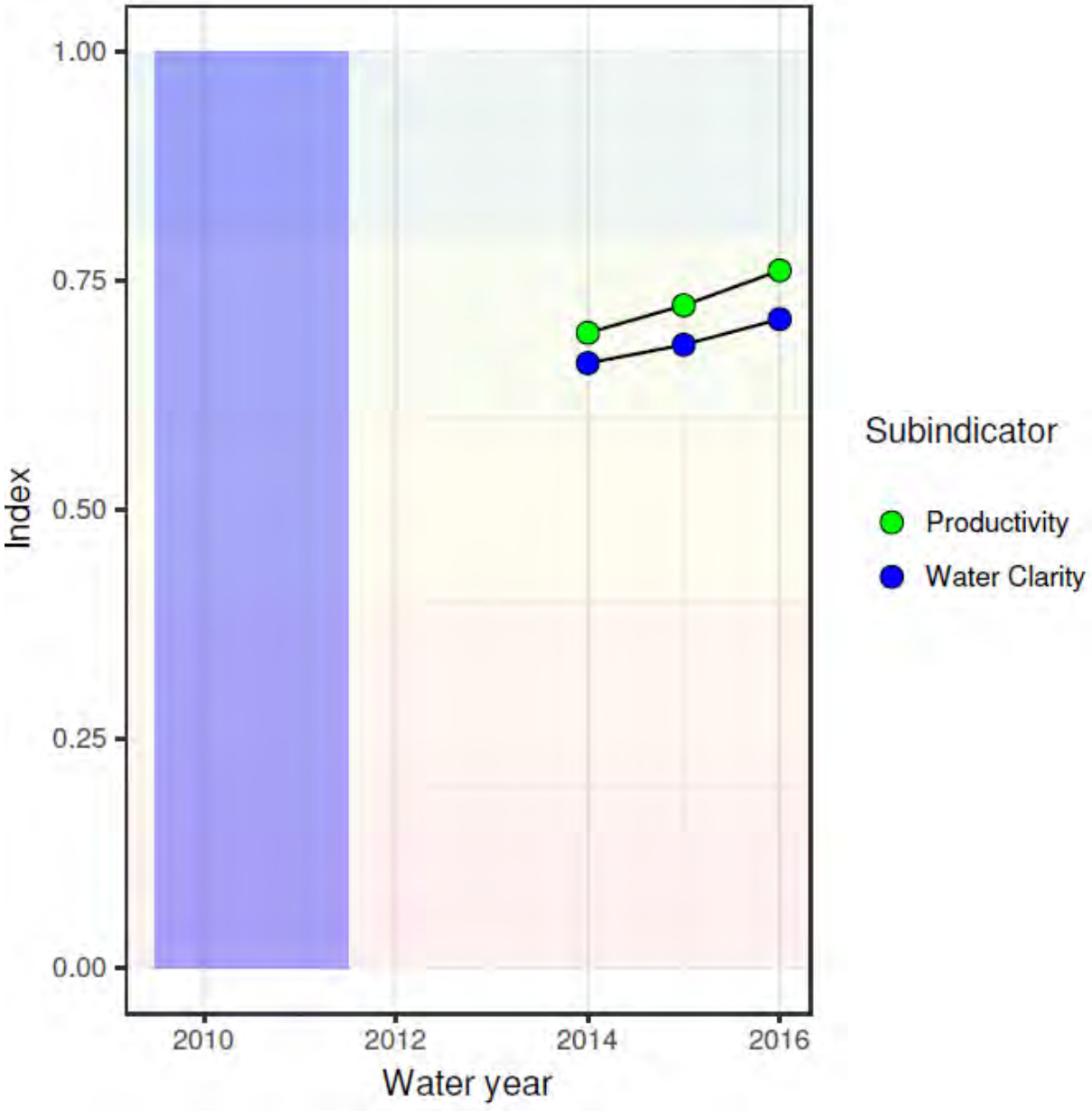


**Figure 103: Time series of fsMAMP Subindicator index scores by GBR (aggregated over management region weighted by area). The blue vertical bar spans from mid 2009 to mid 2011. Faint coloured horizontal bands represent Uniform grade ranges.**

### 4.5.2.2 Mosaic plots

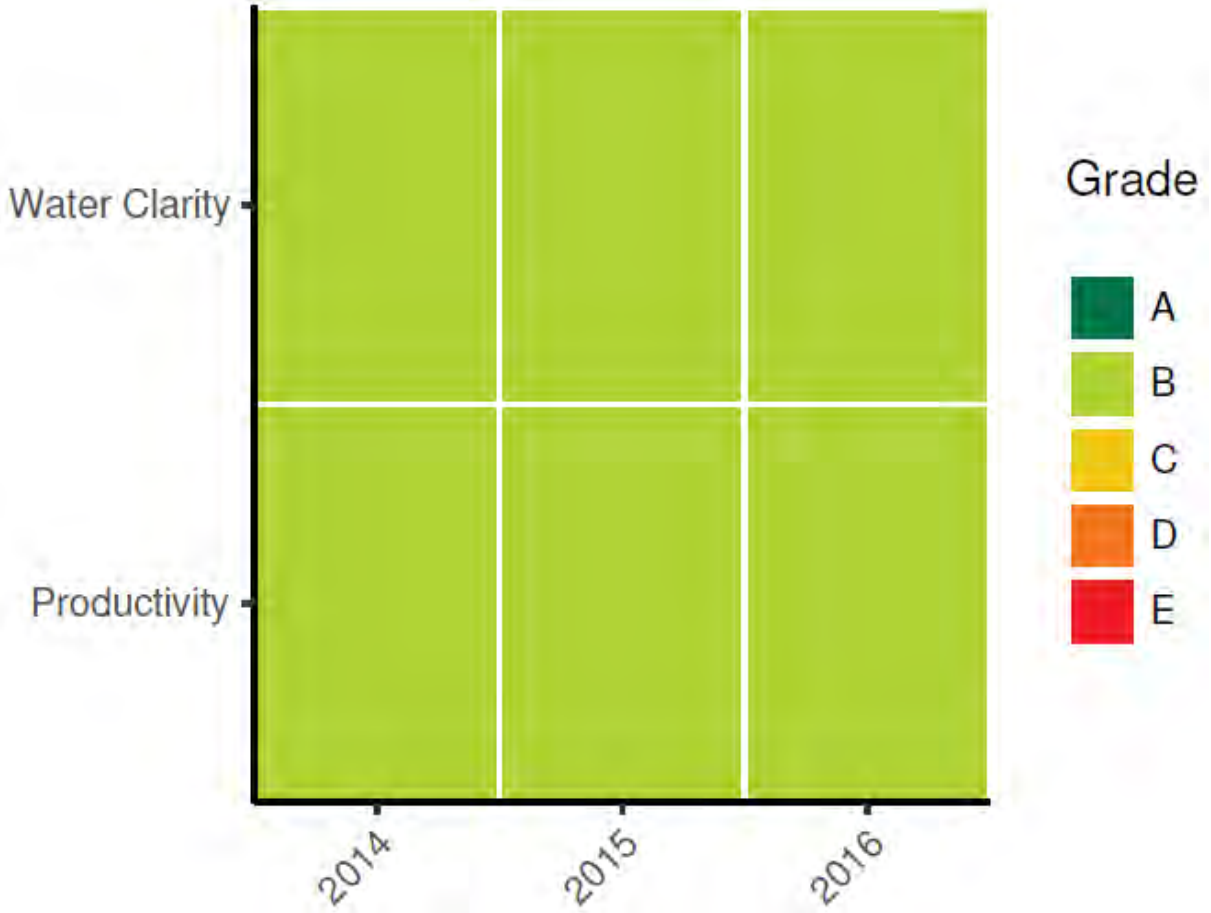


**Figure 104: Simplified (Zone mean) eReefs spatio-temporal fsMAMP Subindicator index grades (Uniform grade type conversion applied).**

### 4.5.3 GBR/Indicator level

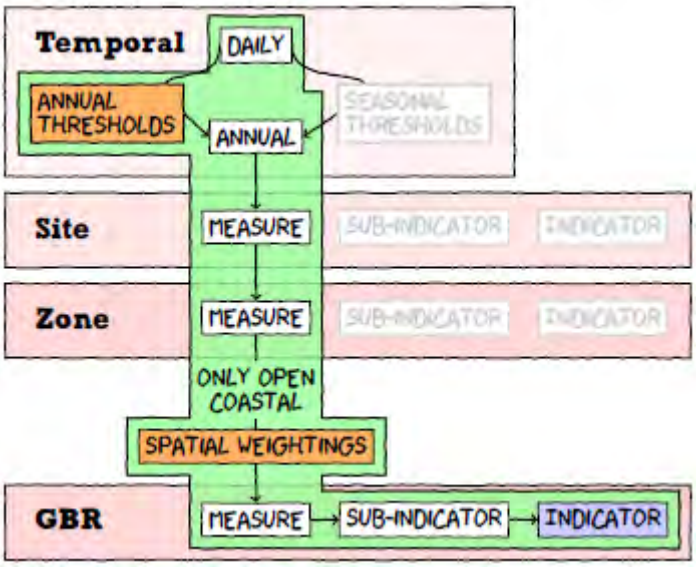

### 4.5.3.1 Simple time series

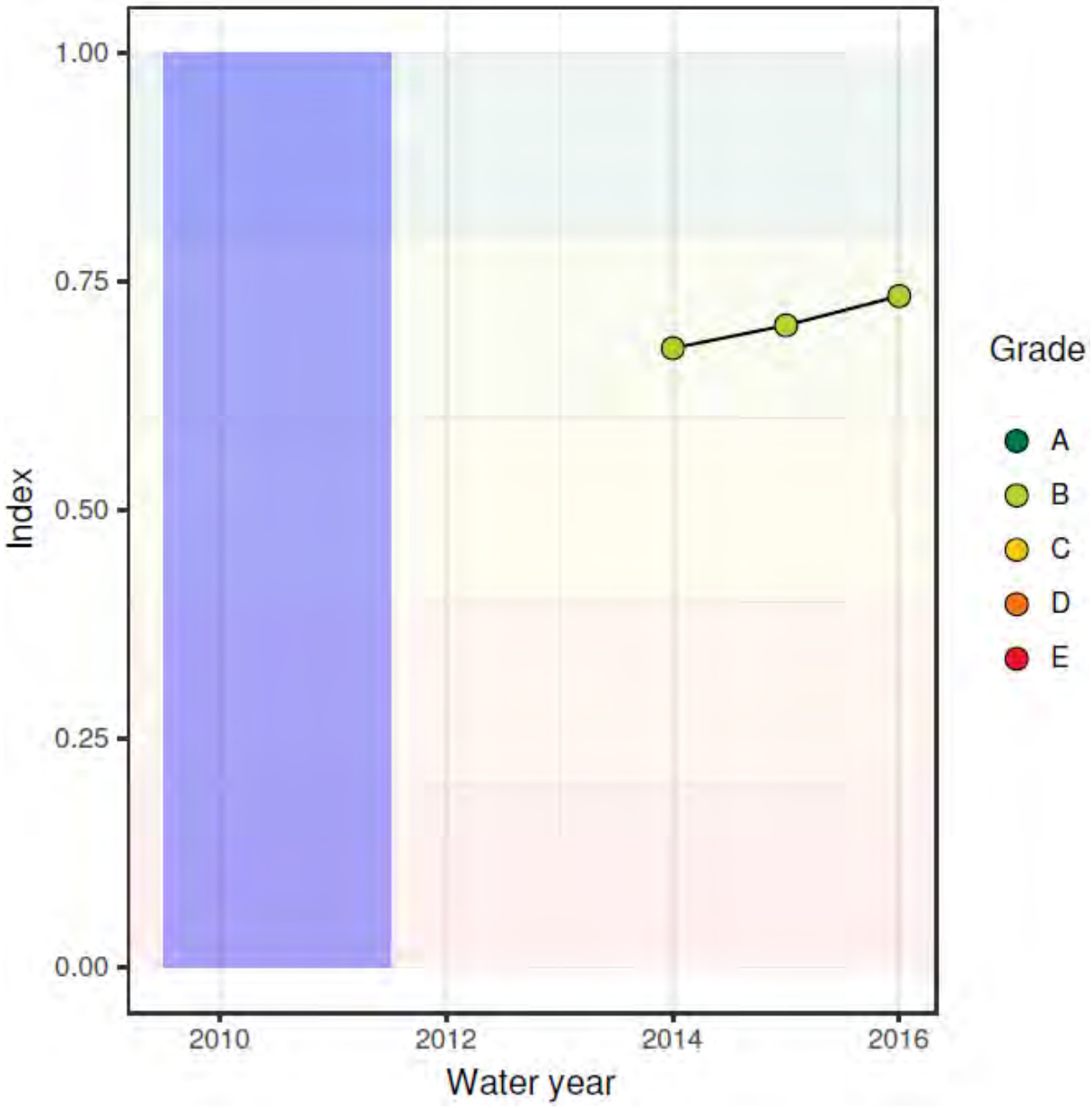


**Figure 105: Time series of fsMAMP Indicator index scores by GBR (aggregated over management region weighted by area). The blue vertical bar spans from mid 2009 to mid 2011. Faint coloured horizontal bands represent Uniform grade ranges.**

### 4.5.3.2 Mosaic plots


**Figure 106: Simplified (Zone mean) eReefs spatio-temporal fsMAMP Indicator index grades (Uniform grade type conversion applied).**

## 4.6 Summary of recommendations

A. Calculation of Zone level Score and Grades

1. Collect raw data (= Measures) for Chlorophyll-a and Secchi depth at each fixed monitoring site and compare individual observations to associated threshold/benchmark/reference or set of expectation ranges
2. Create indexed data as an expression of degree of difference (*scaled modified amplitude method*) to yield a Score for each Measure (Chlorophyll-a and Secchi depth) per sampling location (e.g. Site)
3. Combine Measure Scores into Site-level Sub-indicator (Productivity and Water Clarity) Scores by averaging
4. Combine Sub-indicator Scores into Site-level Indicator (Water Quality) Scores by averaging.
5. Convert Scores into coloured Grades (A-E) for visual presentation in report card

B. Calculation of Zone level Grades

1. Aggregate Site-level *Measure* Scores from step A.1 into Zone-level *Measure* Scores by averaging.
2. Aggregate Zone-level *Measure* Scores into Zone-level *Subindicator* Scores by averaging.
3. Aggregate Zone-level *Subindicator* Scores into Zone-level *Indicator* Scores by averaging.

C. Calculation of Whole GBR Grades

1. Aggregate Zone-level *Measure* Scores for Open Coastal Regions from step B.1 into Whole GBR-level *Measure* Scores by averaging (incorporating spatial weights).
2. Aggregate Whole GBR-level *Measure* Scores into Whole GBR-level *Subindicator* Scores.
3. Aggregate Whole GBR-level *Subindicator* Scores into Whole GBR-level *Indicator* Scores by averaging.

# 5.0 EXPLORATION OF FOCAL AREAS

In addition to working with the 24 large GBRMPA regions and water bodies, it is possible to define very specific spatial and temporal domains that might represent areas of greater focus. For example, it might be of interest to model water quality patterns in a defined area proximal to a source of river discharge as part of an exploration into water quality responses to catchment outcomes.

Small spatial domains also presents an opportunity to explore data assimilation options. The current project has access to four streams of water quality data (discrete AIMS niskin samples, AIMS FLNTU data, Satellite remote sensing and eReefs modelled data). Assimilating eReefs data (4km resolution) and Satellite data (1km resolution) as presented in the eReefs model data represents substantial computational overheads as a result of their high dimensionality. Whilst the discrete AIMS niskin sample is substantially more sparse, it does nonetheless present its own challenges when it comes to assimilation (see below).

We have three choices for combining the discrete AIMS niskin sample data with the eReefs assimilated model data:

1. aggregate together the average discrete (Niskin) sample and the average eReefs data or indices.
2. assimilate via an Ensemble Kalman Filter similar to the eReefs/Satellite data assimilation
3. define a Gaussian Process that incorporates both the discrete AIMS niskin data and eReefs assimilated data
4. assimilate via Fixed Rank Kriging

As a motivating example, we will use the discrete AIMS niskin and eReefs model data surrounding a single Dry Tropics Midshelf AIMS MMP site (Yongala). Yongala is a deep water site and thus the eReefs and discrete AIMS niskin samples are likely to have been collected across a relatively homogeneous bathymetry. Initial discussions will focus only on data from a single day (25/03/2017). The spatial configuration of eReefs observations relative to the AIMS MMP Yongala niskin sampling location is displayed in Figure 107.

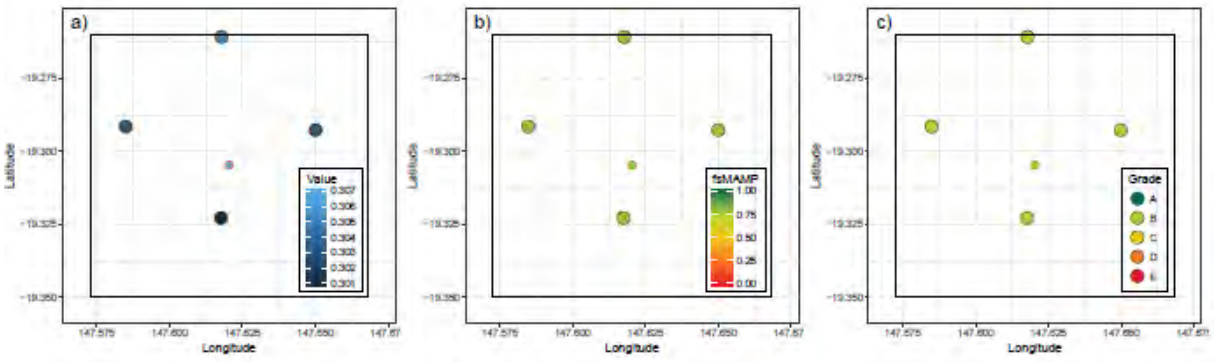


**Figure 107: Spatial distribution of eReefs observation locations within 5km of the Yongala AIMS MMP niskin sampling location (point with red outline). Observations represent a) Chlorophyll-a values and associated b) fsMAMP indices and c) Grades (Uniform conversion) for 25/03/2015.**

Importantly, although the AIMS niskin sample is located geographically roughly in the middle of the eReef locations, its Chlorophyll-a value (and fsMAMP index) is higher (and lower) than the surrounding eReefs values. Although this is only subtle in this example, it will be drawn upon when discussing aggregation options. The fact that the observed AIMS niskin Chlorophyll-a sample collected on 25/03/2015 is higher than the surrounding eReefs estimates might suggest that either or both observation sets are only representative of limited scales. More specifically, it is likely that whilst the AIMS niskin samples only accurately reflect very local conditions, the 4km eReefs data are only likely to be reflective of broad larger scale conditions[24].

The above situation is likely to be exacerbated in highly heterogeneous seascapes. AIMS niskin samples are typically collected in close proximity to coral reefs where the general hydrology and input process might be substantially different to the surrounding deeper water. By contrast, the eReefs model is known to be less reliable in shallow water. Thus, in areas that are heterogeneous with respect to bathymetry and hydrology, the AIMS niskin observations are likely to be representative of only the immediate vicinity (with very similar hydrology etc), whereas the eReefs observations might represent 'average' conditions that are only appropriate when considered on relatively large scales. The 4km resolution of eReefs model is unlikely to present adequate granularity in areas that are heterogeneous with respect to bathymetry and hydrology.

Hence, the scale incompatibilities are likely to limit the ability to combine these two sources of data in a meaningful and reliable manner.

It is also possible that the accuracy of the two sources differ. Unfortunately, in the absence of a 'truth' this is difficult to assess. Nevertheless, since the eReefs data are indirect measures, it is possible that they are not as accurate as the AIMS niskin observations. If we had co-located observations (observations collected at the same locations and times from each source), we could attempt to align or calibrate the sources to one another. However, it is not possible to perform such alignments when data are not co-located and there is suspected differences in their spatial representation envelopes.

## 5.1 Simple aggregation

If we initially ignore all temporal aspects of the data and focus on the single day (25/03/2015), we could aggregate together the single discrete AIMS Niskin sample observation with the average of the four eReefs observations to yield a single Chlorophyll-a estimate for the Yongala focal area (see Figure 108a). Alternatively, we could aggregate Chlorophyll-a indices (see Figure 108b-c).

[24] The eReefs observations represent average modelled conditions within a 4x4km square cell, and therefore whilst potentially broadly reflective of large scale conditions, may not actually be an accurate reflection of anywhere in that 4x4km cell

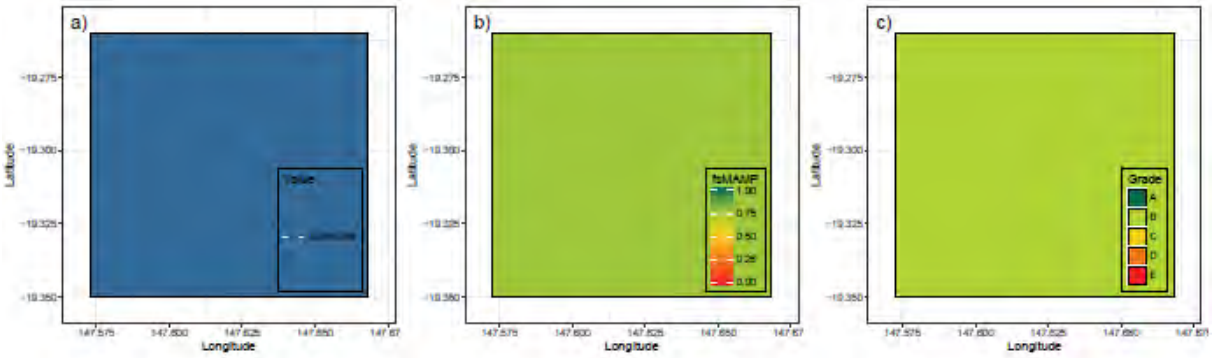


**Figure 108: Yongala focal area aggregated a) Chlorophyll-a values and associated b) fsMAMP indices and c) Grades (Uniform conversion) for 25/03/2015.**

Critically, this technique does assume that the single discrete AIMS niskin sample is representative of the entire spatial domain of the Yongala focal area. That is, we assume that the focal area mean is equal to this single point estimate. As previously discussed, this is likely to be an unrealistic expectation. We currently do not have any information on the spatial envelope represented by discrete samples. It is highly likely that the discrete samples are spatially biased (unrepresentative of the broader area as they are typically designed to sample reefs rather than the general water body. Rather it is likely that the discrete sample only represent the immediate vicinity and uncertainty should decline with increasing distance. That said, the form to which certainty (representation) declines is completely unknown making it impossible to incorporate.

Furthermore, for the purpose of propagating uncertainty, the spatial uncertainty associated with the AIMS niskin sample is assumed to remain constant throughout this focal area. That is, our confidence in the focal mean is informed purely in our confidence in the single observation and that there is no additional loss of confidence associated with increasing distance from the sampling location. Obviously, it is highly unlikely that the reliability of the estimate will remain constant. The same is true for eReefs data, although it is likely to be less of an issue due to the greater sample size and spatial extent.

## 5.2 Ensemble Kalman Filter data assimilation

This is the approach used to assimilate the Satellite data into the eReefs model. Data Assimilation (DA) is a technique with forecasting and reanalysis, the latter of which involves conditioning estimates of state on multiple sources of data. For example, high density modelled data based on thermodynamics and gas laws might be 'calibrated' or augmented by data observed at weather stations. The Kalman filter estimates state as the joint probability distribution ($p(y|x)$ which according to Bayes rule is proportional to the prior probability ($p(x)$) multiplied by the probability (likelihood) of the observational data ($p(y|x)$). The simple Kalman filter provides algebraic expressions that describe the transition of state mean and covariance over time assuming all probability density functions are Gaussian and the transition is linear. If we say we have a prior belief that the state ($x$) has a mean of $\mu$ and covariance of $Q$ and that the data ($d$) have an expected value of $Hx$ and covariance of $R$, it can be shown that the posterior mean ($\hat{\mu}$) and covariance $\hat{Q}$ are:

$$\hat{\mu} = \mu + K(d - Hx), \hat{Q} = (I - KH)Q$$

where *K* (the Kalman gain) is:

$$K = QH^T(HQH^T + R)^{-1}$$

Unfortunately, as the domain of *x* increases (higher dimensionality), the covariance becomes prohibitively large. If however, the state space ($x$) is broken up into a series of states (each perhaps representing a small subset (or ensemble) over time/space), we can replace $Q$ with $C$ (the sample covariance). In either case, we must have estimates of both $C$ and $R$. Whilst we can obtain estimates of $C$, estimates of $R$ are not possible. If we only have a single discrete value within a higher-dimensional model domain, then we have no way of estimating $R$. Furthermore, even in larger focal areas that might contain multiple discrete samples, the samples are too spread out both spatially and temporally to be able to estimate $R$ with any accuracy or reliability. For example, whilst the samples are typically separated in space by 10's of kilometres and months in time, water samples are likely to vary over the scale of meters and hours.

## 5.3 Gaussian Processes

A Gaussian distribution represents the distribution of observations that are themselves the result of an infinite number of influences (or processes). They are widely used to represent the distribution of residuals (unexplained component) when modelling data as it is often assumed that the unexplained component is due to a huge number of additional, unmeasured influences. In traditional linear modelling, we assume that not only are the residuals normally (Gaussian) distributed, we also assume that they are independent (not spatially or temporally correlated) and equally varied around 0.

$$\varepsilon_i \sim N(0, \Sigma) \qquad \Sigma = \begin{pmatrix} \sigma^2 & 0 & \dots & 0 \\ 0 & \sigma^2 & \dots & \vdots \\ \vdots & \dots & \sigma^2 & \vdots \\ 0 & \dots & \dots & \sigma^2 \end{pmatrix}$$

Similarly, rather than express the stochastic elements as a vector of residuals drawn from a normal distribution, we can model the observed data as a multivariate normal (Gaussian) distribution. In this case, we are assuming that each of the observations is drawn from a multivariate normal distribution with different means and covariances). This same argument could be extended to describe the distribution from which functions are drawn. Observed data are the result of the sum of an in infinite number of processes (including measurement error). Many of these processes vary over space and time such that sampling units that are closer together in space and time tend to be more similar to one another than they are to more distant units.

$$y \sim MVN(M, C)$$

A Gaussian Process is largely defined by the covariance matrix ($k(x, x')$). Actually *k* is referred to as the **kernel**. We can define any covariance (kernel) function provided it is semi-definite - essentially that it is a symmetrical matrix.

A few of the popular kernels are described in the following Table 19.

**Table 18: Simple Gaussian Process kernel functions**

| Kernel | Function |
|---|---|
| Linear | $k(x,x') = \sigma_f^2 xx'$ |
| Squared exponential | $k(x,x') = \sigma_f^2 exp\left\lvert\frac{-(x-x')^2}{l^2}\right\rvert$ |
| Periodic | $k(x,x') = \sigma_f^2 exp\left\lvert\frac{-2\sin^2(\pi(x-x')/p}{l^2}\right\rvert$ |
| Periodic exponential | $k(x,x') = \sigma_f^2 exp\left\lvert\frac{-2\sin^2(\pi(x-x')/p}{l_1^2}\right\rvert exp\left\lvert\frac{-(x-x')^2}{l_2^2}\right\rvert$ |
| Matern | $k(x,x') = \sigma_f^2 \frac{1}{\Gamma(v)2^{v-1}}\left\lvert\frac{\sqrt{2v}\lvert(x-x')\rvert}{l}\right\rvert^v K_v\left\lvert\frac{\sqrt{2v}\lvert(x-x')\rvert}{l}\right\rvert$ |

In Table 19, $x$ and $x'$ are vectors of the X variable. $x'$ just indicates a transposed version of the vector. Hence $(x - x')$ indicates the difference (distance) between each pair of x values (they are squared so that they are all positive). When two points are similar $k(x,x')$ approaches 1 (perfect correlation). Smoothing is based on neighbours exerting influence on one another (being correlated). When two points are very distant $k(x,x')$ approaches 0. The *l* are length scale parameters that determines the degree of contagion - that is, they determine the rate that the influence of points deteriorates with distance.

Assuming that the covariance pattern defined by the GP parameters (e.g. $\sigma_f^2$ and *l*) and observation space reliably reflects the underlying processes, the same parameters can be applied to yield a covariance structures for predicting mean and variance across a novel (yet overlapping) space. Specifically, if the covariance across the observed space is $K_{oo}$, the covariance between observed and prediction space is $K_{op}$ and the coavariance across prediction space is $K_{pp}$, then the mean and variance for predicted values are:

$$\hat{y}_p = K_{op}(K_{oo} + \sigma_o^2 I)^{-1} K_{op}^T y_o$$

and

$$var(y_p) = K_{pp} - K_{op}(K_{oo} + \sigma_o^2 I)^{-}1\, K_{op}^T$$

where $\sigma_o^2$ is the estimated variance (uncertainty) in the observations, *I* is an identity matrix of equivalent dimensionality to $K_{oo}$ and $K_{op}^T$ is the transpose of $K_{op}$.

Gaussian Processes could be used to fit smooth multidimensional smoothers separate over each source so as to estimate parameters and uncertainty at any granularity. Whilst this might be appropriate for the eReefs data, it is not possible to build a reasonable Gaussian process via a single point without external estimates of the covariance over functions ($\sigma_f^2$) and the length (wiggliness) of the smoother.

Normally a Gaussian Process is applied to a single source for the purpose of kriging (smoothing). Nevertheless, it could be argued that there are a single set of underlying processes driving spatio-temporal patterns of water quality (e.g. *l* and $\sigma_f^2$) and that the multiple sources (AIMS niskin and eReefs) represent alternative ways to sample observations from those processes. Ideally, any differences between the sources should purely be differences in

accuracy and uncertainty. If this is the case, rather than assume all observations are associated with the same $\sigma_o^2$, we could asssociate one variance to the AIMS niskin observations ($\sigma_n^2$ ) and another to the eReefs observations ($\sigma_e^2$).

Figure 109 illustrates a squared exponential Gaussian Processes with different parameter values applied to a single dimension (Latitude) of the 25/03/2015 Yongala focal area data. In each case, the variability (uncertainty) of the AIMS niskin observations was defined as 10 times lower than than of the eReefs observations. Values of $\sigma_f^2$ and *l* were chosen to represent specific sets of scenarios. For example, lower $\sigma_f^2$ imposes a lower maximum covariance and a lower *l* dictates are more rapid decline in the autocorrelation over distance. Whilst it is possible to apply these functions in an optimizing framework so as to allow the data to determine the most appropriate values for $\sigma_f^2$ and *l*, $\sigma_n^2$ and $\sigma_e^2$ must be supplied based on external estimates.

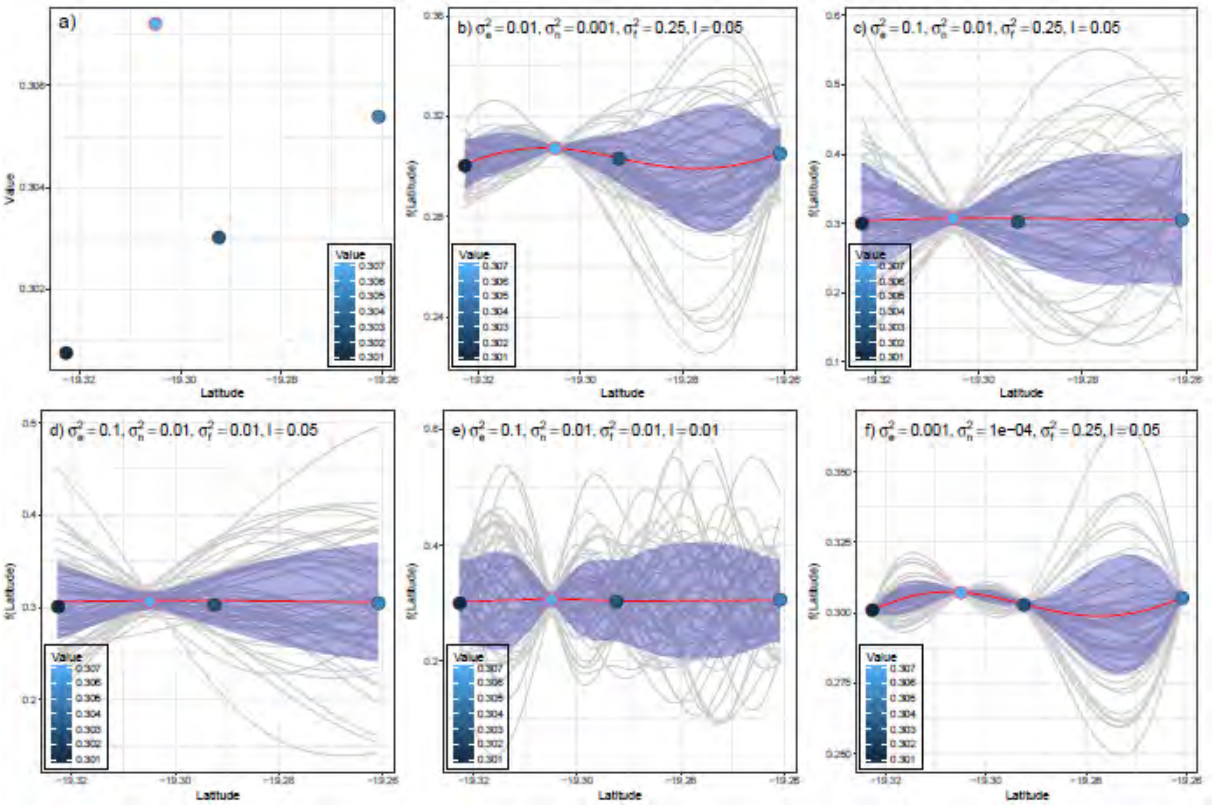


**Figure 109: Illustration of data assimilation via squared exponential Gaussian process applied to a single dimension (Latitude) for the 25/03/2015 Yongala focal area a) Raw Chlorophyll-a values and b-e) different Gaussian Process *parameters.***

Similar to the Kalman Filter, high dimensionality incurs substantial covariance size increases. Every one additional observation results in a doubling of the covariance matrix and a tripling of memory to invert this the covariance matrix. Hence, practical applications employ either ensemble-like approaches or more commonly, sparse covariance matrices[25] to reduce the imposition of dimensionality. Addition of a temporal dimension substantially increases the complexity of the problem. Not only does the covariance structures have to account for

[25] Sparse matrices acknowledge that covariance will decline over time and distance and at some distance, the covariance will effectively be zero.

variability and autocorrelation length over space, it also has to reflect patterns of variability over time. Importantly, it is not just how isolated spatial points change over time. Temporal autocorrelation also occurs between neighbouring points.

## 5.4 Fixed Rank Kriging

Fixed Rank Griging (FRK) is a spatio-temporal modelling and prediction framework in which spatially/temporally correlated random processes are decomposed via linear combinations of basis functions ($\Phi$) along with associated fine-scale variation ($v$) (Cressie and Johannesson, 2008).

$$Y = X\beta + \Phi\alpha + v$$

The use of relatively small numbers of basis functions permits substantial dimensionality reductions that offers a scalable solution for very large data sets. Moreover, the framework facilitates differing spatial support hence allowing some capacity for the 'fusion' of multiple sources with different footprints.

Varying footprints are accommodated by arranging the point-referenced data into grids, the granularity of which is proportional to the footprint or extent of support. For example, the AIMS niskin data and eReefs modelled data could be descretized into a small and set of larger grid squares (see Figure 110b - pale red and blue squares respectively). Whilst the footprint size for the eReefs modelled data was based on the cell grid onto which the model is projected, the AIMS niskin footprint was set to an arbitrarily (smaller) value to illustrate varying degrees of support.

The full spatio-temporal domain is also discretised into a regular grid of smaller cells called *basic areal units* (BAU) which represent the smallest modelling and prediction unit. In this example, we have discretised the spatial domain by hexagonal cells 0.01 degrees longitude by 0.01 degrees latitude (see Figure 110b - black hexagons). Within the model, varying support is then based on the intersection of the square footprints with the BAUs. For this example, we have elected to define two regularly spaced basis functions based on Matern covariance (smoothing parameter of 1.5) to be used in the decomposition of spatio-temporal processes (see Figure 110c).

The multiple resolutions provide a mechanism for estimating the scale of spatio-temporal autocorrelation (however, ideally this requires a substantially larger grid of data than our example).

The basis function covariance matrices and fine-scale variance parameters are estimated via a expectation maximization (EM) algorithm and thereafter used to project predictions onto the scale of the BAU's (see Figure 110d). These predicted values have also been indexed via fsMAMP (see Figure 110e) and converted into Grades (see Figure 110f).

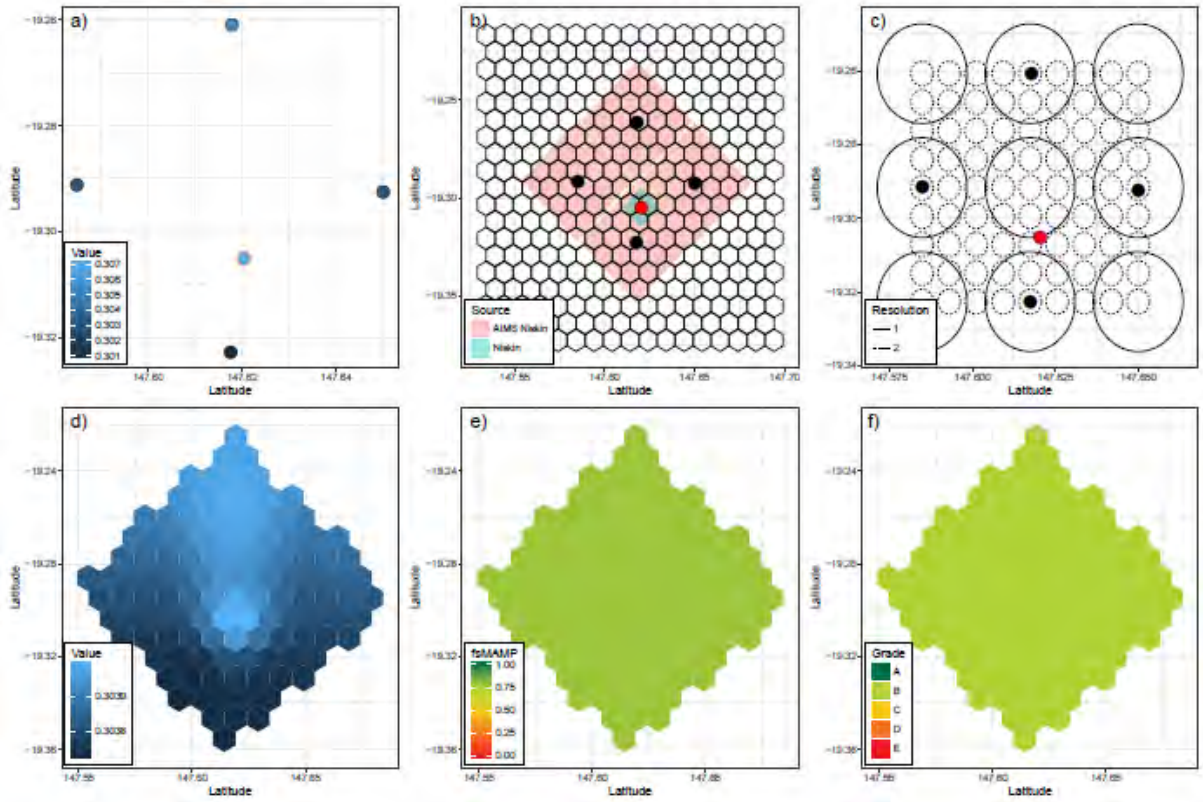


**Figure 110: Illustration of data assimilation via Fixed Rank Kriging applied to spatial data for the 25/03/2015 Yongala focal area a) Raw Chlorophyll-a values (AIMS niskin: red symbol border, eReefs: black symbol border), b) discretization of the spatial domain into a regular hexagonal grid and varying footprints (support) for AIMS niskin (blue) and eReefs (red), d) Matern basis functions of two resolutions, d) predicted values and associated e) fsMAMP indices and f) Grades (Uniform control chart) for 25/03/2015.**

Figure 110 illustrates that whilst fixed rank kriging does offer an option for the assimilation (or fusion) of multiple data sets, in the absence of measurement error, it does assume that all observations are equally accurate. Figure 110d shows a bright spot associated with the higher AIMS niskin Chlorophyll-a value. It is important to reiterate that the extent of this bright spot is due to both the higher Chlorophyll-a observation of the AIMS niskin sample and the arbitrary size of the footprint. To be a meaningful fusion, reasonable estimates of the spatio-temporal extent of representation of the AIMS niskin data will need to be obtained along with estimates of measurement error in both the AIMS niskin and eReefs modelled data.

Spatio-temporal basis functions can be constructed as the tensor product of spatial basis functions and similarly defined temporal basis functions. Measurement error (if known) can also be incorporated.

More recently, Nguyen et al. (2014) has proposed a data assimilation technique for big data that is essentially a blend of fixed rank kriging and Kalman filtering and looks to have some promise.

# REFERENCES

Attard, M., M. Thompson, R. Kelly, and A. Locatelli, 2012. Tamar Estuary Ecosystem Health Assessment Program Monitoring Report 2012. Report to NRM North Tamar Estuary and Esk Rivers Program. Technical report,. Australian and New Zealand Environment and Conservation Council, 2000. Australian Guidelines for Water Quality Monitoring and Reporting. Technical report, Environment Australia, Canberra.

Baird, M. E., N. Cherukuru, E. Jones, N. Margvelashvili, M. Mongin, K. Oubelkheir, P. J. Ralph, F. Rizwi, B. J. Robson, T. Schroeder, J. Skerratt, A. D. L. Steven, and K. A. Wild-Allen. 2016. Remote-sensing reflectance and true colour produced by a coupled hydrodynamic, optical, sediment, biogeochemical model of the Great Barrier Reef, Australia: comparison with satellite data. Env. Model. Software **78**:79–96.

Baird, M. E., P. J. Ralph, F. Rizwi, K. A. Wild-Allen, and A. D. L. Steven. 2013. A dynamic model of the cellular carbon to chlorophyll ratio applied to a batch culture and a continental shelf ecosystem. Limnol. Oceanogr. **58**:1215–1226.

Borja, A., D. M. Dauer, and A. Gremare. 2012. The importance of setting targets and reference conditions in assessing marine ecosystem quality. Ecological Indicators **12**:1 –7. CCME, 2001. Canadian water quality guidelines for the protection of aquatic life: CCME Water Quality Index

1.0, Technical Report. Technical report, CCME, Winnipeg, Manitoba, Canada.

Coates, S., A. Waugh, A. Anwar, and M. Robson. 2007. Efficacy of multimetric fish index as an analysis tool for the transitional fish component of the water framework directive. Marine Pollution Bulletin **55**:255 – 240.

Connolly, R. M., S. Bunn, M. Campbell, B. Escher, J. Hunter, P. Maxwell, T. Page, S. Richmond, D. Rissik, A. Roiko, J. Smart, and P. Teasdale, 2013. Review of the use of report cards for monitoring ecosystem and waterway health. Report to: Gladstone Healthy Harbour Partnership. Technical report, , Queensland, Australia.

Cressie, N., and G. Johannesson. 2008. Fixed rank kriging for very large spatial data sets. Journal of the Royal Statistical Society, B **70**:209–226.

Dauvin, J. C., C. Fisson, J. Garnier, R. Lafite, T. Ruellet, J. Billen, G.and Deloffre, and R. Verney. 2008. A report card and quality indicators for the Seine estuary: From scientific approach to operational tool. Marine Pollution Bulletin **57**:187 – 201.

Dobbie, M. J., and D. Dail. 2013. Robustness and sensitivity of weighting and aggregation in constructing composite indices. Ecological Indicators .

Doran, G. T. 1981. There's a S.M.A.R.T. way to write management's goals and objectives. Management Review (AMA FORUM) **70**:35 – 36.

Emerson, J., A. Hsu, M. Levy, A. de Sherbinin, V. Mara, D. Esty, and M. Jaiteh, 2012. Environmental Performance Index and Pilot Trend Environmental Performance Index. Technical report, Yale Center for Environmental Law and Policy, New Haven. EPA/EC, 1995. State of the Great Lakes 1995. Washington (DC). Technical report, Environmental Protection Agency and Environment Canada,.

Flint, N., J. Rolfe, C. Jones, C. Sellens, A. Rose, and L. Fabbro, 2012. Technical review for the development of an ecosystem health index and report card for the Fitzroy Partnership for river health. Part A: Review of ecosystem health indicators for the Fitzroy Basin. Technical report, Centre for Environmental Management, Central Queensland University.

Ford, D. A., K. P. Edwards, D. Lea, R. M. Barciela, M. J. Martin, and J. Demaria. 2012. Assimilating GlobColour ocean colour data into a pre-operational physical-biogeochemical model. Ocean Sci. **8**:751–771.

Fox, D., 2013. Statistical issues associated with the development of an ecosystem report card. Technical report, Environmetrics Australia. Gladstone Healthy Harbour Partnership, 2016. Technical Report, Gladstone Harbour Report Card 2016, GHHP Technical Report No.3. Technical report, Gladstone Healthy Harbour Partnership, Gladstone.

Hallett, C. S., F. J. Valesini, K. R. Clarke, S. A. Hesp, and S. D. Hoeksema. 2012. Development and validation of fish-based, multimetric indices for assessing the ecological health of Western Australian estuaries. Estuarine, Coastal and Shelf Science **104 – 105**:102 – 113.

Harwell, M., V. Myers, T. Young, A. Bartuska, N. Gassman, J. H. Gentile, S. Appelbaum, J. Barko, B. Causey, C. Johnson, A. McLean, R. Smola, P. Templet, and S. Tosini. 1999. A Framework for an Ecosystem Integrity Report Card: Examples from South Florida show how an ecosystem report card links societal values and scientific information. BioScience **49**:543–556. URL http://www.jstor.org/stable/10.1525/bisi.1999.49.7.543.

Herzfeld, M. 2006. An alternative coordinate system for solving finite difference ocean models. Ocean Modelling **14**:174 – 196.

Herzfeld, M., S. Condie, J. R. Andrewartha, and B. Gorton, 2015. Project ISP007: Development of Connectivity Indicators for the Gladstone Healthy Harbour Report Card Draft Final Technical Report. Technical report, CSIRO.

Hijuelos, A., and D. Reed, 2013. Methodology for Producing a Coastal Louisiana Report Card, September 13, 2013. The Water Institute of the Gulf. Technical report, .

Hurley, T., R. Sadiq, and A. Mazumder. 2012. Adaptation and evaluation of the Canadian Council of Ministers of the Environment Water Quality Index (CCME WQI) for use as an effective tool to characterize drinking source water quality. Water Resources **46**:3544 – 3552.

James, A., C, J. Kershner, J. Samhouri, S. O'Neil, and P. S. Levin. 2012. A Methodology for Evaluating and Ranking Water Quantity Indicators in Support of Ecosystem-Based Management. Envirnmental Management **49**:703 – 719.

Jones, C., J. Flint, Rolfe, C. Sellens, and L. Fabbro, 2013. Technical review for the development of an ecosystem health index and report card for the Fitzroy Partnership for river health. Part B: Methodology and data analysis to support an ecosystem health index and report card for the Fitzroy Basin. Technical report, Centre for Environmental Management, Central Queensland University.

Jones, E. M., M. E. Baird, M. Mongin, J. Parslow, J. Skerratt, J. Lovell, N. Margvelashvili, R. J. Matear, K. Wild- Allen, B. Robson, F. Rizwi, P. Oke, E. King, T. Schroeder, A. Steven, and J. Taylor. 2016. Use of remotesensing reflectance to constrain a data assimilating marine biogeochemical model of the Great Barrier Reef. Biogeosciences **13**:6441–6469.

Kidston, M., R. Matear, and M. E. Baird. 2013. Phytoplankton growth in the Australian sector of the Southern Ocean, examined by optimising ecosystem model parameters. J. Mar. Sys. **128**:123–137.

Lønborg, C., M. Devlin, R. Brinkman, P. Costello, E. da Silva, J. Davidson, K. Gunn, M. Logan, C. Petus, B. Schaffelke, M. Skuza, H. Tonin, D. Tracey, M. Wright, and I. Zagorskis, 2016. Reef Rescue Marine Monitoring Program. Annual Report of AIMS and JCU Activities 2014 to 2015– Inshore water quality monitoring. Report for the Great Barrier Reef Marine Park Authority. Technical report, Australian Institute of Marine Science and JCU TropWATER, Townsville. 170pp.

Margvelashvili, N. 2009. Stretched Eulerian coordinate model of coastal sediment transport. Computer Geosciences **35**:1167–1176.

Margvelashvili, N., M. Herzfeld, F. Rizwi, M. Mongin, M. Baird, E. Jones, B. Schaffelke, E. King, and T. Schroeder. 2016. Emulator-assisted data assimilation in complex models. Ocean Dyn. **66**:1109–1124.

MidCoast Council, 2016. MidCoast Council 2016 Waterway and Catchment Report. Technical report, MidCoast Council, Natural Systems and Estuaries Section. Miller, W. W., H. M. Joung, C. N. Mahannah, and J. R. Garret. 1986. Identification of Water Quality Differences in Nevada Through Index Application1. Journal of Environmental Quality **15**.

Neary, B. P., 2012. A sensitivity analysis of the Canadian Water Quality Index. A report for CCME prepared by Gartner Lee Limited, Ontario, Canada. Technical report, .

Nguyen, H., M. Katzfuss, , N. Cressie, and A. Braverman. 2014. Spatio-temporal data fusion for very large remote sensing datasets. Technometrics **56**:174–175.

Ridgway, K. R., J. R. Dunn, and J. L. Wilkin. 2002. Ocean interpolation by four-dimensional least squares - Application to the waters around Australia. J. Atmos. Ocean. Tech. **19**:1357–1375.

Sakov, P., 2017. EnKF-C user guide version 1.63.0. Technical report, Bureau of Meteorology, https://arxiv.org/pdf/1410.1233.pdf.

Schiller, A., M. Herzfeld, R. Brinkman, and G. Stuart. 2014. Monitoring, predicting and managing one of the seven natural wonders of the world. Bull. Am. Meteor. Soc. pages 23–30.

Schroeder, T., B. Nechad, K. Ruddick, R. Doerffer, M. Schaale, V. Brando, and A. Dekker. 2012. Inter-comparison of MODIS atmospheric correction algorithms for coastal waters using shipborne above water radiometry. pers. comm. .

Skerratt, J., M. Mongin, K. A. Wild-Allen, M. E. Baird, B. J. Robson, B. Schaffelke, M. Soja-Wozniak, N. Margvelashvili, C. H. Davies, A. J. Richardson, and A. D. L. Steven. submitted 9 Nov. 2017. Plankton and nutrient dynamics on the Great Barrier Reef: Skill assessment and analysis of the eReefs biogeochemical model. J. Mar. Sys. •:•.

Walsh, P., and W. Wheeler, 2012. Water quality index aggregation and cost benefit analysis. Working Paper 12- 05. Technical report, U.S. Environmental Protection Agency, National Center for Environmental Economics, Washington, DC.

Waters, D., C. Carroll, R. Ellis, L. Hateley, J. McCloskey, R. Packett, C. Dougall, and B. Fentie, 2014. Modelling reductions of pollutant loads due to improved management practices in the Great Barrier Reef catchments – Whole of GBR. Technical report, Queensland Department of Natural Resources and Mines, Toowoomba, Queensland.

Whittaker, G., S. Lautenbach, and M. Volk, 2012. What is a good index? Problems with statistically based indicators and the Malmquist index as alternative. *in* R. Seppelt, A. A. Voinov, S. Lange, and D. Bankamp, editors. International Environmental Modelling and Software Society (iEMSs) 2012 International Congress on Environmental Modelling and Software Managing Resources of a Limited Planet, Sixth Biennial Meeting. , Leipzig, Germany.

Wood, S. N. 2006. Generalized Additive Models: An Introduction with R. Chapman & Hall/CRC.

# APPENDIX A: THRESHOLDS

Water Quality Threshold values for each Measure in each Zone (Region/Water Body). Thresholds values are similar to annual Guideline values. Wet and Dry represent Wet and Dry season thresholds respectively. Direction of Failure indicates whether a values higher ('H') or lower ('L') than a Threshold would constitute an exceedance. Range From and Range To represent Thresholds for Measures that have a range of optimum values (such as dissolved oxygen or pH).

| Measure | Units | Water Body | Region | Threshold | | | Direction of Faiure | Justification |
|---|---|---|---|---|---|---|---|---|
| | | | | Annual | Dry | Wet | | |
| chl | $\mu gL^{-1}$ | Enclosed Coastal | Cape York | 2.00 | 2.00 | 2.00 | H | QLD WQ guidelines |
| chl | $\mu gL^{-1}$ | Enclosed Coastal | Wet Tropics | 1.10 | 1.10 | 1.10 | H | There is no seasonal adjustment |
| chl | $\mu gL^{-1}$ | Enclosed Coastal | Dry Tropics | 1.00 | 1.00 | 1.00 | H | |
| chl | $\mu gL^{-1}$ | Enclosed Coastal | Mackay Whitsunday | 1.30 | 1.30 | 1.30 | H | |
| chl | $\mu gL^{-1}$ | Enclosed Coastal | Fitzroy | 2.00 | 2.00 | 2.00 | H | |
| chl | $\mu gL^{-1}$ | Enclosed Coastal | Burnett Mary | 2.00 | 2.00 | 2.00 | H | |
| chl | $\mu gL^{-1}$ | Open Coastal | Cape York | 0.45 | 0.63 | 0.32 | H | GBRMPA WQ guidelines |
| chl | $\mu gL^{-1}$ | Open Coastal | Wet Tropics | 0.45 | 0.63 | 0.32 | H | 40% higher in summer, 30% lower in winter |
| chl | $\mu gL^{-1}$ | Open Coastal | Dry Tropics | 0.45 | 0.63 | 0.32 | H | Here summer is taken as Wet Season |
| chl | $\mu gL^{-1}$ | Open Coastal | Mackay Whitsunday | 0.45 | 0.63 | 0.32 | H | and winter is taken as Dry Season |
| chl | $\mu gL^{-1}$ | Open Coastal | Fitzroy | 0.45 | 0.63 | 0.32 | H | |
| chl | $\mu gL^{-1}$ | Open Coastal | Burnett Mary | 0.45 | 0.63 | 0.32 | H | |
| chl | $\mu gL^{-1}$ | Midshelf | Cape York | 0.45 | 0.63 | 0.32 | H | GBRMPA WQ guidelines |
| chl | $\mu gL^{-1}$ | Midshelf | Wet Tropics | 0.45 | 0.63 | 0.32 | H | 40% higher in summer, 30% lower in winter |
| chl | $\mu gL^{-1}$ | Midshelf | Dry Tropics | 0.45 | 0.63 | 0.32 | H | Here summer is taken as Wet Season |
| chl | $\mu gL^{-1}$ | Midshelf | Mackay Whitsunday | 0.45 | 0.63 | 0.32 | H | and winter is taken as Dry Season |
| chl | $\mu gL^{-1}$ | Midshelf | Fitzroy | 0.45 | 0.63 | 0.32 | H | |
| chl | $\mu gL^{-1}$ | Midshelf | Burnett Mary | 0.45 | 0.63 | 0.32 | H | |
| chl | $\mu gL^{-1}$ | Offshore | Cape York | 0.40 | 0.56 | 0.28 | H | GBRMPA WQ guidelines |
| chl | $\mu gL^{-1}$ | Offshore | Wet Tropics | 0.40 | 0.56 | 0.28 | H | 40% higher in summer, 30% lower in winter |
| chl | $\mu gL^{-1}$ | Offshore | Dry Tropics | 0.40 | 0.56 | 0.28 | H | Here summer is taken as Wet Season |
| chl | $\mu gL^{-1}$ | Offshore | Mackay Whitsunday | 0.40 | 0.56 | 0.28 | H | and winter is taken as Dry Season |
| chl | $\mu gL^{-1}$ | Offshore | Fitzroy | 0.40 | 0.56 | 0.28 | H | |
| chl | $\mu gL^{-1}$ | Offshore | Burnett Mary | 0.40 | 0.56 | 0.28 | H | |
| nap | $mgL^{-1}$ | Enclosed Coastal | Cape York | 10.00 | 10.00 | 10.00 | H | QLD WQ guidelines |
| nap | $mgL^{-1}$ | Enclosed Coastal | Wet Tropics | 10.00 | 10.00 | 10.00 | H | There is no seasonal adjustment and |
| nap | $mgL^{-1}$ | Enclosed Coastal | Dry Tropics | 10.00 | 10.00 | 10.00 | H | values for CY and WT are not determined |
| nap | $mgL^{-1}$ | Enclosed Coastal | Mackay Whitsunday | 10.00 | 10.00 | 10.00 | H | Suggest applying same ratio as for turbidity |
| nap | $mgL^{-1}$ | Enclosed Coastal | Fitzroy | 15.00 | 15.00 | 15.00 | H | between CY/WT and others, i.e (15*10)/6=25 |
| nap | $mgL^{-1}$ | Enclosed Coastal | Burnett Mary | 15.00 | 15.00 | 15.00 | H | NAP is taken as = TSS in this context |
| nap | $mgL^{-1}$ | Open Coastal | Cape York | 2.00 | 2.40 | 1.60 | H | GBRMPA WQ guidelines |
| nap | $mgL^{-1}$ | Open Coastal | Wet Tropics | 2.00 | 2.40 | 1.60 | H | 20% higher in summer, 20% lower in winter |
| nap | $mgL^{-1}$ | Open Coastal | Dry Tropics | 2.00 | 2.40 | 1.60 | H | Here summer is taken as Wet Season |
| nap | $mgL^{-1}$ | Open Coastal | Mackay Whitsunday | 2.00 | 2.40 | 1.60 | H | and winter is taken as Dry Season |
| nap | $mgL^{-1}$ | Open Coastal | Fitzroy | 2.00 | 2.40 | 1.60 | H | |
| nap | $mgL^{-1}$ | Open Coastal | Burnett Mary | 2.00 | 2.40 | 1.60 | H | NAP is taken as = TSS in this context |
| nap | $mgL^{-1}$ | Midshelf | Cape York | 2.00 | 2.40 | 1.60 | H | GBRMPA WQ guidelines |
| nap | $mgL^{-1}$ | Midshelf | Wet Tropics | 2.00 | 2.40 | 1.60 | H | 20% higher in summer, 20% lower in winter |
| nap | $mgL^{-1}$ | Midshelf | Dry Tropics | 2.00 | 2.40 | 1.60 | H | Here summer is taken as Wet Season |
| nap | $mgL^{-1}$ | Midshelf | Mackay Whitsunday | 2.00 | 2.40 | 1.60 | H | and winter is taken as Dry Season |
| nap | $mgL^{-1}$ | Midshelf | Fitzroy | 2.00 | 2.40 | 1.60 | H | |

...continued from previous page

| Measure | Units | Water Body | Region | Threshold | | | Direction of Faiure | Justification |
|---|---|---|---|---|---|---|---|---|
| | | | | Annual | Dry | Wet | | |
| nap | $mgL^{-1}$ | Midshelf | Burnett Mary | 2.00 | 2.40 | 1.60 | H | NAP is taken as = TSS in this context |
| nap | $mgL^{-1}$ | Offshore | Cape York | 0.70 | 0.84 | 0.56 | H | GBRMPA WQ guidelines |
| nap | $mgL^{-1}$ | Offshore | Wet Tropics | 0.70 | 0.84 | 0.56 | H | 20% higher in summer, 20% lower in winter |
| nap | $mgL^{-1}$ | Offshore | Dry Tropics | 0.70 | 0.84 | 0.56 | H | Here summer is taken as Wet Season |
| nap | $mgL^{-1}$ | Offshore | Mackay Whitsunday | 0.70 | 0.84 | 0.56 | H | and winter is taken as Dry Season |
| nap | $mgL^{-1}$ | Offshore | Fitzroy | 0.70 | 0.84 | 0.56 | H | |
| nap | $mgL^{-1}$ | Offshore | Burnett Mary | 0.70 | 0.84 | 0.56 | H | NAP is taken as = TSS in this context |
| ntu | NTU | Enclosed Coastal | Cape York | 4.00 | 4.00 | 4.00 | H | QLD WQ guidelines |
| ntu | NTU | Enclosed Coastal | Wet Tropics | 4.00 | 4.00 | 4.00 | H | There is no seasonal adjustment |
| ntu | NTU | Enclosed Coastal | Dry Tropics | 4.00 | 4.00 | 4.00 | H | |
| ntu | NTU | Enclosed Coastal | Mackay Whitsunday | 4.00 | 4.00 | 4.00 | H | Unclear as to why the CY/WT guidelines |
| ntu | NTU | Enclosed Coastal | Fitzroy | 6.00 | 6.00 | 6.00 | H | are higher than Southern regions |
| ntu | NTU | Enclosed Coastal | Burnett Mary | 6.00 | 6.00 | 6.00 | H | |
| ntu | NTU | Open Coastal | Cape York | 1.50 | 1.80 | 1.20 | H | No guideline available but turbidity needed if logger |
| ntu | NTU | Open Coastal | Wet Tropics | 1.50 | 1.80 | 1.20 | H | data is to be integrated. |
| ntu | NTU | Open Coastal | Dry Tropics | 1.50 | 1.80 | 1.20 | H | MMP used a correlation between TSS and NTU |
| ntu | NTU | Open Coastal | Mackay Whitsunday | 1.50 | 1.80 | 1.20 | H | (based on whole of GBR data) which is also used here |
| ntu | NTU | Open Coastal | Fitzroy | 1.50 | 1.80 | 1.20 | H | |
| ntu | NTU | Open Coastal | Burnett Mary | 1.50 | 1.80 | 1.20 | H | Applied 20% higher in summer, 20% lower in winter |
| ntu | NTU | Midshelf | Cape York | 1.50 | 1.80 | 1.20 | H | No guideline available but turbidity needed if logger |
| ntu | NTU | Midshelf | Wet Tropics | 1.50 | 1.80 | 1.20 | H | data is to be integrated. |
| ntu | NTU | Midshelf | Dry Tropics | 1.50 | 1.80 | 1.20 | H | MMP used a correlation between TSS and NTU |
| ntu | NTU | Midshelf | Mackay Whitsunday | 1.50 | 1.80 | 1.20 | H | (based on whole of GBR data) which is also used here |
| ntu | NTU | Midshelf | Fitzroy | 1.50 | 1.80 | 1.20 | H | |
| ntu | NTU | Midshelf | Burnett Mary | 1.50 | 1.80 | 1.20 | H | Applied 20% higher in summer, 20% lower in winter |
| ntu | NTU | Offshore | Cape York | 1.00 | 1.20 | 0.80 | H | No guideline available but turbidity needed if logger |
| ntu | NTU | Offshore | Wet Tropics | 1.00 | 1.20 | 0.80 | H | data is to be integrated. |
| ntu | NTU | Offshore | Dry Tropics | 1.00 | 1.20 | 0.80 | H | MMP used a correlation between TSS and NTU |
| ntu | NTU | Offshore | Mackay Whitsunday | 1.00 | 1.20 | 0.80 | H | (based on whole of GBR data) which is also used here |
| ntu | NTU | Offshore | Fitzroy | 1.00 | 1.20 | 0.80 | H | |
| ntu | NTU | Offshore | Burnett Mary | 1.00 | 1.20 | 0.80 | H | Applied 20% higher in summer, 20% lower in winter |
| sd | m | Enclosed Coastal | Cape York | 1.00 | 1.00 | 1.00 | L | QLD WQ guidelines |
| sd | m | Enclosed Coastal | Wet Tropics | 1.00 | 1.00 | 1.00 | L | There is no seasonal adjustment |
| sd | m | Enclosed Coastal | Dry Tropics | 1.50 | 1.50 | 1.50 | L | |
| sd | m | Enclosed Coastal | Mackay Whitsunday | 1.00 | 1.00 | 1.00 | L | Unclear as to why the CY/WT guidelines |
| sd | m | Enclosed Coastal | Fitzroy | 1.50 | 1.50 | 1.50 | L | are lower than Southern regions |
| sd | m | Enclosed Coastal | Burnett Mary | 1.50 | 1.50 | 1.50 | L | |
| sd | m | Open Coastal | Cape York | 10.00 | 10.00 | 10.00 | L | GBRMPA WQ guidelines |
| sd | m | Open Coastal | Wet Tropics | 10.00 | 10.00 | 10.00 | L | There is no seasonal adjustment |
| sd | m | Open Coastal | Dry Tropics | 10.00 | 10.00 | 10.00 | L | |
| sd | m | Open Coastal | Mackay Whitsunday | 10.00 | 10.00 | 10.00 | L | |
| sd | m | Open Coastal | Fitzroy | 10.00 | 10.00 | 10.00 | L | |
| sd | m | Open Coastal | Burnett Mary | 10.00 | 10.00 | 10.00 | L | |
| sd | m | Midshelf | Cape York | 10.00 | 10.00 | 10.00 | L | GBRMPA WQ guidelines |

*...continued from previous page*

| Measure | Units | Water Body | Region | Threshold | | | Direction of Faiure | Justification |
|---|---|---|---|---|---|---|---|---|
| | | | | Annual | Dry | Wet | | |
| sd | m | Midshelf | Wet Tropics | 10.00 | 10.00 | 10.00 | L | There is no seasonal adjustment |
| sd | m | Midshelf | Dry Tropics | 10.00 | 10.00 | 10.00 | L | |
| sd | m | Midshelf | Mackay Whitsunday | 10.00 | 10.00 | 10.00 | L | |
| sd | m | Midshelf | Fitzroy | 10.00 | 10.00 | 10.00 | L | |
| sd | m | Midshelf | Burnett Mary | 10.00 | 10.00 | 10.00 | L | |
| sd | m | Offshore | Cape York | 17.00 | 17.00 | 17.00 | L | GBRMPA WQ guidelines |
| sd | m | Offshore | Wet Tropics | 17.00 | 17.00 | 17.00 | L | There is no seasonal adjustment |
| sd | m | Offshore | Dry Tropics | 17.00 | 17.00 | 17.00 | L | |
| sd | m | Offshore | Mackay Whitsunday | 17.00 | 17.00 | 17.00 | L | |
| sd | m | Offshore | Fitzroy | 17.00 | 17.00 | 17.00 | L | |
| sd | m | Offshore | Burnett Mary | 17.00 | 17.00 | 17.00 | L | |
| NOx | $\mu gL^{-1}$ | Enclosed Coastal | Cape York | 10.00 | 10.00 | 10.00 | H | Old MMP guidelines |
| NOx | $\mu gL^{-1}$ | Enclosed Coastal | Wet Tropics | 10.00 | 10.00 | 10.00 | H | There is no seasonal adjustment |
| NOx | $\mu gL^{-1}$ | Enclosed Coastal | Dry Tropics | 3.00 | 3.00 | 3.00 | H | |
| NOx | $\mu gL^{-1}$ | Enclosed Coastal | Mackay Whitsunday | 3.00 | 3.00 | 3.00 | H | |
| NOx | $\mu gL^{-1}$ | Enclosed Coastal | Fitzroy | 3.00 | 3.00 | 3.00 | H | |
| NOx | $\mu gL^{-1}$ | Enclosed Coastal | Burnett Mary | 3.00 | 3.00 | 3.00 | H | |
| NOx | $\mu gL^{-1}$ | Open Coastal | Cape York | 2.00 | 2.00 | 2.00 | H | Old MMP guidelines |
| NOx | $\mu gL^{-1}$ | Open Coastal | Wet Tropics | 2.00 | 2.00 | 2.00 | H | There is no seasonal adjustment |
| NOx | $\mu gL^{-1}$ | Open Coastal | Dry Tropics | 3.00 | 3.00 | 3.00 | H | |
| NOx | $\mu gL^{-1}$ | Open Coastal | Mackay Whitsunday | 3.00 | 3.00 | 3.00 | H | |
| NOx | $\mu gL^{-1}$ | Open Coastal | Fitzroy | 3.00 | 3.00 | 3.00 | H | |
| NOx | $\mu gL^{-1}$ | Open Coastal | Burnett Mary | 3.00 | 3.00 | 3.00 | H | |
| NOx | $\mu gL^{-1}$ | Midshelf | Cape York | 2.00 | 2.00 | 2.00 | H | Old guidelines |
| NOx | $\mu gL^{-1}$ | Midshelf | Wet Tropics | 2.00 | 2.00 | 2.00 | H | There is no seasonal adjustment |
| NOx | $\mu gL^{-1}$ | Midshelf | Dry Tropics | 2.00 | 2.00 | 2.00 | H | |
| NOx | $\mu gL^{-1}$ | Midshelf | Mackay Whitsunday | 2.00 | 2.00 | 2.00 | H | |
| NOx | $\mu gL^{-1}$ | Midshelf | Fitzroy | 2.00 | 2.00 | 2.00 | H | |
| NOx | $\mu gL^{-1}$ | Midshelf | Burnett Mary | 2.00 | 2.00 | 2.00 | H | |
| NOx | $\mu gL^{-1}$ | Offshore | Cape York | 2.00 | 2.00 | 2.00 | H | Old MMP guidelines |
| NOx | $\mu gL^{-1}$ | Offshore | Wet Tropics | 2.00 | 2.00 | 2.00 | H | There is no seasonal adjustment |
| NOx | $\mu gL^{-1}$ | Offshore | Dry Tropics | 2.00 | 2.00 | 2.00 | H | |
| NOx | $\mu gL^{-1}$ | Offshore | Mackay Whitsunday | 2.00 | 2.00 | 2.00 | H | |
| NOx | $\mu gL^{-1}$ | Offshore | Fitzroy | 2.00 | 2.00 | 2.00 | H | |
| NOx | $\mu gL^{-1}$ | Offshore | Burnett Mary | 2.00 | 2.00 | 2.00 | H | |

# APPENDIX B: EREEFS MODELS

**Table 19: eReefs regional biogeochemical simulation catalog.**

| Simulation name | Herein name | Date range | Delivery | Notes/Improvements |
|---|---|---|---|---|
| GBR4_H1p85_B1p0_Cbas_Dhnd | eReefs926 | Jan 1, 2011 – Jun 30, 2014 | Available on NCI | Simulation delivered as part of SIEF project (previously known as 926). Skill assessment available in SIEF report. |
| GBR4_H2p0_B2p0_Chyd_Dhnd | | Jan 1, 2011 – present, 2014 | | Second publicly-release (mid 2017) long run being used for GBRF resilience and NESP TWQ Hub projects. |
| GBR4_H2p0_B1p9_Chyd_Dran | eReefs | May 1, 2013 – Oct 1, 2016 | | First application of BGC data assimilation that is being used for GBR report card 7. |

Reef & Rainforest
RESEARCH CENTRE

www.nesptropical.edu.au